Spatial Distribution and Mass Transport of Per- and Polyfluoroalkyl Substances (PFAS) in Surface Water Systems

by

Roger Lopes Viticoski

A dissertation submitted to the Graduate Faculty of
Auburn University
in partial fulfillment of the
requirements for the Degree of
Doctor of Philosophy

Auburn, Alabama
December 10, 2022

Keywords: PFAS, Spatial Distribution, Mass Flux

Approved by

Joel S. Hayworth, Chair, Elton Z. and Lois G. Huff Associate Professor of Civil Engineering
David M. Blersch, Associate Professor of Biosystems Engineering
Mark O. Barnett, Professor of Civil Engineering
Stephanie R. Rogers, Assistant Professor of Geosciences

Abstract

Per- and polyfluoroalkyl substances (PFAS) are a group of nearly 5,000 anthropogenic organic substances produced since the late 1940s. These substances have been used in various consumer products and industrial applications due to their unique chemical properties. The presence of PFAS in the natural environment is particularly concerning because of their recalcitrance and potential adverse health effects on humans and wildlife. Hundreds of studies have contributed to the growing understanding of PFAS, but there are still many unknowns regarding their behavior and fate once in the environment. Thus, this work aims to advance the understanding of the distribution, transport, and fate of PFAS in the environment, with a focus on surface water systems. This dissertation presents three novel research projects aiming to answer similar questions at different geographical scales. First, research data from 228 peer-reviewed journal articles were analyzed to assess the current state of knowledge regarding the global spatial distribution and specific profile of PFAS in the environment and provide guidance regarding environmentally relevant concentrations (ERCs). General information, including location, total and individual PFAS concentrations, author, year, and media, were extracted from these 228 studies. PFAS were detected in 43 countries across all continents between 1999-2021, with ∑PFAS reaching 2,270 μg L^{-1} in surface water, 7,090 μg L^{-1} in groundwater, and 2,450 ng gdw^{-1} in sediment. Worldwide information on PFAS concentrations was used to develop ERCs, recommended not to exceed 2,721 and 48,606 ng L^{-1} in studies evaluating PFAS in surface water and groundwater, respectively, and 137.9 ng gdw^{-1} in sediments to guarantee environmental relevance. ERCs are particularly important in designing controlled studies, in which parameters must mimic environmental conditions to ensure results are meaningful and representative. Furthermore, PFAS have been detected in several areas in the United States, especially in Alabama. Several cities in the state are struggling with PFAS contamination of their drinking water sources, but the overall distribution and sources of PFAS in the state are still mostly unknown. Moreover, tracking the transport of PFAS in the environment has been proven to be challenging, partially due to most studies expressing PFAS contamination solely in terms of aqueous concentration. Seventy-four surface water samples were collected in strategic locations

across all major river systems in Alabama. Samples were filtered, processed in the laboratory through solid phase extraction (SPE), and analyzed using an ultra-high performance liquid chromatography, triple quadrupole mass spectrometer (UHPLC-MS/MS). At least one PFAS was detected in 88% of all samples, with ∑PFAS ranging from non-detect to 237 ng L^{-1}. PFAS distribution was not uniform across the state: while relatively high mean ∑PFAS were detected in the Coosa (191 ng L^{-1}) and Alabama (100 ng L^{-1}) rivers, these substances were not detected in the Conecuh, Escatawpa, and Yellow rivers. Trends in the transport characteristics of PFAS were investigated through a mass flux analysis by multiplying the aqueous concentration by the volumetric flow rate. Consistent increases in the mass fluxes of PFAS were generally observed as rivers flowed through the state, revealing the existence of numerous sources across the state. The highest mass flux (63.3 mg s^{-1}) was detected on the most downstream sampling point in the Alabama River, which eventually discharges into Mobile Bay. Results of this study confirm the ubiquity of PFAS in Alabama and demonstrate that mass flux is a simple and powerful complementary approach that can be used to broadly understand trends in the transport and fate of PFAS in large river systems. Several areas of interest emerged from this project, including a section of the Tallapoosa River Basin downstream from Thurlow Dam and the Chattooga River, part of the Coosa River Basin. This area was used as case study to further elucidate the sources and transport characteristics of PFAS through a mass flux analysis, in which eleven surface water samples were collected in August 2021. Four perfluoroalkyl carboxylic acids (PFCAs) were detected in all eleven samples from the Tallapoosa River Basin, with ∑PFAS ranging from 17.4 to 89.0 ng L^{-1}. Among the potential sources investigated, the Stone's Throw Landfill seems to be a substantial source of PFAS in the Tallapoosa River Basin.

Acknowledgments

First and foremost, I would like to thank my mother Neusa, my husband Clayton, and my sister Vanessa for believing in me and supporting me through this journey. Thank you for all the unconditional love - I could not have done this without you.

I am grateful to have been mentored by great researchers. I would like to thank my advisor, Dr. Joel Hayworth, for the mentorship, opportunity, and for allowing me to pursue my research interests. I could not have completed this work without Dr. Vanisree Mulabagal – thank you for all the inputs and guidance. I would also like to thank my committee members, Dr. David Blersch, Dr. Stephanie Rogers, and Dr. Mark Barnett for their guidance, inspiration, and mentorship. Special thanks to Dr. Soledad Peresin for her role as the University Reader. I would also like to thank my lab mates Meredith Feltman, Danyang Wang, and Ayesha Alam for their help and support with the many hours of sampling and SPE.

Last but not least, I would have been lost without my chosen family. Thank you to all the friends I made along the way in Auburn and San Antonio. Thank you for all the laughs, help with sample collections, dinner parties, barbecues, and companionship. You made this journey much easier.

"Alone we can do so little; together we can do so much"

-Helen Keller

Table of Contents

List of Tables

List of Figures

List of Abbreviations

ADEM	Alabama Department of Environmental Management
AFFF	Aqueous film-forming foam
DF	Detection frequencies
DI	Deionized Water
ERCs	Environmentally relevant concentrations
FDA	Food and Drugs Agency
GAC	Granulated Activated Carbon
HAL	Health advisory limit
MCL	Maximum Contaminant Level
MRM	Multiple reaction monitoring
n.d.	Non-detect
NHANES	National Health and Nutrition Examination Survey
NWM	National Water Model
OECD	Organization for Economic Co-operation and Development
PFAAs	Perfluoroalkyl acids
PFAS	Per- and polyfluoroalkyl Substances
PFCAs	Perfluoroalkyl carboxylic acids
PFPAs	Perfluoroalkyl phosphonic acids
PFPIAs	Perfluoroalkyl phosphinic acids
PFSAs	Perfluoroalkyl sulfonic acids
UHPLC-MSMS/MS	Ultra-high performance liquid chromatography, triple quadrupole mass spectrometer
US EPA	United States Environmental Protection Agency
US NOAA	United States National Oceanic and Atmospheric Administration

USGS	United Stated Geological Survey
WWTPs	Wastewater Treatment Plants
ΣPFAS	Total Concentration of PFAS
$\Phi_{\sum PFAS}$	Mass Flux of PFAS

Chapter 1. Introduction

1.1 PFAS: Forever Chemicals

Chemicals are the basis of our everyday life, contributing to many breakthrough advancements and significant improvements to our quality of life. It is estimated that 150 new substances are developed in the United States yearly, while 2.3 billion tons of synthetic chemicals are produced globally every year (Naidu et al., 2021). Although these anthropogenic substances are extremely useful in many consumer products and industrial applications, they are often employed without fully understanding their potential effects on the environment, humans, and wildlife (Naidu et al., 2021). This is the case of per- and polyfluoroalkyl substances, collectively known as PFAS.

PFAS have been produced since the late 1940s and widely used in a myriad of consumer products, including personal care products, non-stick cookware, food packaging, water- and fire-proof fabrics, firefighting foams, pesticides, among many others (Buck et al., 2011; Lindstrom et al., 2011). PFAS are fluorosurfactants, typically presenting a hydrophilic functional group and a hydro- and lipophobic fluorinated chain. These substances are known as "Forever Chemicals," a term used because of their extreme chemical, biological, and thermal stability. Such stability is related to the presence of stable C-F bonds in their composition (Buck et al., 2011; Guelfo and Adamson, 2018). PFAS were produced and used for decades with limited regulatory oversight. In 1998, 3M reported evidence to the United States Environmental Protection Agency (US EPA) that certain PFAS could bioaccumulate in humans (3M, 1998). Around that time, PFOS, PFOA, PFHxS, and FOSA were detected in the serum of all 1,562 participants collected between 1999-2000 (Calafat et al., 2007). Throughout the last two decades, several studies have observed adverse health effects of PFAS in humans and wildlife, including thyroid disease, high cholesterol, and kidney and testicular cancers, among others (Frisbee et al., 2009; Sunderland et al., 2019). These substances have also been observed to be ubiquitous in the natural environment, being detected in every continent (Kurwadkar et al., 2022). Given the evidence of the omnipresence, recalcitrance, and potential adverse health effects of PFAS, several regulatory agencies started to implement sanctions on the

production and use of PFAS. Due to the unique properties of PFAS, fluorochemical manufacturers started to replace regulated PFAS with new or unregulated fluorinated alternatives (Pan et al., 2018; Wang et al., 2017). As a result, the Organization for Economic Co-operation and Development (OECD) estimated that nearly 5,000 substances present a least one fluorinated moiety (C_nF_{2n-1-}) in their composition (OECD, 2018), while 12,034 substances were listed in the US EPA's Master List of PFAS Substances as of October 2022 (USEPA, 2021).

1.2 Goals

PFAS are recalcitrant, ubiquitous, and present adverse health effects on humans and wildlife. This work aims to better understand their distribution, transport, and fate in the natural environment, with a focus on surface water systems. This dissertation is structured into six chapters, of which three (Chapters 3-5) are novel research manuscripts. These studies aim to answer research questions at different geographical scales, from a global- to a watershed-level analysis.

Hundreds of studies have found PFAS to be omnipresent in the environment. Since these studies are usually focused on localized areas, knowledge of broad trends in the global distribution of PFAS is lacking. Further, information on the concentrations in which PFAS are commonly detected in the environment is paramount to ensure that controlled studies use realistic concentrations and mimic environmental conditions. The lack of a comprehensive analysis of what constitutes environmentally relevant concentrations (ERCs) of PFAS has led many studies to employ elevated concentrations that are not often detected in the environment. In Chapter 3, research data from 228 peer-reviewed journal articles are analyzed to better understand:

1. The global spatial distribution,

2. specific profiles, and

3. ERCs of PFAS in surface water, sediment, and groundwater.

In agreement with what has been observed globally, PFAS have been detected near several source areas in the United States, including Alabama. Notably, one of the first PFAS studies in the United States detected PFOS and PFOA in a portion of the Tennessee River in Alabama in 2002 (Hansen et al., 2002). Currently, many municipalities are challenged by PFAS contamination of their drinking water sources in the state (ADEM, 2022). Despite information on potential hotspots, the overall distribution of PFAS in the state remains largely unknown. Moreover, studies have historically expressed PFAS contamination in terms of aqueous concentrations. Although concentration is an important metric, it might not be sufficient to fully understand the transport of PFAS in the environment, as it is highly influenced by the flow rate. Mass flux analysis can be used as a complementary approach as it integrates aqueous concentration and volumetric flow. In Chapter 4, a statewide analysis of PFAS in Alabama is conducted to investigate:

1. The spatial distribution of seventeen PFAS in surface water in the state.

2. The transport behavior of PFAS in large, interconnected river systems through a mass flux analysis.

3. Identify potential source areas of PFAS in the environment.

PFAS are used in a wide array of consumer products and industrial applications, requiring the use of supplemental analysis and correct sampling to successfully link PFAS contamination to specific sources. Chemical fingerprinting can be used as a tool to complement this analysis (Charbonnet et al., 2021). Once in the environment, successfully understanding the transport mechanisms of PFAS is particularly important to understand their fate. Results from our state-wide analysis of PFAS in Alabama revealed several areas of interest in Alabama and neighboring states, including in a section of the Tallapoosa River. In Chapter 5, a watershed-level analysis of the distribution of PFAS in the Tallapoosa and River is conducted to better understand:

1. The sources of PFAS in the basins through chemical profiling.

2. The transport characteristics of PFAS through a mass flux analysis.

3. Uncertainties and limitations associated with the use of mass flux analysis.

1.3 References

3M. Letter to the US EPA - TSCA Section 8(e) – Perfluorooctane Sulfonate, 1998.

ADEM. Per- and Polyfluoroalkyl Substances (PFAS) in Drinking Water. In: Management ADoE, editor, 2022.

Buck RC, Franklin J, Berger U, Conder JM, Cousins IT, de Voogt P, et al. Perfluoroalkyl and polyfluoroalkyl substances in the environment: terminology, classification, and origins. Integr Environ Assess Manag 2011; 7: 513-41.

Calafat AM, Kuklenyik Z, Reidy JA, Caudill SP, Tully JS, Needham LL. Serum concentrations of 11 polyfluoroalkyl compounds in the US population: data from the National Health and Nutrition Examination Survey (NHANES) 1999− 2000. Environmental science & technology 2007; 41: 2237-2242.

Charbonnet JA, Rodowa AE, Joseph NT, Guelfo JL, Field JA, Jones GD, et al. Environmental Source Tracking of Per- and Polyfluoroalkyl Substances within a Forensic Context: Current and Future Techniques. Environ Sci Technol 2021; 55: 7237-7245.

Frisbee SJ, Brooks AP, Jr., Maher A, Flensborg P, Arnold S, Fletcher T, et al. The C8 health project: design, methods, and participants. Environ Health Perspect 2009; 117: 1873-82.

Guelfo JL, Adamson DT. Evaluation of a national data set for insights into sources, composition, and concentrations of per- and polyfluoroalkyl substances (PFASs) in U.S. drinking water. Environ Pollut 2018; 236: 505-513.

Hansen KJ, Johnson H, Eldridge J, Butenhoff J, Dick L. Quantitative characterization of trace levels of PFOS and PFOA in the Tennessee River. Environmental Science & Technology 2002; 36: 1681-1685.

Kurwadkar S, Dane J, Kanel SR, Nadagouda MN, Cawdrey RW, Ambade B, et al. Per- and polyfluoroalkyl substances in water and wastewater: A critical review of their global occurrence and distribution. Sci Total Environ 2022; 809: 151003.

Lindstrom AB, Strynar MJ, Libelo EL. Polyfluorinated compounds: past, present, and future. Environ Sci Technol 2011; 45: 7954-61.

Naidu R, Biswas B, Willett IR, Cribb J, Kumar Singh B, Paul Nathanail C, et al. Chemical pollution: A growing peril and potential catastrophic risk to humanity. Environ Int 2021; 156: 106616.

OECD. Toward a new comprehensive global database of per-and polyfluoroalkyl substances (PFASs): Summary report on updating the OECD 2007 list of per-and polyfluoroalkyl substances (PFASs). Organisation for Economic Cooperation and Development (OECD) 2018.

Pan Y, Zhang H, Cui Q, Sheng N, Yeung LWY, Sun Y, et al. Worldwide Distribution of Novel Perfluoroether Carboxylic and Sulfonic Acids in Surface Water. Environ Sci Technol 2018; 52: 7621-7629.

Rodgers M. Gadsden Water Works and Sewer Board files lawsuit over water pollution. The Gadsden Times, 2016.

Sunderland EM, Hu XC, Dassuncao C, Tokranov AK, Wagner CC, Allen JG. A review of the pathways of human exposure to poly- and perfluoroalkyl substances (PFASs) and present understanding of health effects. J Expo Sci Environ Epidemiol 2019; 29: 131-147.

USEPA. PFAS Master List of PFAS Substances, 2021.

Wang Z, DeWitt JC, Higgins CP, Cousins IT. A Never-Ending Story of Per- and Polyfluoroalkyl Substances (PFASs)? Environ Sci Technol 2017; 51: 2508-2518.

Chapter 2. Bibliographic Review

2.1 Properties and Use of PFAS

Per- and polyfluoroalkyl substances, collectively known as PFAS, are a large group of emerging persistent organic pollutants. PFAS have surfactant-like properties, presenting a hydrophobic tail, in which one or more carbon-bonded hydrogen atoms have been substituted by fluorine atoms and a hydrophilic head (Figure 2.1). Some substances also present a functional group between the two structures (Buck et al., 2011; Kemi, 2015). PFAS can be divided into two large groups, depending on the presence of carbon-bonded hydrogen atoms in their structure. Perfluoroalkyl substances present fully-fluorinated chains, in which all carbon-bonded hydrogens are replaced by fluorine atoms (Buck et al., 2011; Guelfo and Adamson, 2018). Since carbon-fluorine bonds are the strongest bounds found in organic chemistry (O'Hagan, 2008), perfluoroalkyl substances are highly stable and are not known to degrade under environmental conditions (Buck et al., 2011; Guelfo and Adamson, 2018). They are also highly resistant to thermal, biological, and chemical degradation (Kemi, 2015). On the other hand, polyfluoroalkyl substances still present carbon-hydrogen bonds in their structure and can degrade to perfluoroalkyl substances via biotic and abiotic processes (Buck et al., 2011; Guelfo and Adamson, 2018). For instance, the polyfluoroalkyl 6:2 FTSA has been observed to biodegrade into 5:3 Acid, PFPeA, and PFHxA under aerobic conditions (Zhang et al., 2016a). Fluorotelomer thioether amido sulfonates (FtTAoS) were also observed to biodegrade to a suite of PFAS, including PFBA, PFPeA, PFHxA, PFHpA, and PFOA (Harding-Marjanovic et al., 2015). Since a single polyfluoroalkyl precursor can degrade to several substances, PFAS are usually found in mixtures in the environment (Guelfo and Adamson, 2018).

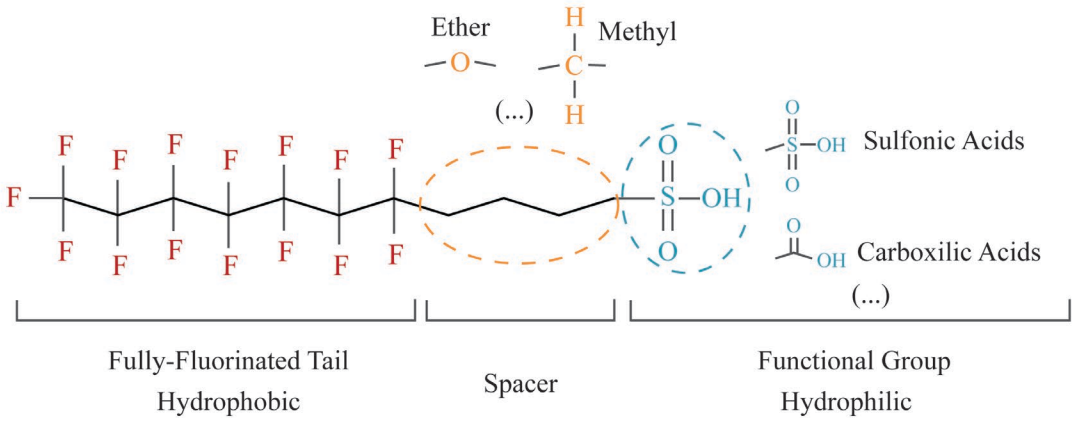

Figure 2.1. General Structure of PFAS. Adapted from Kemi (2015).

PFAS provide unique chemical properties to manufacturers, including high stability and hydro- and oleo-phobic properties (Guelfo and Adamson, 2018). In 1949, 3M started producing perfluorooctanesulfonyl fluoride (POSF) to be used in the formulation of polytetrafluoroethylene (PTFE). Around that time, Dupont introduced Teflon®, a PTFE-based polymer employed in the coating of non-stick cookware. In 1956, 3M introduced Scotchgard™, a stain-repellent line of products containing PFAS, while the United States Food and Drugs Agency (FDA) approved the use of Dupont's Zonyl®, a PFAS-based additive used in the coating of food packaging, in 1962. The United States Navy started using PFAS-containing aqueous film-forming foam (AFFF) fire extinguishers in the 1960s (Lindstrom et al., 2011b; Vecitis et al., 2010). Since then, these substances have been used as fluorosurfactants, emulsifiers, and additives in the production of fluoropolymers, among others. PFAS have been used in the coating of various fabrics, such as water- and fire-repellants in clothing, oil- and stain-repellants in carpets and upholstery, as well as paper treatment in food packaging, and as mist suppressants in the metal plating industry. They have also been used in the formulation of personal care products such as makeup and body lotions, medical devices, building materials, cleaning agents, and even pesticides (DEPA, 2015; Johns and Stead, 2000; Nascimento et al., 2018; Perez et al., 2014; Whitehead et al., 2021). A recent review identified the use of 1,400 PFAS in more than 200 applications, including in ammunition, the coating of windmill blades, and

artificial turf, among others. The authors identified that over 3,000 tons of PFAS were used in producing plastic, rubber, electronics, coatings, and paints between 2000 and 2017 (Gluge et al., 2020).

2.2 Sources and Occurrence of PFAS in the Environment

PFAS can reach the environment through several pathways, including manufacturing facilities that produce or use PFAS in their products, municipal wastewater treatment plants, military bases, airports, firefighting training facilities, landfills, and consumer products (Figure 2.2). Helmer et al. (2022) surveyed 171 contaminated sites in Michigan (US) by source release and found that landfills, AFFF, metal platers, and automotive/metal stamping accounted for 75% of the contamination. Additional sources included sites that produce non-chemical products, manufacturers of specialty chemicals and products such as hydraulic fluid and lubricants, WWTPs, oil refineries, manufacturers of paper products and paints, and tanneries (Helmer et al., 2022).

2.2.1 Industrial Facilities

Direct discharges from manufacturing facilities are one of the primary sources of PFAS into the environment, and several studies have observed extremely high levels of PFAS downstream from them. A fluorochemical facility in China has been linked to extremely high PFAS concentrations in the Xiaoqing River, reaching up to 660,000 ng L^{-1} in surface water (Heydebreck et al., 2015), while PFAS concentrations of up to 6,758 ng L^{-1} were detected downstream from a fluorochemical facility in Germany (Joerss et al., 2020). In the United States, PFAS concentrations up to 750 and 4,696 ng L^{-1} were observed downstream from fluorochemical facilities in the Tennessee and Cape Fear rivers, respectively (Newton et al., 2017; Sun et al., 2016). Concentrations of PFAS up to 876 ng L^{-1} were also detected downstream from a fluorochemical facility in the City of Dordrecht in The Netherlands (Gebbink et al., 2017).

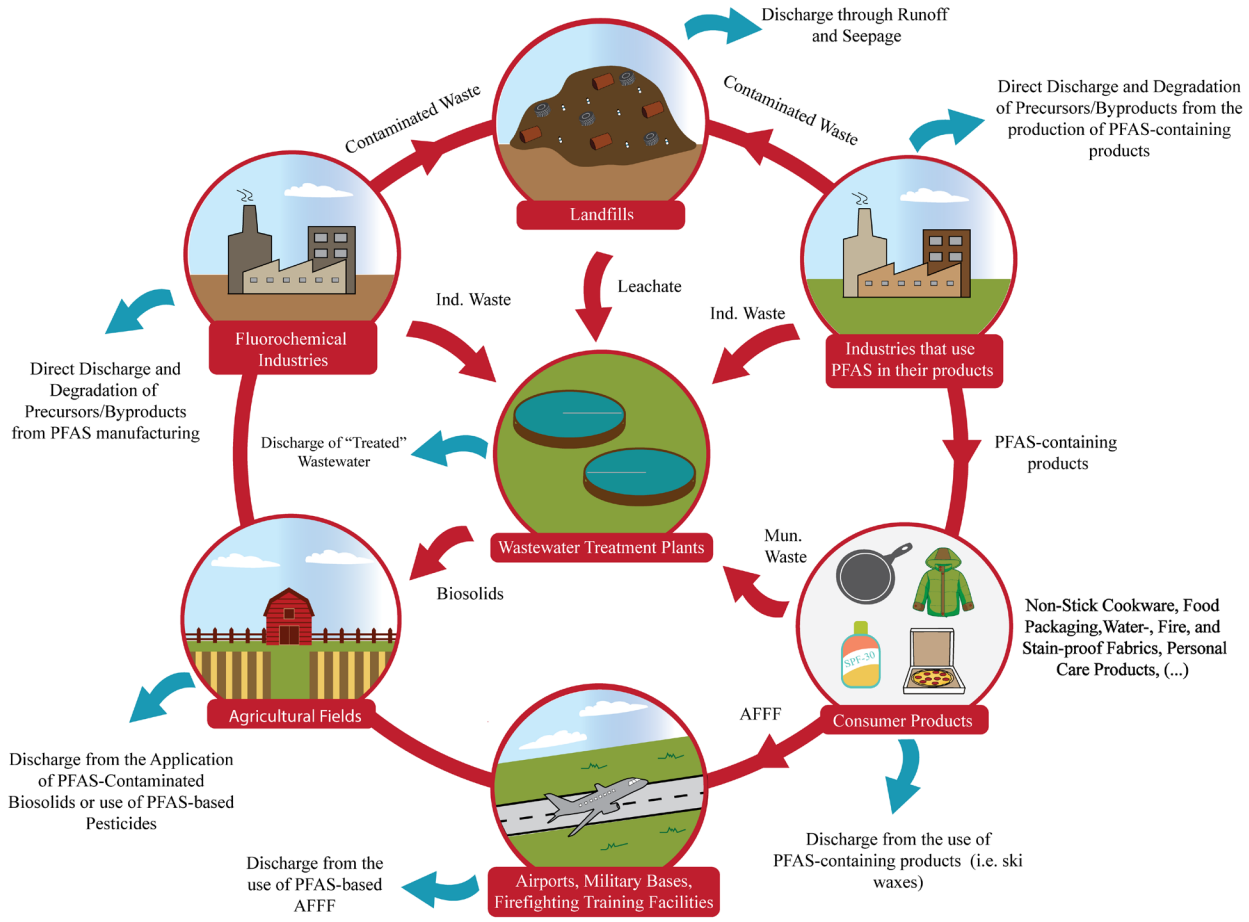

Figure 2.2. Diagram of potential sources of PFAS in the environment. Illustrated sources include fluorochemical and other industrial facilities, landfills, agricultural fields, wastewater treatment plants, consumer products, airports, military bases, and firefighting training facilities.

Industrial facilities of various sectors that use PFAS in their products can also act as significant sources of PFAS in the environment. For instance, Clara et al. (2008) found PFAS in the effluent of nine industrial facilities related to printing, textile, laundry and cleaning, paper, electrical, and metal industries. Metal plating was found to be a major source of PFOS and paper industries of PFOA (Clara et al. 2008). Langberg et al. (2020) also found a manufacturer of paper products to be a significant source of PFAS in a Norwegian lake, related to the use of PFAS in the coating of those products. Liu et al. (2019) conducted a positive matrix factorization-based source analysis of PFAS and found facilities related to erosion inhibitors, AFFF, metal plating, fluoropolymers, and food contact materials to be the primary sources of

PFAS in the coastal areas of Bohai Bay (China). Similarly, Zhang et al. (2016b) surveyed sources in Rhode Island and the New York Metropolitan area and revealed airports, textile mills, atmospheric inputs from the waste sector, and metal smelting facilities to be the primary sources of PFAS. Furthermore, PFAS were identified at concentrations up to 1770 ng L^{-1} in surface water and 13.2 ng gdw^{-1} in sediment in the Conasauga River, downstream from a large number of carpet manufacturers (Konwick et al., 2008; Lasier et al., 2011). PFAS-based products such as 3M's Scotchgard have historically been employed in carpets to provide stain- and water-repellent properties (DEPA, 2015).

2.2.2 Aqueous Film Forming Foam (AFFF)

Facilities that use PFAS-based AFFF can also act as significant sources of PFAS in the environment (Hu et al., 2016). AFFF foams are usually comprised of surfactants, solvents, polymers, and additional additives. PFAS-based AFFFs were first used by the Unites States Navy in the 1960s, but their use was rapidly expanded because of their unique performance in fire suppression (ITRC, 2022; Vecitis et al., 2010). The highest concentration of PFAS ever recorded in surface water was detected in Etobicoke Creek, near Toronto, after an accidental release of 22,000 L of AFFF from the L. B. Pearson International Airport in 2000 (Moody et al., 2002). At that time, Moody and colleagues found the concentration of ΣPFAS in the creek to reach 2,270,000 ng L^{-1}. Awad et al. (2011) monitored the ΣPFAS at the same creek from 2003 to 2009 and found PFAS concentration up to 947 ng L^{-1} in the location closest to the spill a decade after the incident. Firefighting training facilities that have used PFAS-based AFFF are also significant sources of PFAS. For instance, ΣPFAS up to 13,000 ng L^{-1}, one of the highest recorded in Europe, was detected in surface waters downstream from a firefighting training facility in Sweden as part of a nationwide survey of PFAS surface and groundwater (Gobelius et al., 2018). Given the historical use of AFFF in military installations, high concentrations of PFAS have been found in groundwater near these facilities in the United States. Moody and Field (1999) reported ΣPFAS up to 7,090,000 ng L^{-1} and 298,000 ng L^{-1} in the groundwaters near the Naval Air Force Station (Nevada) and Tyndall Air Force Base (Florida), respectively, while Houtz et al. (2013) detected ΣPFAS concentrations up to 1,569,600 ng L^{-1} near the Ellsworth Air Force Base (South Dakota). However, most studies in AFFF-impacted sites have focused on

a limited array of substances, leading to a probable underestimation of the overall PFAS concentration. Barzen-Hanson et al. (2017) discovered 40 new classes of PFAS in the formulation of historical AFFF and AFFF-impacted groundwater. The formulations of most AFFFs have changed to allegedly include less toxic and more degradable PFAS, which are mostly fluorotelomers or short-chain perfluoroalkyl acids (PFAAs) (Mejia-Avendano et al., 2017). However, high levels of PFAS, including legacy long-chain PFAAs, are still being detected near areas where AFFF are used. For instance, Aly et al. (2020) investigated the concentration of PFAS in the Houston Ship Channel after almost 5 million liters of AFFF were employed to suppress a large-scale fire. The authors detected ΣPFAS up to 2,044 ng L^{-1} in surface waters downstream from the incident, with legacy PFOS as one of the major substances.

2.2.3 Landfills

Many of the PFAS-containing products previously described are ultimately disposed in municipal landfills. Liu et al. (2020) evaluated the transformation of commercial (non-industrial) and residential waste from waste collection vehicles to landfills. The authors found that the leachate from collection vehicles was mostly composed of PFAS precursors. In contrast, the majority of PFAS in the leachate from the landfill were perfluoroalkyl acids, suggesting the biotransformation of labile precursors after the disposal of consumer products in landfills (Liu et al., 2020). Lang et al. (2017) conducted a national estimate of PFAS discharge via landfill leachate using data from 18 municipal landfills in the US. The authors estimated that municipal landfills in the US release approximately 600 kg yr^{-1}, which are ultimately sent to WWTPs for treatment. Although the rate of PFAS discharge via landfill leachate was slower than expected, the deterioration of waste is a slow process that can last decades. As noted by the authors, none of the landfills included in the study received industrial waste from PFAS manufacturers or selected industrial sectors traditionally associated with PFAS, such as carpet and textile industries (Lang et al., 2017). In practice, many landfills also accept industrial waste and biosolids from WWTPs that might contain PFAS, which would heavily impact the amount of PFAS in leachate. For instance, Oliaei et al. (2013) found the concentration of PFAS to reach 178,000 ng L^{-1} in the leachate from the Pine Bend Landfill in Minnesota, which received sludge from a 3M WWTP nearby. Ultimately, landfill leachates are usually treated either

on-site or at a municipal WWTP, but studies have shown that most conventional treatments are inefficient in treating PFAS-contaminated waste. In fact, PFAS concentrations were observed to double after the treatment of leachate using membrane bioreactors, with PFAS concentrations reaching up to 3,162 ng L^{-1} after treatment (Fuertes et al., 2017). Surface and groundwater near landfills can also be directly impacted by runoff or seepage (Hepburn et al., 2019; Oliaei et al., 2013).

2.2.4 WWTPs and Biosolids

Municipal and industrial waste and landfill leachate are ultimately sent to WWTPs, resulting in PFAS being widely detected in the influents of WWTPs. Sun et al. (2012) detected ΣPFAS between 200 and 412 ng L^{-1} in the influent of six WWTPs in Tianjin, China, while Sinclair and Kannan (2006) observed PFOA reach up to 1,050 ng L^{-1} in the influent of six WWTPs in New York. Similarly, Coggan et al. (2019) investigated the concentration of PFAS in nineteen WWTPs in Australia, revealing ΣPFAS up to 410 ng L^{-1} in their influents and 520 ng L^{-1} in the effluents. Such an increase in the concentration of PFAS during treatment has been widely observed. For example, Sinclair and Kannan (2006) observed that while primary treatment had no effect on the mass flow of PFAS in WWTPs, secondary treatment using activated sludge led to a significant increase in the mass flows of several PFAAs. A recent study evaluated the mass flow of PFAS through nine sludge treatment systems in Canada, determining that while selected aerobic and anaerobic digestion systems showed up to 40% reduction in the mass flow of PFAS, other systems like alkaline stabilization led to a 99% increase (Lakshminarasimman et al., 2021). This is partially due to the inefficiency of traditional WWTPs in removing PFAS from waste and to the breakdown of labile precursors (Lenka et al., 2021). Unlike PFAAs, many PFAS precursors present weaker bonds, such as C-H, in their main structure and can degrade to PFAAs (Guelfo and Adamson, 2018). An example is described in the work conducted by Chen et al. (2017), in which the authors observed a decrease in the mass loads of selected FTOHs (21-29%) and an increase in the mass of 12 PFAAs (18-165%) in waste subjected to aerobic treatment.

WWTPs are important vectors of PFAS into the environment via the direct discharge of treated waste (Coggan et al., 2019; Lenka et al., 2021). For instance, Moller et al. (2010) observed a sharp increase in the concentration of PFAS in the Rhine River downstream from a WWTP that received industrial waste in Leverkusen (Germany), while Murakami et al. (2008) identified a strong correlation between PFOS, PFHpA, and PFNA and a sewage marker in Japan. Similarly, ΣPFAS up to 1,770 ng L^{-1} were detected in the Conasauga River in Georgia downstream from a municipal WWTP. This WWTP is particularly unique as it receives industrial influents from dozens of carpet manufacturers in the region and sprays the treated waste onto a land-application site for slow discharge (Konwick et al., 2008; Lasier et al., 2011).

Adsorption to sludge is the primary mechanism for PFAS removal in traditional WWTPs (Lenka et al., 2021). This is especially true for longer-chain PFAS, as the length of the fluoroalkyl chain has been widely observed to impact sorption significantly (Coggan et al., 2019). Apart from the chain length, other parameters such as treatment method, soil properties, and pH have been observed to affect sorption. In their study, Ebrahim and colleagues investigated the partitioning behavior of PFAS to various secondary treatment and sludge stabilization methods. The authors observed that sludge stabilization methods and soil characteristics, including the fractions of organic matter, proteins, and lipids, significantly affected the sorption of PFAS to biosolids (Ebrahimi et al., 2021). Because of their partitioning behavior, PFAS have been observed at high concentrations in biosolids samples throughout the world, including in nineteen Australian WWTPs (Coggan et al., 2019), in two large WWTPs in the United Kingdom (Rigby et al., 2021), in two WWTPs in Kentucky and Georgia (Loganathan et al., 2007), and in fifteen WWTPs in Spain and Germany (Gomez-Canela et al., 2012), among others. Biosolids are widely used as soil amendments because they can provide nutrients and organic amendments at a low cost. As a result, PFAS have been detected at high concentrations near agricultural fields that used PFAS-contaminated biosolids as soil amendments. A WWTP in Decatur, AL, distributed over 34,000 metric tons of biosolids contaminated with PFAS to local farmers between 1995 and 2008. PFAS were detected at high levels in surface water (n.d. – 31,906 ng L^{-1}) and groundwater (n.d. – 19,354 ng L^{-1}) samples near fields that received the contaminated

biosolids (Lindstrom et al., 2011a). Apart from the contamination of local groundwater and surface water, land application of contaminated biosolids is concerning due to the uptake potential of PFAS by crops, leading to human and wildlife exposure (Ghisi et al., 2019).

The discharge of improperly or untreated PFAS-contaminated waste from point sources into the environment is partly due to the lack of regulations, the heterogeneity of these substances, and challenges in current remediation technologies. Granulated Activated Carbon (GAC) is currently the most used technology to remove PFAS from water, but it is expensive, generates waste, and may not be appropriate for all PFAS (Eschauzier et al., 2012; Wanninayake, 2021). In recent years, several destructive and immobilizing remediation technologies like combustion and ion exchange have been evaluated for PFAS remediation (Wanninayake, 2021). A recent study by Trang and colleagues revealed a low-temperature mineralization method for removing perfluoroalkyl carboxylic acids (PFCAs) from contaminated water. The authors found that the innovative approach could mineralize PFCAs through a sodium hydroxide-mediated pathway after 24 hours of reaction at 120 °C (Trang et al., 2022). Although promising, emerging technologies have not yet been studied at a full-scale, and more studies are needed to evaluate their true potential.

A complete analysis of the global occurrence of PFAS in surface water, groundwater, and sediment is available in Chapter 3.

2.3 Adverse Health Effects of PFAS in Humans and Wildlife

There are several pathways in which humans can be exposed to PFAS, including consuming contaminated livestock and drinking water, inhaling contaminated air, and contacting contaminated media (Sunderland et al., 2019). Early evidence of PFAS bioaccumulation in humans was made available in the 1960s when scientists detected organic fluorine in human blood (Sunderland et al., 2019). In 1976, Guy and colleagues detected organic fluorine in human plasma from 106 individuals living in five different cities in the United States. The authors identified evidence of *"widespread contamination of human tissues with trace amounts of organic fluorocompounds derived from commercial products"* (Guy et al., 1976). Over

two decades later, data from the National Health and Nutrition Examination Survey (NHANES) illustrated the widespread occurrence of PFAS in the American population. PFOS, PFOA, PFHxS, and FOSA were detected in all 1,562 samples representative of the American population collected between 1999-2000 (Calafat et al., 2007). The latest NHANES biannual data, collected between 2015-2016, examined 10 PFAS in the serum of 1,886 individuals, finding PFHxS, PFOS, PFOA, PFNA, and PFDA to be present in all samples (Xie et al., 2021).

Early studies on the potential effects of PFAS in humans were conducted by 3M using animal specimens. The results of these studies include evidence of carcinogenic effects of N-EtFOSE in rats and lethal effects of Fluorad® Fluorochemical Surfactant FC-95 in monkeys (Sunderland et al., 2019). Since then, the potential adverse health effects of PFAS have been widely explored in laboratory-controlled studies using animal models. Adverse effects in animals include damage to the liver and reproductive system, obesity, tumor induction, endocrine disruption, and immunotoxicity, among others (Fenton et al., 2021). In addition to studies using animal models, epidemiologic studies have also found several links between PFAS exposure and adverse health effects in humans. The C8 Health Project is perhaps the most relevant and comprehensive longitudinal study conducted to this date (Sunderland et al., 2019). This project was created as part of a settlement between Dupont and residents of areas affected by PFOA contamination from the Dupont Washington Works facility in West Virginia (Frisbee et al., 2009). The C8 Health Project evaluated the concentration of ten PFAS in the serum of over 69,000 people between 2005-2006 and identified links between PFOA exposure and six diseases, including thyroid, high cholesterol, and kidney and testicular cancers (Frisbee et al., 2009; Sunderland et al., 2019). A smaller study, named “Isomers of the C8 Health Project”, was conducted on 1,612 Chinese adults and included isomers of PFOS and PFOA and other emerging PFAS (Bao et al., 2017). Results include associations between PFAS exposure and increased hypertension (Bao et al., 2017), increased risk of type 2 diabetes (Zeeshan et al., 2021), thyroid hormone levels (Li et al., 2022), overweight (Tian et al., 2019), among others.

Adverse health effects of PFAS in wildlife include endocrine disruption (Pedersen et al., 2016) and cellular damage (Aquilina-Beck et al., 2020). PFAS have also been observed to bioaccumulate in various animal species, including lake trout (Ren et al., 2022) and polar bears (Boisvert et al., 2019). Moreover, several studies have observed PFAS to biomagnify, including in food webs from Lake Huron (Ren et al., 2022), Barents Sea (Haukas et al., 2007), and St. Lawrence River (Munoz et al., 2022). In contrast, other studies have found no biomagnification potential of PFAS (Goeritz et al., 2013; Lescord et al., 2015). As reviewed by Miranda et al. (2022), biomagnification of PFAS is dependent on several factors, including the location and distance to PFAS sources, length of the food web, and methods used (sampling and analyzed tissues).

2.4 PFAS Regulations and Replacements

For decades, PFAS were used in a myriad of consumer products without much regulatory oversight. This pattern started to change in 1998, when 3M reported to the US EPA that certain PFAS could bioaccumulate in humans (3M, 1998) and vouched to completely phase out the production of PFOS and its related salts by 2002 (3M, 2000). Since then, several studies have reported evidence of adverse health effects of PFAS in humans in wildlife (Fenton et al., 2021; Sunderland et al., 2019), leading to the implementation of regulations and guidelines on the production and use of PFAS worldwide (Figure 2.3). In 2006, the US EPA released a global stewardship program to phase out the production of PFOA and its related salts by 2015 (USEPA, 2006). PFOS and its salts were listed in Annex B of the Stockholm Convention, limiting their production, while PFOA, PFHxS, and their salts were recently added in Annex A, eliminating their production in several countries (Hogue, 2022; Torres et al., 2022). Various agencies have also established standards limiting the amount of certain PFAS in drinking water. For instance, the US EPA implemented a non-enforceable health advisory of 70 ng L^{-1} for the sum of the concentrations of PFOS and PFOA in drinking water in 2016 (USEPA, 2016), while Sweden released a drinking water threshold of no more than 90 ng L^{-1} for the sum of 11 PFAS in that same year (Gobelius et al., 2018). The US EPA recently released updated interim health advisories for PFOS and PFOA of 0.02 and 0.004 ng L^{-1}, respectively, and new health advisories for PFBS and GenX of 2,000 and 10 ng L^{-1}, respectively (USEPA,

2022). These new standards, orders of magnitude lower than the 2016 advisory, underline the potential toxicity of PFOS and PFOA even at extremely low concentrations.

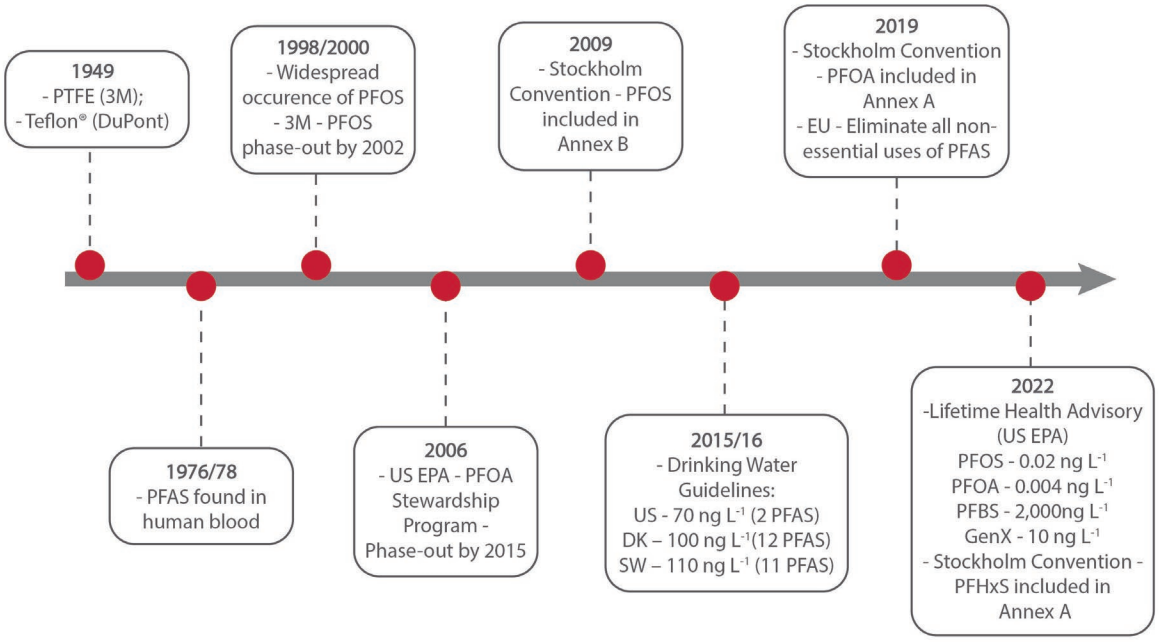

Figure 2.3 Important historical marks on the production, occurrence, and regulatory efforts of PFAS.

Although regulations reduced the production of certain PFAS, manufacturing companies continue to develop new, unregulated fluorinated alternatives. These are usually short-chain (n<6 perfluorinated carbons for PFSAs and n<8 for PFCAs) homologs of long-chain legacy PFAS or present an additional functional group in their composition (DEPA, 2015; Pan et al., 2018; Wang et al., 2017). For example, PFBS and 6:2 Cl-PFESA (trademarked F-53B) have been used as PFSAs alternatives, while HFPO-DA (trademarked Gen-X), ADONA, and PFHxA have been employed as alternatives to PFCAs (Wang et al., 2015). Consequently, it is estimated that approximately 5,000 substances present at least one fluorinated moiety (OECD, 2018), further complicating the PFAS issue.

Fluorochemical manufacturers have argued that emerging alternatives are believed to be less bioaccumulative, as hydrophobicity is directly proportional to chain length, and more easily degradable due to the inclusion of less stable functional groups (DEPA, 2015; Pan et al., 2018). However, the potential adverse health effects of emerging PFAS have not yet been extensively explored (Blum et al., 2015). In

fact, a recent toxicity assessment conducted by the US EPA linked PFBS to significant adverse effects on the thyroid (USEPA, 2021), while the emerging perfluoroether 6:2 Cl-PFESA was observed to present similar acute toxicity of PFOS (Munoz et al., 2019). Emerging PFAS also present higher mobility when compared to their legacy homologs. For example, fluorotelomers and sulfonamides are neutral substances that can volatilize and be atmospherically transported (Cai et al., 2012), while short-chain PFAAs are highly recalcitrant and present higher hydrophobicity (Ateia et al., 2019).

Since the US EPA has not yet developed a comprehensive regulation for PFAS in drinking water in the US, several states have developed state-level regulations for the amount of certain PFAS in drinking water (Table 2.1). Alaska, Colorado, Delaware, Maine, and New Mexico follow the US EPA health advisory of 70 ng L^{-1} for the sum of PFOS and PFOA. Colorado has also implemented a regulation at the point of discharge at specific industries and wastewater treatment plants, limiting the amount of PFAS to reach the environment. Alabama currently has no specific regulation or guidance regarding the amount of PFAS in drinking water.

Table 2.1. State-Level Regulation of PFAS in drinking water and at point of discharge in the US. MCL = Maximum Contaminant Level.

State	Type of Regulation	Limits
Colorado	Point of discharge	PFOS+PFOA+PFNA – 70 ppt, PFHxS – 700 ppt, PFBS - 400,000 ppt
Michigan	MCL – Drinking Water	PFNA – 6 ppt, PFOA – 8 ppt, PFOS - 16 ppt, PFHxS – 51, PFBS – 420, PFHxA – 400,000 HFPO-DA – 370 ppt
Vermont	MCL – Drinking Water	PFOS+PFOA+PFHxS+PFHpA+PFNA – 20 ppt
California	Notification Level – Drinking Water	PFOS – 6.5 ppt and PFOA – 5.1 ppt
	Response Level – Drinking Water	PFOS – 40 ppt and PFOA – 10 ppt
New York	MCL – Drinking Water	PFOS+PFOA – 10 ppt
New Jersey	MCL – Drinking Water	PFOA – 14 ppt, PFOS – 13 ppt, PFNA – 13 ppt
New Hampshire	MCL – Drinking Water	PFOA – 12 ppt, PFOS – 15 ppt, PFNA – 11 ppt, PFHxS – 18 ppt
Minnesota	Guidance - Drinking Water	PFOA = 35 ppt, PFOS – 15 ppt, PFBS – 2,000 ppt, PFHxS – 47 ppt, PFBA – 7,000 ppt
Massachusetts	MCL – Drinking Water	PFOS+PFOA+PFHxS+PFHpA+PFNA+PFDA = 20 ppt

Ohio	Action Level - Drinking Water	PFOS+PFOA = 70 ppt, GenX =700 ppt, PFBS = 140,000 ppt, PFHxS = 140 ppt, PFNA = 21 ppt
Connecticut	Action Level - Drinking Water	PFOS+PFOA+PFHxS+PFHpA+PFNA = 70 ppt
North Carolina	Health Goal – Drinking Water	GenX = 140 ppt

**ppt = ng L^{-1}*

2.5 References

3M. Letter to the US EPA - TSCA Section 8(e) – Perfluorooctane Sulfonate, 1998.

3M. Letter to the US EPA: Phase-out Plan for POSF-Based Products., 2000.

Aly NA, Luo YS, Liu Y, Casillas G, McDonald TJ, Kaihatu JM, et al. Temporal and spatial analysis of per and polyfluoroalkyl substances in surface waters of Houston ship channel following a large-scale industrial fire incident. Environ Pollut 2020; 265: 115009.

Aquilina-Beck AA, Reiner JL, Chung KW, DeLise MJ, Key PB, DeLorenzo ME. Uptake and Biological Effects of Perfluorooctane Sulfonate Exposure in the Adult Eastern Oyster Crassostrea virginica. Arch Environ Contam Toxicol 2020; 79: 333-342.

Ateia M, Maroli A, Tharayil N, Karanfil T. The overlooked short- and ultrashort-chain poly- and perfluorinated substances: A review. Chemosphere 2019; 220: 866-882.

Awad E, Zhang X, Bhavsar SP, Petro S, Crozier PW, Reiner EJ, et al. Long-term environmental fate of perfluorinated compounds after accidental release at Toronto airport. Environ Sci Technol 2011; 45: 8081-9.

Bao WW, Qian ZM, Geiger SD, Liu E, Liu Y, Wang SQ, et al. Gender-specific associations between serum isomers of perfluoroalkyl substances and blood pressure among Chinese: Isomers of C8 Health Project in China. Sci Total Environ 2017; 607-608: 1304-1312.

Barzen-Hanson KA, Roberts SC, Choyke S, Oetjen K, McAlees A, Riddell N, et al. Discovery of 40 Classes of Per- and Polyfluoroalkyl Substances in Historical Aqueous Film-Forming Foams (AFFFs) and AFFF-Impacted Groundwater. Environ Sci Technol 2017; 51: 2047-2057.

Blum A, Balan SA, Scheringer M, Trier X, Goldenman G, Cousins IT, et al. The Madrid Statement on Poly- and Perfluoroalkyl Substances (PFASs). Environ Health Perspect 2015; 123: A107-11.

Boisvert G, Sonne C, Riget FF, Dietz R, Letcher RJ. Bioaccumulation and biomagnification of perfluoroalkyl acids and precursors in East Greenland polar bears and their ringed seal prey. Environ Pollut 2019; 252: 1335-1343.

Buck RC, Franklin J, Berger U, Conder JM, Cousins IT, de Voogt P, et al. Perfluoroalkyl and polyfluoroalkyl substances in the environment: terminology, classification, and origins. Integr Environ Assess Manag 2011; 7: 513-41.

Cai M, Yang H, Xie Z, Zhao Z, Wang F, Lu Z, et al. Per- and polyfluoroalkyl substances in snow, lake, surface runoff water and coastal seawater in Fildes Peninsula, King George Island, Antarctica. J Hazard Mater 2012; 209-210: 335-42.

Calafat AM, Kuklenyik Z, Reidy JA, Caudill SP, Tully JS, Needham LL. Serum concentrations of 11 polyfluoroalkyl compounds in the US population: data from the National Health and Nutrition Examination Survey (NHANES) 1999− 2000. Environmental science & technology 2007; 41: 2237-2242.

Chen H, Peng H, Yang M, Hu J, Zhang Y. Detection, Occurrence, and Fate of Fluorotelomer Alcohols in Municipal Wastewater Treatment Plants. Environ Sci Technol 2017; 51: 8953-8961.

Clara M, Scheffknecht C, Scharf S, Weiss S, Gans O. Emissions of perfluorinated alkylated substances (PFAS) from point sources--identification of relevant branches. Water Sci Technol 2008; 58: 59-66.

Coggan TL, Moodie D, Kolobaric A, Szabo D, Shimeta J, Crosbie ND, et al. An investigation into per- and polyfluoroalkyl substances (PFAS) in nineteen Australian wastewater treatment plants (WWTPs). Heliyon 2019; 5: e02316.

DEPA. Short-chain Polyfluoroalkyl Substances (PFAS). Danish Environmental Protection Agency, 2015, pp. 106.

Ebrahimi F, Lewis AJ, Sales CM, Suri R, McKenzie ER. Linking PFAS partitioning behavior in sewage solids to the solid characteristics, solution chemistry, and treatment processes. Chemosphere 2021; 271: 129530.

Eschauzier C, Beerendonk E, Scholte-Veenendaal P, De Voogt P. Impact of treatment processes on the removal of perfluoroalkyl acids from the drinking water production chain. Environ Sci Technol 2012; 46: 1708-15.

Fenton SE, Ducatman A, Boobis A, DeWitt JC, Lau C, Ng C, et al. Per- and Polyfluoroalkyl Substance Toxicity and Human Health Review: Current State of Knowledge and Strategies for Informing Future Research. Environ Toxicol Chem 2021; 40: 606-630.

Frisbee SJ, Brooks AP, Jr., Maher A, Flensborg P, Arnold S, Fletcher T, et al. The C8 health project: design, methods, and participants. Environ Health Perspect 2009; 117: 1873-82.

Fuertes I, Gomez-Lavin S, Elizalde MP, Urtiaga A. Perfluorinated alkyl substances (PFASs) in northern Spain municipal solid waste landfill leachates. Chemosphere 2017; 168: 399-407.

Gebbink WA, van Asseldonk L, van Leeuwen SPJ. Presence of Emerging Per- and Polyfluoroalkyl Substances (PFASs) in River and Drinking Water near a Fluorochemical Production Plant in the Netherlands. Environ Sci Technol 2017; 51: 11057-11065.

Ghisi R, Vamerali T, Manzetti S. Accumulation of perfluorinated alkyl substances (PFAS) in agricultural plants: A review. Environ Res 2019; 169: 326-341.

Gluge J, Scheringer M, Cousins IT, DeWitt JC, Goldenman G, Herzke D, et al. An overview of the uses of per- and polyfluoroalkyl substances (PFAS). Environ Sci Process Impacts 2020; 22: 2345-2373.

Gobelius L, Hedlund J, Durig W, Troger R, Lilja K, Wiberg K, et al. Per- and Polyfluoroalkyl Substances in Swedish Groundwater and Surface Water: Implications for Environmental Quality Standards and Drinking Water Guidelines. Environ Sci Technol 2018; 52: 4340-4349.

Goeritz I, Falk S, Stahl T, Schäfers C, Schlechtriem C. Biomagnification and tissue distribution of perfluoroalkyl substances (PFASs) in market-size rainbow trout (Oncorhynchus mykiss). Environmental Toxicology and Chemistry 2013; 32: 2078-2088.

Gomez-Canela C, Barth JA, Lacorte S. Occurrence and fate of perfluorinated compounds in sewage sludge from Spain and Germany. Environ Sci Pollut Res Int 2012; 19: 4109-19.

Guelfo JL, Adamson DT. Evaluation of a national data set for insights into sources, composition, and concentrations of per- and polyfluoroalkyl substances (PFASs) in U.S. drinking water. Environ Pollut 2018; 236: 505-513.

Guy W, Taves DR, Brey Jr W. Organic fluorocompounds in human plasma: Prevalence and characterization. ACS Publications, 1976.

Harding-Marjanovic KC, Houtz EF, Yi S, Field JA, Sedlak DL, Alvarez-Cohen L. Aerobic Biotransformation of Fluorotelomer Thioether Amido Sulfonate (Lodyne) in AFFF-Amended Microcosms. Environ Sci Technol 2015; 49: 7666-74.

Haukas M, Berger U, Hop H, Gulliksen B, Gabrielsen GW. Bioaccumulation of per- and polyfluorinated alkyl substances (PFAS) in selected species from the Barents Sea food web. Environ Pollut 2007; 148: 360-71.

Helmer RW, Reeves DM, Cassidy DP. Per- and Polyfluorinated Alkyl Substances (PFAS) cycling within Michigan: Contaminated sites, landfills and wastewater treatment plants. Water Res 2022; 210: 117983.

Hepburn E, Madden C, Szabo D, Coggan TL, Clarke B, Currell M. Contamination of groundwater with per- and polyfluoroalkyl substances (PFAS) from legacy landfills in an urban re-development precinct. Environ Pollut 2019; 248: 101-113.

Heydebreck F, Tang J, Xie Z, Ebinghaus R. Alternative and Legacy Perfluoroalkyl Substances: Differences between European and Chinese River/Estuary Systems. Environ Sci Technol 2015; 49: 8386-95.

Hogue C. Governments agree to eliminate the PFAS chemical PFHxS. Chemical & Engineering News. 100. American Chemical Society, 2022.

Houtz EF, Higgins CP, Field JA, Sedlak DL. Persistence of perfluoroalkyl acid precursors in AFFF-impacted groundwater and soil. Environ Sci Technol 2013; 47: 8187-95.

Hu XC, Andrews DQ, Lindstrom AB, Bruton TA, Schaider LA, Grandjean P, et al. Detection of Poly- and Perfluoroalkyl Substances (PFASs) in U.S. Drinking Water Linked to Industrial Sites,

Military Fire Training Areas, and Wastewater Treatment Plants. Environ Sci Technol Lett 2016; 3: 344-350.

ITRC. Aqueous Film-Forming Foam (AFFF). ITRC PFAS Technical and Regulatory Guidance Document. Interstate Technology Regulatory Council, 2022, pp. 4.

Joerss H, Schramm TR, Sun L, Guo C, Tang J, Ebinghaus R. Per- and polyfluoroalkyl substances in Chinese and German river water - Point source- and country-specific fingerprints including unknown precursors. Environ Pollut 2020; 267: 115567.

Johns K, Stead G. Fluoroproducts—the extremophiles. Journal of Fluorine Chemistry 2000; 104: 5-18.

Kemi S. Occurrence and use of highly fluorinated substances and alternatives. Swedish Chemicals Agency Stockholm, Sweden 2015.

Konwick BJ, Tomy GT, Ismail N, Peterson JT, Fauver RJ, Higginbotham D, et al. Concentrations and patterns of perfluoroalkyl acids in Georgia, USA surface waters near and distant to a major use source. Environmental Toxicology and Chemistry: An International Journal 2008; 27: 2011-2018.

Lakshminarasimman N, Gewurtz SB, Parker WJ, Smyth SA. Removal and formation of perfluoroalkyl substances in Canadian sludge treatment systems - A mass balance approach. Sci Total Environ 2021; 754: 142431.

Lang JR, Allred BM, Field JA, Levis JW, Barlaz MA. National Estimate of Per- and Polyfluoroalkyl Substance (PFAS) Release to U.S. Municipal Landfill Leachate. Environ Sci Technol 2017; 51: 2197-2205.

Langberg HA, Arp HPH, Breedveld GD, Slinde GA, Hoiseter A, Gronning HM, et al. Paper product production identified as the main source of per- and polyfluoroalkyl substances (PFAS) in a Norwegian lake: Source and historic emission tracking. Environ Pollut 2020; 273: 116259.

Lasier PJ, Washington JW, Hassan SM, Jenkins TM. Perfluorinated chemicals in surface waters and sediments from northwest Georgia, USA, and their bioaccumulation in Lumbriculus variegatus. Environ Toxicol Chem 2011; 30: 2194-201.

Lenka SP, Kah M, Padhye LP. A review of the occurrence, transformation, and removal of poly- and perfluoroalkyl substances (PFAS) in wastewater treatment plants. Water Res 2021; 199: 117187.

Lescord GL, Kidd KA, De Silva AO, Williamson M, Spencer C, Wang X, et al. Perfluorinated and polyfluorinated compounds in lake food webs from the Canadian high Arctic. Environ Sci Technol 2015; 49: 2694-702.

Li QQ, Liu JJ, Su F, Zhang YT, Wu LY, Chu C, et al. Chlorinated Polyfluorinated Ether Sulfonates and Thyroid Hormone Levels in Adults: Isomers of C8 Health Project in China. Environ Sci Technol 2022; 56: 6152-6161.

Lindstrom AB, Strynar MJ, Delinsky AD, Nakayama SF, McMillan L, Libelo EL, et al. Application of WWTP biosolids and resulting perfluorinated compound contamination of surface and well water in Decatur, Alabama, USA. Environ Sci Technol 2011a; 45: 8015-21.

Lindstrom AB, Strynar MJ, Libelo EL. Polyfluorinated compounds: past, present, and future. Environ Sci Technol 2011b; 45: 7954-61.

Liu Y, Robey NM, Bowden JA, Tolaymat TM, da Silva BF, Solo-Gabriele HM, et al. From Waste Collection Vehicles to Landfills: Indication of Per- and Polyfluoroalkyl Substance (PFAS) Transformation. Environmental Science & Technology Letters 2020; 8: 66-72.

Liu Y, Zhang Y, Li J, Wu N, Li W, Niu Z. Distribution, partitioning behavior and positive matrix factorization-based source analysis of legacy and emerging polyfluorinated alkyl substances in the dissolved phase, surface sediment and suspended particulate matter around coastal areas of Bohai Bay, China. Environ Pollut 2019; 246: 34-44.

Loganathan BG, Sajwan KS, Sinclair E, Senthil Kumar K, Kannan K. Perfluoroalkyl sulfonates and perfluorocarboxylates in two wastewater treatment facilities in Kentucky and Georgia. Water Res 2007; 41: 4611-20.

Mejia-Avendano S, Munoz G, Vo Duy S, Desrosiers M, Benoi TP, Sauve S, et al. Novel Fluoroalkylated Surfactants in Soils Following Firefighting Foam Deployment During the Lac-Megantic Railway Accident. Environ Sci Technol 2017; 51: 8313-8323.

Miranda DdA, Peaslee GF, Zachritz AM, Lamberti GA. A worldwide evaluation of trophic magnification of per-and polyfluoroalkyl substances in aquatic ecosystems. Integrated Environmental Assessment and Management 2022.

Moller A, Ahrens L, Surm R, Westerveld J, van der Wielen F, Ebinghaus R, et al. Distribution and sources of polyfluoroalkyl substances (PFAS) in the River Rhine watershed. Environ Pollut 2010; 158: 3243-50.

Moody CA, Field JA. Determination of perfluorocarboxylates in groundwater impacted by fire-fighting activity. Environmental science & technology 1999; 33: 2800-2806.

Moody CA, Martin JW, Kwan WC, Muir DC, Mabury SA. Monitoring perfluorinated surfactants in biota and surface water samples following an accidental release of fire-fighting foam into Etobicoke Creek. Environmental science & technology 2002; 36: 545-551.

Munoz G, Liu J, Vo Duy S, Sauvé S. Analysis of F-53B, Gen-X, ADONA, and emerging fluoroalkylether substances in environmental and biomonitoring samples: A review. Trends in Environmental Analytical Chemistry 2019; 23.

Munoz G, Mercier L, Duy SV, Liu J, Sauve S, Houde M. Bioaccumulation and trophic magnification of emerging and legacy per- and polyfluoroalkyl substances (PFAS) in a St. Lawrence River food web. Environ Pollut 2022; 309: 119739.

Murakami M, Imamura E, Shinohara H, Kiri K, Muramatsu Y, Harada A, et al. Occurrence and sources of perfluorinated surfactants in rivers in Japan. Environmental science & technology 2008; 42: 6566-6572.

Nascimento RA, Nunoo DBO, Bizkarguenaga E, Schultes L, Zabaleta I, Benskin JP, et al. Sulfluramid use in Brazilian agriculture: A source of per- and polyfluoroalkyl substances (PFASs) to the environment. Environ Pollut 2018; 242: 1436-1443.

Newton S, McMahen R, Stoeckel JA, Chislock M, Lindstrom A, Strynar M. Novel Polyfluorinated Compounds Identified Using High Resolution Mass Spectrometry Downstream of Manufacturing Facilities near Decatur, Alabama. Environ Sci Technol 2017; 51: 1544-1552.

O'Hagan D. Understanding organofluorine chemistry. An introduction to the C–F bond. Chemical Society Reviews 2008; 37: 308-319.

OECD. Toward a New Comprehensive Global Database of Per- and Polyfluoroalkyl Substances (PFASs): Summary Report on Updating the OECD 2007 List of Per- and Polyfluoroalkyl Substances (PFASs). Series on Risk Management No. 39. Organisation for Economic Co-operation and Development, 2018.

Oliaei F, Kriens D, Weber R, Watson A. PFOS and PFC releases and associated pollution from a PFC production plant in Minnesota (USA). Environ Sci Pollut Res Int 2013; 20: 1977-92.

Pan Y, Zhang H, Cui Q, Sheng N, Yeung LWY, Sun Y, et al. Worldwide Distribution of Novel Perfluoroether Carboxylic and Sulfonic Acids in Surface Water. Environ Sci Technol 2018; 52: 7621-7629.

Pedersen KE, Letcher RJ, Sonne C, Dietz R, Styrishave B. Per- and polyfluoroalkyl substances (PFASs) - New endocrine disruptors in polar bears (Ursus maritimus)? Environ Int 2016; 96: 180-189.

Perez F, Llorca M, Kock-Schulmeyer M, Skrbic B, Oliveira LS, da Boit Martinello K, et al. Assessment of perfluoroalkyl substances in food items at global scale. Environ Res 2014; 135: 181-9.

Ren J, Point AD, Baygi SF, Fernando S, Hopke PK, Holsen TM, et al. Bioaccumulation of polyfluoroalkyl substances in the Lake Huron aquatic food web. Sci Total Environ 2022; 819: 152974.

Rigby H, Dowding A, Fernandes A, Humphries D, Jones NR, Lake I, et al. Concentrations of organic contaminants in industrial and municipal bioresources recycled in agriculture in the UK. Sci Total Environ 2021; 765: 142787.

Sinclair E, Kannan K. Mass loading and fate of perfluoroalkyl surfactants in wastewater treatment plants. Environmental science & technology 2006; 40: 1408-1414.

Sun H, Zhang X, Wang L, Zhang T, Li F, He N, et al. Perfluoroalkyl compounds in municipal WWTPs in Tianjin, China--concentrations, distribution and mass flow. Environ Sci Pollut Res Int 2012; 19: 1405-15.

Sun M, Arevalo E, Strynar M, Lindstrom A, Richardson M, Kearns B, et al. Legacy and Emerging Perfluoroalkyl Substances Are Important Drinking Water Contaminants in the Cape Fear River Watershed of North Carolina. Environmental Science & Technology Letters 2016; 3: 415-419.

Sunderland EM, Hu XC, Dassuncao C, Tokranov AK, Wagner CC, Allen JG. A review of the pathways of human exposure to poly- and perfluoroalkyl substances (PFASs) and present understanding of health effects. J Expo Sci Environ Epidemiol 2019; 29: 131-147.

Tian YP, Zeng XW, Bloom MS, Lin S, Wang SQ, Yim SHL, et al. Isomers of perfluoroalkyl substances and overweight status among Chinese by sex status: Isomers of C8 Health Project in China. Environ Int 2019; 124: 130-138.

Torres F, Guida Y, Weber R, Machado Torres JP. Brazilian overview of per- and polyfluoroalkyl substances listed as persistent organic pollutants in the stockholm convention. Chemosphere 2022; 291: 132674.

Trang B, Li Y, Xue X-S, Ateia M, Houk K, Dichtel WR. Low-temperature mineralization of perfluorocarboxylic acids. Science 2022; 377: 839-845.

USEPA. Fact Sheet: 2010/2015 PFOA Stewardship Program. United States Environmental Protection Agency, 2006.

USEPA. Drinking Water Health Advisories for PFOA and PFOS. United States Environmental Protection Agency, 2016.

USEPA. Human Health Toxicity Values for Perfluorobutane Sulfonic Acid and Related Compound Potassium Perfluorobutane Sulfonate., 2021.

USEPA. EPA Announces New Drinking Water Health Advisories for PFAS Chemicals, $1 Billion in Bipartisan Infrastructure Law Funding to Strengthen Health Protections. In: USEPA, editor, 2022.

Vecitis CD, Wang Y, Cheng J, Park H, Mader BT, Hoffmann MR. Sonochemical degradation of perfluorooctanesulfonate in aqueous film-forming foams. Environmental science & technology 2010; 44: 432-438.

Wang Z, Cousins IT, Scheringer M, Hungerbuehler K. Hazard assessment of fluorinated alternatives to long-chain perfluoroalkyl acids (PFAAs) and their precursors: status quo, ongoing challenges and possible solutions. Environ Int 2015; 75: 172-9.

Wang Z, DeWitt JC, Higgins CP, Cousins IT. A Never-Ending Story of Per- and Polyfluoroalkyl Substances (PFASs)? Environ Sci Technol 2017; 51: 2508-2518.

Wanninayake DM. Comparison of currently available PFAS remediation technologies in water: A review. J Environ Manage 2021; 283: 111977.

Whitehead HD, Venier M, Wu Y, Eastman E, Urbanik S, Diamond ML, et al. Fluorinated Compounds in North American Cosmetics. Environmental Science & Technology Letters 2021; 8: 538-544.

Xie X, Weng X, Liu S, Chen J, Guo X, Gao X, et al. Perfluoroalkyl and Polyfluoroalkyl substance exposure and association with sex hormone concentrations: Results from the NHANES 2015-2016. Environ Sci Eur 2021; 33.

Zeeshan M, Zhang YT, Yu S, Huang WZ, Zhou Y, Vinothkumar R, et al. Exposure to isomers of per- and polyfluoroalkyl substances increases the risk of diabetes and impairs glucose-homeostasis in Chinese adults: Isomers of C8 health project. Chemosphere 2021; 278: 130486.

Zhang S, Lu X, Wang N, Buck RC. Biotransformation potential of 6:2 fluorotelomer sulfonate (6:2 FTSA) in aerobic and anaerobic sediment. Chemosphere 2016a; 154: 224-230.

Zhang X, Lohmann R, Dassuncao C, Hu XC, Weber AK, Vecitis CD, et al. Source attribution of poly- and perfluoroalkyl substances (PFASs) in surface waters from Rhode Island and the New York Metropolitan Area. Environ Sci Technol Lett 2016b; 3: 316-321.

Chapter 3. A global assessment of the spatial distribution and environmentally relevant concentrations of per- and polyfluoroalkyl substances (PFAS) in environmental matrices

Manuscript submitted for publication.

Viticoski, Roger; Feltman, Meredith; Rogers, Stephanie; Wang, Danyang; Mulabagal, Vanisree; Blersch, David; Hayworth, Joel*.

Abstract

This work assessed data from 228 journal articles to better understand the spatial distribution, specific profiles, and environmentally relevant concentrations (ERCs) of per- and polyfluoroalkyl substances (PFAS) in surface water, sediment, and groundwater. PFAS were detected in 43 countries across all continents between 1999-2021. Most studies were focused on the Chinese coastal areas of the Bohai and Yellow seas, Eastern United States, and Western Europe. Overall, ΣPFAS concentrations were observed to reach up to 2,270 μg L^{-1} in surface water, 7,090 μg L^{-1} in groundwater, and 2,450 ng gdw^{-1} in sediment. Multiple sources were linked to the global PFAS contamination, including municipal and industrial waste, landfills, fluorochemical facilities, aqueous film-forming foam (AFFF)-related sites, and atmospheric transport and deposition, among others. Perfluoroalkyl acids (PFAAs) were the most targeted and detected analytes in all analyzed environmental matrices. PFOS had the highest individual concentration in surface water and sediment (2,200 μg L^{-1} and 623 ng gdw^{-1}, respectively), while PFOA had the highest concentration in groundwater (6,600 μg L^{-1}). However, emerging PFAS alternatives, such as short-chain PFAAs and perfluoroethers, have been frequently identified in recent years. Worldwide PFAS concentration data were used to gain insight into ERCs to aid in the design of controlled laboratory studies. ERCs should not exceed 2,721 and 48,606 ng L^{-1} in studies evaluating PFAS in surface water and groundwater, respectively, and 137.9 ng gdw^{-1} in sediments to guarantee environmental relevance. Results from this study enhance the current understanding of the global distribution and profile of PFAS in the

environment and provide data-supported guidance for working with PFAS under controlled experimental conditions.

3.1 Introduction

Many industrial advancements have been facilitated through the development and production of synthetic chemicals, which are often subsequently released into the environment. Per- and polyfluoroalkyl substances (PFAS) have gained global attention because of their utility in many applications and their potential adverse health effects on humans and wildlife. These substances are fluorosurfactants, presenting a hydrophilic functional group and a hydrophobic tail that contains the moiety C_nF_{2n+1}-. The C-F bonds, among the strongest chemical bonds in organic chemistry, provide PFAS with unique chemical, biological, and thermal stability (Buck et al., 2011; Guelfo and Adamson, 2018). Because of their resistance to environmental degradation (Blum et al., 2015), PFAS are also known as "forever chemicals." Manufactured since the late 1940s, PFAS have been used for numerous applications, such as in the coating of non-stick cookware, food packaging materials, and fire-fighting foams (DEPA, 2015; KEMI, 2015; Lindstrom et al., 2011b). Concerns regarding the ubiquity of PFAS came to light in the 1990s when 3M reported evidence of the widespread occurrence of PFAS in human blood bank samples (3M, 1998). Since then, studies have linked PFAS to various health effects in humans, such as testicular and kidney cancers, liver malfunction, and endocrine disruption. Some PFAS have also been observed to be harmful to wildlife, bioaccumulating and biomagnifying in organisms (ATSDR, 2018; Blum et al., 2015; USEPA, 2019). Consequently, regulatory actions have been and continue to be implemented to restrict the production and control the release of these substances globally.

Efforts to limit the release of various PFAS into the environment started in 2000 when 3M, one of the leading manufacturers of PFAS products, announced the phase-out of PFOSF and PFOS-based substances by 2002 (3M, 2000). In 2006, the United States Environmental Protection Agency (US EPA) launched the PFOA Stewardship Program, inviting the eight major producers of PFAS to join a global program to eliminate the emissions of PFOA and its precursors by 2015 (USEPA, 2006). In 2009, PFOS,

its salts, and PFOSF were listed in Annex B of the Stockholm Convention, leading to restrictions on their production in over 100 countries, while PFOA and its salts were listed in Annex A in 2019, eliminating their production in several countries (Torres et al., 2022). There are also many standards for the maximum permissible levels of PFAS in drinking water and consumer products; however, these guidelines vary widely across agencies concerning threshold values and substances. For instance, in 2016, the US EPA issued a non-enforceable health advisory limit (HAL) in which the total or individual levels of PFOS and PFOA should not exceed 70 ng L^{-1} in drinking water (USEPA, 2016). More recently, the US EPA issued updated interim lifetime HALs for PFOS and PFOA of 0.004 and 0.02 ng L^{-1}, respectively, and introduced new HALs for Gen-X and PFBS of 10 and 2,000 ng L^{-1}, respectively (USEPA, 2022). The decrease in PFOS and PFOA health advisories by orders of magnitude highlights the PFAS potential to induce adverse health effects even at very low exposure concentrations. The implementation of health advisory levels for PFAS extends beyond the United States. Denmark released a drinking water threshold of no more than 100 ng L^{-1} for the sum of 12 PFAS in 2015, while in Sweden, the sum of 11 PFAS cannot be higher than 90 ng L^{-1} (Gobelius et al., 2018). In 2019, the Council of the European Union called for a plan to "eliminate all non-essential uses of PFAS" (EUC, 2019). To enlighten the regulative process for PFAS, an improved understanding of their observed levels in the natural environment globally is needed.

Successful regulation of PFAS is complicated, in part, by their vast quantity: thousands of PFAS continuously enter the global market and environment, although not always intentionally (Wang et al., 2017). While PFAS are mainly produced for direct applications, a portion can also be produced as residual intermediates, unintended byproducts, or degradation products (Wang et al., 2017). Since many regulatory efforts have focused on long-chain substances, PFAS manufacturers often replace regulated PFAS with new or otherwise unregulated PFAS. These substances are usually short-chain homologs of long-chain legacy PFAS or present fluorinated segments joined by ether linkages (DEPA, 2015; Pan et al., 2017). For instance, DuPont replaced the legacy PFOA with the perfluoroether HFPO-DA (Gen-X), while 3M replaced PFNA with the perfluoroether ADONA (Munoz et al., 2019b). Although PFAS replacements are expected

to be less bioaccumulative, their toxicity has not been studied nearly as extensively as that of legacy PFAS (DEPA, 2015). Because emerging PFAS are often not as effective as the substances they replaced, many are used in larger concentrations to achieve similar performance. Short-chain PFAS are also generally more resistant to degradation and not easily removed from contaminated matrices, increasing the risk of human and wildlife exposure (Blum et al., 2015). In addition to short-chain and perfluoroether replacements, some manufacturers have begun using certain fluorotelomer and sulfonamide substances as perfluoroalkyl acids (PFAAs) alternatives. However, these replacements can breakdown to the substances they were intended to replace, such as PFOS and PFOA (Buck et al., 2011; Shi et al., 2018). The development of new, often unregulated fluorinated alternatives has led to an increase in the number of PFAS, now estimated to be nearly 5,000 substances (OECD, 2018), many with unique intended and unintended physicochemical and environmental characteristics. As a result, PFAS have been identified across all continents, from Tibet (Yamazaki et al., 2016) and remote areas in Antarctica (Cai et al., 2012; Casal et al., 2017), to highly populated areas in the US (Sinclair et al., 2006; Sun et al., 2016). In fact, based on data from a nationwide PFAS survey in public water systems by the US EPA, it is estimated that over 16.5 million Americans from 33 states are or have been supplied with PFAS-contaminated drinking water (Hu et al., 2016). By aggregating drinking water data from multiple sources, another study estimates that 200 million US residents consume drinking water with a PFOA and PFOS concentration at or above 1 ng L^{-1} (Andrews and Naidenko, 2020).

In addition to the vast amount of PFAS on the global market and the regulatory challenges posed by them, there is considerable uncertainty regarding the concentrations at which they are commonly found in the environment. Most controlled experiments considering the environmental behavior and fate of PFAS, or the effects of exposure to PFAS on humans and wildlife, seek to mimic realistic conditions to ensure that results are meaningful and representative. However, determining what constitutes environmentally relevant concentrations (ERCs) of PFAS has heretofore required estimates by researchers based on a very limited assessment of past observational studies. One outcome of this lack of knowledge regarding ERCs for

individual or mixtures of PFAS is that many controlled PFAS studies have employed elevated concentrations not often seen in the environment. This study used data from 228 peer-reviewed journal articles to enhance understanding of the global distribution of PFAS, identify the groups and individual PFAS most often detected in the environment, and estimate ERCs for these observed PFAS in surface water, sediment, and groundwater. To the best of the authors' knowledge, this is the first study to assess the global spatial distribution of total PFAS based on observational studies and use this information to establish ERCs for the most commonly detected PFAS in the environment.

3.2 Methods

3.2.1 Literature Search and Selection

Studies used in this assessment were first acquired through a search of Google Scholar with the keywords "PFAS in the environment" in November 2019, which resulted in over 10,000 results. Out of these, only studies focused on the occurrence of PFAS in the environment in either surface water, groundwater, or sediment were selected, resulting in 235 studies. Of these, 39 were excluded because 17 did not provide sampling location information and 22 did not provide adequate information on analyte concentrations. A supplementary search was made in the CAB Direct (https://www.cabdirect.org/) in July 2021 on articles from 2019 to 2021, resulting in 32 qualifying studies. Finally, 228 articles from peer-reviewed journals with full-text available in English were selected for this assessment.

3.2.2 Data Extraction

General information, including author, publication year, location, media, number of detected and targeted analytes, and concentrations, were extracted from each article and recorded in an Excel spreadsheet. Both individual concentrations of each substance and the overall average and range of the total PFAS concentrations were extracted from each study. For the purpose of this assessment, mean ΣPFAS refers to the overall average of the total individual PFAS concentrations observed in a given study. For example, for a study with ten sampling locations in a given matrix (surface water, sediment, and groundwater), mean ΣPFAS is the overall average of the ten total PFAS concentrations. For studies that did

not explicitly provide the average and range of ΣPFAS, the same was calculated based on the information provided in the text or supplemental information. In studies where the concentrations of individual analytes per site were not reported, but only the average of each analyte among all sites, individual averages were used to calculate the average ΣPFAS. For studies that reported the concentration of PFAS in surface water or sediment throughout a given depth, only the values corresponding to the surface (or closest to the surface) were used. In long-term studies in which concentrations were measured more than once, the average was used to calculate a single ΣPFAS. The overall distribution of analytes that were targeted and detected was also extracted. From each study, linear and branched isomers of a given analyte were classified as targeted or detected. Targeted analytes encompass all substances that were targeted by a study. In this study, detected analytes are defined as substances with concentrations that were higher than the analytical limits of quantification, and exhibited a detection frequency (DF) higher than 5%. Information was individually recorded for each study and matrix.

3.2.3 Data Analysis

Summary statistics (mean, range, and standard deviation) were calculated in Microsoft Excel. Boxplots were produced using R 3.6.1 (The R Foundation). Analytes were classified following the nomenclature suggested by Buck et al. (2011). A complete list with the names and molecular formulas of all substances mentioned throughout this main text is displayed in Table 3.2. Overall targeted and detected values were calculated for each group. Figures were prepared using Illustrator 2021 (Adobe Co). The area covered by each study was delineated using ArcGIS Pro 2.9 (Environmental Systems Research Institute, Inc.). An ellipse was used to delineate the area covered by each study, using the information provided in the respective study, i.e., maps, coordinates, and location names. To avoid bias in the visual representation, studies that covered large or multiple areas were represented by more than one ellipse, depending on data availability. Author, year, media, description of the location, range, and mean associated with each study area were copied to the attributes table.

3.3 Results and Discussion

3.3.1 PFAS in the Environment: Specific Profiles

Although it is estimated that approximately 5,000 substances contain at least one perfluoroalkyl moiety (OECD, 2018), only a small portion (150 PFAS) were targeted in the assessed studies (Figure 3.1). Most of the assessed studies targeted perfluoroalkyl acids, followed by sulfonamides, fluorotelomers, and perfluoroether substances. Recent studies have discovered novel classes of PFAS through non-targeted analysis (Barzen-Hanson et al., 2017; Newton et al., 2017), which are only partially covered in this assessment. An example is a study by Barzen-Hanson et al. (2017), in which 40 novel classes of PFAS in AFFF-impacted groundwater were discovered (Barzen-Hanson et al., 2017).

Perfluoroalkyl acids (PFAAs) were the most studied PFAS due to their ubiquity in the environment, usefulness in industrial applications, and known/suspected adverse health effects on humans and wildlife. Additionally, there are reliable methods for the analytical quantification of these substances. These substances are highly stable and are usually endpoints in the degradation of PFAS precursors. This group includes perfluoroalkyl carboxylic, sulfonic, phosphonic, phosphinic, and cyclic acids.

Perfluoroalkyl carboxylic acids (PFCAs) are a subgroup of PFAAs that have been used for decades as additives in the manufacture of a myriad of consumer products such as paper and fabric treatments, aqueous fire-fighting foam (AFFF), fluoropolymers, ski waxes, baking paper, carpet, leather, nanosprays, and impregnation sprays, among others (Begley et al., 2008; Choi et al., 2018; Kotthoff et al., 2015; Prevedouros et al., 2006). In the assessed studies, PFOA was the most targeted and frequently detected PFCA in all matrices. PFOA presented the highest concentration in all matrices, reaching up to 579 µg L^{-1} in surface water, 203 ng gdw^{-1} in sediment, and 6,570 µg L^{-1} in groundwater. This is not surprising since PFOA is one of the earliest and most widely studied PFAS and is the target of several regulations (Brennan et al., 2021). PFBA presented the second-highest concentration in surface water and sediment (47,800 ng L^{-1} and 84 ng gdw^{-1}), followed by PFHpA in surface water (42,567 ng L^{-1}) and PFDA in sediment (77.1 ng gdw^{-1}). In groundwater, PFHxA had the second-highest concentration (372 µg L^{-1}), followed by PFPeA

(220 μg L^{-1}). Information on the sources and environmental fate of emerging ultra-short chain PFCAs such as TFA and PFPrA is still lacking, even though they have been found at concentrations up to 35,000 and 2,000 ng L^{-1}, respectively, in surface water downstream of a fluorochemical facility in China (Chen et al., 2018a). In the assessed studies, short-chain PFCAs (<7 perfluorinated carbons) had substantially higher detection frequencies (DF) in surface and groundwater than long-chain PFCAs (≥7 perfluorinated carbons). Short-chain PFCAs had DFs of 90% in surface water and 95% in groundwater, while long-chain PFCAs had 77% and 75%, respectively. This is likely due to the hydrophilic nature of short-chain PFAS (Higgins and Luthy, 2006) and the reduced production of many long-chain PFCAs. In contrast, long-chain PFCAs were detected in 76% of the assessed studies in sediment, while short-chain PFCAs were detected in 66%.

Perfluoroalkyl sulfonic acids (PFSAs) present the general structure $C_nF_{(2n+1)}$-SO_3H and have been used in a variety of products since the 1950s, including metal plating, impregnation, oil production, and AFFF formulations (DEPA, 2015; Wang et al., 2013c). In the assessed studies, PFOS was the most detected PFSA in all matrices, which is expected as PFOS was manufactured for decades and is the target of several regulations (Brennan et al., 2021). PFOS also had the highest concentration in surface water and sediment (2,210 μg L^{-1} and 623 ng gdw^{-1}, respectively), followed by PFHxS and PFBS in surface water (134 μg L^{-1} and 18,000 ng L^{-1}, respectively) and PFBS and PFDS in sediment (114 ng gdw^{-1} and 88.2 ng gdw^{-1}, respectively). In groundwater, PFHxS reached up to 530 μg L^{-1}, followed by PFBS (140 μg L^{-1}) and PFOS (110 μg L^{-1}). Unlike PFCAs, the DF of long-chain (≥6 perfluorinated carbons) and short-chain PFSAs were similar in surface water: 85% and 86%, respectively. However, long-chain PFSAs were detected at much higher frequencies than short-chains in sediment (79% vs. 62%, respectively), likely related to differences in their aqueous solubility (Higgins and Luthy, 2006).

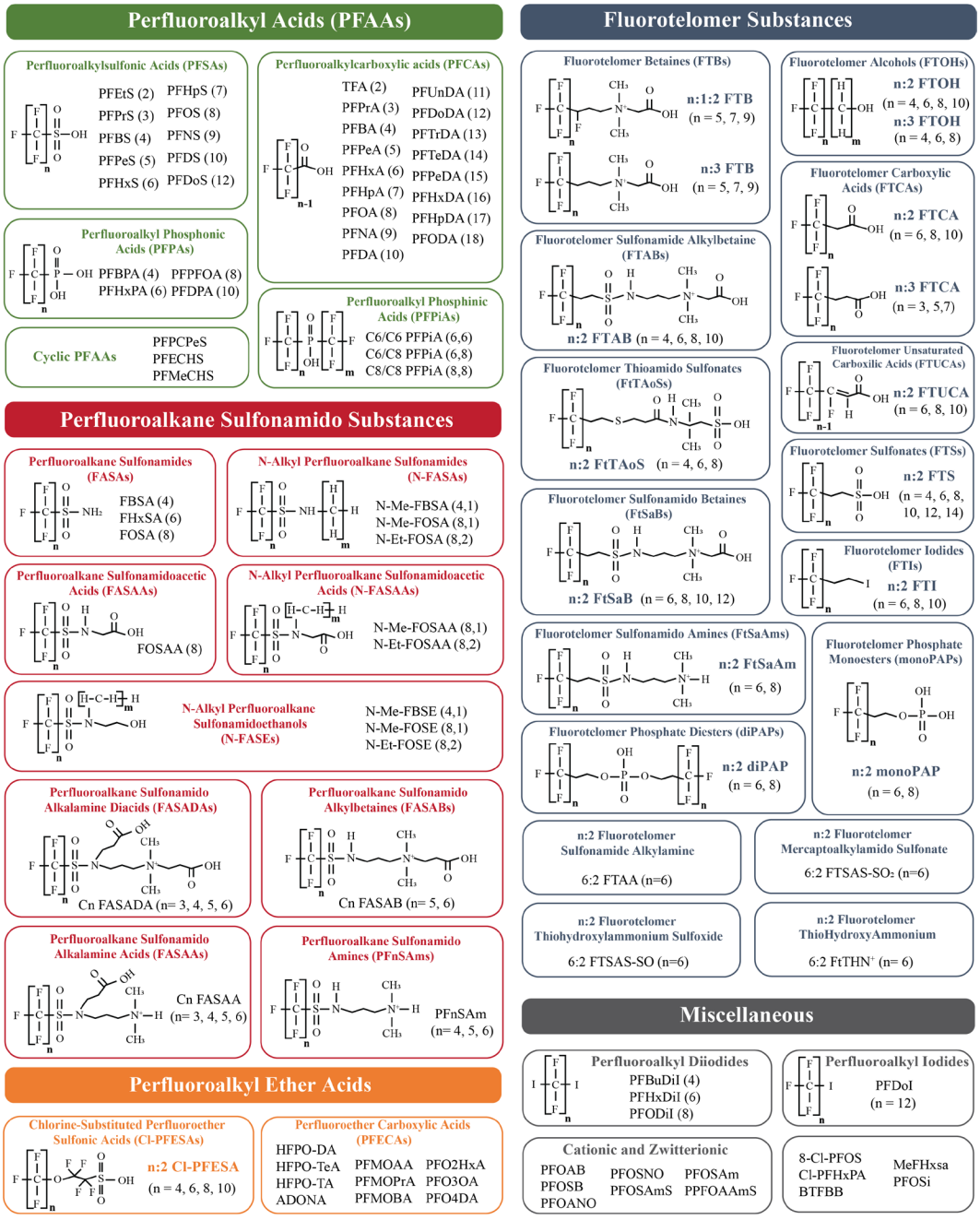

Figure 3.1 Groups and subgroups of PFAS identified in environmental matrices of the assessed studies. When more than two numbers are presented in parenthesis, the first is related to "n" and the second to "m" in the chemical structure. A complete list with names and molecular formulas is displayed in Table 3.2.

Perfluoroalkyl phosphonic (PFPAs) and phosphinic acids (PFPIAs) have been used as surfactants in applications such as leveling and wetting agents. They have also been used as inert ingredients in

pesticides, a practice that is no longer permitted in the United States (D'eon et al., 2009). Between 1998 and 2002, these substances had a production volume of up to 500,000 lbs $year^{-1}$ in North America (Jin et al., 2015). PFPA homologs were targeted in only 6 of the assessed studies, with DF of 60% for PFHxPA and 40% for PFPOA and PFPDA in surface water. PFPIAs were targeted in 4 of the assessed studies, with C6/C6 PFPIA being detected in surface water in 50% of these studies, while C6/C6 and C6/C8 PFPIA were detected in sediment in all four studies. Cyclic PFAAs such as PFECHS and PFMeCHS have been historically used as erosion inhibitors in hydraulic fluids, but little information is known about their usage in consumer products. Although Cyclic PFAAs have been found at high levels in the environment, they have only been targeted by a few studies (De Silva et al., 2011; Wang et al., 2016). Out of those studies, PFPCPeS presented 100% DF in surface water and sediment, and PFECHS and PFMeCHS presented 100% and 83% DF in surface water, respectively.

Perfluoroalkane Sulfonamides are neutral substances that are usually more volatile than PFAAs and can ultimately transform into PFCAs and PFSAs (Ahrens et al., 2009b). For instance, FOSA has been observed to break down into PFOS, and N-FASA and N-FASE to break down into various PFCAs (Buck et al., 2011). These substances are typically used as raw materials for surfactants and surface treatment products (FASE, N-FASE) or are intermediate transformation products of those processes (FASAA, N-FASAA) (Buck et al., 2011). Among the assessed studies, FOSA was the most targeted analyte in all matrices and had the highest DF in surface water (65%), reaching up to 282.5 ng L^{-1} in surface water and 15.1 ng gdw^{-1} in sediment. N-Me-FOSAA had the highest DF (56%) in sediments, and N-Et-FOSAA was detected at a maximum concentration of 286.2 ng gdw^{-1}. C6 FASADA had a DF of 100% in surface water but was only targeted in one of the assessed studies (D'Agostino and Mabury, 2017). The remaining perfluoroalkane sulfonamide substances in the assessed studies had relatively low DF in surface water and sediment. For example, FASAAs, FASABs, and PFnSAms were not detected in any matrices.

Fluorotelomer substances are also neutral and very reactive and are known to degrade to PFAAs (Buck et al., 2011). Due to regulatory restrictions on the use of long-chain PFAAs, fluorotelomer substances

have been widely used as PFAAs replacements, especially in the formulation of AFFF. For instance, 6:2 FTAB is a PFOS replacement and a major component of the AFFF Forafac® 1157 (Shi et al., 2018). Fluorotelomer substances can also be used to produce side-chain fluorinated substances, and diPAPs have been used as defoaming agents in pesticide formulations (Buck et al., 2011). Despite their relevance, the environmental behavior and fate of fluorotelomer substances have not been widely investigated. 6:2 FTS was the most targeted and detected analyte in surface water, sediment, and groundwater, being found in 78%, 50%, and 100% of these respective matrices in the assessed studies. 6:2 FTS was detected at concentrations up to 1,654 ng L^{-1} in surface water and 270 μg L^{-1} in groundwater. A limited number of the assessed studies showed that several analytes from different fluorotelomer subgroups had 100% DF in surface water (FTBs, FTABs, and FtSaAms) and sediment (FTBs, FTABs, and FTSs). Out of the fluorotelomer homologs targeted in groundwater, only 6:2 and 8:2 FTS were detected, at a frequency of 100% and 50%, respectively. The fact that fluorotelomers and most sulfonamides are more reactive than perfluoroalkyl substances (Ahrens et al., 2009b) could, in part, explain their lower detection frequencies in environmental matrices.

Regulatory actions across the globe are reshaping the fluorochemical industry, leading to the development of novel replacements for legacy substances, such as perfluoroethers, under the assumption that ether links make them more easily degradable (Pan et al., 2017). For instance, HFPO-DA (trademarked Gen-X) and ADONA are manufactured by DuPont and 3M, respectively, as PFOA and PFNA replacements in the production of fluoropolymers (Munoz et al., 2019b). Although information on the occurrence and fate of perfluoroethers in the environment is still emerging, these replacement substances accounted for up to 19% of all detected PFAS in a 2018 worldwide survey (Pan et al., 2018). In fact, Pan et al. (2017) detected the emerging perfluoroether HFPO-TA at a peak concentration of 68,500 ng L^{-1} in surface water samples downstream from a fluorochemical facility in China (Pan et al., 2017). Similarly, HFPO-DA and ADONA were detected at 3,800 ng L^{-1} and 2,500 ng L^{-1} in the surface water of Chinese and German rivers, respectively (Joerss et al., 2020). Production of HFPO-DA is permitted by the US EPA under a consent

order that stipulates 99% of HFPO-DA must be captured before wastewater and air discharges. This order, however, does not include HFPO-DA produced as a by-product of other substances (Hopkins et al., 2018). Furthermore, 6:2 Cl-PFESA (trademarked F-53B) is a fluorosurfactant widely used in China in the metal plating industry and has been observed to have acute toxicity similar to PFOS (Munoz et al., 2019b). Among the assessed studies, 6:2 Cl-PFESA and HFPO-DA were the most targeted perfluoroethers in surface water (n=15 and 14, respectively), with a DF of 80% and 86%, respectively. ADONA was targeted in 9 of the assessed studies in surface water and 7 in sediment, with DF of 44% and 14%, respectively.

3.3.2 Global Distribution of PFAS

The 228 studies considered in this assessment reported PFAS in surface water, groundwater, and sediment in 43 countries across all continents over 22 years (1999-2021). Of these, 113 studies focused exclusively on surface water (lakes, rivers, ponds, reservoirs, estuaries, and marine water), 37 on sediment, and 10 on groundwater. Further, 68 focused on more than one matrix, from which 55 analyzed the occurrence of PFAS in sediment and surface water, 8 in surface water and groundwater, and 5 in all three matrices. As shown in Figures 3.2 and 3.3, these studies were not evenly distributed around the globe, as 116 (51%) were focused on Asia, 51 (22%) on Europe, 43 (19%) on The Americas, and less than 5% on the other continents (Oceania, Africa, and Antarctica). Given the complexity and extent of the data presented in this study, an interactive map was developed to better display the global distribution of PFAS (https://storymaps.arcgis.com/stories/06ce7acdad5d4f2fa5fcb10200577225).

A variety of sources are responsible for the widespread global PFAS contamination, including direct and indirect discharges from municipal and industrial waste facilities, landfills, fluorochemical facilities, AFFF sites, and atmospheric transport and deposition, among others. The distribution and potential sources of PFAS associated with each continent are discussed below. A complete list with information and references to all assessed studies is provided in Tables 3.6-3.8.

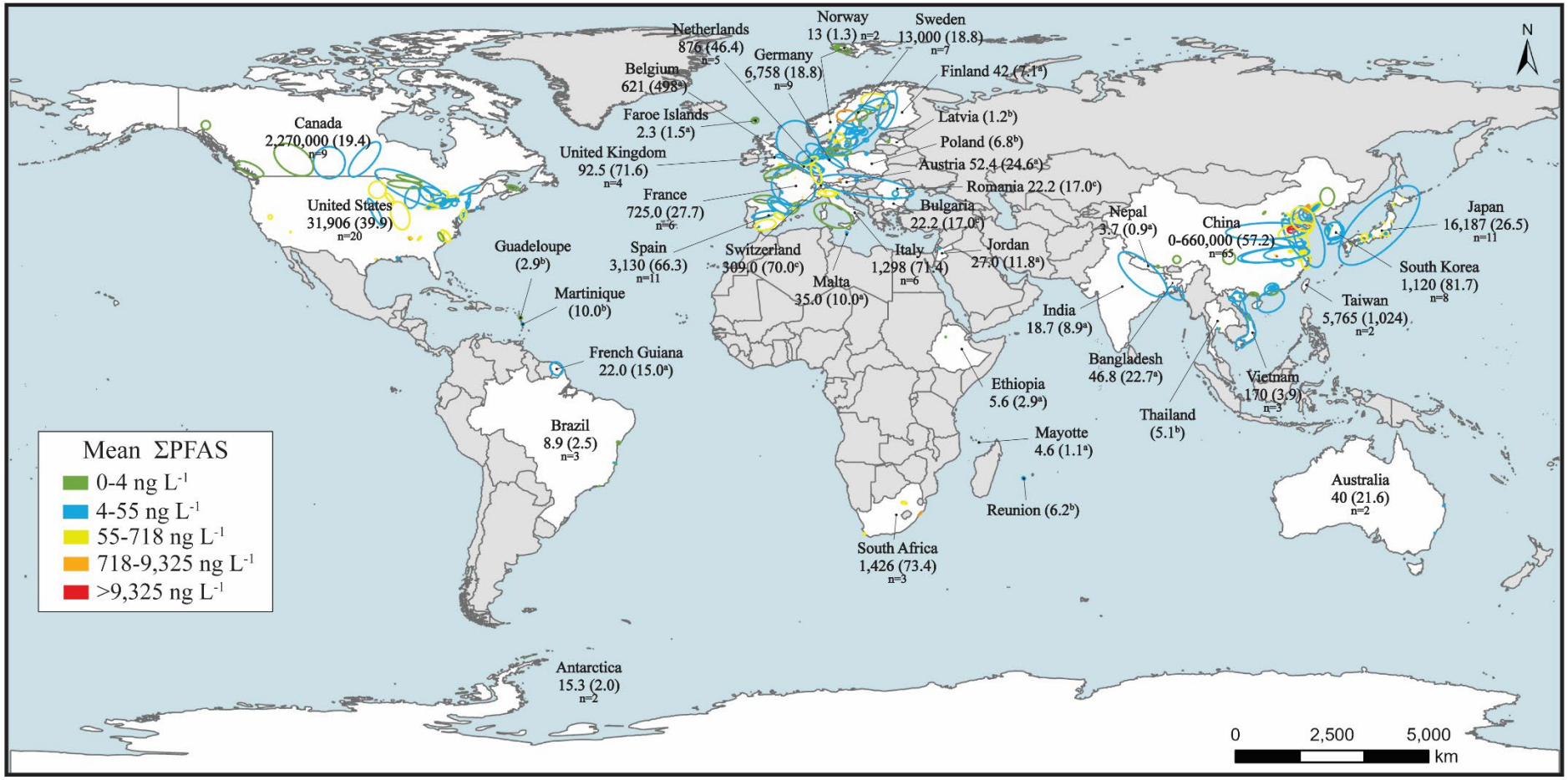

a = average (n=1); b = data reported in a way that only average could be calculated; c = study related to transboundary rivers at the border between neighboring countries.

Figure 3.2 Global distribution of PFAS in surface water. Countries in which at least one study was conducted are illustrated in white. The color of the ellipses represents the mean ΣPFAS in that location. Maximum ΣPFAS, median ΣPFAS, and the number of studies (n) are displayed for each country, when available, in the format: maximum ΣPFAS (median ΣPFAS), with n noted on the following line. Concentrations are expressed in ng L^{-1}.

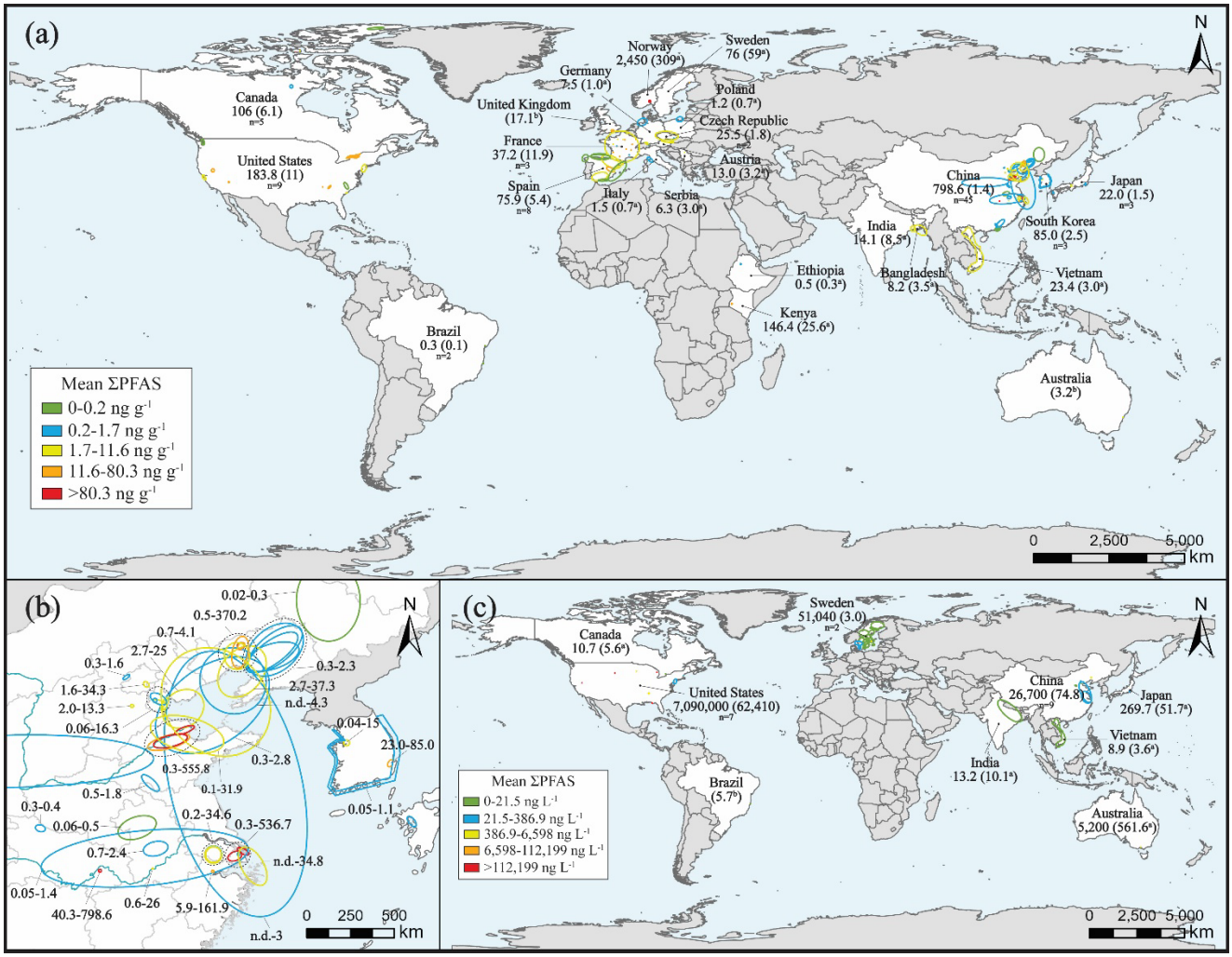

a = average (n=1); b = data reported in a way that only average could be calculated.

Figure 3.3 Global distribution of PFAS in (a) sediment and (c) groundwater. Countries in which at least one study was conducted are illustrated in white. The color of the ellipses represents the mean ΣPFAS in that location. Concentrations are expressed in ng L^{-1} for groundwater and ng gdw^{-1} for sediment. Maximum ΣPFAS, median ΣPFAS, and the number of studies (n) are displayed for each country, when available, in the format: maximum ΣPFAS (median ΣPFAS), with n noted on the following line. Due to data density in this region, the distribution and range of PFAS in sediment in the Bohai Sea area are displayed in more detail in (b), in which major rivers (in blue) and provinces boundaries (in light gray) are shown for spatial reference.

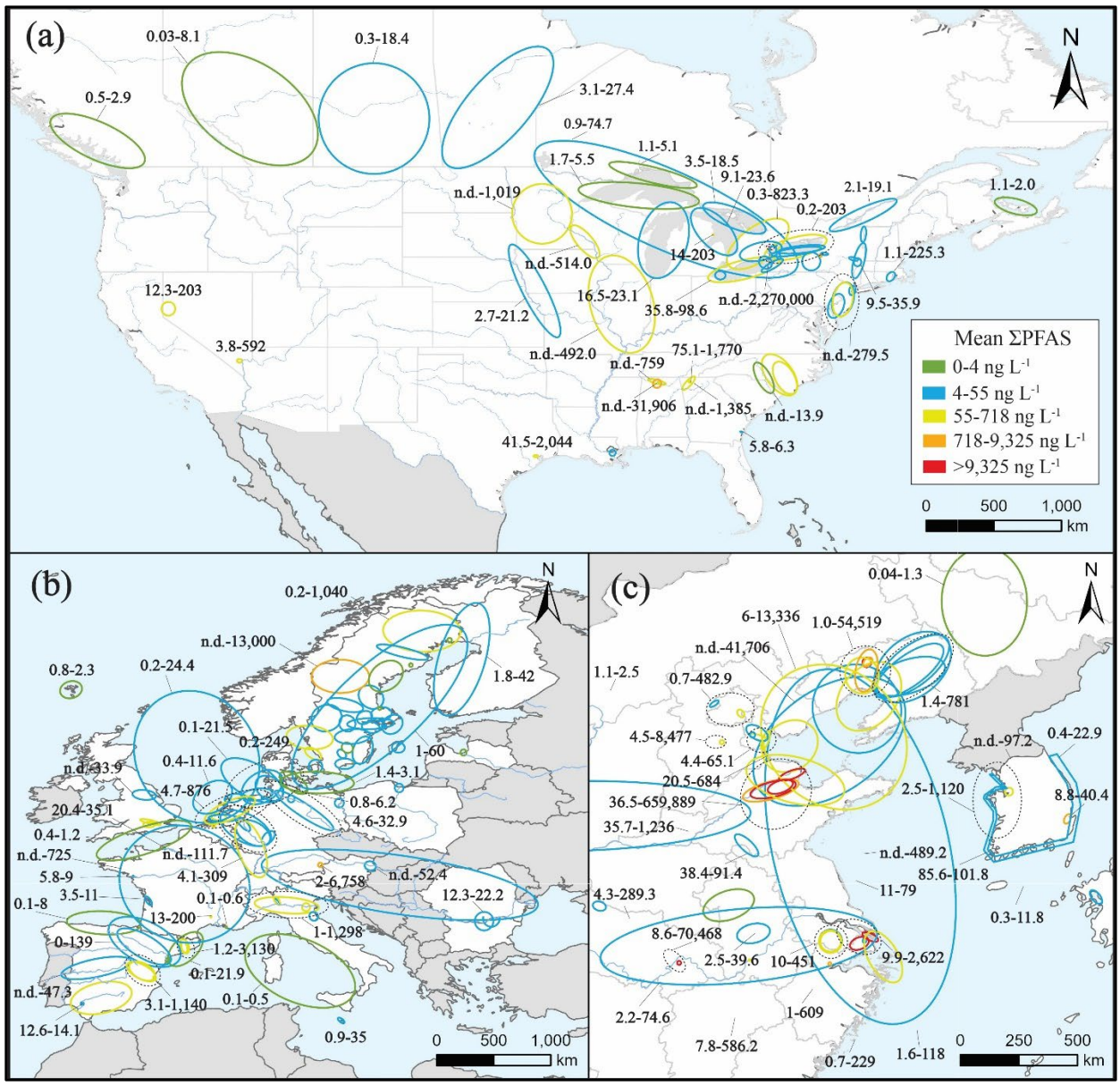

Figure 3.4 Spatial distribution of PFAS in surface water in (a) United States and Southern Canada, (b) Western Europe, and (c) Bohai Sea Area in China and South Korea. Major rivers (in light blue) and states/provinces boundaries (in light gray) are shown for spatial reference. The color of the ellipses represents the mean ΣPFAS in that location, and ΣPFAS ranges (min-max) are also presented when available. Concentrations are expressed in ng L^{-1}.

3.3.2.1 The Americas

A total of 43 assessed studies were conducted across six countries in The Americas, with the majority focusing on surface water. ΣPFAS were observed to range from non-detect (n.d.) to 2,270 μg L^{-1} in surface water (median and mean of 25.1 ng L^{-1} and 1,714 ng L^{-1}, respectively). ΣPFAS in groundwater were higher than in any other continent, ranging from n.d. to 7,090 μg L^{-1} with a median of 3,628 ng L^{-1} and a mean of 257 μg L^{-1}. ΣPFAS in sediment ranged from n.d. to 183.8 ng gdw^{-1}, with a median of 6.1 ng gdw^{-1} and a mean of 14.6 ng gdw^{-1}. The distribution of PFAS in surface water in the United States is displayed in more detail in Figure 3.4a.

The United States has been a major producer and consumer of PFAS since the late 1940s. Although the US EPA has limited or phased out the production of many legacy PFAS (USEPA, 2019), short-chains and other PFAS alternatives are still being produced (Hopkins et al., 2018). Overall, 30 of the assessed studies investigated the distribution of PFAS in the United States between 1999 and 2021, associated with a wide variety of sources. The highest concentration of PFAS in surface water (31,906 ng L^{-1}) in the United States, observed near Decatur, Alabama, was related to the use of previously contaminated wastewater treatment plant (WWTP) biosolids as a soil amendment (Lindstrom et al., 2011a). Two other studies in that same region, published in 2002 and 2017, observed ΣPFAS up to 731 ng L^{-1} and 759 ng L^{-1}, respectively, in the Tennessee River downstream of fluorochemical industrial facilities (Hansen et al., 2002; Newton et al., 2017). Despite phase-out actions and regulations, PFOS and PFOA were still the major contaminants in the most recent study. The 2017 study also identified nine novel PFCAs in the Tennessee River and reported ΣPFAS concentration in sediments as high as 47 ng gdw^{-1}. Direct inputs from fluorochemical facilities were also the most likely primary source of PFAS contamination in the Cape Fear River, North Carolina, where Gen-X reached up to 4,560 ng L^{-1} (Nakayama et al., 2007; Sun et al., 2016). PFAS were also observed at high concentrations (up to 25,300 ng L^{-1}) in groundwater in Minnesota near a historical unlined disposal site that received waste from a fluorochemical facility (Xiao et al., 2015). Industrial effluents from textile facilities in Northwest Georgia were the primary sources of PFAS in the Conasauga

and Coosa rivers, in which ΣPFAS reached up to 1,770 ng L^{-1} in surface water and 39.2 ng gdw^{-1} in sediment (Konwick et al., 2008; Lasier et al., 2011). Multiple sources, including municipal WWTPs, military facilities, runoff, and snowmelt, were linked to PFAS in two urban watersheds in Nevada, in which ΣPFAS reached up to 203 ng L^{-1} in the Truckee River watershed and 592 ng L^{-1} in the Las Vegas Wash watershed. This study also detected ΣPFAS up to 183.8 and 134.2 ng gdw^{-1} in the Truckee River and Las Vegas Wash watersheds, respectively, the highest among all assessed studies in the United States (Bai and Son, 2021). Multiple, yet unspecified, sources were attributed to the relatively high levels (ΣPFAS up to 19.1 ng gdw^{-1}) of PFAS in estuarine sediments near Charleston, SC (White et al., 2015). Relatively low concentrations were detected in surface water and sediment samples of the Yadkin-Pee Dee River in North and South Carolinas (Penland et al., 2020) and sediment samples from Puget Sound, Washington (Long et al., 2013) and San Francisco Bay, California (Higgins et al., 2005).

PFAS, including cyclic PFAAs, were observed in the Great Lakes, with mean ΣPFAS ranging from 3.4 ng L^{-1} in Lake Superior to 107.7 ng L^{-1} in Lake Ontario (Boulanger et al., 2004; De Silva et al., 2011; Sinclair et al., 2006). Yeung et al. (2013) reported relatively high levels of PFAS in the sediments of Lake Ontario, with a mean ΣPFAS of 31.3 ng gdw^{-1} (Yeung et al., 2013). Nakayama et al. (2010) surveyed the Upper Mississippi River Basin and reported ΣPFAS up to 1,019 ng L^{-1} in surface water. The authors conducted a mass flux analysis and observed continuous increases in PFAS loading through the basin, indicating the presence of multiple sources (Nakayama et al., 2010). Several studies evaluated the distribution of PFAS in the Northeastern United States. Zhang et al. (2016) investigated the distribution of PFAS in several waterbodies in Rhode Island and New York, in which ΣPFAS reached 225.3 and 92.6 ng L^{-1}, respectively. This study identified three possible clusters of sources, including airports and textile facilities, atmospheric inputs, and metal smelting facilities (Zhang et al., 2016). High concentrations of PFAS (812.4 ng L^{-1}), especially PFOS and PFOA, were observed in Lake Onondaga (NY), a superfund site that receives inputs from several industries and WWTPs (Sinclair et al., 2006). Kim et al. (2007) evaluated several pathways of PFAS contamination in lakes in Albany (NY) and identified surface runoff and

snowfall/snowmelt as important vectors of PFAS in urban lakes (Kim and Kannan, 2007). ΣPFAS up to 174 ng L^{-1} were observed in raw drinking water in New Jersey in 2013, with AFFF, industrial facilities, and WWTP being the most probable sources (Post et al., 2013). A more recent study published in 2020 detected ΣPFAS up to 279.5 ng L^{-1} in the surface water and 30.9 ng gdw^{-1} in the sediment of several rivers in New Jersey (Goodrow et al., 2020).

The use and release of AFFF have been linked to high concentrations of PFAS in the United States, especially in groundwater near military bases and firefighting training facilities (Houtz et al., 2013; Moody and Field, 1999; Moody et al., 2003; Steele et al., 2018). For instance, ΣPFAS were detected at concentrations up to 7,090 µg L^{-1} at the Naval Air Station in Fallon, Nevada (Moody and Field, 1999), 1,478 µg L^{-1} near the Ellsworth Air Force Base in South Dakota (Houtz et al., 2013), 324 µg L^{-1} at Wurtsmith Air Force Base in Michigan (Moody et al., 2003), and 298 µg L^{-1} at Tyndall Air Force Base in Florida (Moody and Field, 1999). Substantially lower ΣPFAS up to 93.6 ng L^{-1} were detected at Pease Air Force Base in New Hampshire (Steele et al., 2018). Nonetheless, the impact of AFFF is not limited to groundwater. Aly et al. (2020) investigated the temporal and spatial distribution of PFAS in the Houston Ship Channel in Texas following a large-scale industrial fire incident in which 5 million liters of firefighting foams were used. This study observed ΣPFAS reaching 2,044 ng L^{-1} in the weeks following the fire, decreasing substantially within six months after the incident (Aly et al., 2020). Schwichtenberg et al. (2020) detected PFAS in nine pairs of foam and underlying bulk water samples at an AFFF-impacted lake in Michigan. Although ΣPFAS reached up to 108 µg L^{-1} in the foam samples, much lower ΣPFAS up to 203 ng L^{-1} were identified in the underlying bulk water (Schwichtenberg et al., 2020).

Nine assessed studies investigated the distribution of PFAS in the Canadian environment between 2002 and 2019. Notably, a study conducted by Moody et. al (2002) following an AFFF spill in 2000 that released 22,000 L of AFFF from the Toronto Airport into Etobicoke Creek. ΣPFAS reached up to 2,270 µg L^{-1}, the highest concentration yet reported in surface water (Moody et al., 2002). Awad et al. (2011) monitored ΣPFAS in the same creek from 2003 to 2009, and although a drop in the ΣPFAS was observed,

concentrations were still as high as 946.8 ng L^{-1} at the location closest to the spill (Awad et al., 2011). A more recent study reported the widespread occurrence of AFFF-related PFAS, including long-chain PFAAs precursors, in the Welland River area where a maximum ΣPFAS of 823.3 ng L^{-1} was observed (D'Agostino and Mabury, 2017). Relatively high concentrations of PFAS (mean ΣPFAS 5.3-106 ng gdw^{-1}) were also observed in sediments of Canadian Arctic lakes, thought to be related to atmospheric transport and localized inputs (Stock et al., 2007). MacInnis et al. (2019) explored the temporal variation of PFAS in sediment cores from Canadian Arctic lakes, in which exponential increases in the concentration of PFAS were observed over time. The authors observed higher fluxes in the sediments from a high Arctic lake when compared to a low Arctic lake, suggesting the release of PFAS from melting glaciers in the Arctic (MacInnis et al., 2019). D'eon et al. (2009) reported for the first time the presence of perfluorinated phosphonic acids, used in pesticides, in surface water, with urban and rural areas presenting similar levels (D'eon et al., 2009). Scott et al. (2009) sampled a variety of rivers and creeks throughout Canada and observed that levels of PFAAs increased downstream of highly populated areas, with PFOA, PFOS, and PFHxS being predominantly detected (Scott et al., 2009). Meyer et al. (2011) also detected higher PFAS concentrations in the more urbanized portion of the Highland Creek Watershed (Toronto), in which mean ΣPFAS of 37.1 ng L^{-1} were observed (Meyer et al., 2011).

In Latin America, PFAS were detected in surface water in Guadeloupe, Martinique, and French Guiana, where fluorochemical companies are not known to operate (Munoz et al., 2017). In Brazil, PFAS were detected at comparatively low levels, including in rural areas in the state of Bahia (ΣPFAS up to 8.9 ng L^{-1} in surface water and 0.32 ng gdw^{-1} in sediment) (Gilljam et al., 2016; Miranda et al., 2021; Nascimento et al., 2018), and in the heavily urbanized areas of Rio de Janeiro (ΣPFAS up to 3.8 ng L^{-1} in surface water) (Quinete et al., 2009). The presence of PFAS in agricultural areas is thought to be related to the use of the pesticide sulfluramid, which contains N-EtFOSA, a known PFOS and FOSA precursor (Gilljam et al., 2016). Brazil was among the biggest global consumers of PFOS-related compounds between

2003 and 2008 and is estimated to have used 30 tons per year of N-EtFOSA between 2004 and 2015 (Gilljam et al., 2016; Nascimento et al., 2018).

3.3.2.2 Europe

PFAS contamination has been investigated across 20 countries in Europe through 51 of the assessed studies. In surface water, ΣPFAS ranged from n.d. to 13,000 ng L^{-1}, with a median and a mean of 23.4 ng L^{-1} and 132.2 ng L^{-1}, respectively, considerably lower than in the Americas. Only two studies, both conducted in Sweden, evaluated ΣPFAS in European groundwater, ranging from n.d. to 51,040 ng L^{-1}, with a mean of 237.6 ng L^{-1}. Mean and median ΣPFAS in sediment were 16.0 and 5.2 ng gdw^{-1}, respectively, reaching up to 2,450 ng gdw^{-1}. The distribution of PFAS in surface water in Western Europe is displayed in more detail in Figure 3.4b.

In Spain, the maximum ΣPFAS in surface water was observed in the Llobregat River Basin near textile and tannery facilities (3,130 ng L^{-1}), with atmospheric deposition and urbanization thought to be additional potential sources (Campo et al., 2015). Lorenzo et al. (2016) reported mean ΣPFAS levels of 260.9 ng L^{-1} in surface water and 5.8 ng gdw^{-1} in sediments of the Guadalquivir River, where sources were related to textile and olive oil industries, WWTPs, and a military facility. The authors also identified ski waxes used at resorts as a source of PFAS in the Ebro River Basin, in which mean ΣPFAS of 51.9 ng L^{-1} and 7.8 ng gdw^{-1}, were observed in surface water and sediment, respectively (Lorenzo et al., 2016). ΣPFAS up to 217 ng L^{-1} were observed in the L'Albufera Natural Park, likely due to industrial and WWTPs inputs (Lorenzo et al., 2019; Pico et al., 2012). Campo et al. (2016) reported ΣPFAS up to 1,140 ng L^{-1} and 75.9 ng gdw^{-1} in surface water and sediment of the Jucar River Basin, respectively, with dams acting as potential sinks (Campo et al., 2016). The presence of PFAS in other Spanish waterbodies such as the Cantabrian Sea, Catalan Coast, Tagus River, and Ebro Delta was also investigated but mean ΣPFAS were relatively low (<12 ng L^{-1}) (Gomez et al., 2011; Navarro et al., 2020; Pignotti et al., 2017; Sanchez-Avila et al., 2010). Leon et al. (2020) also detected relatively low PFAS in sediment samples from four Spanish coastal regions, in which ΣPFAS did not exceed 0.4 ng gdw^{-1} (Leon et al., 2020).

In Italy, the highest concentration of PFAS in surface water was observed in the Po River basin, with ΣPFAS reaching up to 1,298 ng L^{-1} (mean 114.6 ng L^{-1}) (Loos et al., 2008). Similar levels (ΣPFAS up to 889 ng L-1) were observed in the Lambro River Basin, which discharges into the Po River, likely due to industrial discharges (Castiglioni et al., 2015), although a more recent study detected PFAS at concentrations below 40 ng L^{-1} (Castiglioni et al., 2018). Brumovsky et al. (2016) investigated the distribution of PFAS in the Western Mediterranean Sea and detected ΣPFAS ranging between 0.063 and 0.52 ng L^{-1}. This study found relatively similar concentrations in a deep-water sample, attributing this observation to water renewal through downwelling events (Brumovsky et al., 2016). Pignotti et al. (2018) investigated the partition of several endocrine disruptors, including PFAS, between water and sediment in the Romagna Area in Northern Italy. Although PFOS and PFOA were identified in surface water samples (mean ΣPFAS 14.7 ng L^{-1}), they were usually below detection limits in sediment samples (Pignotti and Dinelli, 2018).

Munoz et al. (2015) sampled 133 lakes and rivers as part of a National French Survey and observed ΣPFAS ranging from n.d. to 725 ng L^{-1} in surface water and from n.d. to 25 ng gdw^{-1} in sediment. The highest concentrations were observed near industrial and urban areas, and grain size and organic carbon were observed to affect PFAS levels in sediments (Munoz et al., 2015). A subset (n=12) of those samples was further analyzed to assess the presence of a wide array of analytes, including zwitterionic, cationic, and anionic PFAS in sediment, in which maximum ΣPFAS of 37.2 ng gdw^{-1} were observed (Munoz 2016). Schmidt et al. (2019) reported ΣPFAS up to 200 ng L^{-1} in the Rhone River, possibly from several textile facilities in that region (Schmidt et al., 2019). In England, samples from the Thames River were reported in two studies published in 2007 and 2018 as part of larger international sampling campaigns. Although mean ΣPFAS of 59.4 and 83.8 ng L^{-1} were reported in these studies, potential sources were not clearly identified (McLachlan et al., 2007; Pan et al., 2018). A nationwide survey of PFAS distribution in riverine sediments in the Czech Republic revealed ΣPFAS between 0.4 ng gdw^{-1} and 25.5 ng gdw^{-1}, potentially due to industrial inputs (Hlouskova et al., 2014). ΣPFAS up to 6.8 ng gdw^{-1} were observed in sediment samples

of an industrial area in the Morava River Catchment, in which seasonal variations were correlated to high flow events in the basin (Becanova et al., 2016).

Several studies investigated the distribution of PFAS in the Rhine River Basin, spanning several countries, including the Netherlands, France, Switzerland, and Germany. Moller et al. (2010) conducted a thorough survey of the watershed, from its headwaters to its discharge into the North Sea. This study reported ΣPFAS ranging between 0.35 and 621 ng L^{-1}, with a sharp increase after discharges from an industrial WWTP in the German city of Leverkusen. The highest ΣPFAS (621 ng L^{-1}) was found in the River Scheldt in Belgium, linked to industrial inputs, including a fluorochemical facility (Moller et al., 2010). Four other studies investigated the distribution of PFAS in the Rhine River basin as part of larger sampling campaigns and detected mean ΣPFAS between 24.2 and 47.1 ng L^{-1} (Heydebreck et al., 2015; Joerss et al., 2020; McLachlan et al., 2007; Pan et al., 2018). The Rhine River ultimately discharges into the North Sea, in which yearly ΣPFAS mass discharges of 17 tons were previously estimated (Moller et al., 2010). Other German rivers such as the Ems, Weser, and Elbe also discharge into the North Sea. ΣPFAS of 249 ng L^{-1} were reported at one sampling location along the Elbe River, which is believed to be related to an influx of PFBS from industrial waste (Zhao et al., 2015a). Mean ΣPFAS were generally below 25 ng L^{-1} in the Ems and Weser rivers (Ahrens et al., 2010a; Heydebreck et al., 2015; McLachlan et al., 2007; Zhao et al., 2015a). ΣPFAS up to 39.1 ng L^{-1} were detected near coastal areas in the North Sea (Heydebreck et al., 2015) but sharply decreased as seawater dilution increased (Ahrens et al., 2009b; Ahrens et al., 2010a; Heydebreck et al., 2015).

The highest ΣPFAS (6,758 ng L^{-1}) in surface water in Germany was detected in the Alz River, downstream from a fluorochemical facility. Interestingly, the perfluoroethers ADONA and HFPO-DA accounted for most of that concentration (Joerss et al., 2020). In the Netherlands, ΣPFAS up to 876 ng L^{-1} were detected near a fluorochemical plant (Gebbink et al., 2017). Gobelius et al. (2018) investigated the distribution of PFAS in Swedish surface and groundwater in 450 samples and reported high mean ΣPFAS of 110 ng L^{-1} and 49 ng L^{-1}, respectively, but much lower medians of 3.9 ng L^{-1} and 0.04 ng L^{-1}, indicating

considerable variability in the data. This study reported ΣPFAS up to 13,000 ng L^{-1} in surface water, the highest in Europe, which was attributed to discharges from firefighting training facilities (Gobelius et al., 2018). In fact, the use and release of AFFF is a significant source of PFAS in the Swedish environment. For instance, Mussabek et al. (2019) reported a maximum ΣPFAS of 1,700 ng L^{-1} in surface water and 76.0 ng gdw^{-1} in sediment near a firefighting training facility in northern Sweden (Mussabek et al., 2019), while Filipovic et al. (2015) reported ΣPFAS up to 51,040 ng L^{-1} in groundwater samples near a military airport (Filipovic et al., 2015). Koch et al. (2021) also reported a maximum ΣPFAS of 2,870 ng L^{-1} in a constructed wetland near the Ronneby Airport (Koch et al., 2021). Skaar et al. (2019) reported ΣPFAS up to 120 ng L^{-1} in surface water runoff samples near a firefighting training facility in the Norwegian Svalbard Islands, but much lower ΣPFAS (n.d.-13 ng L^{-1}) in marine and freshwater samples (Skaar et al., 2019). Langberg et al. (2020) examined historical discharges of PFAS into a freshwater lake in Southern Norway and detected ΣPFAS up to 2,450 ng gdw^{-1} in a sediment core, with the temporal profile matching the historical use of PFAS in the production of paper products(Langberg et al., 2020).

PFAS were detected in surface water samples in the Danube River in Austria (mean ΣPFAS 24.6 ng L^{-1}) (Clara et al., 2009), several waterbodies in Malta (mean ΣPFAS 10 ng L^{-1}) (Sammut et al., 2017) and Finland (mean ΣPFAS 7.1 ng L^{-1}) (Junttila et al., 2019), and in four freshwater lakes in the Faroe Islands (mean ΣPFAS 1.5 ng L^{-1}) (Eriksson et al., 2013). Waterbodies in other European countries, including the Vistula River in Poland, the Danube River in Romania, and the Daugava River in Latvia, were included in a European survey conducted by McLachlan et al. (2007) with ΣPFAS below 17 ng L^{-1} (McLachlan et al., 2007). PFAS were also identified in sediment from alpine lakes in Austria (Clara et al., 2009), the Gulf of Gdansk in Poland (Falandysz et al., 2012), and a wastewater canal in Serbia (Beskoski et al., 2013) with mean ΣPFAS were below 4 ng gdw^{-1}.

3.3.2.3 Asia

The highest number of the assessed studies was concentrated in Asia (n=116), encompassing ten countries, with the majority (n=85) in China. ΣPFAS ranged from n.d. to 659,889 ng L^{-1} in Asian surface

water, with a mean and a median of 2,457 ng L^{-1} and 44.4 ng L^{-1}, respectively, the highest global median levels. ΣPFAS reached up to 798.6 ng gdw^{-1} in sediment, the highest observed concentration globally, with a mean of 26.4 ng gdw^{-1} but a much lower median of 1.8 ng gdw^{-1}. In addition, ΣPFAS up to 26,700 ng L^{-1} were reported in groundwater, with a mean of 1,691 ng L^{-1} and a median of 61.6 ng L^{-1}.

Relatively high PFAS concentrations were observed on the West Coast of South Korea. So et al. (2004) reported ΣPFAS up to 1,120 ng L^{-1} in Gyeonggi Bay (So et al., 2004), while Rostkowski et al. (2006) and Naile et al. (2010) observed much lower concentrations in that area (Naile et al., 2010; Rostkowski et al., 2006). However, the 2006 study reported ΣPFAS up to 867.1 ng L^{-1} in the streams discharging into Lake Shihwa and Gyeonggi Bay (Rostkowski et al., 2006). This region of South Korea is highly industrialized, with steel, electrical, and petrochemical companies being the main industries (Rostkowski et al., 2006). ΣPFAS were also observed to decrease in Asan Lake from 695 ng L^{-1}, reported by Naile et al. (2010) to 94 ng L^{-1}, reported by Lee et al. (2020) (Lee et al., 2020b; Naile et al., 2010). Despite this decline, elevated ΣPFAS (467 ng L^{-1}) were observed in the Jinwi River, an Asan Lake tributary (Lee et al., 2020b). Mean ΣPFAS were generally lower in other parts of South Korea (Lam et al., 2016; Lee et al., 2020a; Seo et al., 2019; So et al., 2004), except in sediment samples from the Hyung-San River, in which maximum ΣPFAS of 85 ng gdw^{-1} were detected (Seo et al., 2019).

In India, low mean ΣPFAS of 8.9 ng L^{-1} and 10.1 ng L^{-1} were found in surface and groundwater, respectively, in the Ganges River Basin, despite increasing industrialization in recent years (Sharma et al., 2016). However, PFOA reached up to 14.1 ng gdw^{-1} in sediment samples from the Sundarban wetland, which receives inputs from the Ganges (Corsolini et al., 2012). In Thailand, low mean ΣPFAS of 9 and 1.2 ng L^{-1} were reported in the Chao Phraya and Bang Pakong rivers, respectively (Kunacheva et al., 2009). Duong et al. (2015) reported ΣPFAS between n.d. and 46 ng L^{-1} in several waterbodies in Vietnam, likely due to industrial and municipal inputs. This study also observed substantially higher ΣPFAS in the wet season, indicating that stormwater runoff might be an important vector of PFAS into the sampled waterways (Lam et al., 2017). Lam et al. (2017) conducted a nationwide survey of PFAS in major river basins in

Vietnam and detected ΣPFAS up to 107 ng L^{-1} in surface water and 23.4 ng gdw^{-1} in sediment, with PFOA being the predominant analyte in surface water and PFOS and PFHxS in sediment (Lam et al., 2017). Further, Kim et al. (2013) reported ΣPFAS up to 170 ng L^{-1} downstream of an electronic-waste recycling site in Bui Dau, Vietnam (Kim et al., 2013).

A nationwide survey of PFOS in 142 Japanese surface water samples was conducted by Saito et al. (2003), in which concentrations ranging from 0.2 to 25.2 ng L^{-1} were reported in coastal water samples and 0.3 to 157 ng L^{-1} in freshwater samples (Saito et al., 2003). Similarly, Murakami et al. (2008) surveyed 9 PFAS in 18 rivers, reporting ΣPFAS up to 315.7 ng L^{-1}. This study found a strong correlation between the levels of PFOS, PFHpA, and PFNA to those of a sewage marker, indicating these substances were most likely derived from sewage inputs. The same was not observed for PFOA, which had the highest individual concentration in this study (Murakami et al., 2008). PFOA also had the highest concentration in a survey of multiple rivers in the Kyoto City area, reaching up to 110 ng L^{-1} in surface water samples (Senthilkumar et al., 2007). The highest ΣPFAS (16,187 ng L^{-1}) in surface water in Japan was detected in the Samondogawa River, downstream of a fluororesin manufacturer. PFHxA accounted for most of the contamination (16,000 ng L^{-1}), indicating a possible shift towards PFOA alternatives (Takemine et al., 2014). Although mean ΣPFAS in surface water samples from Tokyo Bay were somewhat low (11.0-33.1 ng L^{-1}) (Benskin et al., 2010; Sakurai et al., 2010; Takazawa et al., 2009), Zushi et al. (2011) reported ΣPFAS up to 6,047 ng L^{-1} in the Chiba area, part of the Tokyo Bay Basin (Zushi et al., 2011). Benskin et al. (2010) detected high ΣPFAS (819.6 ng L^{-1}) in Tomakomai Bay, which were related to an AFFF spill event prior to sampling (Benskin et al., 2010).

While regulatory and voluntary phase-out actions are driving the development of novel fluorinated substances in some countries, an increase in the production volume of many legacy and novel PFAS has been observed in other countries (Shi et al., 2015; Zhu et al., 2015). For example, the production of PFOS-related chemicals in China increased from an estimated 30 tons in 2001 to more than 250 tons in 2006-2011 (Wang et al., 2015). As a result, some of the highest concentrations ever recorded in surface water and

sediment were detected in the Chinese environment. The majority of the assessed studies in China were concentrated in the coastal areas of the Bohai Sea and the Yellow Sea (Figures 3.3b and 3.4c). Several studies have linked fluorochemical facilities to extremely high PFAS concentrations in the Xiaoqing River. Mean ΣPFAS ranging from 13,133 ng L^{-1} to 121 μg L^{-1} were observed in this river, and maximum ΣPFAS in one of its tributary downstream of fluorochemical facilities reached 660 μg L^{-1} (Heydebreck et al., 2015; Pan et al., 2017; Shi et al., 2015; Song et al., 2018). PFAS were also detected in sediments of the Xiaoqing River, with a mean ΣPFAS of 555.8 ng gdw^{-1} (Song et al., 2018). Although PFOA was still the most detected PFAS in surface water in this area, novel PFAS including HFPO-DA and HFPO-TA, the latter detected for the first time in the environment, were also major components (Pan et al., 2017). The City of Fuxin, located on the northeastern side of the Bohai Sea, is home to several fluorochemical facilities attracted by the vast natural abundance of mineral fluorine in the area (Bao et al., 2011). A temporal increase in the concentration of PFAS in surface water was observed in this area, from a maximum ΣPFAS of 713 ng L^{-1} in 2009 (Bao et al., 2011) to over 54,000 ng L^{-1} in 2016 (Chen et al., 2018a). Although levels of various PFAS in environmental matrices substantially increased over time in this area, PFBS and PFBA were consistently the major PFAS in surface water (Bao et al., 2011; Chen et al., 2018a; Wang et al., 2015; Zhu et al., 2015). As a result of robust industrial activity in Fuxin, groundwater and sediment were also observed to be contaminated with high levels of PFAS, in which ΣPFAS reached up to 26,700 ng L^{-1} in groundwater (Bao et al., 2011; Bao et al., 2019; Chen et al., 2018a) and 370.2 ng gdw^{-1} in sediment (Bao et al., 2011; Chen et al., 2018a; Wang et al., 2015). Several studies also investigated the distribution of PFAS in the Yangtze River and detected highly variable mean ΣPFAS between 20 and 456 ng L^{-1} (Joerss et al., 2020; Pan et al., 2014a; Pan and You, 2010; Pan et al., 2018; So et al., 2007; Tan et al., 2018). The highest reported concentrations (ΣPFAS 2,622 ng L^{-1} in surface water and 536.7 ng gdw^{-1} in sediment) were detected downstream of a chemical park in Shanghai, near its discharge point to the Yellow Sea (Joerss et al., 2020; Pan and You, 2010). The distribution of PFAS in surface water and sediment in Taihu Lake near Shanghai has also been widely investigated (Chen et al., 2018b; Chen et al., 2015b; Guo et al., 2015; Ma et al., 2018; Pan et al., 2018; Yang et al., 2011; Yu et al., 2013). In addition to a variation in PFAS concentrations over

time (ΣPFAS 53-224.6 ng L^{-1} in surface water and 0.7-18.7 ng gdw^{-1} in sediment), a shift in the aqueous homologs was observed. Two independent studies conducted in 2009 reported PFOS and PFOA as the major PFAS (Qiu et al., 2010; Yang et al., 2011), while two studies conducted in 2015 reported a shift towards PFHxS (Chen et al., 2018b; Ma et al., 2018). Extremely high ΣPFAS up to 70,468 ng L^{-1} and 798.6 ng gdw^{-1} were observed in surface water and sediment, respectively, in Tangxun Lake south of Wuhan, most likely related to municipal and industrial inputs (Zhou et al., 2013).

Assessed studies in other regions of China had PFAS concentrations in environmental matrices much lower than the highly elevated concentrations noted above. For instance, mean ΣPFAS in sediment samples from the Huangpu River (Bao et al., 2010), Daliao River Basin (Bao et al., 2009), Bohai Sea (Chen et al., 2016a; Gao et al., 2014; Wang et al., 2011b), Pearl River Delta (Chen et al., 2019; Gao et al., 2015), Songhua River (Dong et al., 2018), Danjiangkou Reservoir (He et al., 2018), Huai River Basin (Meng et al., 2014), Liao River (Pan et al., 2015; Yang et al., 2011), Dongijang River (Pan et al., 2015) and Guanting Reservoir (Wang et al., 2011a) were below 1 ng gdw^{-1}. Similarly, low mean ΣPFAS between 0.6-11.1 ng L^{-1} were detected in coastal surface waters from Dalian Bay (Ding et al., 2018; Ju et al., 2008), Jiaozhou Bay (Han et al., 2020), Beibu Gulf (Pan et al., 2019), South China Sea (Wang et al., 2019a), and between 0.6-19.4 ng L^{-1} in freshwater samples from the Songhua River (Dong et al., 2018), Lake Chaohu (Liu et al., 2015b), Guanting Reservoir (Wang et al., 2011a), Pearl River Delta (Liu et al., 2015a; Zhang et al., 2013), and Tibet (Yamazaki et al., 2016).

3.3.2.4 Africa, Oceania, and Antarctica

As only eleven of the 228 assessed studies were conducted in Africa, Oceania, and Antarctica, information on the distribution of PFAS in these regions is limited. In the African continent, Ahrens et al. (2016) investigated the presence of PFAS in the surface water and sediments of Lake Tana in Ethiopia, where mean ΣPFAS of 2.9 ng L^{-1} and 0.3 ng gdw^{-1} were reported, respectively. The short-chains PFBA and PFHxA were the dominant PFAS in this study, linked to WWTPs inputs (Ahrens et al., 2016). PFOS and PFOA were found in the sediments of Lake Victoria in Kenya (maximum ΣPFAS of 146.4 ng gdw^{-1}), with

industrial and municipal waste identified as the major sources (Orata et al., 2011). As part of a French national survey, the presence of PFAS in the French territories of Reunion and Mayotte was investigated, revealing low mean ΣPFAS (1.1-6.2 ng L^{-1}) in surface water samples (Munoz et al., 2017). ΣPFAS up to 1,426 ng L^{-1} were found in the surface water of two South African estuaries, with PFOA and PFBA as the major analytes (Fauconier et al., 2020). Concentrations of PFOS and PFOA in three rivers in Cape Town (South Africa) averaged 69.5 ng L^{-1}, with a maximum concentration of 415.2 ng L^{-1}, most likely due to inputs from WWTPs and landfill leachate (Mudumbi et al., 2014). Groffen et al. (2018) reported ΣPFAS up to 122 ng L^{-1} near Johannesburg, South Africa (Groffen et al., 2018).

Thompson et al. (2011) reported mean ΣPFAS of 32.3 ng L^{-1} in surface water and 3.2 ng gdw^{-1} in sediment within Sydney Harbor in Australia. Given the absence of local point sources, the authors linked the observed PFAS contamination to either diffuse non-point sources or long-range transport (Thompson et al., 2011). Gallen et al. (2014) also detected PFAS in Moreton Bay near Brisbane after a major flood event, suggesting urban runoff as a possible source of the observed PFAS (Gallen et al., 2014). PFAS were also detected in Australian groundwater near historical landfills, with ΣPFAS reaching up to 5,200 ng L^{-1} (Hepburn et al., 2019). In the Antarctic region, Cai et al. (2012) reported mean ΣPFAS of 3.9 ng L^{-1} in surface water on King George Island (Shetland Islands, 65 miles north of the Antarctic Peninsula), attributed to inputs from a small WWTP and atmospheric transport (Cai et al., 2012). PFAS were also identified on Livingston Island (Shetland Islands), attributed to atmospheric and oceanic transport, since no local sources were identified (Casal et al., 2017).

3.3.3 Environmentally Relevant Concentrations

One goal of the work presented here is to address the lack of knowledge regarding ERCs of PFAS in a way that provides data-supported guidance for working with PFAS under controlled experimental conditions. Figure 3.5 illustrates the broad global range and distribution of ΣPFAS observed in surface water, groundwater, and sediment, based on overall means and maximum ΣPFAS from each assessed

study/location. Mean (50th percentile), 75th and 90th percentiles, minimum/maximum values, and outliers are shown for each category.

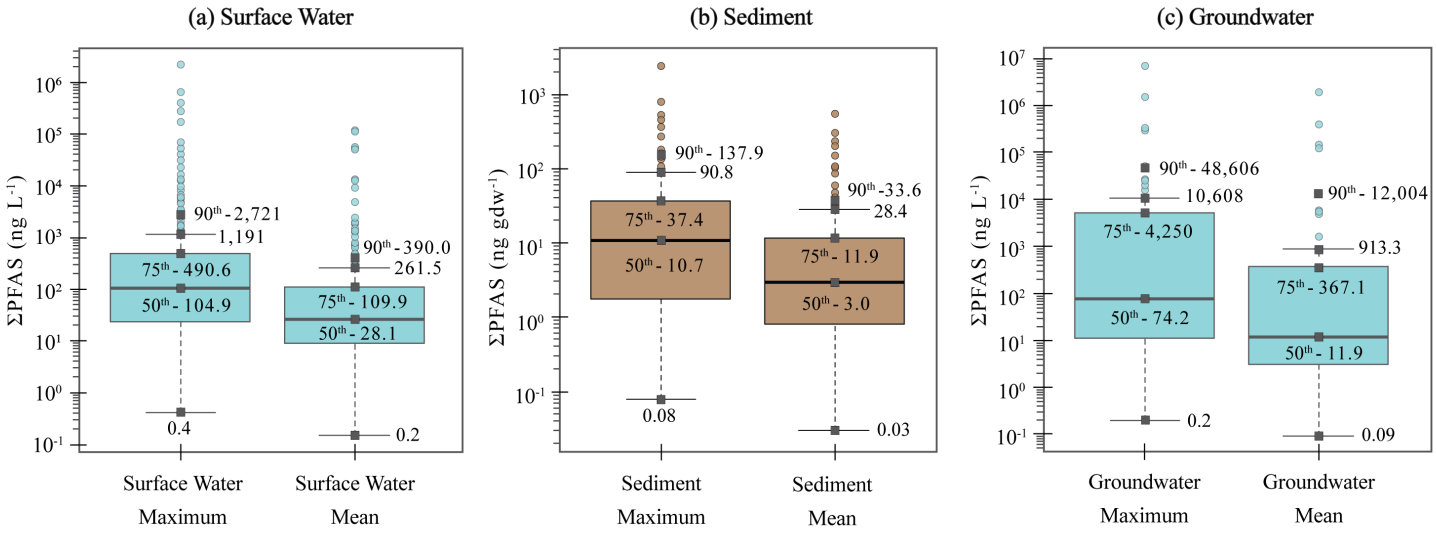

Figure 3.5 Distribution of ΣPFAS in (a) surface water, (b) sediment, and (c) groundwater. "Maximum" and "Mean" values were calculated based on maximum and mean ΣPFAS from each assessed study/location, respectively. The vertical axis is logarithmically scaled. Summary statistics, including median (50th percentile) and 75th and 90th percentiles, are presented for each plot. Whiskers represent the addition/subtraction of the respective quartile by 1.5 times the interquartile range.

For the observational dataset, mean ∑PFAS in surface water ranged from 0.2 ng L^{-1} to 121 µg L^{-1}, with a maximum ∑PFAS of 2,270 µg L^{-1}. Overall ∑PFAS in surface water averaged 1,509 ng L^{-1} and 16,891 ng L^{-1} based on mean and maximum total concentrations, respectively. Most ∑PFAS in surface water were observed to be below 1,192 ng L^{-1}. In fact, 75% of the concentrations were below 490.6 ng L^{-1} for maximum and 109.9 ng L^{-1} for mean ∑PFAS. Although median ∑PFAS in groundwater were lower than in surface water, average ∑PFAS were higher (222 µg L^{-1} for maximum and 60 µg L^{-1} for mean total concentrations). Maximum levels were also much higher in groundwater: 7,090 µg L^{-1} and 1,908 µg L^{-1}, based on maximum and mean total concentrations. The third quartile was also higher in groundwater (4,250 ng L^{-1} for maximum and 367.1 ng L^{-1} for mean total concentrations). In sediments, ∑PFAS usually did not

exceed 90.8 ng gdw^{-1} and 28.4 ng gdw^{-1}, based on maximum and mean concentrations, respectively. The results of this study provide observational data-supported ERCs for ∑PFAS (Table 3.1). When working with PFAS in controlled experiments, ∑PFAS not exceeding the 90th percentile (i.e., within 90% of previously observed concentrations) assure environmental relevance. Thus, maximum ERCs should not exceed 2,721 ng L^{-1} and 48,606 ng L^{-1} in studies evaluating ∑PFAS in surface water and groundwater, respectively, and 137.9 ng gdw^{-1} in sediment (Table 3.1).

Table 3.1 Mean, median (50th percentile), and 75th and 90th percentiles based on overall means and maximum ΣPFAS from each assessed study/location. It is recommended that ∑PFAS does not exceed the 90th percentile (i.e., within 90% of previously observed concentrations) in controlled studies to ensure environmental relevance.

Matrix	Mean	50th	75th	90th
Surface Water (ng L^{-1})				
Mean ∑PFAS	1,509	28.1	109.2	390.0
Max. ∑PFAS	16,891	104.9	490.6	2,721
Sediment (ng gdw^{-1})				
Mean ∑PFAS	20.9	3.0	11.9	33.6
Max. ∑PFAS	78.9	10.7	37.4	137.9
Groundwater (ng L^{-1})				
Mean ∑PFAS	60,479	11.9	367.1	12,004
Max. ∑PFAS	222,479	74.2	4,250	48,606

It is important to emphasize that the ERCs noted above are based on ∑PFAS in a given environmental matrix, not the concentration of an individual PFAS analyte. In the assessed studies, ∑PFAS were based on an average of ten individual, quantified PFAS analytes in surface water and nine in groundwater and sediment. Moreover, in the assessed studies, the number of individual PFAS analytes was not generally directly related to the total ∑PFAS concentration. To investigate concentrations of individual PFAS, information on the individual concentrations of the most frequently targeted analytes in each media was also extracted from each study, when available (Figure 3.6). In surface water, PFOS ranged from n.d. to 2,210 µg L^{-1} with the highest mean (1,525 ng L^{-1}), followed by PFOA (mean 841.7 ng L^{-1} and maximum 579 µg L^{-1}) and PFHxS (mean 141.2 ng L^{-1} and maximum 134 µg L^{-1}). PFOS also had the highest mean in sediment of 3.9 ng gdw^{-1} (n.d.-623 ng gdw^{-1}), followed by PFBS (mean 1.5 ng gdw^{-1} and maximum 114 ng

gdw^{-1}) and PFBA (mean 1.4 ng gdw^{-1} and maximum 84 ng gdw^{-1}). The fact that PFBS and PFBA had some of the highest mean concentrations of PFAS in sediment is surprising, as short-chain PFAS are generally more hydrophilic than their longer-chain homologs (Higgins and Luthy, 2006). In groundwater, PFOA had the highest mean concentration of 8,045 ng L^{-1} (n.d.- 6,570 µg L^{-1}), while PFHxA and 6:2 FTS came next with mean concentrations of 5,510 ng L^{-1} (n.d.- 372 µg L^{-1}) and 5,064 ng L^{-1} (n.d.- 270 µg L^{-1}), respectively.

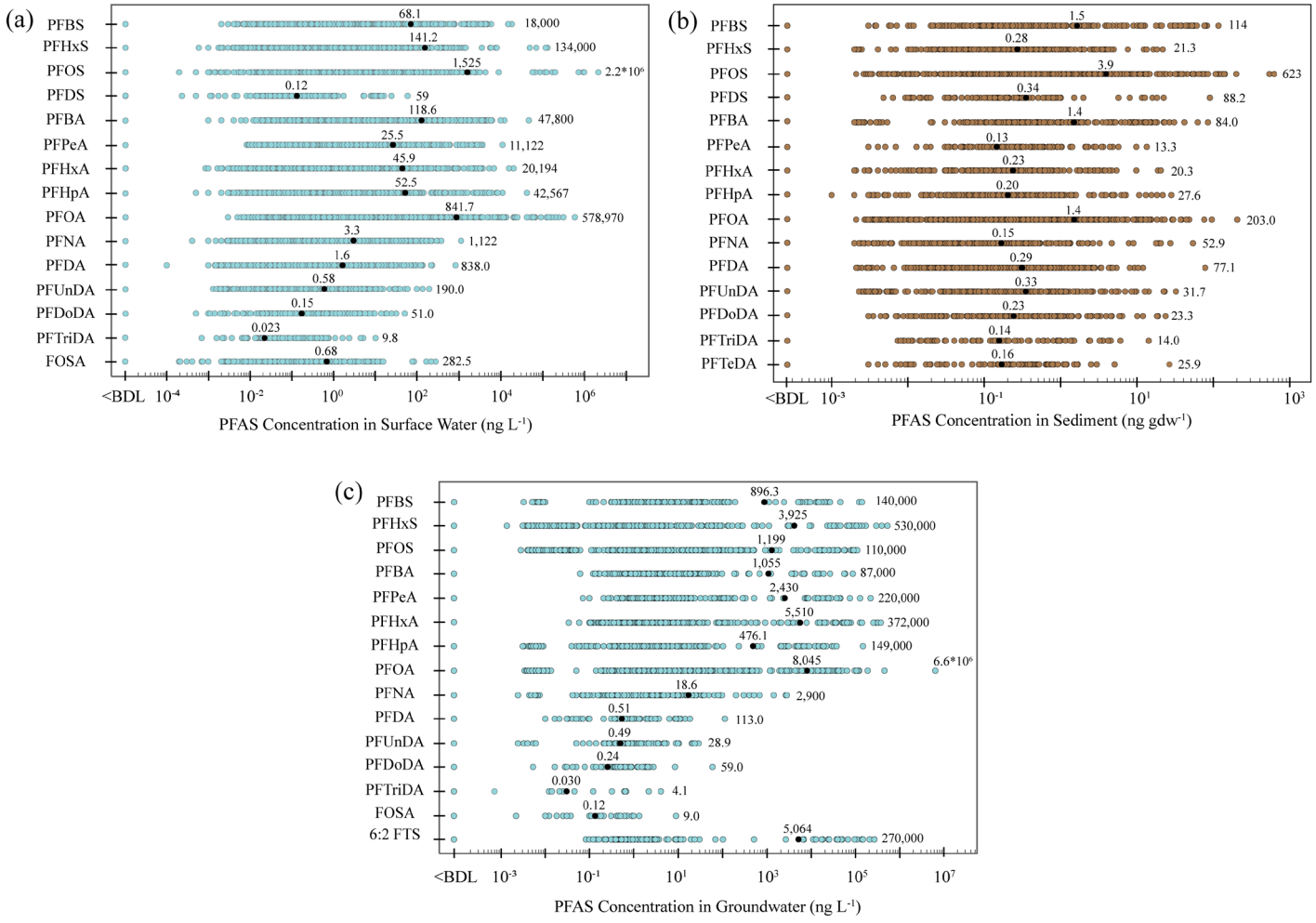

Figure 3.6. Overall concentrations of the 15 most detected PFAS in (a) surface water, (b) sediment, and (c) groundwater based on assessed studies. Mean and maximum concentrations are displayed for each analyte.

The assessed studies demonstrate the global extent of PFAS contamination and provide several key insights that can help guide future PFAS research. Many developing countries have a limited number of studies despite increasing industrial activity and urbanization, which suggests that the extent of PFAS contamination in these countries remains largely unknown. Legacy PFAS comprise the bulk of PFAS observed in the assessed studies and are likely to remain in the environment for a considerable amount of time regardless of reductions in production and use. However, novel (emerging) PFAS such as HFPO-DA, HFPO-TA, F-53B, 6:2 FTS, TFA, PFPrA, and FHxSA were also identified as major contributors to PFAS contamination in many of the assessed studies (Chen et al., 2018a; Pan et al., 2017; Pan et al., 2018). Thus, future studies must keep pace with the changes in PFAS manufacturing and use. While re-sampling areas where PFAS were previously detected is important to understand the temporal variation of PFAS concentrations and profile, locations with no existing PFAS data should be prioritized to better understand the true scope of PFAS pollution worldwide. Additionally, developing new methods for identifying sources of PFAS in the environment (for example, isomer profiling) is necessary. Finally, the ERCs provided here based on an assessment of observational PFAS studies can be used in the design of controlled experiments considering the environmental behavior and fate of PFAS, as well as the effects of PFAS exposure on humans and wildlife.

3.4 Supporting Information

Table 3.2. List of analytes targeted in the assessed studies. Analytes were classified into subgroups based on information presented in their respective studies, nomenclature suggested by Buck et al. (2011), and available information in the CompTox database (Williams et al., 2017).

Perfluoroalkyl Acids (PFAAs)				
Subgroup	(n,m)	Analyte	Name	Molecular Formula
Perfluoroalkyl Sulfonic Acids (PFSAs)	2	PFEtS	Perfluoroethanesulfonic acid	$C_2F_5(SO_3H)$
	3	PFPrS	Perfluoropropanesulfonic acid	$C_3F_7(SO_3H)$
	4	PFBS	Perfluorobutanesulfonic acid	$C_4F_9(SO_3H)$
	5	PFPeS	Perfluoropentanesulfonic acid	$C_5F_{11}(SO_3H)$

	6	PFHxS	Perfluorohexanesulfonic acid	$C_6F_{13}(SO_3H)$
	7	PFHpS	Perfluoroheptanesulfonic acid	$C_7F_{15}(SO_3H)$
	8	PFOS	Perfluorooctanesulfonic acid	$C_8F_{17}(SO_3H)$
	9	PFNS	Perfluorononanesulfonic acid	$C_9F_{19}(SO_3H)$
	10	PFDS	Perfluorodecanesulfonic acid	$C_{10}F_{21}(SO_3H)$
	12	PFDoS	Perfluorododecanesulfonic acid	$C_{12}F_{25}(SO_3H)$
Perfluoroalkyl Carboxylic Acids (PFCAs)	2	TFA	Trifluoroacetic Acid	$CF_3(COOH)$
	3	PFPrA	Perfluoropropanoic acid	$C_2F_5(COOH)$
	4	PFBA	Perfluorobutanoic acid	$C_3F_7(COOH)$
	5	PFPeA	Perfluoropentanoic acid	$C_4F_9(COOH)$
	6	PFHxA	Perfluorohexanoic acid	$C_5F_{11}(COOH)$
	7	PFHpA	Perfluoroheptanoic acid	$C_6F_{13}(COOH)$
	8	PFOA	Perfluorooctanoic acid	$C_7F_{15}(COOH)$
	9	PFNA	Perfluorononanoic acid	$C_8F_{17}(COOH)$
	10	PFDA	Perfluorodecanoic acid	$C_9F_{19}(COOH)$
	11	PFUnDA	Perfluoroundecanoic acid	$C_{10}F_{21}(COOH)$
	12	PFDoDA	Perfluorododecanoic acid	$C_{11}F_{23}(COOH)$
	13	PFTrDA	Perfluorotridecanoic acid	$C_{12}F_{25}(COOH)$
	14	PFTeDA	Perfluorotetradecanoic acid	$C_{13}F_{27}(COOH)$
	15	PFPeDA	Perfluoropentadecanoic acid	$C_{14}F_{29}(COOH)$
	16	PFHxDA	Perfluorohexadecanoic acid	$C_{15}F_{31}(COOH)$
	17	PFHpDA	Perfluoroheptadecanoic acid	$C_{16}F_{33}(COOH)$
	18	PFODA	Perfluorooctadecanoic acid	$C_{17}F_{35}(COOH)$
Perfluoroalkyl Phosphonic Acids (PFPAs)	4	PFBPA	Perfluorobutylphosphonic acid	$C_4F_9(P=O)(OH)_2$
	6	PFHxPA	Perfluorohexylphosphonic acid	$C_6F_{13}(P=O)(OH)_2$
	8	PFPFOA	Perfluorooctylphosphonic acid	$C_8F_{17}(P=O)(OH)_2$
	10	PFDPA	Perfluorodecylphosphonic acid	$C_{10}F_{21}(P=O)(OH)_2$
Perfluoroalkyl Phosphinic Acids (PFPIAs)	6,6	C6/C6 PFPiA	Bis(Perfluorohexyl) phosphinic acid	$C_6F_{13}(P=O)(OH)(C_6F_{13})$
	6,8	C6/C8 PFPiA	Perfluorohexylperfluorooctyl phosphinic acid	$C_6F_{13}(P=O)(OH)(C_8F_{17})$
	8,8	C8/C8 PFPiA	Bis(Perfluorooctyl) phosphinic acid	$C_8F_{17}(P=O)(OH)(C_8F_{17})$
Cyclic PFAAs	8	PFPCPeS	Perfluoropropylcyclopentane sulfonate	$C_5F_8C_3F_7SO_3$
	8	PFECHS	Perfluoro-4-ethylcyclohexane sulfonate	$C_6F_{10}C_2F_5SO_3$
	7	PFMeCHS	Perfluoromethylcyclohexane sulfonate	$C_6F_{10}CF_3SO_3$
Perfluoroalkane Sulfonamido Substances				

Subgroup	(n,m)	Analyte	Name	Molecular Formula
Perfluoroalkane Sulfonamides (FASAs)	4	FBSA	Perfluorobutane sulfonamide	$C_4F_9(SO_2NH_2)$
	6	FHxSA	Perfluorohexanesulfonamide	$C_6F_{13}(SO_2NH_2)$
	8	FOSA	Perfluorooctanesulfonamide	$C_8F_{17}(SO_2NH_2)$
N-Alkyl Perfluoroalkane Sulfonamides (N-FASAs)	4,1	N-Me-FBSA	N-Methylperfluorobutane sulfonamide	$C_4F_9SO_2NHCH_3$
	8,1	N-Me-FOSA	N-Methylperfluorooctane sulfonamide	$C_8F_{17}SO_2NHCH_3$
	8,2	N-Et-FOSA	N-Ethylperfluorooctane sulfonamide	$C_8F_{17}SO_2NHC_2H_5$
Perfluoroalkane Sulfonamidoacetic Acids (FASAAs)	8	FOSAA	Perfluorooctanesulfonamidoacetic acid	$C_8F_{17}SO_2NH(CH_2)(C=O)(OH)$
N-Alkyl Perfluoroalkane Sulfonamidoacetic Acids (N-FASAAs)	8,1	N-Me-FOSAA	2-(N-Methylperfluorooctane sulfonamido)acetic acid	$C_8F_{17}SO_2NCH_3(CH_2)(C=O)(OH)$
	8,2	N-Et-FOSAA	2-(N-Ethylperfluorooctane sulfonamido)acetic acid	$C_8F_{17}SO_2NC_2H_5(CH_2)(C=O)(OH)$
N-Alkyl Perfluoroalkane Sulfonamidoethanols (N-FASE)	4,1	N-Me-FBSE	N-methylperfluorobutane sulfonamidoethanol	$C_4F_9SO_2NCH_3C_2H_4OH$
	8,1	N-Me-FOSE	N-Methylperfluorooctane sulfonamidoethanol	$C_8F_{17}SO_2NCH_3C_2H_4OH$
	8,2	N-Et-FOSE	N-Ethylperfluorooctane sulfonamidoethanol	$C_8F_{17}SO_2NC_2H_5C_2H_4OH$
Perfluoroalkane Sulfonamido Alkalamine Diacids (FASADAs)	3	C3 FASADA	C3 Perfluoroalkane Sulfonamido Alkalamine Diacid	$C_3F_7SO_2(N_2C_{11}H_{22}O_4)$
	4	C4 FASADA	C4 Perfluoroalkane Sulfonamido Alkalamine Diacid	$C_4F_9SO_2(N_2C_{11}H_{22}O_4)$
	5	C5 FASADA	C5 Perfluoroalkane Sulfonamido Alkalamine Diacid	$C_5F_{11}SO_2(N_2C_{11}H_{22}O_4)$
	6	C6 FASADA	C6 Perfluoroalkane Sulfonamido Alkalamine Diacid	$C_6F_{13}SO_2(N_2C_{11}H_{22}O_4)$
Perfluoroalkane Sulfonamido Alkalamine Acids (FASAAs)	3	C3 FASAA	C3 Perfluoroalkane Sulfonamido Alkalamine Acid	$C_3F_7SO_2(N_2C_8H_{18}O_2)$
	4	C4 FASAA	C4 Perfluoroalkane Sulfonamido Alkalamine Acid	$C_4F_9SO_2(N_2C_8H_{18}O_2)$
	5	C5 FASAA	C5 Perfluoroalkane Sulfonamido Alkalamine Acid	$C_5F_{11}SO_2(N_2C_8H_{18}O_2)$
	6	C6 FASAA	C6 Perfluoroalkane Sulfonamido Alkalamine Acid	$C_6F_{13}SO_2(N_2C_8H_{18}O_2)$
Perfluoroalkane Sulfonamido Alkylbetaines (FASABs)	5	C5 FASAB	C5 Perfluoroalkane Sulfonamido Alkylbetaine	$C_5F_{11}SO_2(N_2C_8H_{18}O_2)$
	6	C6 FASAB	C6 Perfluoroalkane Sulfonamido Alkylbetaine	$C_6F_{13}SO_2(N_2C_8H_{18}O_2)$
Perfluoroalkane Sulfonamido Amines (PFnSAm)	4	PFBSAm	Perfluorobutane Sulfonamido Amine	$C_4F_9SO_2(N_2C_5H_{14})$
	5	PFPeSAm	Perfluoropentane Sulfonamido Amine	$C_5F_{11}SO_2(N_2C_5H_{14})$

	6	PFHxSAm	Perfluorohexane Sulfunamido Amine	$C_6F_{13}SO_2(N_2C_5H_{14})$
Fluorotelomer Substances				
Subgroup	(n,m)	Analyte	Name	Molecular Formula
Fluorotelomer Betaines (FTBs)	5,1,2	5:1:2 FTB	5:1:2 Fluorotelomer Betaine	$C_5F_{11}C_3FH_5(NC_4H_9O_2)$
	7,1,2	7:1:2 FTB	7:1:2 Fluorotelomer Betaine	$C_7F_{15}C_3FH_5(NC_4H_9O_2)$
	9,1,2	9:1:2 FTB	9:1:2 Fluorotelomer Betaine	$C_9F_{19}C_3FH_5(NC_4H_9O_2)$
	5,3	5:3 FTB	5:3 Fluorotelomer Betaine	$C_5F_{11}C_3H_6(NC_4H_9O_2)$
	7,3	7:3 FTB	7:3 Fluorotelomer Betaine	$C_7F_{15}C_3H_6(NC_4H_9O_2)$
	9,3	9:3 FTB	9:3 Fluorotelomer Betaine	$C_9F_{19}C_3H_6(NC_4H_9O_2)$
Fluorotelomer Sulfonamide Alkylbetaines (FTABs)	4,2	4:2 FTAB	4:2 Fluorotelomer Sulfonamide Alkylbetaine	$C_4F_9C_2H_4SO_2(N_2C_7H_{16}O_2)$
	6,2	6:2 FTAB	6:2 Fluorotelomer Sulfonamide Alkylbetaine	$C_6F_{13}C_2H_4SO_2(N_2C_7H_{16}O_2)$
	8,2	8:2 FTAB	8:2 Fluorotelomer Sulfonamide Alkylbetaine	$C_8F_{17}C_2H_4SO_2(N_2C_7H_{16}O_2)$
	10,2	10:2 FTAB	10:2 Fluorotelomer Sulfonamide Alkylbetaine	$C_{10}F_{21}C_2H_4SO_2(N_2C_7H_{16}O_2)$
	12,2	12:2 FTAB	12:2 Fluorotelomer Sulfonamide Alkylbetaine	$C_{12}F_{25}C_2H_4SO_2(N_2C_7H_{16}O_2)$
Fluorotelomer Alcohols (FTOHs)	4,2	4:2 FTOH	4:2 Fluorotelomer alcohol	$C_4F_9C_2H_4(OH)$
	6,2	6:2 FTOH	6:2 Fluorotelomer alcohol	$C_6F_{13}C_2H_4(OH)$
	8,2	8:2 FTOH	8:2 Fluorotelomer alcohol	$C_6F_{13}C_2H_4(OH)$
	10,2	10:2 FTOH	10:2 Fluorotelomer alcohol	$C_6F_{13}C_2H_4(OH)$
	4,3	4:3 FTOH	4:3 Fluorotelomer alcohol	$C_4F_9C_3H_6(OH)$
	6,3	6:3 FTOH	6:3 Fluorotelomer alcohol	$C_6F_{13}C_3H_6(OH)$
	8,3	8:3 FTOH	8:3 Fluorotelomer alcohol	$C_8F_{17}C_3H_6(OH)$
Fluorotelomer carboxylic acids (FTCAs)	6,2	6:2 FTCA	6:2 Fluorotemer carboxylic acid	$C_6F_{13}CH_2(COOH)$
	8,2	8:2 FTCA	8:2 Fluorotemer carboxylic acid	$C_8F_{17}CH_2(COOH)$
	10,2	10:2 FTCA	10:2 Fluorotemer carboxylic acid	$C_{10}F_{21}CH_2(COOH)$
	3,3	3:3 FTCA	3:3 Fluorotemer carboxylic acid	$C_3F_7C_2H_4(COOH)$
	5,3	5:3 FTCA	5:3 Fluorotemer carboxylic acid	$C_5F_{11}C_2H_4(COOH)$
	7,3	7:3 FTCA	7:3 Fluorotemer carboxylic acid	$C_7F_{15}C_2H_4(COOH)$
Fluorotelomer Unsaturated Carboxilic Acids (FTUCAs)	6,2	6:2 FTUCA	6:2 Fluorotelomer unsaturated acid	$C_5F_{11}CF{=}CH(COOH)$
	8,2	8:2 FTUCA	8:2 Fluorotelomer unsaturated acid	$C_7F_{15}CF{=}CH(COOH)$
	10,2	10:2 FTUCA	10:2 Fluorotelomer unsaturated acid	$C_9F_{19}CF{=}CH(COOH)$
Fluorotelomer Sulfonates (FTSs)	4,2	4:2 FTS	4:2 Fluorotelomer sulfonate	$C_4F_9C_2H_4(SO_3H)$
	6,2	6:2 FTS	6:2 Fluorotelomer sulfonate	$C_6F_{13}C_2H_4(SO_3H)$

	8,2	8:2 FTS	8:2 Fluorotelomer sulfonate	$C_8F_{17}C_2H_4(SO_3H)$
	10,2	10:2 FTS	10:2 Fluorotelomer sulfonate	$C_{10}F_{21}C_2H_4(SO_3H)$
	12,2	12:2 FTS	12:2 Fluorotelomer sulfonate	$C_{12}F_{25}C_2H_4(SO_3H)$
	14,2	14:2 FTS	14:2 Fluorotelomer sulfonate	$C_{14}F_{29}C_2H_4(SO_3H)$
Fluorotelomer Iodides	6,2	6:2 FTI	6:2 Fluorotelomer iodide	$C_6F_{13}C_2H_4(I)$
	8,2	8:2 FTI	8:2 Fluorotelomer iodide	$C_8F_{17}C_2H_4(I)$
	10,2	10:2 FTI	10:2 Fluorotelomer iodide	$C_{10}F_{21}C_2H_4(I)$
Fluorotelomer thioamido Sulfonates (FtTAoSs)	4,2	4:2 FtTAoS	4:2 Fluorotelomer Thioamido Sulfonate	$C_4F_9C_2H_4(C_7H_{14}NSO_4)$
	6,2	6:2 FtTAoS	6:2 Fluorotelomer Thioamido Sulfonate	$C_6F_{13}C_2H_4(C_7H_{14}NSO_4)$
	8,2	8:2 FtTAoS	8:2 Fluorotelomer Thioamido Sulfonate	$C_8F_{17}C_2H_4(C_7H_{14}NSO_4)$
Fluorotelomer Sulfonamido Betaines (FtSaBs)	6,2	6:2 FtSaB	6:2 Fluorotelomer Sulfonamido Betaine	$C_6F_{13}C_2H_4(C_7H_{16}N_2SO_4)$
	8,2	8:2 FtSaB	8:2 Fluorotelomer Sulfonamido Betaine	$C_8F_{17}C_2H_4(C_7H_{16}N_2SO_4)$
	10,2	10:2 FtSaB	10:2 Fluorotelomer Sulfonamido Betaine	$C_{10}F_{21}C_2H_4(C_7H_{16}N_2SO_4)$
	12,2	12:2 FtSaB	12:2 Fluorotelomer Sulfonamido Betaine	$C_{12}F_{25}C_2H_4(C_7H_{16}N_2SO_4)$
Fluorotelomer Sulfonamido Amines (FtSaAms)	6,2	6:2 FtSaAm	6:2 Fluorotelomer Sulfonamido Amine	$C_6F_{13}C_2H_4(C_5H_{14}N_2SO_2)$
	8,2	8:2 FtSaAm	8:2 Fluorotelomer Sulfonamido Amine	$C_8F_{17}C_2H_4(C_5H_{14}N_2SO_2)$
Fluorotelomer Phosphate Monoesters (monoPAPs)	6,2	6:2 monoPAP	6:2 Fluorotelomer phosphate monoester	$C_6F_{13}C_2H_4(POO(OH)_2)$
	8,2	8:2 monoPAP	8:2 Fluorotelomer phosphate monoester	$C_8F_{17}C_2H_4(POO(OH)_2)$
Fluorotelomer phosphate diesters	6,2	6:2 diPAP	6:2 Fluorotelomer phosphate diester	$(C_6F_{13}C_2H_4)_2(POOOH)$
	8,2	8:2 diPAP	8:2 Fluorotelomer phosphate diester	$(C_8F_{17}C_2H_4)_2(POOOH)$
	10,2	10:2 diPAP	10:2 Fluorotelomer phosphate diester	$(C_{10}F_{21}C_2H_4)_2(POOOH)$
Fluorotelomer Sulfonamide Alkylamine	6	6:2 FTAA	6:2 Fluorotelomer Sulfonamide Alkylamine	n.a.
Fluorotelomer Mercaptoalkylamido Sulfonate	6	6:2 FTSAS-SO_2	6:2 Fluorotelomer Mercaptoalkylamido Sulfonate	n.a.
Fluorotelomer Thiohydroxylammonium Sulfoxide	6	6:2 FTSAS-SO	6:2 Fluorotelomer Thiohydroxylammonium Sulfoxide	n.a.
Fluorotelomer ThioHydroxyAmmonium	6	6:2 FtTHN+	6:2 Fluorotelomer ThioHydroxyAmmonium	n.a.
Perfluoroalkyl Ether Acids				
Subgroup	(n,m)	Analyte	Name	Molecular Formula
Chlorine-Substituted Perfluoroether Sulfonic Acids (Cl-PFESAs)	6	4:2 Cl-PFESA	4:2 chlorinated polyfluorinated ether sulfonate	$C_6F_{12}Cl(SO_4)$
	8	6:2 Cl-PFESA	6:2 chlorinated polyfluorinated ether sulfonate	$C_8F_{16}Cl(SO_4)$

	10	8:2 Cl-PFESA	8:2 chlorinated polyfluorinated ether sulfonate	$C_{10}F_{20}Cl(SO_4)$
	12	10:2 Cl-PFESA	10:2 chlorinated polyfluorinated ether sulfonate	$C_{12}F_{24}Cl(SO_4)$
Perfluoroether Carboxylic Acids (PFECAs)	5	HFPO-DA	Hexafluoropropylene Oxide-dimer Acid	$C_5F_{11}O(COOH)$
	8	HFPO-TA	Hexafluoropropylene Oxide-Trimer Acid	$C_8F_{17}O_2(COOH)$
	11	HFPO-TeA	Perfluoro (2, 5, 8-trimethyl-3, 6, 9-trioxadecanoic)	$C_{11}F_{23}O_3(COOH)$
	6	ADONA	Dodecafluoro-3H-4,8-dioxanonanoate	$C_6HF_{12}O_2(COOH)$
	2	PFMOAA	Perfluoro-2-methoxyacetic acid	$C_2F_5O(COOH)$
	3	PFMOPrA	Perfluoro-3-methoxypropanoic acid	$C_3F_7O(COOH)$
	4	PFMOBA	Perfluoro-4-methoxybutanoic acid	$C_4F_9O(COOH)$
	3	PFO2HxA	Perfluoro(3,5-dioxahexanoic) acid	$C_3F_7O_2(COOH)$
	4	PFO3OA	Perfluoro(3,5,7-trioxaoctanoic) acid	$C_4F_9O_3(COOH)$
	5	PFO4DA	Perfluoro(3,5,7,9-tetraoxadecanoic) acid	$C_5F_{11}O_4(COOH)$
Miscellaneous				
Subgroup	(n,m)	Analyte	Name	Molecular Formula
Perfluoroalkyl Iodides	12	PFDoI	Perfluorododecyl iodide	$C_{12}F_{25}(I)$
Perfluoroalkyl Diiodides	4	PFBuDiI	Octafluoro-1,4-diiodobutane	$(I)C_4F_9(I)$
	6	PFHxDiI	Dodecafluoro-1,6-diiodohexane	$(I)C_6F_{13}(I)$
	8	PFODiI	Hexadecafluoro-1,8-diiodooctane	$(I)C_8F_{17}(I)$
Cationic and Zwitterionic	n.a.	PFOAB	2-(dimethyl(3-(perfluorooctanamido) propyl)ammonio) acetate	$C_{15}H_{15}F_{15}N_2O_3$
	n.a.	PFOSB	2-(dimethyl(3-(perfluorooctylsulfonamido) propyl)ammonio) acetate	$C_{15}H_{15}F_{17}N_2O_4S$
	n.a.	PFOANO	N,N-dimethyl-3-(perfluorooctanamido) propan-1-amine oxide	$C_{13}H_{13}F_{15}N_2O_2$
	n.a.	PFOSNO	N,N-dimethyl-3-(perfluorooctylsulfonamido)propan-1-amine oxide	$C_{13}H_{13}F_{17}N_2O_3S$
	n.a.	PFOSAmS	N,N,N-trimethyl-3-(perfluorooctylsulfonamido)propan-1-aminium	$C_{14}H_{16}F_{17}N_2O_2S^+$
	n.a.	PFOAAmS	N,N,N-trimethyl-perfluorooctanamido)propan-1-aminium	$C_{14}H_{16}F_{15}N_2O^+$
	n.a.	PFOSAm	N-(3-(Dimethylamino)propyl)-perfluorooctane-1-sulfonamide	$C_{13}H_{13}F_{17}N_2O_2S$

n.a. – information not available

Table 3.3. Summary Statistics (range, mean, median, and number of studies) for the distribution of PFAS in Surface Water (ng L^{-1}) by country.

The Americas					
Country	Min	Max	Mean	Median	Number of Studies
Brazil	n.d.	8.9	2.2	2.5	3
Canada	n.d.	2,270,000	4,573	19.4	9
French Guiana	9	22.0	15.0	n.a	1
Guadeloupe	n.a.	n.a.	2.9	n.a	1
Martinique	n.a.	n.a.	10.00	n.a	1
United States	n.d.	31,906	188.4	40.0	21
Europe					
Country	Min	Max	Mean	Median	Number of Studies
Austria	n.d.	52.4	24.6	n.a	1
Belgium	233	621	498	n.a	1
Faroe Islands	0.82	2.3	1.5	n.a	1
Finland	1.8	42	7.1	n.a	1
France	n.d.	725	37.7	27.7	6
Germany	n.d.	6,758	165.8	18.8	9
Italy	0.063	1,298	83.9	71.4	6
Latvia	n.a.	n.a.	1.2	n.a	1
Malta	0.89	35.0	10.0	n.a	1
Netherlands	0.35	876	68.7	46.4	5
Norway	n.d.	13	1.3	1.3	2
Poland	n.a.	n.a.	6.8	n.a	1
Romania	12.3	22.2	17.0	n.a*	1
Bulgaria	12.3	22.2	17.0	n.a*	1
Spain	n.d.	3,130	106.7	66.3	11
Sweden	n.d.	13,000	210.2	18.8	7
UK	n.d.	62.0	62.3	71.6	4
Switzerland	4.08	309	70.03	n.a*	1
Asia					
Country	Min	Max	Mean	Median	Number of Studies
Bangladesh	10.6	46.8	22.7	n.a	1
China	n.d.	659,889	4,117	57.5	
India	1.8	18.7	8.9	n.a	1
Japan	n.d.	16,187	80.9	26.5	11
Jordan	n.d.	27	11.8	n.a	1
Nepal	n.d.	3.7	0.89	n.a	1
South Korea	n.d.	1,120	84.9	81.7	8

Taiwan	0.1	5,765	1024.3	1024.3	2
Thailand			5.1	n.a	1
Vietnam	n.d.	170	6.9	3.9	3
Antarctica, Africa, and Oceania					
Country	Min	Max	Mean	Median	Number of Studies
Antarctica	0.094	15.3	2.0	2.0	2
Australia	0.8	40.0	21.6	21.6	2
Ethiopia	0.073	5.6	2.9	n.a	1
Mayotte	n.d.	4.6	1.1	n.a	1
Reunion	n.a.	n.a.	6.2	n.a	1
South Africa	2	1,426	306.3	73.4	3

n.d. – not detected/below detections limits/below reporting limits; n.a. – information not available; n.a. study related to transboundary river on the border between neighboring countries.*

Table 3.4. Summary Statistics (range, mean, median, and number of studies) for the distribution of PFAS in Sediment (ng g^{-1}) by country.

The Americas					
Country	Min	Max	Mean	Median	Number of Studies
Brazil	n.d.	0.32	0.12	0.12	2
Canada	n.d.	106.0	19.4	6.1	5
USA	n.d.	183.8	13.6	11.0	9
Europe					
Country	Min	Max	Mean	Median	Number of Studies
Austria	1.4	13.0	3.2	n.a	1
Czech Republic	n.d.	25.5	1.8	1.8	2
France	n.d.	37.2	12.1	11.9	3
Germany	0.056	7.5	1.0	n.a	1
Italy	n.d.	1.5	0.7	n.a	1
Norway	5.3	2,450	309.0	n.a	1
Poland	0.3	1.2	0.7	n.a	1
Serbia	0.56	6.29	3.0	n.a	1
Spain	n.d.	75.9	5.1	5.4	8
Sweden	42.0	76.0	59.0	n.a	1
UK	n.a.	n.a.	17.1	n.a	1
Asia					
Country	Min	Max	Mean	Median	Number of Studies
Bangladesh	1.1	8.2	3.5	n.a	1
China	n.d.	798.6	29.5	1.4	45
India	n.d.	14.1	8.5	n.a	1
Japan	n.d.	22.0	2.8	1.5	3
South Korea	0.040	85.0	17.0	2.5	3

Vietnam	n.d.	23.4	3.0	n.a	1
Africa and Oceania					
Country	Min	Max	Mean	Median	Number of Studies
Australia	n.a.	n.a.	3.2	n.a	1
Ethiopia	0.23	0.50	0.30	n.a	1
Kenya	n.d.	146.4	25.6	n.a	1

n.d. – not detected/below detections limits/below reporting limits; n.a. – information not available

Table 3.5. Summary Statistics (range, mean, median, and number of studies) for the distribution of PFAS in Groundwater (ng L^{-1}) by country.

The Americas					
Country	Min	Max	Mean	Median	Number of Studies
Brazil	n.a.	n.a.	5.7	n.a	1
Canada	2.1	10.7	5.6	n.a	1
USA	n.d.	7,090,000	321,811	62,410	7
Europe					
Country	Min	Max	Mean	Median	Number of Studies
Sweden	n.d.	51,040	237.6	3.0	2
Asia					
Country	Min	Max	Mean	Median	Number of Studies
China	n.d.	26,700	2,248	74.8	9
India	7.5	13.2	10.1	n.a	1
Japan	1.9	269.7	51.7	n.a	1
Vietnam	n.d.	8.9	3.6	n.a	1
Oceania					
Country	Min	Max	Mean	Median	Number of Studies
Australia	26.0	5,200	561.6	n.a	1

n.d. – not detected/below detections limits/below reporting limits; n.a. – information not available

Table 3.6. Global distribution of PFAS in Surface Water. Information on location, media, mean and range ∑PFAS in surface water (ng L^{-1}) is provided.

The Americas						
Location	Country	Media	Min	Max	Mean	Reference
Guanabara Bay	Brazil	Brackish Water	1.48	3.82	2.5	(Quinete et al., 2009)
Paraiba do Sul River	Brazil	Brackish/Freshwater	n.d.	2	0.88	
Baia de Todos os Santos, Bahia	Brazil	Brackish/Freshwater	0.31	4.88	2.55	(Lofstedt Gilljam et al., 2016)

Intanhem River	Brazil	Brackish/Freshwater	0.33	8.93	5.01	(Nascimento et al., 2018)
Caravelas Estuary	Brazil	Brackish Water	n.d.	1.02	0.15	(Nascimento et al., 2018)
Etobicoke Creek/Toronto Airport	Canada	Freshwater	n.d.	946.8	141.04	(Awad et al., 2011)
Toronto/Lake Ontario Area	Canada	Freshwater	12.82	37.07	24.32	(Meyer et al., 2011)
Prince Edward Island	Canada	Freshwater	1.11	2.03	1.58	(Scott et al., 2009)
Quebec	Canada	Freshwater	2.14	19.14	10.14	
Ontario	Canada	Freshwater	0.93	74.71	10.15	
Manitoba	Canada	Freshwater	3.1	27.36	7.36	
Saskatchewan	Canada	Freshwater	0.29	18.44	6.31	
Alberta	Canada	Freshwater	0.033	8.05	3.11	
British Columbia	Canada	Freshwater	0.52	2.89	1.36	
Yukon	Canada	Freshwater	1.763	6.14	3.95	
Welland River + Nearby creeks and lake	Canada	Freshwater	0.31	823.34	224.51	(D'Agostino and Mabury, 2017)
Resolute Lake	Canada	Freshwater	98.78	167.56	133.17	
Meretta Lake	Canada	Freshwater	n.a.	n.a.	235.02	
Several Waterbodies near Lake Ontario	Canada	Freshwater	0.23	141.51	25.45	(D'eon et al., 2009)
Etobicoke Creek	Canada	Freshwater	n.d.	2270000	112974.1	(Moody et al., 2002)
Lake Superior	Canada	Freshwater	1.14	5.07	3.1	(De Silva et al., 2011)
Lake Huron	Canada	Freshwater	3.49	18.45	13.31	
Lake Erie	Canada	Freshwater	18.35	20.42	19.39	
Lake Ontario	Canada	Freshwater	14.92	32.44	21.59	
Resolute Lake	Canada	Freshwater	49.9	157.7	101.41	(Stock et al., 2007)
Char Lake	Canada	Freshwater	11.2	25.7	18.85	
Meretta Lake and Tributaries	Canada	Freshwater	121	158.2	136.05	
Amituk Lake	Canada	Freshwater	9.9	15.9	12.57	
French Guiana	French Guiana	Freshwater	9	22	15	(Munoz et al., 2017)
Guadeloupe	Guadeloupe	Freshwater	n.a.	n.a.	2.9	
Martinique	Martinique	Freshwater	n.a.	n.a.	10	
Near Albany, NY	USA	Freshwater	9.49	35.9	21.8	(Kim and Kannan, 2007)
Lake Michigan	USA	Freshwater	16.52	23.05	18.46	(De Silva et al., 2011)
Tennessee River (North Alabama)	USA	Freshwater	16.8	731	244.24	(Hansen et al., 2002)
Conasauga River and Dalton	USA	Freshwater	75.1	1770	703.26	(Konwick et al., 2008)

Atamaha River	USA	Brackish/Freshwater	5.75	6.32	6.02	
Conasauga and Coosa River	USA	Freshwater	n.d.	1385	635.25	(Lasier et al., 2011)
Decatur Area	USA	Freshwater	n.d.	31906	2440.32	(Lindstrom et al., 2011a)
Upper Mississippi - Minnesota	USA	Freshwater	n.d.	1019.26	71.52	(Nakayama et al., 2010)
Upper Mississippi - Wisconsin	USA	Freshwater	n.d.	514.04	60.13	
Upper Mississippi - Illinois	USA	Freshwater	n.d.	492.03	66.89	
Missouri River	USA	Freshwater	2.73	21.22	8.66	
Decatur Area - Tennessee River	USA	Freshwater	n.d.	759	129.11	(Newton et al., 2017)
NJ State Raw Drinking Water Source	USA	Freshwater	n.d.	174	40.91	(Post et al., 2013)
Rhode Island	USA	Freshwater	1.13	225.25	27.9	(Zhang et al., 2016)
New York Metropolitan Area	USA	Freshwater	3.88	92.59	31.57	
Mississippi River	USA	Freshwater	n.a.	n.a.	25.11	(Benskin et al., 2010)
Cape Fear River Basin, NC	USA	Freshwater	n.a.	n.a.	198.82	(Nakayama et al., 2007)
Intake from WTP from 3 communities along the CRB	USA	Freshwater	n.a.	n.a.	375.67	(Sun et al., 2016)
Lake Ontario	USA	Freshwater	n.a.	n.a.	27.3	(Sinclair et al., 2006)
Niagara River	USA	Freshwater	n.a.	n.a.	25.7	
Lake Erie	USA	Freshwater	n.a.	n.a.	19.2	
Finger Lakes	USA	Freshwater	n.a.	n.a.	16.5	
Lake Onondaga	USA	Freshwater	n.a.	n.a.	812.4	
Lake Oneida	USA	Freshwater	n.a.	n.a.	23.4	
Erie Canal	USA	Freshwater	n.a.	n.a.	39	
Lake Champlain	USA	Freshwater	n.a.	n.a.	28	
Hudson River	USA	Freshwater	n.a.	n.a.	37.6	
Delaware River	USA	Brackish/Freshwater	n.a.	n.a.	44.15	(Pan et al., 2018)
Houston Ship Channel	USA	Brackish/Freshwater	41.54	2044.08	661.05	(Aly et al., 2020)
Selected Waterbodies in New Jersey	USA	Freshwater	22.9	279.5	93.9	(Goodrow et al., 2020)
Yadkin-Pee Dee River	USA	Freshwater	n.d.	13.86	2.78	(Penland et al., 2020)

Van Etten Lake (Michigan)	USA	Freshwater	14	203	76.67	(Schwichtenberg et al., 2020)
Truckee River, Nevada	USA	Freshwater	12.3	203	55.21	(Bai and Son, 2021)
Las Vegas Wash, Nevada	USA	Freshwater	3.8	592	223.5	
Lake Superior	USA	Freshwater	1.69	5.45	3.44	(De Silva et al., 2011)
Lake Huron	USA	Freshwater	9.07	23.58	16.31	
Lake Erie	USA	Freshwater	n.a.	n.a.	14.68	
Lake Ontario	USA	Freshwater	15.53	33.87	21.55	
Lake Ontario	USA/Canada	Freshwater	30	203	107.68	(Boulanger et al., 2004)
Lake Erie	USA/Canada	Freshwater	35.8	98.6	80.16	
Europe						
Location	Country	Media	Min	Max	Mean	Reference
Danube River Basin	Austria	Freshwater	n.d.	52.4	24.58	(Clara et al., 2009)
Scheldt River	Belgium	Freshwater	233	621	498	(Moller et al., 2010)
LakeLeitisvatn, Havnadal, Kornvatn, and Á Mýrana	Faroe Islands	Freshwater	0.82	2.26	1.5	(Eriksson et al., 2013)
Finnish Environment	Finland	Freshwater	1.8	42	7.07	(Junttila et al., 2019)
Orge River	France	Freshwater	n.a.	n.a.	73	(Labadie and Chevreuil, 2011)
Loire River	France	Freshwater	5.8	9.03	8.01	(McLachlan et al., 2007)
Seine River	France	Freshwater	20.42	35.12	27.12	
Gironde Estuary	France	Brackish/Freshwater	3.5	11	6.5	(Munoz et al., 2019a)
Bay of Marseille	France	Brackish	0.11	0.59	0.27	(Schmidt et al., 2019)
Rhone River	France	Freshwater	13	200	88.31	
French National Survey	France	Freshwater	n.d.	725	28.2	(Munoz et al., 2015)
Elbe River	Germany	Freshwater	4.64	27.24	16.75	(Heydebreck et al., 2015)
Elbe, lower Weser and North Sea	Germany	Freshwater/Coastal Seawater	0.15	249	8.7	(Zhao et al., 2015a)
Elbe River	Germany	Freshwater	19.33	32.9	25.75	(McLachlan et al., 2007)
Baltic Sea	Germany	Coastal Seawater	0.79	6.15	2.73	(Ahrens et al., 2010a)
North Sea	Germany	Coastal Seawater	0.07	21.53	9.155	
Hesse River	Germany	Freshwater	n.d.	88	20.78	(Llorca et al., 2012)

German Bight	Germany	Coastal Seawater	9.36	31.18	15.89	(Ahrens et al., 2009b)
Alz River	Germany	Freshwater	2	6758.35	2003.61	(Joerss et al., 2020)
Main, Ruhr, and Rine Rivers	Germany	Freshwater	17.62	87.47	37.53	
Ems/North Sea	Germany	Freshwater/Coastal Seawater	3.9	39.1	13.06	(Heydebreck et al., 2015)
Rhine River	Germany	Freshwater	18.85	111.66	42.86	
Rhine River	Germany/ Netherlands	Freshwater	n.a.	n.a.	47.14	(Pan et al., 2018)
Oder River	Germany/ Poland	Freshwater	n.a.	n.a.	7.46	(McLachlan et al., 2007)
Rhine River Basin	Germany/ Switzerland/ France	Freshwater	4.08	309	70.03	(Moller et al., 2010)
Western Mediterranean Sea	Italy	Coastal Seawater	0.063	0.52	0.31	(Brumovsky et al., 2016)
Po River and Tributaries	Italy	Freshwater	1	1298	114.61	(Loos et al., 2008)
Romagna Area	Italy	Freshwater	n.a.	n.a.	14.7	(Pignotti and Dinelli, 2018)
River Lambro Basin	Italy	Freshwater	17	40	28.14	(Castiglioni et al., 2018)
Milan Area - Italy	Italy	Freshwater	14	889	118.32	(Castiglioni et al., 2015)
Po River	Italy	Freshwater	222.9	231.21	227.06	(McLachlan et al., 2007)
Daugava River	Latvia	Freshwater	n.a.	n.a.	1.22	(McLachlan et al., 2007)
Malta and Gozo	Malta	Freshwater	0.89	35.02	10.03	(Sammut et al., 2017)
Several waterbodies near Fluorochemical Plant	Netherlands	Freshwater	38	876	180.83	(Gebbink et al., 2017)
Rhine River	Netherlands	Freshwater	20.27	31.95	24.22	(McLachlan et al., 2007)
Ems/North Sea	Netherlands	Freshwater/Coastal Seawater	4.7	25.8	11.34	(Heydebreck et al., 2015)
Rhine River	Netherlands	Freshwater	26.82	104.87	46.42	
Meuse Delta Area	Netherlands	Freshwater	20.8	287	166.43	(Moller et al., 2010)
North Sea	Netherlands	Coastal Seawater	0.35	11.6	4.43	
Svalbard Archipelago	Norway	Freshwater/Coastal Seawater	n.d.	13	2.33	(Skaar et al., 2019)
Kongsfjorden marine environment - Svalbard	Norway	Brackish Water	n.d.	2.4	0.24	(Ademollo et al., 2021)

Vistula River	Poland	Freshwater	n.a.	n.a.	6.14	(McLachlan et al., 2007)
Danube River	Romania/Bulgaria	Freshwater	12.26	22.2	16.96	(McLachlan et al., 2007)
Llobregat Basin	Spain	Freshwater	21.3	3130	295	(Campo et al., 2015)
Cantabrian Sea	Spain	Brackish/Freshwater	0.06	8	0.55	(Gomez et al., 2011)
Guadalquivir River Basin	Spain	Freshwater	n.a.	n.a.	260.9	(Lorenzo et al., 2016)
Ebro River Basin	Spain	Freshwater	n.a.	n.a.	51.9	
Tagus River Watershed	Spain	Freshwater	n.d.	47.3	12.28	(Navarro et al., 2020)
L'Albufera Natural Park - Spain	Spain	Freshwater	3.05	217	77.81	(Pico et al., 2012)
Ebro Delta	Spain	Brackish/Freshwater	n.a.	n.a.	3.49	(Pignotti et al., 2017)
Guadalquivir River	Spain	Freshwater	12.56	14.14	13.35	(McLachlan et al., 2007)
Catalan Coast	Spain	Brackish/Freshwater	0.07	21.9	2.83	(Sanchez-Avila et al., 2010)
Jucar River Basin	Spain	Freshwater	21.1	1140	91.8	(Campo et al., 2016)
Xúquer River Basin	Spain	Freshwater	20	378	95.67	(Llorca et al., 2012)
Ebro River	Spain	Freshwater	n.d.	139	54.82	
Llobregat River	Spain	Freshwater	1.2	2878	435	
Albufera Natural Park	Spain	Freshwater	n.a.	n.a.	98.3	(Lorenzo et al., 2019)
Blekinge	Sweden	Freshwater	1.4	13	5.45	(Gobelius et al., 2018)
Dalarna	Sweden	Freshwater	0.09	33	8.91	
Gävleborg	Sweden	Freshwater	0.1	72	9.19	
Gotland	Sweden	Freshwater	n.d.	170	30.03	
Halland	Sweden	Freshwater	0.9	760	77.34	
Jämtland	Sweden	Freshwater	n.d.	13000	1896.86	
Jönköping	Sweden	Freshwater	n.d.	220	27.58	
Kalmar	Sweden	Freshwater	0.3	51	7.97	
Kronoberg	Sweden	Freshwater	1.2	2	1.6	
Norrbotten	Sweden	Freshwater	0.2	1040	104.51	
Örebro	Sweden	Freshwater	0.3	153	23.99	
Östergötland	Sweden	Freshwater	1.6	19	5.27	
Skåne	Sweden	Freshwater	n.d.	150	22.76	
Södermanland	Sweden	Freshwater	0.5	180	37.06	
Stockholm	Sweden	Freshwater	0.2	180	31.04	
Uppsala	Sweden	Freshwater	0.2	126	13.44	

Värmland	Sweden	Freshwater	0.3	120	18.81	
Västerbotten	Sweden	Freshwater	2.8	94	48.4	
Västernorrland	Sweden	Freshwater	0.1	34	3.48	
Västmanland	Sweden	Freshwater	0.9	31	18.67	
Västra Götaland	Sweden	Freshwater	1.4	3300	192.28	
Near Military Airport Stockholm	Sweden	Freshwater	n.d.	79	25.32	(Filipovic et al., 2015)
Dalalven River	Sweden	Freshwater	n.a.	n.a.	0.36	(McLachlan et al., 2007)
Vindelalven River	Sweden	Freshwater	n.a.	n.a.	0.42	
Kalix Alv River	Sweden	Freshwater	n.a.	n.a.	0.26	
Near Airport in Luleå, Sweden	Sweden	Freshwater	1400	1700	1550	(Mussabek et al., 2019)
Malaren Lake	Sweden	Freshwater	n.a.	n.a.	18.7	(Pan et al., 2018)
Pond near Ronneby airport	Sweden	Freshwater	286	2870	1908.67	(Koch et al., 2021)
East Sweden	Sweden	Brackish/Freshwater	1	60	8.3	(Nguyen et al., 2017)
Blackwater River, River Bourne, Hogsmill River	UK	Freshwater	n.a.	n.a.	92.49	(Wilkinson et al., 2017)
Thames River	UK	Freshwater	56.78	61.99	59.39	(McLachlan et al., 2007)
Aire and Calder rivers	UK	Freshwater	n.d.	33.85	13.69	(Earnshaw et al., 2014)
Thames River	UK	Freshwater	n.a.	n.a.	83.81	(Pan et al., 2018)
Danube River Basin	Several (Europe)	Freshwater	n.a.	n.a.	25.5	(Loos et al., 2017)
Asia						
Location	Country	Media	Min	Max	Mean	Reference
Bay of Bengal	Bangladesh	Brackish Water	10.6	46.8	22.74	(Habibullah-Al-Mamun et al., 2016)
Jiulong River Estuary, China	China	Brackish/Freshwater	n.d.	110.4	30.87	(Cai et al., 2018)
East China Sea Coastal Area	China	Freshwater	n.d.	489.2	145.29	(Chen et al., 2016b)
Bohai Sea	China	Brackish Water	n.d.	99.4	10.57	(Chen et al., 2016a)
Bohai Sea	China	Brackish/Freshwater	5.03	41706	727.27	(Chen et al., 2017)
Fuxin Area	China	Freshwater	807.82	54518.46	9442.66	(Chen et al., 2018a)

Baiyangdian Lake + Tributaries	China	Freshwater	4.46	8476.69	1330.3	(Cui et al., 2018)
Dalian Bay	China	Brackish Water	7.89	13.69	11.15	(Ding et al., 2018)
Songhua River	China	Freshwater	0.037	1.34	0.62	(Dong et al., 2018)
Xiaoqing River	China	Freshwater	42.4	659889	53583.9	(Heydebreck et al., 2015)
Dalian Bay	China	Brackish/Coastal Seawater	0.27	38.51	3.21	(Ju et al., 2008)
South China Sea	China	Coastal Seawater	2.26	14.54	4.91	(Kwok et al., 2015)
Pearl River Delta Area	China	Freshwater	1.51	33.5	7.57	(Liu et al., 2015a)
Coastal Areas of Bohai Bay	China	Brackish/Freshwater	20.5	684	147	(Liu et al., 2019c)
Baiyangdian Lake	China	Freshwater	469	3462	1305	(Liu et al., 2019a)
Eastern China	China	Brackish/Freshwater	0.68	229	70.18	(Lu et al., 2015)
Qiantang River	China	Freshwater	0.98	609	174.4	(Zhang et al., 2015)
Yangtze River Estuary	China	Brackish Water	36.3	703.3	231.3	(Pan and You, 2010)
Yangtze River	China	Freshwater	2.2	74.56	20.29	(Pan et al., 2014a)
Beibu Gulf	China	Brackish/Freshwater	0.61	4.92	3.08	(Pan et al., 2019)
Grand Canal - China	China	Freshwater	7.8	218	44.6	(Piao et al., 2017)
Shuangtaizi Estuary	China	Brackish/Freshwater	66.17	184.72	114.08	(Shao et al., 2016)
Xiaoqing River	China	Freshwater	36.5	169000	13132.63	(Shi et al., 2015)
Xiaoqing River	China	Freshwater	n.a.	n.a.	49533.98	(Song et al., 2018)
Several waterbodies in Shenyang	China	Freshwater	n.a.	n.a.	18.97	(Sun et al., 2011)
Hangpu River	China	Freshwater	39.8	596.2	226.3	(Sun et al., 2017)
Yangtze River	China	Freshwater	7.8	586.2	44.6	(Tan et al., 2018)
North Bohai Sea Area	China	Brackish/Freshwater	n.d.	121	18.4	(Wang et al., 2011b)
Guanting Reservoir	China	Freshwater	0.75	3.1	1.7	(Wang et al., 2012a)
Liaoning River Area	China	Freshwater	3.2	121	39	

Tianjin	China	Freshwater	4.4	25	13	
Hohhot	China	Freshwater	1.1	2.5	1.8	
Hanjiang River	China	Freshwater	8.6	568	204	(Wang et al., 2013a)
Yellow River Estuary	China	Freshwater	82.3	261.8	157.48	(Wang et al., 2013b)
Beijing Airport Area	China	Freshwater	22.93	482.85	121.29	(Wang et al., 2016)
Beijing Urban Area	China	Freshwater	2.88	222.57	45.39	(Wang et al., 2019b)
South China Sea Coastal Region	China	Coastal Seawater	0.02	1.89	0.6	(Wang et al., 2019a)
Tibet	China	Freshwater	0.16	2.56	0.94	(Yamazaki et al., 2016)
Chengdu and Eastern Tibet	China	Freshwater	0.6	7.76	3.33	
Taihu Lake	China	Freshwater	17.8	449	53.01	(Yang et al., 2011)
Liao River	China	Freshwater	1.4	131	44.29	
Pearl River	China	Freshwater	3	52	19.46	(Zhang et al., 2013)
Shandong Province	China	Freshwater	35.71	1236.21	235.47	(Zhang et al., 2019)
Bohai Sea, Yellow Sea, Yangtze River	China	Brackish/Coastal Seawater	1.6	118	11.75	(Zhao et al., 2017)
Daling River	China	Freshwater	1.77	9540	1328.25	(Zhu et al., 2015)
Nansi Lake	China	Freshwater	38.4	91.43	67.05	(Cao et al., 2015)
Liadong Bay Basin	China	Freshwater	2.52	210.9	22.69	(Chen et al., 2015a)
Liao River	China	Freshwater	44.4	781	165	(Chen et al., 2015b)
Taihu Lake	China	Freshwater	17.2	94.4	64	
Taihu Lake	China	Freshwater	96.3	330	148	(Chen et al., 2018b)
Taihu Lake	China	Freshwater	10.03	119.81	56.86	(Guo et al., 2015)
Lake Chaohu	China	Freshwater	2.47	39.57	14.46	(Liu et al., 2015b)
Lake Taihu + Tributaries	China	Freshwater	19.3	451	146.5	(Ma et al., 2018)
Lake Taihu	China	Freshwater	163.7	299.6	224.56	(Pan et al., 2014b)
Guanting Reservoir	China	Freshwater	0.7	3.1	1.66	(Wang et al., 2011a)
Tianjin	China	Freshwater	4.4	25	12.54	(Wang et al., 2012b)

Tangxun Lake	China	Freshwater	4574.06	70467.55	12485.2	(Zhou et al., 2013)
Baiyangdian Lake	China	Freshwater	14.8	95.6	46.96	(Zhou et al., 2012)
Several waterbodies in Shanghai	China	Freshwater	113.38	362.37	171.65	(Sun et al., 2018)
Baihe River	China	Freshwater	41	72.6	57.45	(Liu et al., 2018)
River Xi, Fuxin	China	Freshwater	370	713	495.57	(Bao et al., 2011)
Xiaoqing River	China	Freshwater	48.4	282000	55565.8	(Pan et al., 2017)
Liao River	China	Freshwater	n.a.	n.a.	25.74	(Pan et al., 2018)
Chao Lake	China	Freshwater	n.a.	n.a.	273.49	
Taihu Lake	China	Freshwater	n.a.	n.a.	167.68	
Huai River	China	Freshwater	n.a.	n.a.	27.29	
Pearl River	China	Freshwater	n.a.	n.a.	35.75	
Yellow River	China	Freshwater	n.a.	n.a.	21.95	
Yangtze River	China	Freshwater	n.a.	n.a.	38.56	
Daling River Basin	China	Freshwater	1.01	4742	1041.48	(Wang et al., 2015)
Taihu Lake	China	Freshwater	60	126	101.88	(Yu et al., 2013)
Huai River Basin	China	Freshwater	11	79	27.78	
Xi-Daling River	China	Freshwater	47.99	4775.56	2006.41	(Gao et al., 2020)
Jiaozhou Bay	China	Brackish Water	5.54	205.3	16.07	(Han et al., 2020)
Xiaoqing River	China	Freshwater	96.99	415371	121058.5	(Joerss et al., 2020)
Xi River	China	Freshwater	144.6	23004.95	4796.87	
Yangtze River	China	Freshwater	46.62	2621.67	457.88	
Bohai Bay and Tributaries	China	Brackish/Freshwater	6.04	13336.4	396.2	(Zhao et al., 2020)
Northwest of downtown Hangzhou City	China	Freshwater	110	236.27	158.02	(Xu et al., 2021)
Yangtze River	China	Freshwater	4.25	289.25	40.89	(So et al., 2007)
Pearl River Delta	China	Freshwater	2.24	99.84	30.92	
Suzhou Area	China	Freshwater	9.91	588.59	350.78	(Wei et al., 2018)
Tianjin	China	Freshwater	7.48	65.09	23.79	(Pan et al., 2011)
Ganges basin	India	Freshwater	1.79	18.65	8.92	(Sharma et al., 2016)

Tokyo Bay	Japan	Brackish/Freshwater	n.a.	n.a.	10.95	(Benskin et al., 2010)
Tomakomai Bay	Japan	Brackish/Freshwater	45.36	819.63	432.49	
R. Tokorogawa	Japan	Freshwater	n.a.	n.a.	158.65	(Murakami et al., 2008)
R. Sarugawa	Japan	Freshwater	n.a.	n.a.	2.64	
R. Yoneshirogawa	Japan	Freshwater	n.a.	n.a.	26.45	
R. Narusegawa	Japan	Freshwater	n.a.	n.a.	110.7	
R. Nakagawa	Japan	Freshwater	n.a.	n.a.	10.2	
R. Tamagawa	Japan	Freshwater	56.87	315.66	219.38	
R. Arakawa	Japan	Freshwater	n.a.	n.a.	91.5	
R. Kurobegawa	Japan	Freshwater	n.a.	n.a.	1.73	
R. Shounaigawa	Japan	Freshwater	n.a.	n.a.	100.21	
R. Abegawa	Japan	Freshwater	n.a.	n.a.	71.93	
R. Yuragawa	Japan	Freshwater	n.a.	n.a.	66	
R. Yamatogawa	Japan	Freshwater	n.a.	n.a.	222.1	
R. Asahikawa	Japan	Freshwater	n.a.	n.a.	198.42	
R. Ashidagawa	Japan	Freshwater	n.a.	n.a.	25.19	
R. Niyodogawa	Japan	Freshwater	n.a.	n.a.	1.99	
R. Monobegawa	Japan	Freshwater	n.a.	n.a.	4.9	
R. Oonogawa	Japan	Freshwater	n.a.	n.a.	2.64	
R. Kimotsukigawa	Japan	Freshwater	n.a.	n.a.	10	
Tokyo Bay	Japan	Brackish Water	14.3	30.5	21.54	(Sakurai et al., 2010)
Tama River, Tokyo	Japan	Freshwater	3.8	38	23	(Ye et al., 2014)
Tokyo Bay Surrounding Areas	Japan	Freshwater	2.25	6046.94	156.43	(Zushi et al., 2011)
Tokyo Bay Area	Japan	Freshwater	0.4	151	33.08	(Takazawa et al., 2009)
Yodo River Basin	Japan	Freshwater	1	89.7	11.2	(Niisoe et al., 2015)
Japan National Survey	Japan	Brackish/Freshwater	0.2	157	7.83	(Saito et al., 2003)
Several rives in the Kyoto City Area	Japan	Freshwater	7.9	120	64.08	(Senthilkumar et al., 2007)
Harima Sea and Osaka Bay Area	Japan	Brackish/Freshwater	n.d.	16186.7	249.19	(Takemine et al., 2014)
Lake Biwa	Japan	Freshwater	n.a.	n.a.	11.52	(Tsuda et al., 2010)
Zarqa River	Jordan	Freshwater	n.d.	27	11.79	(Shigei et al., 2020)
Mt. Everest - Streams	Nepal	Freshwater	n.d.	3.68	0.89	(Miner et al., 2021)
Asan Lake Area	South Korea	Freshwater	17.7	467	172	(Lee et al., 2020b)

Gyeonggi Bay, South Korea	South Korea	Brackish/Freshwater	4.31	867.09	91.46	(Rostkowski et al., 2006)
Pohang/Gyeongju	South Korea	Freshwater	8.79	40.43	22.07	(Seo et al., 2019)
South Coast - South Korea	South Korea	Coastal Seawater	0.28	11.84	6.02	(So et al., 2004)
West Coast - South Korea	South Korea	Coastal Seawater	2.49	1120.33	227.48	
YeongSangang	South Korea	Brackish/Freshwater	85.6	101.84	93.72	(Naile et al., 2010)
Geumgang	South Korea	Brackish/Freshwater	77.15	121.88	99.52	
Han River	South Korea	Freshwater	n.a.	n.a.	23.97	(Pan et al., 2018)
Coastal Water in South Korea	South Korea	Coastal Seawater	0.39	22.9	4.46	(Lee et al., 2020a)
Major Rivers, Rice Fields, and Bays	South Korea	Brackish/Freshwater	n.d.	97.2	13.01	(Lam et al., 2016)
Lake Shihua	South Korea	Brackish Water	19.43	129.62	81.72	(Naile et al., 2010)
Asan and SapGyo	South Korea	Brackish Water	87.04	694.92	248.9	
SinDuri, ManLipo, and AnMyundo (Beach)	South Korea	Coastal Seawater	10.05	36.71	19.46	
Near Hsinchu Science Park	Taiwan	Freshwater	110.6	5764.6	1997.73	(Lin et al., 2009)
Baoshan Reservoir	Taiwan	Freshwater	0.1	212	50.9	(Jiang et al., 2021)
Bangaponk River	Thailand	Freshwater	n.a.	n.a.	1.2	(Kunacheva et al., 2009)
Chao Phraya River	Thailand	Freshwater	n.a.	n.a.	9	
Vietnam (RU, MD, BR, ER)	Vietnam	Freshwater	n.d.	170	24.92	(Kim et al., 2013)
Da Nang	Vietnam	Freshwater	n.d.	16.84	1.8	(Duong et al., 2015)
Hue	Vietnam	Freshwater	n.d.	3.65	0.98	
Ho Chi Minh City	Vietnam	Freshwater	0.13	46.03	6.03	
Hanoi	Vietnam	Freshwater	0.11	3.28	1.42	
Nationwide Survey	Vietnam	Freshwater	n.d.	107	6.19	(Lam et al., 2017)
Antarctica, Africa, and Oceania						
Location	Country	Media	Min	Max	Mean	Reference
King George Island	Antarctica	Brackish/Freshwater	0.53	15.28	3.87	(Cai et al., 2012)
Livingston Island	Antarctica	Coastal Seawater	0.094	0.42	0.19	(Casal et al., 2017)
Brisbane River system	Australia	Brackish/Freshwater	0.83	40	10.94	(Gallen et al., 2014)

Sydney Harbor	Australia	Freshwater	n.a.	n.a.	32.3	(Thompson et al., 2011)
Lake Tana	Ethiopia	Freshwater	0.073	5.6	2.88	(Ahrens et al., 2016)
Martinique	Martinique	Freshwater	n.a.	n.a.	10	(Munoz et al., 2017)
Mayotte	Mayotte	Freshwater	n.d.	4.6	1.1	
Vaal River, near Johannesburg	South Africa	Freshwater	11.4	122	73.43	(Groffen et al., 2018)
Eerste, Diep, and Salt Rivers	South Africa	Freshwater	2	415.2	69.46	(Mudumbi et al., 2014)
KwaZulu-Natal coastline	South Africa	Brackish Water	188.87	1425.66	776.14	(Fauconier et al., 2020)
Reunion	Reunion	Freshwater	n.a.	n.a.	6.2	(Munoz et al., 2017)
Maritime Environment (Ocean/Sea)						
Location	Country	Media	Min	Max	Mean	Reference
Antarctic Ocean	-	Seawater	0.33	0.61	0.46	(Yamazaki et al., 2021)
Arctic Ocean	-	Seawater	n.a.	n.a.	0.42	(Li et al., 2018)
Atlantic and Arctic Seawater	-	Seawater	0.01	1.15	0.098	(Benskin et al., 2012)
Atlantic Ocean	-	Seawater	n.d.	1.12	0.16	(Ahrens et al., 2009a)
Bering Sea	-	Seawater	n.a.	n.a.	0.5	(Li et al., 2018)
Chukchi Sea	-	Seawater	n.a.	n.a.	0.51	
East and South China Sea	-	Seawater	n.d.	2.61	0.43	(Zheng et al., 2017)
East China Sea	-	Seawater	0.64	4.39	2.26	(Yamazaki et al., 2019)
East China Sea	-	Seawater	n.a.	n.a.	2.79	(Li et al., 2018)
English Channel	-	Coastal Seawater	0.35	1.2	0.59	(Theobald et al., 2011)
Greenland Sea, Atlantic Ocean and Southern Ocean	-	Seawater	n.d.	0.65	0.11	(Zhao et al., 2012)
Japan Sea	-	Seawater	0.1	1.05	0.42	(Yamazaki et al., 2019)
Japan Sea	-	Seawater	11.21	11.34	11.28	(Benskin et al., 2010)
Japan Sea	-	Seawater	n.a.	n.a.	0.83	(Li et al., 2018)
Mediterranean Sea	-	Seawater	0.18	0.33	0.23	(Yamazaki et al., 2019)

North Sea	-	Coastal Seawater	0.18	24.37	4.67	(Theobald et al., 2011)
Northern Europe, Atlantic and Southern Ocean	-	Seawater	n.d.	1.004	0.27	(Ahrens et al., 2010b)
Norwegian Sea	-	Seawater	0.01	1.67	0.74	(Ahrens et al., 2010a)
Sea of Okhotsk	-	Seawater	n.a.	n.a.	0.52	(Li et al., 2018)
Taiwan Strait	-	Seawater	1.53	1.91	1.72	(Yamazaki et al., 2019)
Taiwan Western Strait	-	Seawater	0.35	3.73	1.18	(Yamazaki et al., 2021)
Tropical and Subtropical Surface Oceans	-	Seawater	n.d.	10.9	1.18	(Gonzalez-Gaya et al., 2014)
Western Arctic Ocean	-	Seawater	0.3	0.65	0.43	(Yamazaki et al., 2021)
Western Baltic Sea	-	Coastal Seawater	1.4	3.13	1.86	(Theobald et al., 2011)

n.d. – not detected/below detections limits/below reporting limits; n.a. – information not available

Table 3.7. Global distribution of PFAS in Sediment. Information on location, media, mean and range ∑PFAS in sediment (ng g^{-1}) is provided.

The Americas						
Location	Country	Media	Min	Max	Mean	Reference
Subae Estuary	Brazil	Sediment	n.d.	0.32	0.15	(Miranda et al., 2021)
Caravelas Estuary	Brazil	Sediment	n.d.	0.2	0.085	(Nascimento et al., 2018)
Etobicoke Creek/Toronto Airport Area	Canada	Sediment	n.d.	15.67	2.04	(Awad et al., 2011)
Big Creek and Welland River	Canada	Sediment	0.93	13.2	7.62	(D'Agostino and Mabury, 2017)
Lake Hazen	Canada	Sediment	n.a.	n.a.	0.16	(MacInnis et al., 2019)
Lake B35	Canada	Sediment	n.a.	n.a.	1.52	
Amituk Lake	Canada	Sediment	n.a.	n.a.	6.96	(Stock et al., 2007)
Char Lake	Canada	Sediment	n.a.	n.a.	5.3	
Resolute Lake	Canada	Sediment	n.a.	n.a.	106	
Lake Ontario	Canada	Sediment	1.12	73.17	25.82	(Yeung et al., 2013)

Truckee River, Nevada	USA	Sediment	1.8	183.8	34.11	(Bai and Son, 2021)
Las Vegas Wash	USA	Sediment	n.d.	134.2	26.69	
Selected Waterbodies in New Jersey	USA	Sediment	n.d.	30.9	6.96	(Goodrow et al., 2020)
San Francisco Bay Area	USA	Sediment	0.14	6.51	2.21	(Higgins et al., 2005)
Conasauga and Coosa River	USA	Sediment	0.29	39.2	15.04	(Lasier et al., 2011)
Pudget Sound, WA	USA	Sediment	n.a.	n.a.	0.16	(Long et al., 2013)
Decatur Area - Tennessee River	USA	Sediment	n.d.	47	16.05	(Newton et al., 2017)
Yadkin-Pee Dee River	USA	Sediment	n.d.	n.d.	n.d.	(Penland et al., 2020)
Charleston, SC	USA	Sediment	0.22	19.2	3.79	(White et al., 2015)
Lake Ontario	USA	Sediment	9.42	76.5	31.32	(Yeung et al., 2013)
Europe						
Location	Country	Media	Min	Max	Mean	Reference
Lake Constance	Austria	Sediment	1.69	4.17	2.92	(Clara et al., 2009)
Lake Luner	Austria	Sediment	n.a.	n.a.	1.88	
Lake Formarin	Austria	Sediment	n.a.	n.a.	4.33	
Lake Tilisuna	Austria	Sediment	n.a.	n.a.	1.44	
Danube River	Austria	Sediment	1.38	12.95	5.33	
Zlin Area, Czech Republic	Czech Republic	Sediment	n.d.	6.8	0.95	(Becanova et al., 2016)
Czech Republic	Czech Republic	Sediment	0.41	25.5	2.71	(Hlouskova et al., 2014)
Orge River	France	Sediment	n.a.	n.a.	8.4	(Labadie and Chevreuil, 2011)
Escault River	France	Sediment	n.a.	n.a.	8.15	(Munoz et al., 2016)
Meurthe River	France	Sediment	n.a.	n.a.	12.2	
Risle River	France	Sediment	n.a.	n.a.	1.74	
Yerres River	France	Sediment	n.a.	n.a.	13.36	
Bedat River	France	Sediment	n.a.	n.a.	17.95	
Clain River	France	Sediment	n.a.	n.a.	0.86	
Layon River	France	Sediment	n.a.	n.a.	11.51	
Garonne River	France	Sediment	n.a.	n.a.	13.33	
Ouche River	France	Sediment	n.a.	n.a.	37.21	
Rhone River	France	Sediment	n.a.	n.a.	12.73	
Avene River	France	Sediment	n.a.	n.a.	1.59	

Bordeaux Lake	France	Sediment	n.a.	n.a.	28.3	
National French Survey	France	Sediment	n.d.	25	1.77	(Munoz et al., 2015)
German Bight	Germany	Sediment	0.056	7.5	1	(Zhao et al., 2015b)
Tuscan Archipelago National Park - Italy	Italy	Sediment	n.d.	1.5	0.71	(Perra et al., 2013)
Lake Tyrifjorden	Norway	Sediment	5.3	2450.2	309	(Langberg et al., 2020)
Gulf of Gdank, Baltic Sea	Poland	Sediment	0.33	1.21	0.74	(Falandysz et al., 2012)
Pancevo Industrial Area	Serbia	Sediment	0.562	6.29	3.02	(Beskoski et al., 2013)
Llobregat Basin	Spain	Sediment	8.35	37.5	8.19	(Campo et al., 2015)
Jucar River Basin	Spain	Sediment	14.3	75.9	21.8	(Campo et al., 2016)
Cantabrian Sea	Spain	Sediment	n.d.	0.13	0.039	(Gomez et al., 2011)
Strait-Alboran - Coastal	Spain	Sediment	n.d.	0.2	0.1	(Leon et al., 2020)
Levantine-Balearic (Medit Sea)	Spain	Sediment	0.1	0.4	0.2	
Bay of Biscay/Cantabrian	Spain	Sediment	n.d.	n.d.	n.d.	
Galician/Atlantic Ocean	Spain	Sediment	n.d.	n.d.	n.d.	
Guadalquivir River Basin	Spain	Sediment	n.a.	n.a.	5.76	(Lorenzo et al., 2016)
Ebro River Basin	Spain	Sediment	n.a.	n.a.	7.84	
Albufera National Park	Spain	Sediment	n.a.	n.a.	5.77	(Lorenzo et al., 2019)
L'Albufera Natural Park - Spain	Spain	Sediment	0.25	17.38	6.23	(Pico et al., 2012)
Ebro Delta	Spain	Sediment	n.a.	n.a.	5.03	(Pignotti et al., 2017)
Near Airport in Luleå, Sweden	Sweden	Sediment	42	76	59	(Mussabek et al., 2019)
Blackwater River, River Bourne, Hogsmill River	UK	Sediment	n.a.	n.a.	17.05	(Wilkinson et al., 2018)
Asia						
Location	Country	Media	Min	Max	Mean	Reference
Bay of Bengal	Bangladesh	Sediment	1.07	8.15	3.46	(Habibullah-Al-Mamun et al., 2016)

Hangpu River	China	Sediment	0.25	1.1	0.62	(Bao et al., 2010)
Zhujiang River	China	Sediment	0.09	3.6	1.25	
Daliao River System	China	Sediment	0.29	1.03	0.61	(Bao et al., 2009)
River Xi, Fuxin	China	Sediment	0.48	90	18.79	(Bao et al., 2011)
Nansi Lake, China	China	Sediment	0.47	1.81	1.09	(Cao et al., 2015)
Bohai Sea	China	Sediment	0.33	2.78	0.67	(Chen et al., 2016a)
Fuxin Area	China	Sediment	5.21	370.17	85.35	(Chen et al., 2018a)
Liadong Bay Basin	China	Sediment	2.65	37.34	6.09	(Chen et al., 2015a)
Pearl River Delta	China	Sediment	0.024	0.18	0.1	(Chen et al., 2019)
Taihu Lake	China	Sediment	0.623	5.55	2.15	(Chen et al., 2018b)
Liao River	China	Sediment	0.54	2.34	1.03	(Chen et al., 2015b)
Taihu Lake	China	Sediment	0.57	17.9	4.12	
Songhua River	China	Sediment	0.021	0.34	0.092	(Dong et al., 2018)
Bohai Sea, Yellow Sea, and East China Sea	China	Sediment	n.d.	2.98	0.55	(Gao et al., 2014)
Pearl River Estuary	China	Sediment	n.d.	2.41	0.79	(Gao et al., 2015)
Xi-Daling River	China	Sediment	2.14	40.33	13.92	(Gao et al., 2020)
Taihu Lake	China	Sediment	1.11	8.21	2.43	(Guo et al., 2015)
Danjiangkou Reservoir	China	Sediment	0.27	0.4	0.32	(He et al., 2018)
Hangpu River and Dianshan Lake	China	Sediment	62.5	276	105.53	(Li et al., 2010)
Urban Lakes Anqing City	China	Sediment	0.6	26	9.1	(Li et al., 2017)
Baiyangdian Lake	China	Sediment	1.97	13.3	6.53	(Liu et al., 2019a)
Coastal Areas of Bohai Bay	China	Sediment	2.69	25	6.76	(Liu et al., 2019c)
Huai River Watershed	China	Sediment	0.06	0.46	0.19	(Meng et al., 2014)
Yangtze River	China	Sediment	0.05	1.44	0.395	(Pan et al., 2014a)

Hai River and Tributaries	China	Sediment	n.a.	n.a.	0.79	(Pan et al., 2015)
Liao River	China	Sediment	n.a.	n.a.	0.48	
Zhujiang River	China	Sediment	n.a.	n.a.	1.3	
Dongijang River	China	Sediment	n.a.	n.a.	0.69	
Yellow River	China	Sediment	n.a.	n.a.	1.12	
Yangtze River Estuary	China	Sediment	72.9	536.7	236.2	(Pan and You, 2010)
Lake Taihu	China	Sediment	5.8	34.6	18.7	(Pan et al., 2014b)
Tianjin	China	Sediment	0.062	8.54	1.33	(Pan et al., 2011)
Lake Chaohu Area	China	Sediment	0.72	2.43	1.449	(Qi et al., 2015)
Xiaoqing River	China	Sediment	0.33	107	18.21	(Shi et al., 2015)
Xiaoqing River	China	Sediment	n.a.	n.a.	555.79	(Song et al., 2018)
Daling River Basin	China	Sediment	3.76	55.08	10.68	(Wang et al., 2015)
South China Sea Coastal Region	China	Sediment	0.0032	0.079	0.025	(Wang et al., 2019a)
Yellow River Estuary	China	Sediment	75.48	456.98	198.81	(Wang et al., 2013b)
North Bohai Sea Area	China	Sediment	n.d.	4.31	0.62	(Wang et al., 2011b)
Tianjin, China	China	Sediment	1.5	7.8	3.74	(Wang et al., 2012b)
Guanting Reservoir	China	Sediment	0.27	1.6	0.69	(Wang et al., 2011a)
Beijing Airport Area	China	Sediment	1.6	34.32	6.79	(Wang et al., 2016)
Northwest of downtown Hangzhou City	China	Sediment	5.85	161.86	40.8	(Xu et al., 2021)
East China Sea	China	Sediment	n.d.	34.8	9	(Yan et al., 2015)
Taihu Lake	China	Sediment	0.23	1.3	0.69	(Yang et al., 2011)
Liao River	China	Sediment	0.25	1.1	0.5	
Huaihe River	China	Sediment	0.52	16.33	3.47	(Zhao et al., 2014a)
Pearl River Delta	China	Sediment	n.d.	3.11	1.32	(Zhao et al., 2014b)
Bohai Bay and Tributaries	China	Sediment	0.7	4.13	1.78	(Zhao et al., 2020)

Dayan River	China	Sediment	0.01	3.72	0.63	(Zheng et al., 2015)
Tangxun Lake	China	Sediment	40.25	798.56	150.04	(Zhou et al., 2013)
South Bohai Coastal Rivers	China	Sediment	0.098	31.92	1.8	(Zhu et al., 2014)
Bay of Bengal	India	Sediment	n.d.	14.09	8.51	(Corsolini et al., 2012)
Ariake Sea	Japan	Sediment	n.a.	n.a.	1.5	(Nakata et al., 2006)
Tokyo Bay	Japan	Sediment	0.29	1.69	0.76	(Sakurai et al., 2010)
Several Rivers in the Kyoto City Area	Japan	Sediment	n.d.	22	6.02	(Senthilkumar et al., 2007)
Coastal Waters of South Korea	South Korea	Sediment	0.045	1.13	0.33	(Lee et al., 2020a)
Asan Lake Area	South Korea	Sediment	0.04	15	2.51	(Lee et al., 2020b)
Pohang/Gyeongju	South Korea	Sediment	22.96	84.96	48.2	(Seo et al., 2019)
Nationwide Survey	Vietnam	Sediment	n.d.	23.4	3.02	(Lam et al., 2017)
Africa and Oceania						
Location	Country	Media	Min	Max	Mean	Reference
Sydney Harbor	Australia	Sediment	n.a.	n.a.	3.16	(Thompson et al., 2011)
Lake Tana	Ethiopia	Sediment	0.23	0.5	0.3	(Ahrens et al., 2016)
Lake Victoria	Kenya	Sediment	n.d.	146.4	25.59	(Orata et al., 2011)
Maritime Environment (Ocean/Sea)						
Location	Country	Media	Min	Max	Mean	Reference
North Bering Sea	-	Sediment	0.55	1.2	0.85	(Kahkashan et al., 2019)
Chukchi Sea	-	Sediment	0.8	2.67	1.27	
Bering Sea	-	Sediment	0.06	1.73	0.79	(Lin et al., 2020)
Chukchi Sea	-	Sediment	0.11	1.54	0.6	
Canadian Basin	-	Sediment	0.06	0.63	0.19	

n.d. – not detected/below detections limits/below reporting limits; n.a. – information not available

Table 3.8. Global distribution of PFAS in Groundwater. Information on location, media, mean and range ∑PFAS in groundwater (ng L^{-1}) is provided.

The Americas						
Location	Country	Media	Min	Max	Mean	Reference
Itanhem River Basin	Brazil	Groundwater	n.a.	n.a.	5.73	(Nascimento et al., 2018)
Toronto/Lake Ontario Area	Canada	Groundwater	2.11	10.71	5.57	(Meyer et al., 2011)
Decatur Area	USA	Groundwater	n.d.	19354.1	1637.4	(Lindstrom et al., 2011a)
Naval Air Station Fallon	USA	Groundwater	n.d.	7090000	1907500	(Moody and Field, 1999)
Tyndall Air Force Base	USA	Groundwater	n.d.	298000	145250	
Wurtsmith Air Force Base	USA	Groundwater	13000	324000	119200	(Moody et al., 2003)
NJ State Raw Drinking Water Source	USA	Groundwater	n.d.	138	30.78	(Post et al., 2013)
Ellsworth Air Force Base, SD	USA	Groundwater	200	1477600	395226.9	(Houtz et al., 2013)
Pease Air Force Base	USA	Groundwater	n.d.	93.6	22.19	(Steele et al., 2018)
Near Twin Cities	USA	Groundwater	n.d.	25300	5619.44	(Xiao et al., 2015)
Europe						
Location	Country	Media	Min	Max	Mean	Reference
Blekinge	Sweden	Groundwater	n.d.	14	6.84	(Gobelius et al., 2018)
Dalarna	Sweden	Groundwater	n.d.	0.2	0.2	
Gävleborg	Sweden	Groundwater	n.d.	34	2.69	
Gotland	Sweden	Groundwater	n.d.	34	1.33	
Halland	Sweden	Groundwater	0.2	270	36.23	
Jämtland	Sweden	Groundwater	n.d.	3.2	0.48	
Jönköping	Sweden	Groundwater	n.d.	n.d.	n.d.	
Kalmar	Sweden	Groundwater	n.d.	49	10.48	
Kronoberg	Sweden	Groundwater	0.1	0.4	0.7	
Norrbotten	Sweden	Groundwater	n.d.	101	11.89	
Örebro	Sweden	Groundwater	0.4	2.7	1.55	
Östergötland	Sweden	Groundwater	0.3	11	3.33	
Skåne	Sweden	Groundwater	0.2	160	53.14	

Södermanland	Sweden	Groundwater	n.d.	21	7.45	
Stockholm	Sweden	Groundwater	n.d.	22	8.58	
Uppsala	Sweden	Groundwater	n.d.	5.6	1.68	
Värmland	Sweden	Groundwater	n.d.	0.2	0.09	
Västerbotten	Sweden	Groundwater	n.d.	n.d.	n.d.	
Västernorrland	Sweden	Groundwater	0.3	6.5	1.79	
Västmanland	Sweden	Groundwater	n.d.	32	6.97	
Västra Götaland	Sweden	Groundwater	n.d.	6400	249.07	
Near Military Airport Stockholm	Sweden	Groundwater	1.3	51040	4823.56	(Filipovic et al., 2015)
Asia						
Location	Country	Media	Min	Max	Mean	Reference
East China Sea Coastal Area	China	Groundwater	n.d.	614.1	74.82	(Chen et al., 2016b)
Yellow Sea Coastal Region	China	Groundwater	2.7	1224.19	111.59	(Wei et al., 2018)
Fuxin Area	China	Groundwater	1038.38	15729.4	5934.59	(Chen et al., 2018a)
Tianjin Urban Area	China	Groundwater	0.32	8.3	2.4	(Qi et al., 2016)
Fluorotelomer Industrial Park near Fuxin	China	Groundwater	216	26700	13521	(Bao et al., 2019)
Shijiazhuang Area	China	Groundwater	0.56	13.34	2.35	(Liu et al., 2019b)
Baihe River Area	China	Groundwater	2.1	54.7	28.86	(Liu et al., 2018)
River Xi, Fuxin	China	Groundwater	6.03	1400	485.21	(Bao et al., 2011)
Northwest of downtown Hangzhou City	China	Groundwater	17.29	163.24	71.5	(Xu et al., 2021)
Ganges basin	India	Groundwater	7.46	13.2	10.14	(Sharma et al., 2016)
Tokyo Bay Area	Japan	Groundwater	1.87	269.65	51.65	(Murakami et al., 2009)
Nationwide Survey	Vietnam	Groundwater	n.d.	8.88	3.55	(Lam et al., 2017)
Oceania						
Location	Country	Media	Min	Max	Mean	Reference
Port Melbourne Area	Australia	Groundwater	26	5200	561.62	(Hepburn et al., 2019)

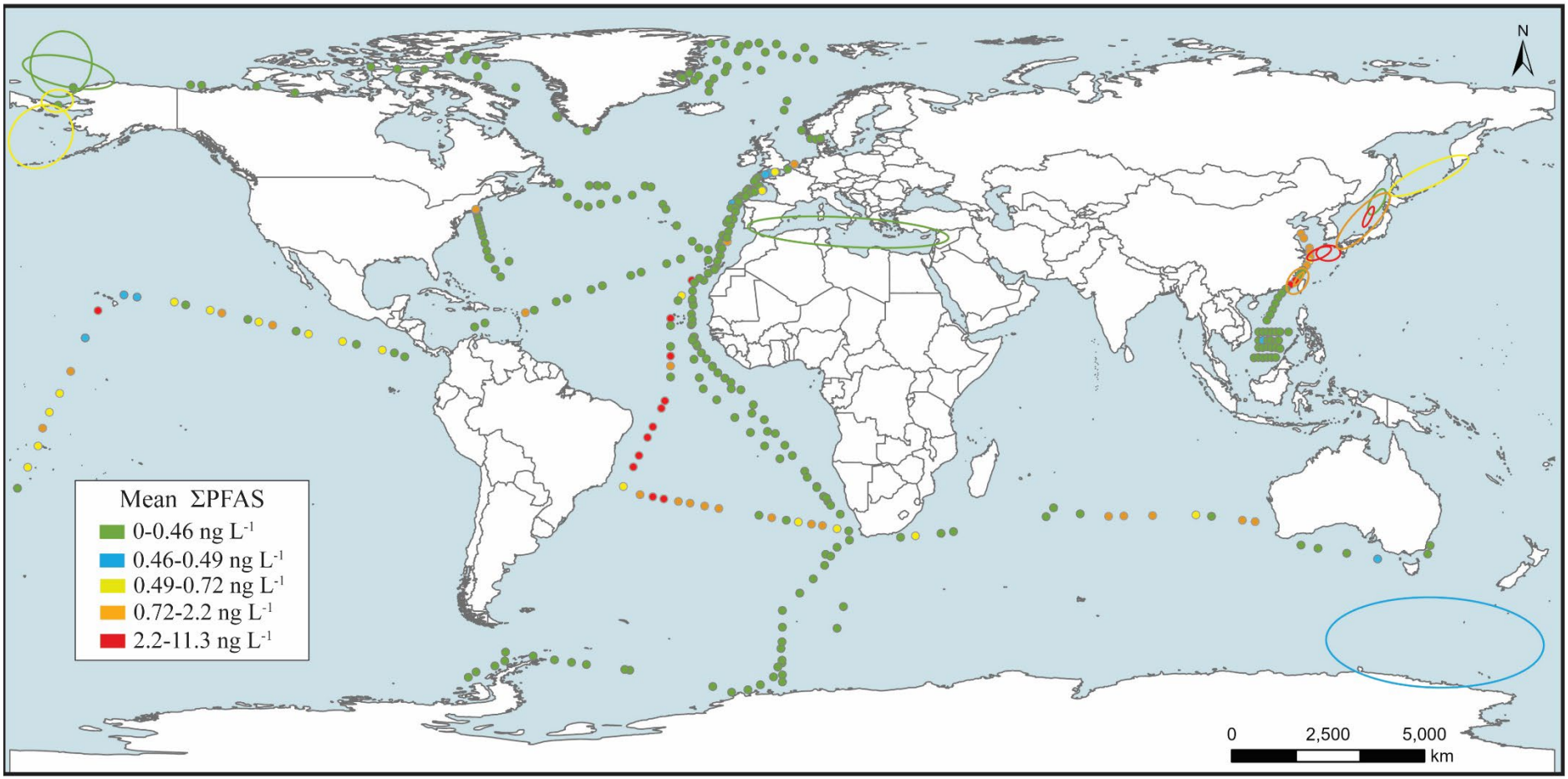

Figure 3.7. Global Distribution of PFAS in Maritime Environments. Concentrations are expressed in ng L^{-1}.

Table 3.9. Summary Statistics (range, mean, median, and percentile) for the concentrations of the 15 most targeted analytes in Surface Water. Concentrations are expressed in ng L^{-1}.

Substance	Min	Max	Mean	Median	75th	90th
PFBS	n.d.	18,000	68.1	0.27	2.1	11.9
PFHxS	n.d.	134,000	141.2	0.20	1.3	8.4
PFOS	n.d.	2,210,000	1524.5	1.1	5.7	27.9
PFDS	n.d.	59.0	0.12	n.d.	n.d.	0.020
PFBA	n.d.	47,800	118.6	0.48	3.9	28.9
PFPeA	n.d.	11,122	25.5	0.37	2.6	12.4
PFHxA	n.d.	20,194	45.9	1.1	5.0	18.0
PFHpA	n.d.	42,567	52.5	0.58	2.5	8.9
PFOA	n.d.	578,970	841.6	3.3	13.8	58.8
PFNA	n.d.	1,122	3.3	0.21	1.0	3.6
PFDA	n.d.	838.0	1.6	0.020	0.40	1.6
PFUnDA	n.d.	190.0	0.58	n.d.	0.052	0.45
PFDoDA	n.d.	51.0	0.15	n.d.	n.d.	0.032
PFTriDA	n.d.	9.8	0.024	n.d.	n.d.	0.019
FOSA	n.d.	282.5	0.68	n.d.	0.060	0.35

Table 3.10. Summary Statistics (range, mean, and quartiles) of the concentration of the 15 most targeted analytes in Sediment. Concentrations are expressed in ng g^{-1}.

Substance	Min	Max	Mean	Median	75th	90th
PFBS	n.d.	114.0	1.5	n.d.	0.18	0.64
PFHxS	n.d.	21.3	0.28	n.d.	0.10	0.34
PFOS	n.d.	623.0	3.9	0.18	0.79	4.2
PFDS	n.d.	88.2	0.34	n.d.	0.006	0.10
PFBA	n.d.	84.0	1.4	n.d.	0.29	1.79
PFPeA	n.d.	13.3	0.13	n.d.	0.050	0.23
PFHxA	n.d.	20.3	0.23	n.d.	0.074	0.32
PFHpA	n.d.	21.8	0.19	n.d.	0.070	0.31
PFOA	n.d.	203.0	1.4	0.10	0.56	1.77
PFNA	n.d.	19.0	0.15	n.d.	0.10	0.27
PFDA	n.d.	77.1	0.29	0.010	0.12	0.34
PFUnDA	n.d.	31.7	0.33	0.004	0.13	0.43
PFDoDA	n.d.	23.3	0.23	n.d.	0.08	0.23
PFTriDA	n.d.	14.0	0.14	n.d.	0.012	0.14
PFTeDA	n.d.	25.9	0.16	n.d.	0.006	0.20

Table 3.11. Summary Statistics (range, mean, and quartiles) of the concentration of the 15 most targeted analytes in Groundwater. Concentrations are expressed in ng L^{-1}.

Substance	Min	Max	Mean	Median	75th	90th
PFBS	n.d.	896.3	n.d.	140,000	8.0	0.71
PFHxS	n.d.	3,925	1.1	530,000	26.0	12.0
PFOS	n.d.	1,199	3.8	110,000	37.8	12.0
PFBA	n.d.	1,055	0.39	87,000	33.5	4.6
PFPeA	n.d.	2,430	0.20	220,000	54.5	5.3
PFHxA	n.d.	5,510	0.44	372,000	121.0	4.0
PFHpA	n.d.	476.1	n.d.	149,000	6.0	0.52
PFOA	n.d.	8,045	n.d.	6,570,000	149.0	6.2
PFNA	n.d.	18.6	n.d.	2,900	1.3	0.090
PFDA	n.d.	0.51	n.d.	113.0	0.41	n.d.
PFUnDA	n.d.	0.49	n.d.	28.9	0.73	n.d.
PFDoDA	n.d.	0.24	n.d.	59.0	0.19	n.d.
PFTriDA	n.d.	0.030	n.d.	4.1	n.d.	n.d.
FOSA	n.d.	0.12	n.d.	9.0	0.30	0.10
6:2 FTS	n.d.	5,064	n.d.	270,000	11.7	0.88

3.5 References

3M. Letter to the US EPA - TSCA Section 8(e) -- Perfluorooctane Sulfonate 1998.

3M. Letter to the US EPA: Phase-out Plan for POSF-Based Products, 2000.

Ademollo N, Spataro F, Rauseo J, Pescatore T, Fattorini N, Valsecchi S, et al. Occurrence, distribution and pollution pattern of legacy and emerging organic pollutants in surface water of the Kongsfjorden (Svalbard, Norway): Environmental contamination, seasonal trend and climate change. Mar Pollut Bull 2021; 163: 111900.

Ahrens L, Barber JL, Xie Z, Ebinghaus R. Longitudinal and latitudinal distribution of perfluoroalkyl compounds in the surface water of the Atlantic Ocean. Environmental science & technology 2009a; 43: 3122-3127.

Ahrens L, Felizeter S, Ebinghaus R. Spatial distribution of polyfluoroalkyl compounds in seawater of the German Bight. Chemosphere 2009b; 76: 179-84.

Ahrens L, Gashaw H, Sjoholm M, Gebrehiwot SG, Getahun A, Derbe E, et al. Poly- and perfluoroalkylated substances (PFASs) in water, sediment and fish muscle tissue from Lake Tana, Ethiopia and implications for human exposure. Chemosphere 2016; 165: 352-357.

Ahrens L, Gerwinski W, Theobald N, Ebinghaus R. Sources of polyfluoroalkyl compounds in the North Sea, Baltic Sea and Norwegian Sea: Evidence from their spatial distribution in surface water. Mar Pollut Bull 2010a; 60: 255-60.

Ahrens L, Xie Z, Ebinghaus R. Distribution of perfluoroalkyl compounds in seawater from northern Europe, Atlantic Ocean, and Southern Ocean. Chemosphere 2010b; 78: 1011-6.

Aly NA, Luo YS, Liu Y, Casillas G, McDonald TJ, Kaihatu JM, et al. Temporal and spatial analysis of per and polyfluoroalkyl substances in surface waters of Houston ship channel following a large-scale industrial fire incident. Environ Pollut 2020; 265: 115009.

Andrews DQ, Naidenko OV. Population-Wide Exposure to Per- and Polyfluoroalkyl Substances from Drinking Water in the United States. Environmental Science & Technology Letters 2020; 7: 931-936.

ATSDR. ATSDR's Minimal Risk Levels (MRLs) and Environmental Media Evaluation Guides (EMEGs) for PFAS, 2018.

Awad E, Zhang X, Bhavsar SP, Petro S, Crozier PW, Reiner EJ, et al. Long-term environmental fate of perfluorinated compounds after accidental release at Toronto airport. Environ Sci Technol 2011; 45: 8081-9.

Bai X, Son Y. Perfluoroalkyl substances (PFAS) in surface water and sediments from two urban watersheds in Nevada, USA. Sci Total Environ 2021; 751: 141622.

Bao J, Jin Y, Liu W, Ran X, Zhang Z. Perfluorinated compounds in sediments from the Daliao River system of northeast China. Chemosphere 2009; 77: 652-7.

Bao J, Liu W, Liu L, Jin Y, Dai J, Ran X, et al. Perfluorinated compounds in the environment and the blood of residents living near fluorochemical plants in Fuxin, China. Environ Sci Technol 2011; 45: 8075-80.

Bao J, Liu W, Liu L, Jin Y, Ran X, Zhang Z. Perfluorinated compounds in urban river sediments from Guangzhou and Shanghai of China. Chemosphere 2010; 80: 123-30.

Bao J, Yu WJ, Liu Y, Wang X, Jin YH, Dong GH. Perfluoroalkyl substances in groundwater and home-produced vegetables and eggs around a fluorochemical industrial park in China. Ecotoxicol Environ Saf 2019; 171: 199-205.

Barzen-Hanson KA, Roberts SC, Choyke S, Oetjen K, McAlees A, Riddell N, et al. Discovery of 40 Classes of Per- and Polyfluoroalkyl Substances in Historical Aqueous Film-Forming Foams (AFFFs) and AFFF-Impacted Groundwater. Environ Sci Technol 2017; 51: 2047-2057.

Becanova J, Komprdova K, Vrana B, Klanova J. Annual dynamics of perfluorinated compounds in sediment: A case study in the Morava River in Zlin district, Czech Republic. Chemosphere 2016; 151: 225-33.

Begley TH, Hsu W, Noonan G, Diachenko G. Migration of fluorochemical paper additives from food-contact paper into foods and food simulants. Food Addit Contam Part A Chem Anal Control Expo Risk Assess 2008; 25: 384-90.

Benskin JP, Ahrens L, Muir DC, Scott BF, Spencer C, Rosenberg B, et al. Manufacturing origin of perfluorooctanoate (PFOA) in Atlantic and Canadian Arctic seawater. Environ Sci Technol 2012; 46: 677-85.

Benskin JP, Yeung LW, Yamashita N, Taniyasu S, Lam PK, Martin JW. Perfluorinated acid isomer profiling in water and quantitative assessment of manufacturing source. Environmental science & technology 2010; 44: 9049-9054.

Beskoski VP, Takemine S, Nakano T, Slavkovic Beskoski L, Gojgic-Cvijovic G, Ilic M, et al. Perfluorinated compounds in sediment samples from the wastewater canal of Pancevo (Serbia) industrial area. Chemosphere 2013; 91: 1408-15.

Blum A, Balan SA, Scheringer M, Trier X, Goldenman G, Cousins IT, et al. The Madrid Statement on Poly- and Perfluoroalkyl Substances (PFASs). Environ Health Perspect 2015; 123: A107-11.

Boulanger B, Vargo J, Schnoor JL, Hornbuckle KC. Detection of perfluorooctane surfactants in Great Lakes water. Environmental science & technology 2004; 38: 4064-4070.

Brennan NM, Evans AT, Fritz MK, Peak SA, von Holst HE. Trends in the Regulation of Per- and Polyfluoroalkyl Substances (PFAS): A Scoping Review. Int J Environ Res Public Health 2021; 18.

Brumovsky M, Karaskova P, Borghini M, Nizzetto L. Per- and polyfluoroalkyl substances in the Western Mediterranean Sea waters. Chemosphere 2016; 159: 308-316.

Buck RC, Franklin J, Berger U, Conder JM, Cousins IT, de Voogt P, et al. Perfluoroalkyl and polyfluoroalkyl substances in the environment: terminology, classification, and origins. Integr Environ Assess Manag 2011; 7: 513-41.

Cai M, Yang H, Xie Z, Zhao Z, Wang F, Lu Z, et al. Per- and polyfluoroalkyl substances in snow, lake, surface runoff water and coastal seawater in Fildes Peninsula, King George Island, Antarctica. J Hazard Mater 2012; 209-210: 335-42.

Cai Y, Wang X, Wu Y, Zhao S, Li Y, Ma L, et al. Temporal trends and transport of perfluoroalkyl substances (PFASs) in a subtropical estuary: Jiulong River Estuary, Fujian, China. Sci Total Environ 2018; 639: 263-270.

Campo J, Lorenzo M, Perez F, Pico Y, Farre M, Barcelo D. Analysis of the presence of perfluoroalkyl substances in water, sediment and biota of the Jucar River (E Spain). Sources, partitioning and relationships with water physical characteristics. Environ Res 2016; 147: 503-12.

Campo J, Perez F, Masia A, Pico Y, Farre M, Barcelo D. Perfluoroalkyl substance contamination of the Llobregat River ecosystem (Mediterranean area, NE Spain). Sci Total Environ 2015; 503-504: 48-57.

Cao Y, Cao X, Wang H, Wan Y, Wang S. Assessment on the distribution and partitioning of perfluorinated compounds in the water and sediment of Nansi Lake, China. Environ Monit Assess 2015; 187: 611.

Casal P, Zhang Y, Martin JW, Pizarro M, Jimenez B, Dachs J. Role of Snow Deposition of Perfluoroalkylated Substances at Coastal Livingston Island (Maritime Antarctica). Environ Sci Technol 2017; 51: 8460-8470.

Castiglioni S, Davoli E, Riva F, Palmiotto M, Camporini P, Manenti A, et al. Mass balance of emerging contaminants in the water cycle of a highly urbanized and industrialized area of Italy. Water Res 2018; 131: 287-298.

Castiglioni S, Valsecchi S, Polesello S, Rusconi M, Melis M, Palmiotto M, et al. Sources and fate of perfluorinated compounds in the aqueous environment and in drinking water of a highly urbanized and industrialized area in Italy. J Hazard Mater 2015; 282: 51-60.

Chen H, Han J, Zhang C, Cheng J, Sun R, Wang X, et al. Occurrence and seasonal variations of per- and polyfluoroalkyl substances (PFASs) including fluorinated alternatives in rivers, drain outlets and the receiving Bohai Sea of China. Environ Pollut 2017; 231: 1223-1231.

Chen H, Sun R, Zhang C, Han J, Wang X, Han G, et al. Occurrence, spatial and temporal distributions of perfluoroalkyl substances in wastewater, seawater and sediment from Bohai Sea, China. Environ Pollut 2016a; 219: 389-398.

Chen H, Yao Y, Zhao Z, Wang Y, Wang Q, Ren C, et al. Multimedia Distribution and Transfer of Per- and Polyfluoroalkyl Substances (PFASs) Surrounding Two Fluorochemical Manufacturing Facilities in Fuxin, China. Environ Sci Technol 2018a; 52: 8263-8271.

Chen H, Zhang C, Han J, Sun R, Kong X, Wang X, et al. Levels and spatial distribution of perfluoroalkyl substances in China Liaodong Bay basin with concentrated fluorine industry parks. Mar Pollut Bull 2015a; 101: 965-71.

Chen L, Tsui MMP, Lam JCW, Wang Q, Hu C, Wai OWH, et al. Contamination by perfluoroalkyl substances and microbial community structure in Pearl River Delta sediments. Environ Pollut 2019; 245: 218-225.

Chen M, Wang Q, Shan G, Zhu L, Yang L, Liu M. Occurrence, partitioning and bioaccumulation of emerging and legacy per- and polyfluoroalkyl substances in Taihu Lake, China. Sci Total Environ 2018b; 634: 251-259.

Chen S, Jiao XC, Gai N, Li XJ, Wang XC, Lu GH, et al. Perfluorinated compounds in soil, surface water, and groundwater from rural areas in eastern China. Environ Pollut 2016b; 211: 124-31.

Chen X, Zhu L, Pan X, Fang S, Zhang Y, Yang L. Isomeric specific partitioning behaviors of perfluoroalkyl substances in water dissolved phase, suspended particulate matters and sediments in Liao River Basin and Taihu Lake, China. Water Res 2015b; 80: 235-44.

Choi H, Bae IA, Choi JC, Park SJ, Kim M. Perfluorinated compounds in food simulants after migration from fluorocarbon resin-coated frying pans, baking utensils, and non-stick baking papers on the Korean market. Food Addit Contam Part B Surveill 2018; 11: 264-272.

Clara M, Gans O, Weiss S, Sanz-Escribano D, Scharf S, Scheffknecht C. Perfluorinated alkylated substances in the aquatic environment: an Austrian case study. Water Res 2009; 43: 4760-8.

Corsolini S, Sarkar SK, Guerranti C, Bhattacharya BD, Rakshit D, Jonathan MP, et al. Perfluorinated compounds in surficial sediments of the Ganges River and adjacent Sundarban mangrove wetland, India. Mar Pollut Bull 2012; 64: 2829-33.

Cui Q, Pan Y, Zhang H, Sheng N, Dai J. Elevated concentrations of perfluorohexanesulfonate and other per- and polyfluoroalkyl substances in Baiyangdian Lake (China): Source characterization and exposure assessment. Environ Pollut 2018; 241: 684-691.

D'Agostino LA, Mabury SA. Certain Perfluoroalkyl and Polyfluoroalkyl Substances Associated with Aqueous Film Forming Foam Are Widespread in Canadian Surface Waters. Environ Sci Technol 2017; 51: 13603-13613.

D'eon JC, Crozier PW, Furdui VI, Reiner EJ, Libelo EL, Mabury SA. Perfluorinated phosphonic acids in Canadian surface waters and wastewater treatment plant effluent: discovery of a new class of perfluorinated acids. Environmental Toxicology and Chemistry: An International Journal 2009; 28: 2101-2107.

De Silva AO, Spencer C, Scott BF, Backus S, Muir DC. Detection of a cyclic perfluorinated acid, perfluoroethylcyclohexane sulfonate, in the Great Lakes of North America. Environ Sci Technol 2011; 45: 8060-6.

DEPA. Short-chain Polyfluoroalkyl Substances (PFAS). Danish Environmental Protection Agency, 2015, pp. 106.

Ding G, Xue H, Yao Z, Wang Y, Ge L, Zhang J, et al. Occurrence and distribution of perfluoroalkyl substances (PFASs) in the water dissolved phase and suspended particulate matter of the Dalian Bay, China. Chemosphere 2018; 200: 116-123.

Dong W, Liu B, Song Y, Zhang H, Li J, Cui X. Occurrence and Partition of Perfluorinated Compounds (PFCs) in Water and Sediment from the Songhua River, China. Arch Environ Contam Toxicol 2018; 74: 492-501.

Duong HT, Kadokami K, Shirasaka H, Hidaka R, Chau HTC, Kong L, et al. Occurrence of perfluoroalkyl acids in environmental waters in Vietnam. Chemosphere 2015; 122: 115-124.

Earnshaw MR, Paul AG, Loos R, Tavazzi S, Paracchini B, Scheringer M, et al. Comparing measured and modelled PFOS concentrations in a UK freshwater catchment and estimating emission rates. Environ Int 2014; 70: 25-31.

Eriksson U, Karrman A, Rotander A, Mikkelsen B, Dam M. Perfluoroalkyl substances (PFASs) in food and water from Faroe Islands. Environ Sci Pollut Res Int 2013; 20: 7940-8.

EUC. Towards a Sustainable Chemicals Policy Strategy of the Union Council conclusions. Council of the European Union, 2019.

Falandysz J, Rostkowski P, Jarzynska G, Falandysz JJ, Taniyasu S, Yamashita N. Determination of perfluorinated alkylated substances in sediments and sediment core from the Gulf of Gdansk, Baltic Sea. J Environ Sci Health A Tox Hazard Subst Environ Eng 2012; 47: 428-34.

Fauconier G, Groffen T, Wepener V, Bervoets L. Perfluorinated compounds in the aquatic food chains of two subtropical estuaries. Sci Total Environ 2020; 719: 135047.

Filipovic M, Woldegiorgis A, Norstrom K, Bibi M, Lindberg M, Osteras AH. Historical usage of aqueous film forming foam: a case study of the widespread distribution of perfluoroalkyl acids from a military airport to groundwater, lakes, soils and fish. Chemosphere 2015; 129: 39-45.

Gallen C, Baduel C, Lai FY, Thompson K, Thompson J, Warne M, et al. Spatio-temporal assessment of perfluorinated compounds in the Brisbane River system, Australia: impact of a major flood event. Mar Pollut Bull 2014; 85: 597-605.

Gao L, Liu J, Bao K, Chen N, Meng B. Multicompartment occurrence and partitioning of alternative and legacy per- and polyfluoroalkyl substances in an impacted river in China. Sci Total Environ 2020; 729: 138753.

Gao Y, Fu J, Meng M, Wang Y, Chen B, Jiang G. Spatial distribution and fate of perfluoroalkyl substances in sediments from the Pearl River Estuary, South China. Mar Pollut Bull 2015; 96: 226-34.

Gao Y, Fu J, Zeng L, Li A, Li H, Zhu N, et al. Occurrence and fate of perfluoroalkyl substances in marine sediments from the Chinese Bohai Sea, Yellow Sea, and East China Sea. Environ Pollut 2014; 194: 60-68.

Gebbink WA, van Asseldonk L, van Leeuwen SPJ. Presence of Emerging Per- and Polyfluoroalkyl Substances (PFASs) in River and Drinking Water near a Fluorochemical Production Plant in the Netherlands. Environ Sci Technol 2017; 51: 11057-11065.

Gilljam J, Leonel J, Cousins IT, Benskin JP. Is Ongoing Sulfluramid Use in South America a Significant Source of Perfluorooctanesulfonate (PFOS)? Production Inventories, Environmental Fate, and Local Occurrence. Environ Sci Technol 2016; 50: 653-9.

Gobelius L, Hedlund J, Durig W, Troger R, Lilja K, Wiberg K, et al. Per- and Polyfluoroalkyl Substances in Swedish Groundwater and Surface Water: Implications for Environmental Quality Standards and Drinking Water Guidelines. Environ Sci Technol 2018; 52: 4340-4349.

Gomez C, Vicente J, Echavarri-Erasun B, Porte C, Lacorte S. Occurrence of perfluorinated compounds in water, sediment and mussels from the Cantabrian Sea (North Spain). Mar Pollut Bull 2011; 62: 948-55.

Gonzalez-Gaya B, Dachs J, Roscales JL, Caballero G, Jimenez B. Perfluoroalkylated substances in the global tropical and subtropical surface oceans. Environ Sci Technol 2014; 48: 13076-84.

Goodrow SM, Ruppel B, Lippincott RL, Post GB, Procopio NA. Investigation of levels of perfluoroalkyl substances in surface water, sediment and fish tissue in New Jersey, USA. Sci Total Environ 2020; 729: 138839.

Groffen T, Wepener V, Malherbe W, Bervoets L. Distribution of perfluorinated compounds (PFASs) in the aquatic environment of the industrially polluted Vaal River, South Africa. Sci Total Environ 2018; 627: 1334-1344.

Guelfo JL, Adamson DT. Evaluation of a national data set for insights into sources, composition, and concentrations of per- and polyfluoroalkyl substances (PFASs) in U.S. drinking water. Environ Pollut 2018; 236: 505-513.

Guo C, Zhang Y, Zhao X, Du P, Liu S, Lv J, et al. Distribution, source characterization and inventory of perfluoroalkyl substances in Taihu Lake, China. Chemosphere 2015; 127: 201-7.

Habibullah-Al-Mamun M, Ahmed MK, Raknuzzaman M, Islam MS, Negishi J, Nakamichi S, et al. Occurrence and distribution of perfluoroalkyl acids (PFAAs) in surface water and sediment of a tropical coastal area (Bay of Bengal coast, Bangladesh). Sci Total Environ 2016; 571: 1089-104.

Han T, Gao L, Chen J, He X, Wang B. Spatiotemporal variations, sources and health risk assessment of perfluoroalkyl substances in a temperate bay adjacent to metropolis, North China. Environ Pollut 2020; 265: 115011.

Hansen KJ, Johnson H, Eldridge J, Butenhoff J, Dick L. Quantitative characterization of trace levels of PFOS and PFOA in the Tennessee River. Environmental Science & Technology 2002; 36: 1681-1685.

He X, Li A, Wang S, Chen H, Yang Z. Perfluorinated substance assessment in sediments of a large-scale reservoir in Danjiangkou, China. Environ Monit Assess 2018; 190: 66.

Hepburn E, Madden C, Szabo D, Coggan TL, Clarke B, Currell M. Contamination of groundwater with per- and polyfluoroalkyl substances (PFAS) from legacy landfills in an urban re-development precinct. Environ Pollut 2019; 248: 101-113.

Heydebreck F, Tang J, Xie Z, Ebinghaus R. Alternative and Legacy Perfluoroalkyl Substances: Differences between European and Chinese River/Estuary Systems. Environ Sci Technol 2015; 49: 8386-95.

Higgins CP, Field JA, Criddle CS, Luthy RG. Quantitative determination of perfluorochemicals in sediments and domestic sludge. Environmental science & technology 2005; 39: 3946-3956.

Higgins CP, Luthy RG. Sorption of perfluorinated surfactants on sediments. Environmental science & technology 2006; 40: 7251-7256.

Hlouskova V, Lankova D, Kalachova K, Hradkova P, Poustka J, Hajslova J, et al. Brominated flame retardants and perfluoroalkyl substances in sediments from the Czech aquatic ecosystem. Sci Total Environ 2014; 470-471: 407-16.

Hopkins ZR, Sun M, DeWitt JC, Knappe DR. Recently detected drinking water contaminants: GenX and other per-and polyfluoroalkyl ether acids. Journal-American Water Works Association 2018; 110: 13-28.

Houtz EF, Higgins CP, Field JA, Sedlak DL. Persistence of perfluoroalkyl acid precursors in AFFF-impacted groundwater and soil. Environ Sci Technol 2013; 47: 8187-95.

Hu XC, Andrews DQ, Lindstrom AB, Bruton TA, Schaider LA, Grandjean P, et al. Detection of Poly- and Perfluoroalkyl Substances (PFASs) in U.S. Drinking Water Linked to Industrial Sites, Military Fire Training Areas, and Wastewater Treatment Plants. Environ Sci Technol Lett 2016; 3: 344-350.

Jiang JJ, Okvitasari AR, Huang FY, Tsai CS. Characteristics, pollution patterns and risks of Perfluoroalkyl substances in drinking water sources of Taiwan. Chemosphere 2021; 264: 128579.

Jin H, Zhang Y, Zhu L, Martin JW. Isomer profiles of perfluoroalkyl substances in water and soil surrounding a chinese fluorochemical manufacturing park. Environ Sci Technol 2015; 49: 4946-54.

Joerss H, Schramm TR, Sun L, Guo C, Tang J, Ebinghaus R. Per- and polyfluoroalkyl substances in Chinese and German river water - Point source- and country-specific fingerprints including unknown precursors. Environ Pollut 2020; 267: 115567.

Ju X, Jin Y, Sasaki K, Saito N. Perfluorinated surfactants in surface, subsurface water and microlayer from Dalian coastal waters in China. Environmental science & technology 2008; 42: 3538-3542.

Junttila, Vähä, Perkola, Räike, Siimes, Mehtonen, et al. PFASs in Finnish Rivers and Fish and the Loading of PFASs to the Baltic Sea. Water 2019; 11.

Kahkashan S, Wang X, Chen J, Bai Y, Ya M, Wu Y, et al. Concentration, distribution and sources of perfluoroalkyl substances and organochlorine pesticides in surface sediments of the northern Bering Sea, Chukchi Sea and adjacent Arctic Ocean. Chemosphere 2019; 235: 959-968.

KEMI. Occurrence and use of highly fluorinated substances and alternatives. Swedish Chemical Agency, 2015, pp. 112.

Kim JW, Tue NM, Isobe T, Misaki K, Takahashi S, Viet PH, et al. Contamination by perfluorinated compounds in water near waste recycling and disposal sites in Vietnam. Environ Monit Assess 2013; 185: 2909-19.

Kim S-K, Kannan K. Perfluorinated acids in air, rain, snow, surface runoff, and lakes: relative importance of pathways to contamination of urban lakes. Environmental science & technology 2007; 41: 8328-8334.

Koch A, Yukioka S, Tanaka S, Yeung LWY, Karrman A, Wang T. Characterization of an AFFF impacted freshwater environment using total fluorine, extractable organofluorine and suspect per- and polyfluoroalkyl substance screening analysis. Chemosphere 2021; 276: 130179.

Konwick BJ, Tomy GT, Ismail N, Peterson JT, Fauver RJ, Higginbotham D, et al. Concentrations and patterns of perfluoroalkyl acids in Georgia, USA surface waters near and distant to a major use source. Environmental Toxicology and Chemistry: An International Journal 2008; 27: 2011-2018.

Kotthoff M, Muller J, Jurling H, Schlummer M, Fiedler D. Perfluoroalkyl and polyfluoroalkyl substances in consumer products. Environ Sci Pollut Res Int 2015; 22: 14546-59.

Kunacheva C, Boontanon SK, Fujii S, Tanaka S, Musirat C, Artsalee C, et al. Contamination of perfluorinated compounds (PFCs) in Chao Phraya River and Bangpakong River, Thailand. Water Sci Technol 2009; 60: 975-82.

Kwok KY, Wang XH, Ya M, Li Y, Zhang XH, Yamashita N, et al. Occurrence and distribution of conventional and new classes of per- and polyfluoroalkyl substances (PFASs) in the South China Sea. J Hazard Mater 2015; 285: 389-97.

Labadie P, Chevreuil M. Partitioning behaviour of perfluorinated alkyl contaminants between water, sediment and fish in the Orge River (nearby Paris, France). Environ Pollut 2011; 159: 391-7.

Lam NH, Cho CR, Kannan K, Cho HS. A nationwide survey of perfluorinated alkyl substances in waters, sediment and biota collected from aquatic environment in Vietnam: Distributions and bioconcentration profiles. J Hazard Mater 2017; 323: 116-127.

Lam NH, Min B-K, Cho C-R, Park K-H, Ryu J-S, Kim P-J, et al. Distribution of perfluoroalkyl substances in water from industrialized bays, rivers and agricultural areas in Korea. Toxicology and Environmental Health Sciences 2016; 8: 43-55.

Langberg HA, Arp HPH, Breedveld GD, Slinde GA, Hoiseter A, Gronning HM, et al. Paper product production identified as the main source of per- and polyfluoroalkyl substances (PFAS) in a Norwegian lake: Source and historic emission tracking. Environ Pollut 2020; 273: 116259.

Lasier PJ, Washington JW, Hassan SM, Jenkins TM. Perfluorinated chemicals in surface waters and sediments from northwest Georgia, USA, and their bioaccumulation in Lumbriculus variegatus. Environ Toxicol Chem 2011; 30: 2194-201.

Lee JW, Lee HK, Lim JE, Moon HB. Legacy and emerging per- and polyfluoroalkyl substances (PFASs) in the coastal environment of Korea: Occurrence, spatial distribution, and bioaccumulation potential. Chemosphere 2020a; 251: 126633.

Lee YM, Lee JY, Kim MK, Yang H, Lee JE, Son Y, et al. Concentration and distribution of per- and polyfluoroalkyl substances (PFAS) in the Asan Lake area of South Korea. J Hazard Mater 2020b; 381: 120909.

Leon VM, Vinas L, Concha-Grana E, Fernandez-Gonzalez V, Salgueiro-Gonzalez N, Moscoso-Perez C, et al. Identification of contaminants of emerging concern with potential environmental risk in Spanish continental shelf sediments. Sci Total Environ 2020; 742: 140505.

Li F, Huang H, Xu Z, Ni H, Yan H, Chen R, et al. Investigation of Perfluoroalkyl Substances (PFASs) in Sediments from the Urban Lakes of Anqing City, Anhui Province, China. Bull Environ Contam Toxicol 2017; 99: 760-764.

Li F, Zhang C, Qu Y, Chen J, Chen L, Liu Y, et al. Quantitative characterization of short- and long-chain perfluorinated acids in solid matrices in Shanghai, China. Sci Total Environ 2010; 408: 617-23.

Li L, Zheng H, Wang T, Cai M, Wang P. Perfluoroalkyl acids in surface seawater from the North Pacific to the Arctic Ocean: Contamination, distribution and transportation. Environ Pollut 2018; 238: 168-176.

Lin AY, Panchangam SC, Lo CC. The impact of semiconductor, electronics and optoelectronic industries on downstream perfluorinated chemical contamination in Taiwanese rivers. Environ Pollut 2009; 157: 1365-72.

Lin Y, Jiang JJ, Rodenburg LA, Cai M, Wu Z, Ke H, et al. Perfluoroalkyl substances in sediments from the Bering Sea to the western Arctic: Source and pathway analysis. Environ Int 2020; 139: 105699.

Lindstrom AB, Strynar MJ, Delinsky AD, Nakayama SF, McMillan L, Libelo EL, et al. Application of WWTP biosolids and resulting perfluorinated compound contamination of surface and well water in Decatur, Alabama, USA. Environ Sci Technol 2011a; 45: 8015-21.

Lindstrom AB, Strynar MJ, Libelo EL. Polyfluorinated compounds: past, present, and future. Environ Sci Technol 2011b; 45: 7954-61.

Liu B, Zhang H, Xie L, Li J, Wang X, Zhao L, et al. Spatial distribution and partition of perfluoroalkyl acids (PFAAs) in rivers of the Pearl River Delta, southern China. Sci Total Environ 2015a; 524-525: 1-7.

Liu J, Zhao X, Liu Y, Qiao X, Wang X, Ma M, et al. High contamination, bioaccumulation and risk assessment of perfluoroalkyl substances in multiple environmental media at the Baiyangdian Lake. Ecotoxicol Environ Saf 2019a; 182: 109454.

Liu WX, He W, Qin N, Kong XZ, He QS, Yang B, et al. Temporal-spatial distributions and ecological risks of perfluoroalkyl acids (PFAAs) in the surface water from the fifth-largest freshwater lake in China (Lake Chaohu). Environ Pollut 2015b; 200: 24-34.

Liu Y, Li X, Wang X, Qiao X, Hao S, Lu J, et al. Contamination Profiles of Perfluoroalkyl Substances (PFAS) in Groundwater in the Alluvial-Pluvial Plain of Hutuo River, China. Water (Basel) 2019b; 11: 1-2316.

Liu Y, Ma L, Yang Q, Li G, Zhang F. Occurrence and spatial distribution of perfluorinated compounds in groundwater receiving reclaimed water through river bank infiltration. Chemosphere 2018; 211: 1203-1211.

Liu Y, Zhang Y, Li J, Wu N, Li W, Niu Z. Distribution, partitioning behavior and positive matrix factorization-based source analysis of legacy and emerging polyfluorinated alkyl substances in the dissolved phase, surface sediment and suspended particulate matter around coastal areas of Bohai Bay, China. Environ Pollut 2019c; 246: 34-44.

Llorca M, Farre M, Pico Y, Muller J, Knepper TP, Barcelo D. Analysis of perfluoroalkyl substances in waters from Germany and Spain. Sci Total Environ 2012; 431: 139-50.

Lofstedt Gilljam J, Leonel J, Cousins IT, Benskin JP. Is Ongoing Sulfluramid Use in South America a Significant Source of Perfluorooctanesulfonate (PFOS)? Production Inventories, Environmental Fate, and Local Occurrence. Environ Sci Technol 2016; 50: 653-9.

Long ER, Dutch M, Weakland S, Chandramouli B, Benskin JP. Quantification of pharmaceuticals, personal care products, and perfluoroalkyl substances in the marine sediments of Puget Sound, Washington, USA. Environ Toxicol Chem 2013; 32: 1701-10.

Loos R, Locoro G, Huber T, Wollgast J, Christoph EH, de Jager A, et al. Analysis of perfluorooctanoate (PFOA) and other perfluorinated compounds (PFCs) in the River Po watershed in N-Italy. Chemosphere 2008; 71: 306-13.

Loos R, Tavazzi S, Mariani G, Suurkuusk G, Paracchini B, Umlauf G. Analysis of emerging organic contaminants in water, fish and suspended particulate matter (SPM) in the Joint Danube Survey using solid-phase extraction followed by UHPLC-MS-MS and GC-MS analysis. Sci Total Environ 2017; 607-608: 1201-1212.

Lorenzo M, Campo J, Farre M, Perez F, Pico Y, Barcelo D. Perfluoroalkyl substances in the Ebro and Guadalquivir river basins (Spain). Sci Total Environ 2016; 540: 191-9.

Lorenzo M, Campo J, Morales Suarez-Varela M, Pico Y. Occurrence, distribution and behavior of emerging persistent organic pollutants (POPs) in a Mediterranean wetland protected area. Sci Total Environ 2019; 646: 1009-1020.

Lu Z, Song L, Zhao Z, Ma Y, Wang J, Yang H, et al. Occurrence and trends in concentrations of perfluoroalkyl substances (PFASs) in surface waters of eastern China. Chemosphere 2015; 119: 820-827.

Ma X, Shan G, Chen M, Zhao J, Zhu L. Riverine inputs and source tracing of perfluoroalkyl substances (PFASs) in Taihu Lake, China. Sci Total Environ 2018; 612: 18-25.

MacInnis JJ, Lehnherr I, Muir DCG, Quinlan R, De Silva AO. Characterization of perfluoroalkyl substances in sediment cores from High and Low Arctic lakes in Canada. Sci Total Environ 2019; 666: 414-422.

McLachlan MS, Holmström KE, Reth M, Berger U. Riverine discharge of perfluorinated carboxylates from the European continent. Environmental Science & Technology 2007; 41: 7260-7265.

Meng J, Wang T, Wang P, Giesy JP, Lu Y. Perfluoroalkyl substances and organochlorine pesticides in sediments from Huaihe watershed in China. J Environ Sci (China) 2014; 26: 2198-206.

Meyer T, De Silva AO, Spencer C, Wania F. Fate of perfluorinated carboxylates and sulfonates during snowmelt within an urban watershed. Environ Sci Technol 2011; 45: 8113-9.

Miner KR, Clifford H, Taruscio T, Potocki M, Solomon G, Ritari M, et al. Deposition of PFAS 'forever chemicals' on Mt. Everest. Sci Total Environ 2021; 759: 144421.

Miranda DA, Benskin JP, Awad R, Lepoint G, Leonel J, Hatje V. Bioaccumulation of Per- and polyfluoroalkyl substances (PFASs) in a tropical estuarine food web. Sci Total Environ 2021; 754: 142146.

Moller A, Ahrens L, Surm R, Westerveld J, van der Wielen F, Ebinghaus R, et al. Distribution and sources of polyfluoroalkyl substances (PFAS) in the River Rhine watershed. Environ Pollut 2010; 158: 3243-50.

Moody CA, Field JA. Determination of perfluorocarboxylates in groundwater impacted by fire-fighting activity. Environmental science & technology 1999; 33: 2800-2806.

Moody CA, Hebert GN, Strauss SH, Field JA. Occurrence and persistence of perfluorooctanesulfonate and other perfluorinated surfactants in groundwater at a fire-training area at Wurtsmith Air Force Base, Michigan, USA. J Environ Monit 2003; 5: 341-5.

Moody CA, Martin JW, Kwan WC, Muir DC, Mabury SA. Monitoring perfluorinated surfactants in biota and surface water samples following an accidental release of fire-fighting foam into Etobicoke Creek. Environmental science & technology 2002; 36: 545-551.

Mudumbi JB, Ntwampe SK, Muganza FM, Okonkwo JO. Perfluorooctanoate and perfluorooctane sulfonate in South African river water. Water Sci Technol 2014; 69: 185-94.

Munoz G, Budzinski H, Babut M, Lobry J, Selleslagh J, Tapie N, et al. Temporal variations of perfluoroalkyl substances partitioning between surface water, suspended sediment, and biota in a macrotidal estuary. Chemosphere 2019a; 233: 319-326.

Munoz G, Duy SV, Labadie P, Botta F, Budzinski H, Lestremau F, et al. Analysis of zwitterionic, cationic, and anionic poly- and perfluoroalkyl surfactants in sediments by liquid chromatography polarity-switching electrospray ionization coupled to high resolution mass spectrometry. Talanta 2016; 152: 447-56.

Munoz G, Giraudel JL, Botta F, Lestremau F, Devier MH, Budzinski H, et al. Spatial distribution and partitioning behavior of selected poly- and perfluoroalkyl substances in freshwater ecosystems: a French nationwide survey. Sci Total Environ 2015; 517: 48-56.

Munoz G, Labadie P, Botta F, Lestremau F, Lopez B, Geneste E, et al. Occurrence survey and spatial distribution of perfluoroalkyl and polyfluoroalkyl surfactants in groundwater, surface water, and sediments from tropical environments. Sci Total Environ 2017; 607-608: 243-252.

Munoz G, Liu J, Vo Duy S, Sauvé S. Analysis of F-53B, Gen-X, ADONA, and emerging fluoroalkylether substances in environmental and biomonitoring samples: A review. Trends in Environmental Analytical Chemistry 2019b; 23.

Murakami M, Imamura E, Shinohara H, Kiri K, Muramatsu Y, Harada A, et al. Occurrence and sources of perfluorinated surfactants in rivers in Japan. Environmental science & technology 2008; 42: 6566-6572.

Murakami M, Kuroda K, Sato N, Fukushi T, Takizawa S, Takada H. Groundwater pollution by perfluorinated surfactants in Tokyo. Environmental science & technology 2009; 43: 3480-3486.

Mussabek D, Ahrens L, Persson KM, Berndtsson R. Temporal trends and sediment-water partitioning of per- and polyfluoroalkyl substances (PFAS) in lake sediment. Chemosphere 2019; 227: 624-629.

Naile JE, Khim JS, Wang T, Chen C, Luo W, Kwon BO, et al. Perfluorinated compounds in water, sediment, soil and biota from estuarine and coastal areas of Korea. Environ Pollut 2010; 158: 1237-44.

Nakata H, Kannan K, Nasu T, Cho H-S, Sinclair E, Takemura A. Perfluorinated contaminants in sediments and aquatic organisms collected from shallow water and tidal flat areas of the Ariake

Sea, Japan: environmental fate of perfluorooctane sulfonate in aquatic ecosystems. Environmental science & technology 2006; 40: 4916-4921.

Nakayama S, Strynar MJ, Helfant L, Egeghy P, Ye X, Lindstrom AB. Perfluorinated compounds in the Cape Fear drainage basin in North Carolina. Environmental science & technology 2007; 41: 5271-5276.

Nakayama SF, Strynar MJ, Reiner JL, Delinsky AD, Lindstrom AB. Determination of perfluorinated compounds in the Upper Mississippi River Basin. Environmental science & technology 2010; 44: 4103-4109.

Nascimento RA, Nunoo DBO, Bizkarguenaga E, Schultes L, Zabaleta I, Benskin JP, et al. Sulfluramid use in Brazilian agriculture: A source of per- and polyfluoroalkyl substances (PFASs) to the environment. Environ Pollut 2018; 242: 1436-1443.

Navarro I, de la Torre A, Sanz P, Martinez MLA. Perfluoroalkyl acids (PFAAs): Distribution, trends and aquatic ecological risk assessment in surface water from Tagus River basin (Spain). Environ Pollut 2020; 256: 113511.

Newton S, McMahen R, Stoeckel JA, Chislock M, Lindstrom A, Strynar M. Novel Polyfluorinated Compounds Identified Using High Resolution Mass Spectrometry Downstream of Manufacturing Facilities near Decatur, Alabama. Environ Sci Technol 2017; 51: 1544-1552.

Nguyen MA, Wiberg K, Ribeli E, Josefsson S, Futter M, Gustavsson J, et al. Spatial distribution and source tracing of per- and polyfluoroalkyl substances (PFASs) in surface water in Northern Europe. Environ Pollut 2017; 220: 1438-1446.

Niisoe T, Senevirathna ST, Harada KH, Fujii Y, Hitomi T, Kobayashi H, et al. Perfluorinated carboxylic acids discharged from the Yodo River Basin, Japan. Chemosphere 2015; 138: 81-8.

OECD. Toward a New Comprehensive Global Database of Per- and Polyfluoroalkyl Substances (PFASs): Summary Report on Updating the OECD 2007 List of Per- and Polyfluoroalkyl Substances (PFASs). Series on Risk Management No. 39. Organisation for Economic Co-operation and Development, 2018.

Orata F, Maes A, Werres F, Wilken RD. Perfluorinated Compounds Distribution and Source Identification in Sediments of Lake Victoria Gulf Basin. Soil and Sediment Contamination: An International Journal 2011; 20: 129-141.

Pan CG, Ying GG, Zhao JL, Liu YS, Jiang YX, Zhang QQ. Spatiotemporal distribution and mass loadings of perfluoroalkyl substances in the Yangtze River of China. Sci Total Environ 2014a; 493: 580-7.

Pan CG, Ying GG, Zhao JL, Liu YS, Liu SS, Du J, et al. Spatial distribution of perfluoroalkyl substances in surface sediments of five major rivers in China. Arch Environ Contam Toxicol 2015; 68: 566-76.

Pan CG, Yu KF, Wang YH, Zhang W, Zhang J, Guo J. Perfluoroalkyl substances in the riverine and coastal water of the Beibu Gulf, South China: Spatiotemporal distribution and source identification. Sci Total Environ 2019; 660: 297-305.

Pan G, You C. Sediment-water distribution of perfluorooctane sulfonate (PFOS) in Yangtze River Estuary. Environ Pollut 2010; 158: 1363-7.

Pan G, Zhou Q, Luan X, Fu QS. Distribution of perfluorinated compounds in Lake Taihu (China): impact to human health and water standards. Sci Total Environ 2014b; 487: 778-84.

Pan Y, Shi Y, Wang J, Jin X, Cai Y. Pilot investigation of perfluorinated compounds in river water, sediment, soil and fish in Tianjin, China. Bull Environ Contam Toxicol 2011; 87: 152-7.

Pan Y, Zhang H, Cui Q, Sheng N, Yeung LWY, Guo Y, et al. First Report on the Occurrence and Bioaccumulation of Hexafluoropropylene Oxide Trimer Acid: An Emerging Concern. Environ Sci Technol 2017; 51: 9553-9560.

Pan Y, Zhang H, Cui Q, Sheng N, Yeung LWY, Sun Y, et al. Worldwide Distribution of Novel Perfluoroether Carboxylic and Sulfonic Acids in Surface Water. Environ Sci Technol 2018; 52: 7621-7629.

Penland TN, Cope WG, Kwak TJ, Strynar MJ, Grieshaber CA, Heise RJ, et al. Trophodynamics of Per- and Polyfluoroalkyl Substances in the Food Web of a Large Atlantic Slope River. Environ Sci Technol 2020; 54: 6800-6811.

Perra G, Focardi SE, Guerranti C. Levels and spatial distribution of perfluorinated compounds (PFCs) in superficial sediments from the marine reserves of the Tuscan Archipelago National Park (Italy). Mar Pollut Bull 2013; 76: 379-82.

Piao HT, Jiao XC, Gai N, Chen S, Lu GH, Yin XC, et al. Perfluoroalkyl substances in waters along the Grand Canal, China. Chemosphere 2017; 179: 387-394.

Pico Y, Blasco C, Farre M, Barcelo D. Occurrence of perfluorinated compounds in water and sediment of L'Albufera Natural Park (Valencia, Spain). Environ Sci Pollut Res Int 2012; 19: 946-57.

Pignotti E, Casas G, Llorca M, Tellbuscher A, Almeida D, Dinelli E, et al. Seasonal variations in the occurrence of perfluoroalkyl substances in water, sediment and fish samples from Ebro Delta (Catalonia, Spain). Sci Total Environ 2017; 607-608: 933-943.

Pignotti E, Dinelli E. Distribution and partition of endocrine disrupting compounds in water and sediment: Case study of the Romagna area (North Italy). Journal of Geochemical Exploration 2018; 195: 66-77.

Post GB, Louis JB, Lippincott RL, Procopio NA. Occurrence of perfluorinated compounds in raw water from New Jersey public drinking water systems. Environ Sci Technol 2013; 47: 13266-75.

Prevedouros K, Cousins IT, Buck RC, Korzeniowski SH. Sources, fate and transport of perfluorocarboxylates. Environmental science & technology 2006; 40: 32-44.

Qi Y, Hu S, Huo S, Xi B, Zhang J, Wang X. Spatial distribution and historical deposition behaviors of perfluoroalkyl substances (PFASs) in sediments of Lake Chaohu, a shallow eutrophic lake in Eastern China. Ecological Indicators 2015; 57: 1-10.

Qi Y, Huo S, Hu S, Xi B, Su J, Tang Z. Identification, characterization, and human health risk assessment of perfluorinated compounds in groundwater from a suburb of Tianjin, China. Environmental Earth Sciences 2016; 75.

Qiu Y, Jing H, Shi H. Perfluorocarboxylic acids (PFCAs) and perfluoroalkyl sulfonates (PFASs) in surface and tap water around Lake Taihu in China. Frontiers of Environmental Science & Engineering in China 2010; 4: 301-310.

Quinete N, Wu Q, Zhang T, Yun SH, Moreira I, Kannan K. Specific profiles of perfluorinated compounds in surface and drinking waters and accumulation in mussels, fish, and dolphins from southeastern Brazil. Chemosphere 2009; 77: 863-9.

Rostkowski P, Yamashita N, So IMK, Taniyasu S, Lam PKS, Falandysz J, et al. Perfluorinated compounds in streams of the Shihwa industrial zone and Lake Shihwa, South Korea. Environmental Toxicology and Chemistry: An International Journal 2006; 25: 2374-2380.

Saito N, Sasaki K, Nakatome K, Harada K, Yoshinaga T, Koizumi A. Perfluorooctane sulfonate concentrations in surface water in Japan. Arch Environ Contam Toxicol 2003; 45: 149-58.

Sakurai T, Serizawa S, Isobe T, Kobayashi J, Kodama K, Kume G, et al. Spatial, phase, and temporal distributions of perfluorooctane sulfonate (PFOS) and perfluorooctanoate (PFOA) in Tokyo Bay, Japan. Environmental science & technology 2010; 44: 4110-4115.

Sammut G, Sinagra E, Helmus R, de Voogt P. Perfluoroalkyl substances in the Maltese environment - (I) surface water and rain water. Sci Total Environ 2017; 589: 182-190.

Sanchez-Avila J, Meyer J, Lacorte S. Spatial distribution and sources of perfluorochemicals in the NW Mediterranean coastal waters (Catalonia, Spain). Environ Pollut 2010; 158: 2833-40.

Schmidt N, Fauvelle V, Castro-Jimenez J, Lajaunie-Salla K, Pinazo C, Yohia C, et al. Occurrence of perfluoroalkyl substances in the Bay of Marseille (NW Mediterranean Sea) and the Rhone River. Mar Pollut Bull 2019; 149: 110491.

Schwichtenberg T, Bogdan D, Carignan CC, Reardon P, Rewerts J, Wanzek T, et al. PFAS and Dissolved Organic Carbon Enrichment in Surface Water Foams on a Northern U.S. Freshwater Lake. Environ Sci Technol 2020; 54: 14455-14464.

Scott BF, Spencer C, Lopez E, Muir DC. Perfluorinated alkyl acid concentrations in Canadian rivers and creeks. Water Quality Research Journal 2009; 44: 263-277.

Senthilkumar K, Ohi E, Sajwan K, Takasuga T, Kannan K. Perfluorinated compounds in river water, river sediment, market fish, and wildlife samples from Japan. Bull Environ Contam Toxicol 2007; 79: 427-31.

Seo SH, Son MH, Shin ES, Choi SD, Chang YS. Matrix-specific distribution and compositional profiles of perfluoroalkyl substances (PFASs) in multimedia environments. J Hazard Mater 2019; 364: 19-27.

Shao M, Ding G, Zhang J, Wei L, Xue H, Zhang N, et al. Occurrence and distribution of perfluoroalkyl substances (PFASs) in surface water and bottom water of the Shuangtaizi Estuary, China. Environ Pollut 2016; 216: 675-681.

Sharma BM, Bharat GK, Tayal S, Larssen T, Becanova J, Karaskova P, et al. Perfluoroalkyl substances (PFAS) in river and ground/drinking water of the Ganges River basin: Emissions and implications for human exposure. Environ Pollut 2016; 208: 704-13.

Shi G, Xie Y, Guo Y, Dai J. 6:2 fluorotelomer sulfonamide alkylbetaine (6:2 FTAB), a novel perfluorooctane sulfonate alternative, induced developmental toxicity in zebrafish embryos. Aquat Toxicol 2018; 195: 24-32.

Shi Y, Vestergren R, Xu L, Song X, Niu X, Zhang C, et al. Characterizing direct emissions of perfluoroalkyl substances from ongoing fluoropolymer production sources: A spatial trend study of Xiaoqing River, China. Environ Pollut 2015; 206: 104-12.

Shigei M, Ahrens L, Hazaymeh A, Dalahmeh SS. Per- and polyfluoroalkyl substances in water and soil in wastewater-irrigated farmland in Jordan. Sci Total Environ 2020; 716: 137057.

Sinclair E, Mayack DT, Roblee K, Yamashita N, Kannan K. Occurrence of perfluoroalkyl surfactants in water, fish, and birds from New York State. Arch Environ Contam Toxicol 2006; 50: 398-410.

Skaar JS, Raeder EM, Lyche JL, Ahrens L, Kallenborn R. Elucidation of contamination sources for poly- and perfluoroalkyl substances (PFASs) on Svalbard (Norwegian Arctic). Environ Sci Pollut Res Int 2019; 26: 7356-7363.

So M, Taniyasu S, Yamashita N, Giesy J, Zheng J, Fang Z, et al. Perfluorinated compounds in coastal waters of Hong Kong, South China, and Korea. Environmental Science & Technology 2004; 38: 4056-4063.

So MK, Miyake Y, Yeung WY, Ho YM, Taniyasu S, Rostkowski P, et al. Perfluorinated compounds in the Pearl River and Yangtze River of China. Chemosphere 2007; 68: 2085-95.

Song X, Vestergren R, Shi Y, Huang J, Cai Y. Emissions, Transport, and Fate of Emerging Per- and Polyfluoroalkyl Substances from One of the Major Fluoropolymer Manufacturing Facilities in China. Environ Sci Technol 2018; 52: 9694-9703.

Steele M, Griffith C, Duran C. Monthly Variations in Perfluorinated Compound Concentrations in Groundwater. Toxics 2018; 6.

Stock NL, Furdui VI, Muir DC, Mabury SA. Perfluoroalkyl contaminants in the Canadian Arctic: evidence of atmospheric transport and local contamination. Environmental science & technology 2007; 41: 3529-3536.

Sun H, Li F, Zhang T, Zhang X, He N, Song Q, et al. Perfluorinated compounds in surface waters and WWTPs in Shenyang, China: mass flows and source analysis. Water Res 2011; 45: 4483-90.

Sun M, Arevalo E, Strynar M, Lindstrom A, Richardson M, Kearns B, et al. Legacy and Emerging Perfluoroalkyl Substances Are Important Drinking Water Contaminants in the Cape Fear River Watershed of North Carolina. Environmental Science & Technology Letters 2016; 3: 415-419.

Sun R, Wu M, Tang L, Li J, Qian Z, Han T, et al. Perfluorinated compounds in surface waters of Shanghai, China: Source analysis and risk assessment. Ecotoxicol Environ Saf 2018; 149: 88-95.

Sun Z, Zhang C, Yan H, Han C, Chen L, Meng X, et al. Spatiotemporal distribution and potential sources of perfluoroalkyl acids in Huangpu River, Shanghai, China. Chemosphere 2017; 174: 127-135.

Takazawa Y, Nishino T, Sasaki Y, Yamashita H, Suzuki N, Tanabe K, et al. Occurrence and Distribution of Perfluorooctane Sulfonate and Perfluorooctanoic Acid in the Rivers of Tokyo. Water, Air, and Soil Pollution 2009; 202: 57-67.

Takemine S, Matsumura C, Yamamoto K, Suzuki M, Tsurukawa M, Imaishi H, et al. Discharge of perfluorinated compounds from rivers and their influence on the coastal seas of Hyogo prefecture, Japan. Environ Pollut 2014; 184: 397-404.

Tan KY, Lu GH, Yuan X, Zheng Y, Shao PW, Cai JY, et al. Perfluoroalkyl Substances in Water from the Yangtze River and Its Tributaries at the Dividing Point Between the Middle and Lower Reaches. Bull Environ Contam Toxicol 2018; 101: 598-603.

Theobald N, Caliebe C, Gerwinski W, Huhnerfuss H, Lepom P. Occurrence of perfluorinated organic acids in the North and Baltic seas. Part 1: distribution in sea water. Environ Sci Pollut Res Int 2011; 18: 1057-69.

Thompson J, Roach A, Eaglesham G, Bartkow ME, Edge K, Mueller JF. Perfluorinated alkyl acids in water, sediment and wildlife from Sydney Harbour and surroundings. Mar Pollut Bull 2011; 62: 2869-75.

Torres F, B., M., Guida Y, Weber R, Machado Torres JP. Brazilian overview of per- and polyfluoroalkyl substances listed as persistent organic pollutants in the stockholm convention. Chemosphere 2022; 291: 132674.

Tsuda T, Inoue A, Igawa T, Tanaka K. Seasonal changes of PFOS and PFOA concentrations in Lake Biwa water. Bull Environ Contam Toxicol 2010; 85: 593-7.

USEPA. Fact Sheet: 2010/2015 PFOA Stewardship Program. United States Environmental Protection Agency, 2006.

USEPA. Drinking Water Health Advisories for PFOA and PFOS. United States Environmental Protection Agency, 2016.

USEPA. EPA's Per- and Polyfluoroalkyl Substances Action Plan. US EPA, 2019, pp. 72.

USEPA. EPA Announces New Drinking Water Health Advisories for PFAS Chemicals, $1 Billion in Bipartisan Infrastructure Law Funding to Strengthen Health Protections. In: USEPA, editor, 2022.

Wang B, Cao M, Zhu H, Chen J, Wang L, Liu G, et al. Distribution of perfluorinated compounds in surface water from Hanjiang River in Wuhan, China. Chemosphere 2013a; 93: 468-73.

Wang P, Lu Y, Wang T, Zhu Z, Li Q, Zhang Y, et al. Transport of short-chain perfluoroalkyl acids from concentrated fluoropolymer facilities to the Daling River estuary, China. Environ Sci Pollut Res Int 2015; 22: 9626-36.

Wang Q, Tsui MMP, Ruan Y, Lin H, Zhao Z, Ku JPH, et al. Occurrence and distribution of per- and polyfluoroalkyl substances (PFASs) in the seawater and sediment of the South China sea coastal region. Chemosphere 2019a; 231: 468-477.

Wang S, Wang H, Deng W. Perfluorooctane sulfonate (PFOS) distribution and effect factors in the water and sediment of the Yellow River Estuary, China. Environ Monit Assess 2013b; 185: 8517-24.

Wang T, Chen C, Naile JE, Khim JS, Giesy JP, Lu Y. Perfluorinated compounds in water, sediment and soil from Guanting Reservoir, China. Bull Environ Contam Toxicol 2011a; 87: 74-9.

Wang T, Khim JS, Chen C, Naile JE, Lu Y, Kannan K, et al. Perfluorinated compounds in surface waters from Northern China: comparison to level of industrialization. Environ Int 2012a; 42: 37-46.

Wang T, Lu Y, Chen C, Naile JE, Khim JS, Giesy JP. Perfluorinated compounds in a coastal industrial area of Tianjin, China. Environ Geochem Health 2012b; 34: 301-11.

Wang T, Lu Y, Chen C, Naile JE, Khim JS, Park J, et al. Perfluorinated compounds in estuarine and coastal areas of north Bohai Sea, China. Mar Pollut Bull 2011b; 62: 1905-14.

Wang Y, Shi Y, Cai Y. Spatial distribution, seasonal variation and risks of legacy and emerging per- and polyfluoroalkyl substances in urban surface water in Beijing, China. Sci Total Environ 2019b; 673: 177-183.

Wang Y, Vestergren R, Shi Y, Cao D, Xu L, Cai Y, et al. Identification, Tissue Distribution, and Bioaccumulation Potential of Cyclic Perfluorinated Sulfonic Acids Isomers in an Airport Impacted Ecosystem. Environ Sci Technol 2016; 50: 10923-10932.

Wang Z, Cousins IT, Scheringer M, Hungerbuhler K. Fluorinated alternatives to long-chain perfluoroalkyl carboxylic acids (PFCAs), perfluoroalkane sulfonic acids (PFSAs) and their potential precursors. Environ Int 2013c; 60: 242-8.

Wang Z, DeWitt JC, Higgins CP, Cousins IT. A Never-Ending Story of Per- and Polyfluoroalkyl Substances (PFASs)? Environ Sci Technol 2017; 51: 2508-2518.

Wei C, Wang Q, Song X, Chen X, Fan R, Ding D, et al. Distribution, source identification and health risk assessment of PFASs and two PFOS alternatives in groundwater from non-industrial areas. Ecotoxicol Environ Saf 2018; 152: 141-150.

White ND, Balthis L, Kannan K, De Silva AO, Wu Q, French KM, et al. Elevated levels of perfluoroalkyl substances in estuarine sediments of Charleston, SC. Sci Total Environ 2015; 521-522: 79-89.

Wilkinson JL, Hooda PS, Swinden J, Barker J, Barton S. Spatial distribution of organic contaminants in three rivers of Southern England bound to suspended particulate material and dissolved in water. Sci Total Environ 2017; 593-594: 487-497.

Wilkinson JL, Hooda PS, Swinden J, Barker J, Barton S. Spatial (bio)accumulation of pharmaceuticals, illicit drugs, plasticisers, perfluorinated compounds and metabolites in river sediment, aquatic plants and benthic organisms. Environ Pollut 2018; 234: 864-875.

Williams AJ, Grulke CM, Edwards J, McEachran AD, Mansouri K, Baker NC, et al. The CompTox Chemistry Dashboard: a community data resource for environmental chemistry. Journal of cheminformatics 2017; 9: 1-27.

Xiao F, Simcik MF, Halbach TR, Gulliver JS. Perfluorooctane sulfonate (PFOS) and perfluorooctanoate (PFOA) in soils and groundwater of a U.S. metropolitan area: migration and implications for human exposure. Water Res 2015; 72: 64-74.

Xu C, Liu Z, Song X, Ding X, Ding D. Legacy and emerging per- and polyfluoroalkyl substances (PFASs) in multi-media around a landfill in China: Implications for the usage of PFASs alternatives. Sci Total Environ 2021; 751: 141767.

Yamazaki E, Falandysz J, Taniyasu S, Hui G, Jurkiewicz G, Yamashita N, et al. Perfluorinated carboxylic and sulphonic acids in surface water media from the regions of Tibetan Plateau: Indirect evidence on photochemical degradation? J Environ Sci Health A Tox Hazard Subst Environ Eng 2016; 51: 63-9.

Yamazaki E, Taniyasu S, Ruan Y, Wang Q, Petrick G, Tanhua T, et al. Vertical distribution of perfluoroalkyl substances in water columns around the Japan sea and the Mediterranean Sea. Chemosphere 2019; 231: 487-494.

Yamazaki E, Taniyasu S, Wang X, Yamashita N. Per- and polyfluoroalkyl substances in surface water, gas and particle in open ocean and coastal environment. Chemosphere 2021; 272: 129869.

Yan H, Zhang C, Zhou Q, Yang S. Occurrence of perfluorinated alkyl substances in sediment from estuarine and coastal areas of the East China Sea. Environ Sci Pollut Res Int 2015; 22: 1662-9.

Yang L, Zhu L, Liu Z. Occurrence and partition of perfluorinated compounds in water and sediment from Liao River and Taihu Lake, China. Chemosphere 2011; 83: 806-14.

Ye F, Tokumura M, Islam MS, Zushi Y, Oh J, Masunaga S. Spatial distribution and importance of potential perfluoroalkyl acid precursors in urban rivers and sewage treatment plant effluent--case study of Tama River, Japan. Water Res 2014; 67: 77-85.

Yeung LW, De Silva AO, Loi EI, Marvin CH, Taniyasu S, Yamashita N, et al. Perfluoroalkyl substances and extractable organic fluorine in surface sediments and cores from Lake Ontario. Environ Int 2013; 59: 389-97.

Yu N, Shi W, Zhang B, Su G, Feng J, Zhang X, et al. Occurrence of perfluoroalkyl acids including perfluorooctane sulfonate isomers in Huai River Basin and Taihu Lake in Jiangsu Province, China. Environ Sci Technol 2013; 47: 710-7.

Zhang G, Pan Z, Wu Y, Shang R, Zhou X, Fan Y. Distribution of Perfluorinated Compounds in Surface Water and Soil in Partial Areas of Shandong Province, China. Soil and Sediment Contamination: An International Journal 2019; 28: 502-512.

Zhang M, Tang F, Yu Y, Xu J-f, Li H, Wu M-h, et al. Residue concentration and distribution characteristics of perfluorinated compounds in surface water from Qiantang River in Hangzhou section. Environmental Science 2015; 36: 4471-4478.

Zhang X, Lohmann R, Dassuncao C, Hu XC, Weber AK, Vecitis CD, et al. Source attribution of poly- and perfluoroalkyl substances (PFASs) in surface waters from Rhode Island and the New York Metropolitan Area. Environ Sci Technol Lett 2016; 3: 316-321.

Zhang Y, Lai S, Zhao Z, Liu F, Chen H, Zou S, et al. Spatial distribution of perfluoroalkyl acids in the Pearl River of southern China. Chemosphere 2013; 93: 1519-25.

Zhao X, Xia X, Zhang S, Wu Q, Wang X. Spatial and vertical variations of perfluoroalkyl substances in sediments of the Haihe River, China. J Environ Sci (China) 2014a; 26: 1557-66.

Zhao YG, Wan HT, Wong MH, Wong CK. Partitioning behavior of perfluorinated compounds between sediment and biota in the Pearl River Delta of South China. Mar Pollut Bull 2014b; 83: 148-54.

Zhao Z, Cheng X, Hua X, Jiang B, Tian C, Tang J, et al. Emerging and legacy per- and polyfluoroalkyl substances in water, sediment, and air of the Bohai Sea and its surrounding rivers. Environ Pollut 2020; 263: 114391.

Zhao Z, Tang J, Mi L, Tian C, Zhong G, Zhang G, et al. Perfluoroalkyl and polyfluoroalkyl substances in the lower atmosphere and surface waters of the Chinese Bohai Sea, Yellow Sea, and Yangtze River estuary. Sci Total Environ 2017; 599-600: 114-123.

Zhao Z, Xie Z, Moller A, Sturm R, Tang J, Zhang G, et al. Distribution and long-range transport of polyfluoroalkyl substances in the Arctic, Atlantic Ocean and Antarctic coast. Environ Pollut 2012; 170: 71-7.

Zhao Z, Xie Z, Tang J, Sturm R, Chen Y, Zhang G, et al. Seasonal variations and spatial distributions of perfluoroalkyl substances in the rivers Elbe and lower Weser and the North Sea. Chemosphere 2015a; 129: 118-25.

Zhao Z, Xie Z, Tang J, Zhang G, Ebinghaus R. Spatial distribution of perfluoroalkyl acids in surface sediments of the German Bight, North Sea. Sci Total Environ 2015b; 511: 145-52.

Zheng H, Hu G, Xu Z, Li H, Zhang L, Zheng J, et al. Characterization and distribution of heavy metals, polybrominated diphenyl ethers and perfluoroalkyl substances in surface sediment from the Dayan River, South China. Bull Environ Contam Toxicol 2015; 94: 503-10.

Zheng H, Wang F, Zhao Z, Ma Y, Yang H, Lu Z, et al. Distribution profiles of per- and poly fluoroalkyl substances (PFASs) and their re-regulation by ocean currents in the East and South China Sea. Mar Pollut Bull 2017; 125: 481-486.

Zhou Z, Liang Y, Shi Y, Xu L, Cai Y. Occurrence and transport of perfluoroalkyl acids (PFAAs), including short-chain PFAAs in Tangxun Lake, China. Environ Sci Technol 2013; 47: 9249-57.

Zhou Z, Shi Y, Li W, Xu L, Cai Y. Perfluorinated compounds in surface water and organisms from Baiyangdian Lake in North China: source profiles, bioaccumulation and potential risk. Bull Environ Contam Toxicol 2012; 89: 519-24.

Zhu Z, Wang T, Meng J, Wang P, Li Q, Lu Y. Perfluoroalkyl substances in the Daling River with concentrated fluorine industries in China: seasonal variation, mass flow, and risk assessment. Environ Sci Pollut Res Int 2015; 22: 10009-18.

Zhu Z, Wang T, Wang P, Lu Y, Giesy JP. Perfluoroalkyl and polyfluoroalkyl substances in sediments from South Bohai coastal watersheds, China. Mar Pollut Bull 2014; 85: 619-27.

Zushi Y, Ye F, Motegi M, Nojiri K, Hosono S, Suzuki T, et al. Spatially detailed survey on pollution by multiple perfluorinated compounds in the Tokyo Bay basin of Japan. Environ Sci Technol 2011; 45: 2887-93.

Chapter 4. Spatial Distribution and Mass Transport of Perfluoroalkyl Substances (PFAS) in Surface Water: a Statewide Evaluation of PFAS Occurrence and Fate in Alabama.

Roger L. Viticoski[a]; Denying Wang[a]; Meredith A. Feltman[a]; Vanisree Mulabagal[a]; Stephanie R. Rogers[b]; David M. Blersch[c]; Joel S. Hayworth[a]*

Department of Civil and Environmental Engineering[a], Department of Geosciences[b], Department of Biosystems Engineering[c], Auburn University, Auburn, Alabama - 36849, United States

Published in Science of The Total Environment, 836 (2022) 155524

Abstract

Per- and polyfluoroalkyl substances (PFAS) have been previously detected near suspected sources in Alabama, but the overall extent of contamination across the state is unknown. This study evaluated the spatial distribution of 17 PFAS within the ten major river basins in Alabama and provided insights into their transport and fate through a mass flux analysis. Six PFAS were identified in 65 out of the 74 riverine samples, with mean $\sum_6$PFAS levels of 35.2 ng L^{-1}. The highest $\sum_6$PFAS concentration of 237 ng L^{-1} was detected in the Coosa River, a transboundary river that receives discharges from multiple sources in Alabama and Georgia. PFAS distribution was not observed to be uniform across the state: while the Coosa, Alabama, and Chattahoochee rivers presented relatively high mean $\sum_6$PFAS concentrations of 191, 100 and 28.8 ng L^{-1}, respectively, PFAS were not detected in the Conecuh, Escatawpa, and Yellow rivers. Remaining river systems presented mean $\sum_6$PFAS concentrations between 7.94 and 24.7 ng L^{-1}. Although the short-chain perfluoropentanoic acid (PFPeA) was the most detected analyte (88%), perfluorobutanesulfonic acid (PFBS) was the substance with the highest individual concentration of 79.4 ng L^{-1}. Consistent increases in the mass fluxes of PFAS were observed as the rivers flowed through Alabama, reaching up to 63.3 mg s^{-1}, indicating the presence of numerous sources across the state. Most of the mass inputs would not have been captured if only aqueous concentrations were evaluated, since

concentration is usually heavily impacted by environmental conditions. Results of this study demonstrate that mass flux is a simple and powerful complementary approach that can be used to broadly understand trends in the transport and fate of PFAS in large river systems.

4.1 Introduction

Per- and polyfluoroalkyl substances (PFAS) are the focus of thousands of studies due to their adverse health effects in humans and wildlife. PFAS encompass a large group of anthropogenic organic substances widely used in industrial applications and consumer products, including in the coating of cookware and food packaging, stain- and water-repellent products and fabrics, as well as in the formulation of aqueous film forming foam (AFFF) fire extinguishers, ski wax, and much more (Johns and Stead, 2000; KEMI, 2015; Pan et al., 2018). In the late 1990s, 3M reported to the United States Environmental Protection Agency (US EPA) evidence that certain PFAS could bioaccumulate in humans (3M, 1998) and agreed to end the production of perfluorooctanesulfonic acid (PFOS) and its related salts by 2002 (3M, 2000). Since then, several studies have reported that certain PFAS might have negative health impacts in humans, including carcinogenic (Steenland and Winquist, 2021) and endocrine disrupting (Gong et al., 2019) effects, increased blood cholesterol levels (Seo et al., 2018), and obesity (Braun, 2017). In wildlife, PFAS can bioaccumulate and biomagnify through food chains (Xu et al., 2014), inhibit growth (McCarthy et al., 2017), and act as endocrine disruptors (Pedersen et al., 2016). Thus, the presence of PFAS in aquatic environments is of great concern.

Due to their stability and heterogeneity, the remediation of PFAS-contaminated waste is challenging (Ross et al., 2018), and PFAS are often discharged into the environment without proper treatment. Sources include municipal wastewater treatment plants (WWTPs), industrial facilities, landfills, airports, military bases, and firefighting training facilities, among others (Hu et al., 2016). As a result, PFAS have been identified on every continent, from remote Antarctica (Casal et al., 2017) to populous areas of Asia (Pan et al., 2017; Zushi et al., 2011) and Europe (Gobelius et al., 2018; Munoz et al., 2015). In the US, Alabama is a particular hotspot for PFAS. Previous studies, conducted in 2002 and 2017, identified an area

of increased PFAS concentration in the Tennessee River downstream of several chemical facilities, including a 3M plant (Hansen et al., 2002; Newton et al., 2017). The 2017 study also identified nine previously unknown PFAS and two other novel substances that were structurally similar to existing PFAS (Newton et al., 2017). Even more troublesome, the Decatur WWTP distributed over 34,000 metric tons of biosolids contaminated with PFAS to local farmers between 1995 and 2008 (Lindstrom et al., 2011). Lindstrom et al. (2011) found PFAS levels up to 31,906 ng L^{-1} in surface water near fields that received the contaminated biosolids. In response, the Alabama Department of Environmental Management (ADEM) announced a consent order with 3M, stating that the company must remediate contaminated sites in the Decatur area, as well as "monitor, test, and research impacts of exposure" (ADEM, 2020). Similarly, high levels of PFAS were also identified in the Coosa River (Lasier et al., 2011) – the main drinking water source for several cities in Alabama. The City of Gadsden, AL is currently litigating against more than 30 textile companies located in Georgia, arguing that these companies are responsible for the high levels of PFAS in the Coosa River. Recently, ADEM conducted a survey in 290 public water systems (PWS) for 18 PFAS (ADEM, 2021). According to their report, PFAS were found in 57 PWS, with ∑PFAS reaching up to 384 ng L^{-1}, indicating the presence of PFAS in their corresponding source waters, as these substances are not likely to be removed through conventional treatment processes (Crone et al., 2019).

While previous studies have greatly enhanced the understanding on PFAS sources and their overall distribution, much remains unknown regarding their transport and fate in the environment. This is partially related to the fact that most studies express PFAS contamination in terms of concentration, which is not sufficient to track contamination in large river systems. This is because aqueous concentrations are affected by a variety of environmental factors, such as precipitation and stormwater runoff. Thus, considering aqueous concentration alone can lead to erroneous conclusions regarding the amount and transport of contaminant mass through interconnected river systems. Moreover, identification of sources can be difficult, as variable environmental conditions may mask potential PFAS inputs. Mass flux analysis is a simple complimentary approach that combines volumetric discharge and aqueous concentration. Most

studies have used the concept of mass flux to estimate yearly mass discharge of tributaries into lakes or bays, using an annual average flow rate. For instance, Ma et al. (2018) calculated the fluxes of tributaries discharging into Taihu Lake and used them to determine sources, while Zhao et al. (2020) calculated the mass discharge of tributaries into the Bohai Sea. Results from those studies enhanced the understanding of the fate of PFAS in the environment, but not so much about their transport behavior. On the other hand, Nakayama et al. (2010) performed a mass flux analysis to track the mass transport of PFAS in the Upper Mississippi River Basin, by calculating the mass flux for sampling points using a 72-h average volumetric flow rate.

The ultimate fate of PFAS in the environment remains unclear. Studies have shown that some PFAS can be removed from water by partitioning to sediments and suspended particulates, volatilization, and sequestration by biota and wildlife (Casal et al., 2017; Liu et al., 2019; Munoz et al., 2019), depending on their chemical properties. Regardless of the environmental compartment, most terminal (stable) PFAS will persist virtually unchanged (Guelfo and Adamson, 2018), hence their nickname “forever chemicals”. Thus, this study aims to determine the spatial distribution of seventeen PFAS in surface water in Alabama and identify trends in their transport behavior through a mass flux analysis. Results of the mass flux analysis were also used to identify locations within the state serving as potential PFAS source areas. This is the first study to use mass flux analysis to systematically track PFAS contamination in multiple river systems at a state level in the US and demonstrates that mass flux analysis is a broadly applicable, reasonably simple approach for capturing large-scale trends in the transport of PFAS through interconnected surface water systems.

4.2 Methods

4.2.1 Chemicals and Reagents

Target analytes include six perfluorocarboxylic acids (PFBA, PFPeA, PFHxA, PFHpA, PFOA, and PFNA), six perfluorosulfonic acids (PFBS, PFPeS, PFHxS, PFHpS, PFOS, and PFNS), and five perfluoroethers (HFPO-DA, NaDONA, PF4OPeA, PF5OHxA, and 3,6-OPFHpA). For the above analytes,

eleven are considered short-chain PFAS (PFBA, PFPeA, PFHxA, PFHpA, PFBS, PFPeS, and all the perfluoroethers). Analytical grade PFAS standards were purchased from Wellington Laboratories (Ontario, Canada). The molecular weight, chemical structure, nomenclature, and CAS of analytes are listed in Table 4.2. High purity LC-MS grade solvents (water, methanol, and acetonitrile) were purchased from VWR international (Suwanee, GA), and mobile phase modifiers (ammonium formate) were purchased from Agilent Technologies (Wilmington, DE).

4.2.2 Field Sampling

Given the geographic scale of this project, individual major river systems were not extensively sampled. Instead, sample locations were strategically determined to capture inlets and outlets of each river basin, confluence of rivers, changes in land use (agricultural vs. urban vs. forested), zones of hydrographical and geographical relevance, and inputs from industrial and municipal wastewater (see S2 for more details). Based on these criteria, 74 sampling locations were selected from fourteen river systems across ten river basins, namely the Alabama (AC-1,6), Black Warrior (BT-1,6), Cahaba (AC-7,10), Chattahoochee (CH-1,8), Choctawhatchee (CW-1,5), Conecuh (CO-1,4), Coosa (CT-1,5), Escatawpa (ES-1,2), Perdido (FP-2,5), Tallapoosa (CT-6,9), Tennessee (TN-1,9), Tombigbee (BT-7,8 and TM-1,3), and Yellow rivers (FP-1), and Mobile River and Tributaries (TM-4,12).

Samples were collected between June 27th and August 30th, 2020, during seven sampling events, with each trip covering at least one river basin. A complete list of geographical coordinates and time/date of sampling is available in Table 4.3. Samples were collected from bridges, public access areas, and boat ramps. A sampling device consisting of a 1-gallon high-density polyethylene (HDPE) storage bottle attached to a 100 ft rope and 5 lb weight was developed (Figure 4.5). At each location, the sampling device was used to collect 2 L of surface water, which was transferred to a labeled HDPE storage bottle. One sample was collected in each location, as previous studies conducted by the authors suggest little to no variation in replicates (Mulabagal et al., 2018). Water parameters such as temperature, pH, and conductivity were measured in-situ using a Hanna HI98130 combo tester (Hanna Instruments, Inc.). To avoid cross-

contamination between samples, the sampling device was thoroughly rinsed with deionized water (DI water) before and after each sampling collection. In between excursions, the sampler was rinsed with methanol and DI water in the laboratory. For quality control, a field blank was collected at each sampling excursion by transferring 2 L of DI water from the sampler to a labeled HDPE storage bottle. Samples and field blanks were transferred to the laboratory in coolers (-4 °C).

4.2.3 Quantitative Analysis

Surface water samples (2 L) were filtered under vacuum through 0.7 µm GE Whatman glass microfiber filters (GE, Boston, MA, USA) to remove suspended particulates and large debris. Filtration was conducted within 48 hours of samples arriving at the laboratory, and samples were either immediately processed or stored at -20 °C. Samples were processed through solid phase extraction (SPE) following a previously published method (Mulabagal et al., 2018), with slight modifications. Briefly, 500 mL were loaded into Oasis WAX cartridges (6cc, 150 mg; Waters Corporation, Milford, MA, US) pre-conditioned with 0.1% ammonium hydroxide in methanol (4 mL), methanol (4 mL), and LC grade water (4 mL). After loading, the cartridges were washed with a 25 mM ammonium acetate buffer (pH 4.0) in LC grade water (4 mL) and dried under vacuum. Target analytes were then extracted from SPE cartridges with methanol (1.5 mL) followed by 0.1% ammonium hydroxide in methanol (1.5 mL). Final extracts were filtered through 0.2 µm Agilent glass fiber nylon syringe filters. Samples were spiked with a mass-labeled internal standard (MPFOS) before analysis. While MPFOS was spiked after extraction, previous recovery experiments for target PFAS have indicated that SPE performance was within acceptable limits (Table 4.5). Further, quantitation using an electrospray ion source requires an internal standard-based approach to minimize variation of ionization during analysis of the target analytes and ideally, multiple isotopically-labelled standards would be employed. Although MPFOS was used to quantify all 17 target analytes in this study, detection response of MPFOS in calibration solutions and analytical samples was similar over several sample batches, indicating a consistent internal standard performance. A series of calibration levels spiked with MPFOS were analyzed by measuring the peak response ratio for the target analytes and MPFOS. PFAS calibration curves were tested for linearity, accuracy, and precision, presenting r^2>0.994 and accuracy

ranging from 83% to 113% (Table 4.5). Target analytes were then quantified using an Agilent ultra-high performance liquid chromatography, triple quadrupole mass spectrometer (UHPLC-MS/MS), composed of a 1290 Infinity II high-speed pump (Model G7120) coupled to a triple quadrupole mass spectrometer (Model G6460) and Jet-Stream Electrospray Ionization source. Water samples were analyzed in multiple reaction monitoring (MRM) mode. Each sample was analyzed five times, with two method blanks (acetonitrile:water 80:20) in between each sample. A 7-point calibration was also run for each batch. Additional information is provided in S3.

4.2.4 Data Analysis

Statistical analyses were conducted using R v.4.0.2 (R Foundation for Statistical Computing). Concentrations below detection limits were treated as zero for summary statistics. Possible correlations among the concentration of the different detected PFAS were evaluated through the Spearman correlation method. LC-MS/MS data was processed using Agilent Mass Hunter software version B.07.1. Spatial analyses were conducted using ArcMap v 10.7.1 (Esri - Environmental Systems Research Institute). Information related to spatial analyses and data sources is presented in S4. Mass flux of PFAS ($\Phi_{\sum PFAS}$) was calculated by multiplying the sum of PFAS concentration ($\sum$PFAS) at a given location by the 48-h average volumetric flow rate ($\overline{Q}$), as shown in equation (1). Volumetric flow rate data were acquired from the United Stated Geological Survey (USGS), when stations were located near sampling points, or from the National Water Model (NWM) supported by the US National Oceanic and Atmospheric Administration (US-NOAA), within 48h of sampling (S6). Mass fluxes were estimated based on point concentration at one location across the entire cross-section of a given river. An important assumption in this approach is that PFAS originating from upstream sources are well-mixed in both the vertical and transverse (perpendicular to river flow) directions at any given sampling location. This assumption is reasonably valid for vertical mixing but may be less valid in the transverse direction for sampling locations in close proximity to PFAS sources (Fischer et al., 1979; Lane et al., 2008; Pouchoulin et al., 2020; Wu and Wu, 2019). Determining the longitudinal extent of a transverse mixing zone for PFAS introduced into natural surface water channels

requires information on channel geometry, transverse water velocity and PFAS concentration distributions, and other location-specific conditions in the vicinity of each sample location, which was well outside the scope of this study. Thus, this study assumes that uncertainties associated with potentially incomplete transverse mixing at some sampling locations in close proximity to PFAS source areas do not invalidate the overall trends in PFAS mass transport for interconnected river systems within a large geographic area.

$$\Phi_{\sum \mathrm{PFAS}} [mg\ s^{-1}] = \sum \mathrm{PFAS} * \overline{\mathrm{Q}} \quad (1)$$

4.3 Results and Discussion

4.3.1 PFAS Profile in Alabama

Of the seventeen target analytes, only six were detected, including three short-chain and one long-chain perfluorocarboxylic acids (PFCAs): PFPeA, PFHxA, PFHpA, and PFOA, and one short-chain and one-long chain perfluorosulfonic acids (PFSAs), PFBS and PFOS. The perfluoroethers were not found in any of the samples. Despite the relatively low number of detected analytes, at least one PFAS was found in 88% (n=65) of all surface water samples. The short-chain PFPeA was the most detected substance, found in 88% of all samples in a range of 2.11 to 54.9 ng L^{-1}. PFPeA was also found to be among the highest detected PFAS in several previous studies, including in two urban watersheds in Nevada, US (Bai and Son, 2021) and in the Asan Lake area in South Korea (Lee et al., 2020). PFOA and PFHxA were detected in 74 and 58% of samples, respectively, with concentrations ranging between 0.24-30.2 and 0.88-39.1 ng L^{-1}, respectively. PFOS and PFHpA were detected at lower frequencies (22 and 19%, respectively) with a concentration range of 7.39-30.7 and 5.26-13.1 ng L^{-1}, respectively. Although PFBS was only quantified in 15% of samples, it was the substance with the highest individual concentration of 79.4 ng L^{-1}.

Despite the fact that the PFAS profile varied substantially among the river basins in Alabama (Table 4.1), a significant ($p<0.05$) correlation in their concentration was observed among all analytes. Spearman coefficients ranged from 0.59 for PFOS and PFPeA to 0.90 for PFHpA and PFBS (see Table 4.7 for correlation matrix). The high correlation between PFHpA and PFBS might be linked to their use in the carpet industry, since PFHpA is a breakdown product of stain- and grease-repellent coatings for carpets (Wang et al., 2015), and PFBS is used as a PFOS alternative in the production of stain-repellent fabric

protectors (DEPA, 2015). This hypothesis is further supported by the fact that both substances were mostly detected in the Coosa and Alabama Rivers, which are suspected to receive discharges from carpet manufacturers in Georgia. PFPeA and PFHxA also presented a high correlation (0.85), which could be related to the fact that both analytes are the degradation products of several precursors, including the fluorotelomers 6:2 FTOH (Liu et al., 2010) and 6:2 FTSA (Wang et al., 2011).

In terms of PFAS families, PFCAs were quantified much more frequently (88%) than PFSAs (22%). This pattern has been widely observed, as PFSAs are more likely to be removed from water by partitioning to sediments and suspended particulate matter than PFCAs (Ahrens et al., 2010; Higgins and Luthy, 2006). Moreover, short-chain (PFBS, PFPeA, PFHxA, and PFHpA) and long-chain PFAS (PFOS and PFOA) were detected at similar frequencies (88 and 74%). However, their contributions to the overall concentration differed: concentrations of short-chain PFAS were, on average, three times higher than long-chains. This is further evidenced when computing the concentration ratio of long-chain PFAS to their shorter-chain replacements: PFPeA/PFOA and PFBS/PFOS averaged 2.58 ± 2.87 and 2.98 ± 0.78, respectively. This is likely a reflection of the restrictions in the production of many long-chain PFAS and their subsequent replacement by shorter-chain PFAS. For example, after PFOS production was phased-out in the US in 2002, PFBS has been used as its alternative in several products, including 3M's Scotchgard®, a stain-repellent fabric protector (DEPA, 2015; Wang et al., 2013). The prevalence of short-chain PFAS was also observed in previous studies. For instance, Gao et al. (2020) observed PFBA and PFBS to be the most detected analytes in the Xi River (China), while Bai and Son (2021) found PFHxA and PFPeA to be predominant in their study in Nevada (US). The dominance of short-chain PFAS is to be expected since they are generally more easily transported, more stable, and presently used in higher amounts when compared to their long-chain homologues (Blum et al., 2015). Although short-chain PFAS are widespread, fluorochemical manufacturers have suggested that short-chain PFAS are less likely to bioaccumulate in humans and wildlife. However, the potential toxicity effects of short-chain PFAS should not neglected. For

instance, the US EPA recently released a toxicity assessment for PFBS, linking several adverse health effects, especially to the thyroid, to PFBS exposure (USEPA, 2021).

Table 4.1. Range (min-max) and average (in parenthesis) of analytes for each of the analyzed rivers. Overall detection frequencies (D.F.) are also displayed. Concentrations are expressed in ng L^{-1}.

River Basin	PFBS	PFPeA	PFHxA	PFHpA	PFOA	PFOS	∑PFAS
Alabama	28.2-33.3 (30.1)	20.8-23.5 (21.9)	13.2-15.3 (14.1)	7.55-8.18 (7.78)	14.0-15.3 (14.6)	10.7-13.0 (11.7)	96.4-108 (100)
Black Warrior	n.d.	2.11-23.1 (8.66)	n.d.-11.5 (1.93)	n.d.	0.243-6.14 (1.99)	n.d.	2.35-40.76 (12.6)
Cahaba	n.d.	8.50-15.0 (10.9)	n.d.-7.31 (2.79)	n.d.	n.d.-7.11 (3.85)	n.d.	8.50-29.4 (17.6)
Chattahoochee	n.d.	8.40-17.5 (12.30)	3.56-10.8 (6.51)	n.d.-6.22 (2.11)	4.33-10.2 (7.91)	n.d.	21.4-43.5 (28.8)
Choctawhatchee	n.d.	n.d.-15.7 (7.42)	n.d.-15.0 (3.00)	n.d.	n.d.-14.0 (2.80)	n.d.-19.1 (3.82)	n.d.-63.8 (17.0)
Conecuh	n.d.	n.d.	n.d.	n.d.	n.d.	n.d.	n.d.
Coosa	52.8-79.4 (63.9)	33.8-54.9 (42.1)	22.5-39.3 (30.4)	8.83-13.1 (11.1)	18.3- 30.2 (23.7)	11.0-29.6 (19.9)	155-237 (191)
Escatawpa	n.d.	n.d.	n.d.	n.d.	n.d.	n.d.	n.d.
Mobile Bay	n.d.	4.39-14.7 (11.4)	n.d.-6.50 (4.17)	n.d.	2.68-7.53 (5.73)	n.d.-30.7 (3.41)	8.48-56.7 (24.7)
Perdido	n.d.	4.16-13.9 (10.4)	n.d.-6.07 (3.68)	n.d.	2.59-9.01 (6.46)	n.d.	6.75-29.0 (20.5)
Tallapoosa	n.d.	5.56-8.55 (6.95)	n.d.	n.d.	n.d.-5.78 (2.80)	n.d.	5.56-14.0 (9.76)
Tennessee	n.d.	5.26-8.78 (7.38)	0.882-7.02 (4.54)	n.d.	3.02-10.70 (5.58)	n.d.-9.51 (2.89)	9.17-35.6 (20.4)
Tombigbee	n.d.	5.78-9.05 (7.75)	n.d.	n.d.	n.d.-0.554 (0.191)	n.d.	6.33-9.05 (7.94)
Yellow	n.d.	n.d.	n.d.	n.d.	n.d.	n.d.	n.d.
D.F. (%)	14.9	87.8	58.1	18.9	74.3	21.6	87.8

n.d.= not detected

4.3.2 Spatial Distribution of PFAS in Alabama

Results from this study confirmed the ubiquity of PFAS in sampled river systems in Alabama. $\sum_6$PFAS levels ranged from below detection limits to 237 ng L^{-1} (Figure 4.1), while mean and median $\sum_6$PFAS were equal to 35.2 and 17.8 ng L^{-1}, respectively. The highest $\sum_6$PFAS concentration of 237 ng L^{-1} was found in the Coosa River (CT-3), with PFBS and PFPeA as the predominant analytes. The Coosa River was previously sampled for PFAS at a similar location to CT-1, the first sampling location in Figure 4.1. In that study, Lasier et al. (2011) detected ∑PFAS concentration of 564 ng L^{-1} and PFOS and PFBS as

major analytes, compared to the 155 ng L^{-1} found in this study. The authors linked the contamination to carpet manufacturers in Dalton, GA that have their effluents treated by a municipal wastewater treatment plant. Carpet and textile industries are known to be potential sources of PFAS, due to the use of PFAS as stain-, fire-, and water-repellents in fabrics (Zheng and Salamova, 2020; Zhu et al., 2021). The fact that PFBS, used as a PFOS-alternative in the formulation of these products (DEPA, 2015), was found at high concentrations in the Coosa River further supports the hypothesis that carpet industries in Georgia are a major source of PFAS in the Coosa River. The Alabama and Chattahoochee rivers also presented relatively high mean $\sum_6$PFAS concentrations of 100 and 28.8 ng L^{-1}, respectively. Aqueous concentrations were fairly uniform across the course of both the Alabama and Chattahoochee, with slight increases after the cities of Montgomery and Columbus, respectively. The highest $\sum_6$PFAS concentration of 40.8 ng L^{-1} in the Black Warrior River basin was detected in Locust Fork (BT-1), a tributary that receives inputs from the Birmingham area, including a WWTP and a large landfill. PFAS profile in Locust Fork included PFPeA, PFHxA, and PFOA, the same observed in the Cahaba River, which flows through the eastern side of Birmingham.

Concentration of $\sum_6$PFAS in the Tennessee River averaged 20.4 ± 10.2 ng L^{-1}, ranging from 9.17 ng L^{-1} at the first sampling point (TN-1) to 35.6 ng L^{-1} after the Wheeler Lake Dam (TN-7). PFAS levels in the Tennessee River were previously studied by Hansen et al. (2002) and Newton et al. (2017), in which they reported $\sum$PFAS up to 731 and 750 ng L^{-1}, respectively, directly downstream from fluorochemical plants in Decatur, AL. In this study, low levels of PFAS ($\sum_6$PFAS = 15.9 ng L^{-1}) were detected downstream from Decatur (TN-6). This difference is likely related to the fact that sample TN-6 was collected on the northern side of a wide (3 km) section of the Tennessee River, opposite from the Decatur industries and discharges from these industries were most likely not completely mixed across the entire river width. One of the assumptions of this study is that the sampled rivers are well-mixed systems and variation in concentration at any cross-section is negligible. However, this assumption is not true in reservoirs such as Wheeler Lake, where some of the Tennessee River samples were collected. Even for well-mixed systems,

PFAS concentrations have been observed to exponentially decrease as distance from sources increases. For instance, Chen et al. (2018) observed the concentration of certain PFAS to decrease by an average of 75% within 5 km from a fluorochemical manufacturing park in Fuxin, China, which further supports our hypothesis. Although PFOA was detected in all samples in the Tennessee River, PFOS was only observed in TN-7,9, after the Wheeler Lake Dam. This raises questions regarding the role of dams in the transport of PFAS. It is possible that certain PFAS will accumulate more easily behind dams due to the increase in water residence time. In fact, Nakayama et al. (2010) noticed an increase in the concentration of PFOA in samples collected on the Mississippi River immediately downstream from a dam, relating it to possible increased vertical mixing and resuspension of previously deposited material. More research is needed to understand the effects of dams on the transport of PFAS.

Selected tributaries to Mobile Bay were also sampled. The $\sum_6$PFAS levels in these tributaries were very similar, between 24.2 and 28.0 ng L^{-1} (TM-5,7). The eastern side of the bay is mainly composed of residential and forested areas and sampled tributaries presented low $\sum_6$PFAS levels, ranging between 8.48 and 10.1 ng L^{-1}. The western side, where the city of Mobile is located, is much more industrialized. As expected, $\sum_6$PFAS levels were much higher in those tributaries, ranging from 22.2 to 56.7 ng L^{-1}. Although PFOA was detected in all tributaries, PFOS was only found in one sample (TM-10, PFOS concentration of 30.7 ng L^{-1}), in the Deer River, downstream of several chemical industries. The fact that PFOS was identified does not necessarily mean that those facilities are discharging PFOS into the river, since PFAS precursors like several sulfonamides can breakdown into PFOS (Benskin et al., 2012; Gilljam et al., 2016). However, the detection of PFOS is a potential concern as it can pose a risk to wildlife in the bay, as PFOS was observed to cause developmental effects in several fish species (Wang et al., 2011) and to cause cellular damage to oysters (Aquilina-Beck et al., 2020). The Conecuh, Escatawpa, and Yellow Rivers did not present any measurable amounts of the 17 target PFAS.

PFAS have been identified on every continent around the globe, with concentrations ranging from pg L^{-1} (Brumovsky et al., 2016) to mg L^{-1} (Moody et al., 2002), and given the geographic scale of this

project, comparisons to other large-scale studies are more appropriate. For instance, Gobelius et al. (2018) conducted a nationwide survey of 26 PFAS in Sweden, with ∑PFAS concentrations reaching up to 13,000 ng L^{-1}, but a median ∑PFAS of 3.9 ng L^{-1} in the 289 surface water samples. While mean concentration of PFOS (24 ng L^{-1}) and PFHxA (13 ng L^{-1}) in Swedish surface waters were considerably higher than in Alabama (3.31 ng L^{-1} for PFOS and 5.74 ng L^{-1} for PFHxA), mean concentrations of PFOA were similar (6.2 ng L^{-1} versus 6.14 ng L^{-1} in this study). Similarly, Munoz et al. (2015) conducted a survey of 22 PFAS in France and detected at least one PFAS in 89% of the 333 samples, with ∑PFAS reaching up to 725 ng L^{-1} and a mean and median of 28 and 7.9 ng L^{-1}, respectively. The authors detected the highest mean individual concentrations of PFOS (5.14 ng L^{-1}), PFHxS (4.72 ng L^{-1}), PFHxA (3.56 ng L^{-1}), and PFOA (2.54 ng L^{-1}), compared to 3.31, <BDL, 5.74, and 6.14 ng L^{-1} found in this study. However, concentrations of PFPeA (1.66 ng L^{-1}) and PFBS (1.27 ng L^{-1}) in French waterbodies were considerably lower than in Alabama (11.6 and 6.74 ng L^{-1} for PFPeA and PFBS, respectively). Pan et al. (2018) conducted a worldwide survey of 24 PFAS in surface water, including some of the emerging ethers targeted in this study. Mean concentrations of PFOA, PFHxA, PFOS, and PFBS of 8.19, 4.74, 4.39, and 5.65 ng L^{-1}, respectively, found in that study are comparable to what was observed in Alabama (6.14, 5.74, 3.31, and 6.76 ng L^{-1}, respectively). However, the authors detected PFHxS and HFPO-DA at high frequencies, which were not detected above detection limits in any of the samples from Alabama.

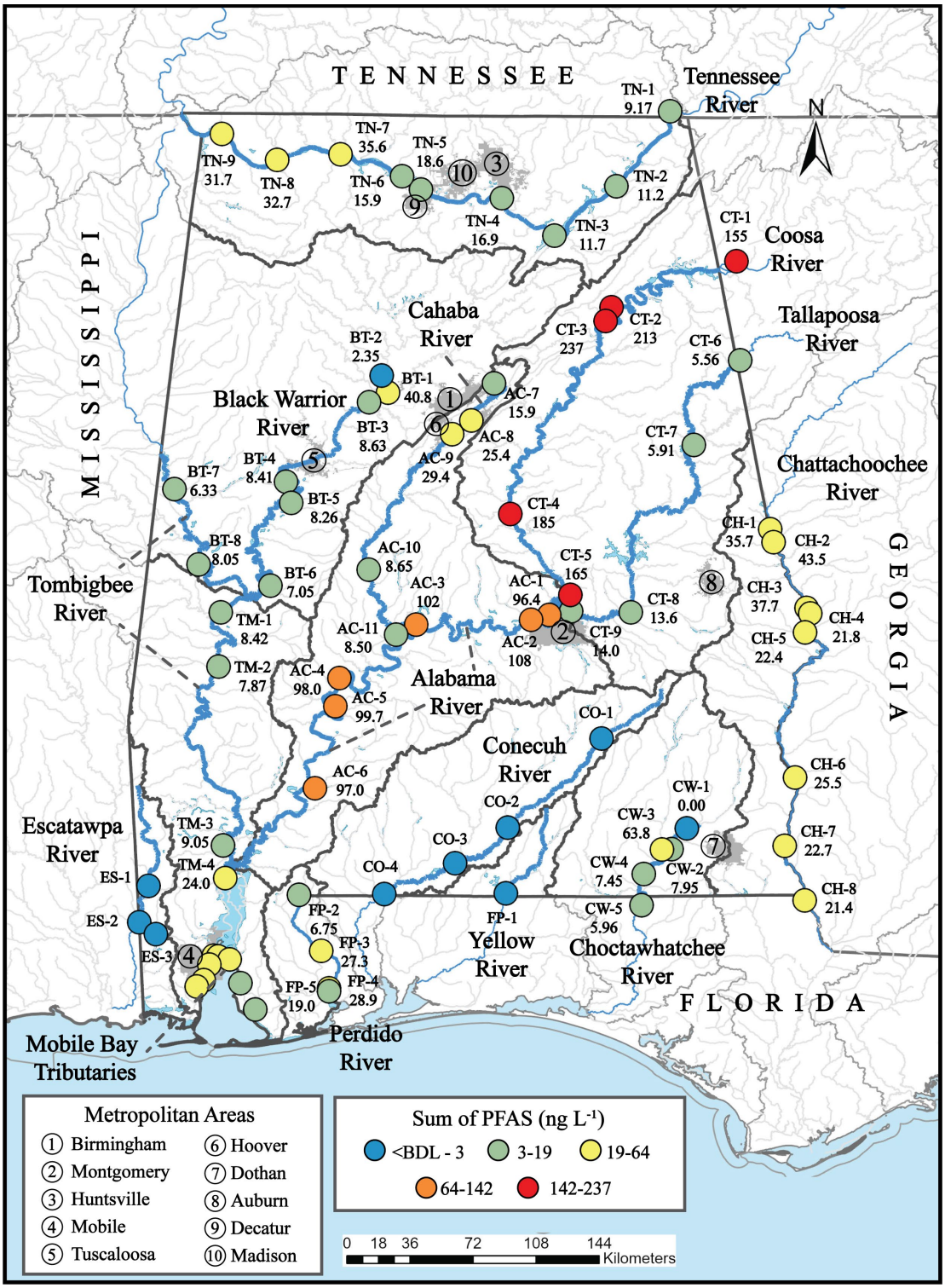

Figure 4.1. Spatial Distribution of PFAS in Alabama. $\sum_6$PFAS concentrations (in ng L^{-1}) are displayed for sampling locations, ranging from below detection limits (<BDL) to 237 ng L^{-1}. The 10 largest metropolitan areas are indicated for reference. WGS84 projection.

4.3.3 Mass Flux of PFAS in Alabama

One of the main goals of this study was to conduct a mass flux analysis to broadly identify trends in the transport of PFAS in Alabama. Mass fluxes were calculated by multiplying the $\sum_6$PFAS concentration by the 48-h average discharge rate at each sampling location, and results are displayed in Figures 4.2 and 4.3. These figures show that transboundary rivers, either flowing into Alabama or at the border with its neighboring states, are an important vector of PFAS contamination into the state. For instance, the first sampling point on the Coosa River, CT-1, indicates a mass flux of PFAS ($\Phi_{\sum PFAS}$) of 23.3 mg s^{-1} from Georgia into Alabama, while $\Phi_{\sum PFAS}$ in CT-2 (30.7 mg s^{-1}) also reflects possible inputs through tributaries from Georgia, including the Chattooga River. Moreover, sources in neighboring states are also contributing to the PFAS contamination in the Chattahoochee and Perdido Rivers, transboundary rivers located at the border with Georgia and Florida, respectively. Other rivers, such as the Tallapoosa and Tombigbee, generally presented lower background fluxes of 0.0350 and 0.550 mg s^{-1}, representing inputs from Georgia and Mississippi, respectively. The issue of the movement of PFAS mass through transboundary rivers is not confined to Alabama or the US and exemplifies the need for inter-state and international strategies to mitigate PFAS contamination.

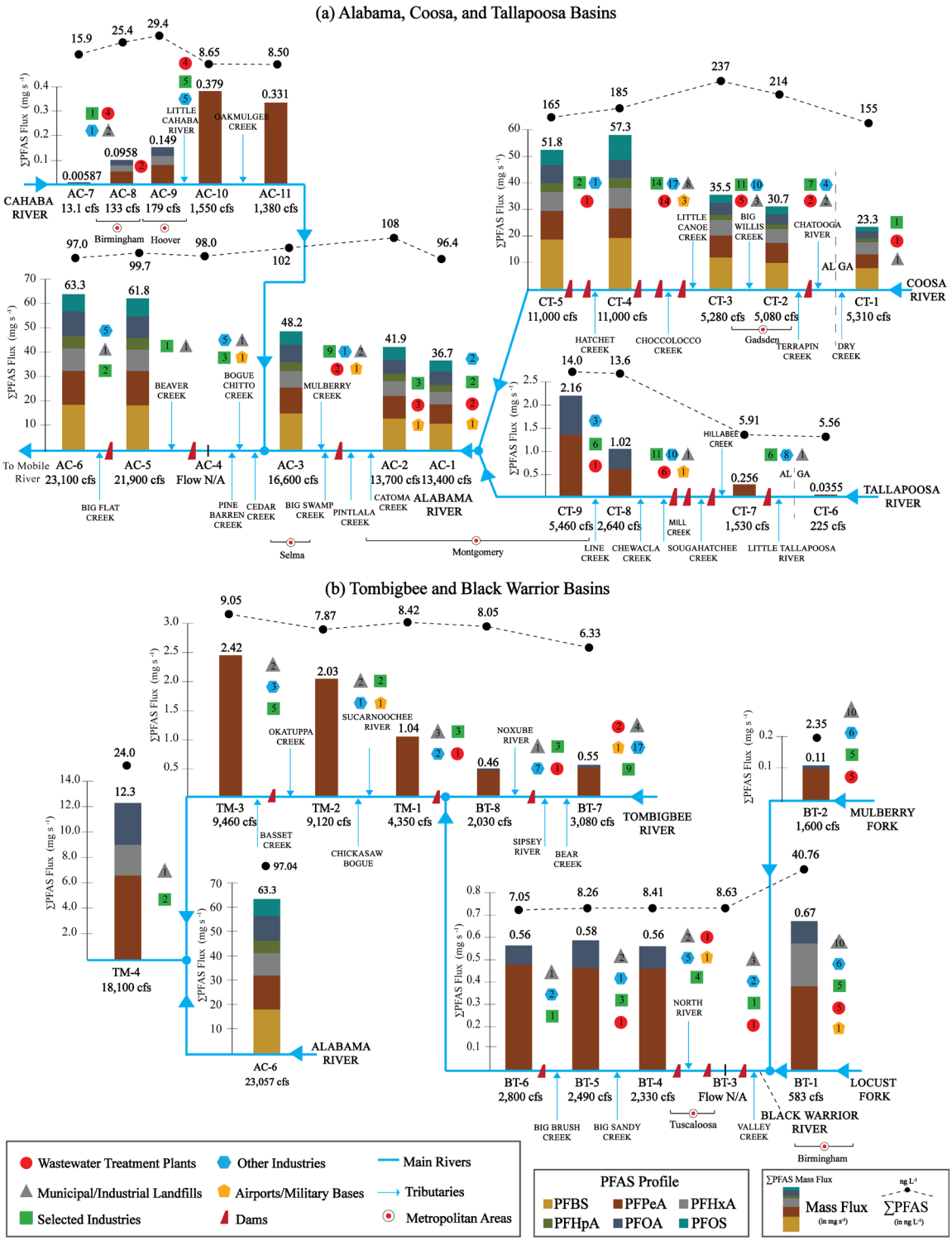

Figure 4.2. Schematic diagram of $\sum_6$PFAS mass flux (vertical bars, expressed in mg s^{-1}) and aqueous concentration (black circles, expressed in ng L^{-1}) for the (a) Alabama, Coosa, and Tallapoosa and

(b) Tombigbee and Black Warrior River Basins. The fluxes of individual PFAS are also displayed for each sampling point. Main metropolitan areas, dams, and likely sources are also displayed. Selected industries (green squares) include sectors that have been previously related to PFAS use, such as paper, automotive, plastics/packaging, chemical, flooring/tile, and textile/carpets. Respective number on icons represent the number of potential sources within the catchment associated with that category. Distances between sampling points are not to scale.

In addition to the background flux from neighboring states, consistent increases in the mass fluxes of PFAS were generally observed as the rivers flowed through Alabama. Considerable increases were observed in the Coosa and Alabama Rivers, in which the mass flux increased by 2.2 and 1.7 folds, respectively, as the rivers progressed through the basins. Sources in the Upper Coosa River were most likely related to inputs from carpet industries and WWTPs, expanding to other industries, WWTPs, landfills, and military bases as the river moved through the basin. In the Alabama River, WWTPs, landfills, and the Maxwell Air Force Base are potential sources in the upper section of the river, while various paper industries seem to be the major contributors of PFAS in the lower section. Previous studies have suggested that facilities that produce paper products could be major sources of PFAS in the environment (Clara et al., 2008; Langberg et al., 2020). Langberg et al. (2020) also noticed that paper fibers from paper mills can be a major vector for the transport and exposure of PFAS. It is also worth noting that the major mass inputs from these potential sources would not have been captured if only aqueous concentrations were considered. For instance, $\sum_6$PFAS concentrations across the Alabama River are fairly constant, with a variation of only 0.642 ng L^{-1} between the first and last sampling point. A similar trend was also observed in the Chattahoochee River, where the $\Phi_{\sum PFAS}$ more than doubled between samples CH-4 and 8 while the aqueous concentration was fairly constant. Such differences exemplify the usefulness of the mass flux analysis in tracking PFAS contamination in large river systems.

Similarly, a consistent increase in the $\Phi_{\sum PFAS}$ was observed in the Tallapoosa River, reaching up to 2.16 mg s^{-1} before it merged with the Coosa River. Interestingly, PFOA was only identified after sample

location CT_7, after potential inputs from the Auburn area discharged through the Chewacla and Saugahatchee creeks, local inputs from a large sewage pond in Tallassee, and inputs from a large landfill. Landfills are a major source of PFAS to the environment due to the disposal of many PFAS-containing products and waste (Lang et al., 2017). Alabama has 173 operating landfills, with many of them located in poor rural areas and accepting toxic waste from all states in the US (Milman, 2019). Further, low $\Phi_{\sum PFAS}$ of 0.55 and 0.46 mg s^{-1} were detected in the first two sampling points in the Tombigbee River, prior to discharges from the Black Warrior River. A consistent increase in the $\Phi_{\sum PFAS}$ was observed between samples TM-1,3, reaching 2.42 mg s^{-1}. Although the Tombigbee River watershed is primarily rural, samples TM-1 and 2 were sampled immediately downstream from paper industries, and TM-3 from a chemical facility, which could have contributed to the increase in mass.

The Claybank Creek, located in the Choctawhatchee River watershed, was sampled to assess the accuracy of the mass flux. A mass flux of 0.198 mg s^{-1} was calculated for sample CW-3 in Claybank Creek (Figure 4.3b), downstream from the Fort Rucker military base and the City of Enterprise WWTP. High concentrations of PFAS, primarily in groundwater, have been found near military installations in the US due to the use of AFFF (Barzen-Hanson et al., 2017; Moody and Field, 1999). The next sample, CW-4, captured the fluxes of both CW-2 and CW-3. CW-4 presented a $\Phi_{\sum PFAS}$ of 0.179 mg s^{-1}, lower than what would have been estimated by simply adding fluxes from the upstream samples. This difference, however, is explained by flow inputs from tributaries between those points. For instance, CW-2 and CW-3 presented flow rates of 496 and 109 cfs, while the flow rate in CW-4 was 850 cfs. This indicates that the inflow from tributaries of about 245 cfs contained little to no PFAS.

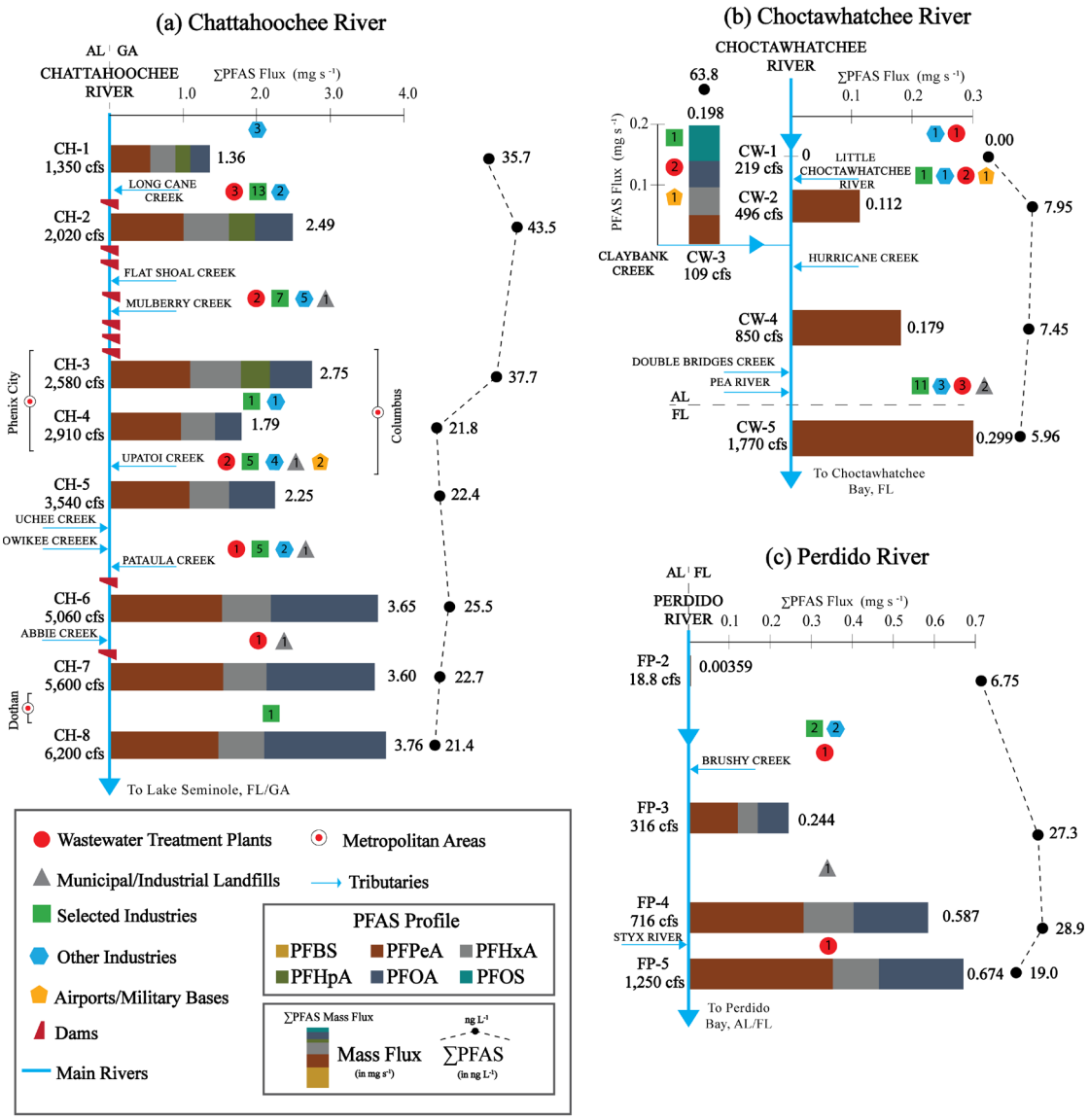

Figure 4.3. Schematic diagram of $\sum_6$PFAS mass flux (vertical bars, expressed in mg s^{-1}) and aqueous concentration (black circles, expressed in ng L^{-1}) for the (a) Chattahoochee, (b) Choctawhatchee, and (c) Perdido River Basins. The fluxes of individual PFAS are also displayed for each sampling point. Main metropolitan areas, dams, and likely sources are also displayed. Selected industries (green squares) include sectors that have been previously related to PFAS use, such as paper, automotive, plastics/packaging, chemical, flooring/tile, and textile/carpets. Respective number on icons represent the number of potential sources within the catchment associated with that category. Distances between sampling points are not to scale.

Finally, most of the state drains into Mobile Bay, especially through the Alabama and Tombigbee Rivers. A mass flux of 63.3 mg s^{-1}, the highest in the state, was detected in the last sampling point in the Alabama River, right upstream of the confluence with the Tombigbee River. After the merge, the Mobile River is formed, captured by the sample TM-4, in which a flux of 12.3 mg s^{-1} was detected. The $\Phi_{\sum PFAS}$ in TM-4 is substantially lower than the fluxes in the upstream rivers. A possible explanation for this decrease could be the high-water exchange in the region, as the area is dominated by wetlands. The Mobile River is further divided into several tributaries before reaching Mobile Bay. The $\sum_6$PFAS levels in these tributaries were very similar, between 24.2 and 28.0 ng L^{-1} (TM-5,7).

4.4 Conclusions

The results of this study raise important considerations for the possible implications of PFAS to humans and wildlife in Alabama. PFAS were found to be ubiquitous in the majority of rivers and tributaries sampled, being detected in 88% of surface water samples, even in less industrialized areas, with $\sum_6$PFAS levels reaching up to 237 ng L^{-1}. PFAS can pose a risk to wildlife, especially in rivers where PFAS were found at higher concentrations. This could also indirectly affect humans that consume PFAS-contaminated wildlife, as some PFAS are known or suspected to bioaccumulate and biomagnify through food webs (Xu et al., 2014). Since these samples were taken from riverine water, the results of this work are not directly applicable to human exposure through drinking water. However, many of the sampled rivers are used as drinking water sources, and several studies have considered the inability of conventional water treatment facilities to remove PFAS from water (Crone et al., 2019).

This study also exemplifies the usefulness of the mass flux analysis in tracking PFAS contamination in interconnected river systems flowing through large geographical areas. Although background fluxes from neighboring states are an important vector of PFAS into the state, consistent increases in the mass fluxes were generally observed as the rivers flowed through Alabama. These increases suggest the existence of a considerable number of local sources within catchments and river basins. As demonstrated, mass inputs from these sources would not have been captured if only aqueous concentrations

were observed. Results from the mass flux analysis also provide empirical evidence of the long-range transport of PFAS, especially short-chain analytes, in interconnected river systems. Finally, most of the PFAS contamination in Alabama is ultimately being discharged into bays and other coastal areas, which poses a risk for those ecosystems.

4.5 Supporting Information

S1. Target Analytes

Table 4.2. Molecular weight, formula, nomenclature, and CAS of the substances targeted in this study and internal standard (MPFOS)

Substance	Nomenclature	Molecular Weight	CAS	Molecular Formula
PFBA	Perfluorobutanoic acid	214.04	375-22-4	C_3F_7COOH
PFPeA	Perfluoropentanoic acid	264.05	2706-90-3	C_4F_9COOH
PFHxA	Perfluorohexanoic acid	314.05	307-24-4	$C_5F_{11}COOH$
PFHpA	Perfluoroheptanoic acid	364.06	375-85-9	$C_6F_{13}COOH$
PFOA	Perfluorooctanoic acid	414.07	335-67-1	$C_7F_{15}COOH$
PFNA	Perfluorononanoic acid	464.08	375-95-1	$C_8F_{17}COOH$
PFBS	Perfluorobutanesulfonic acid	300.10	375-73-5	$C_4F_9SO_3H$
PFPeS	Perfluoropentanesulfonic acid	350.11	2706-91-4	$C_5F_{11}SO_3H$
PFHxS	Perfluorohexanesulfonic acid	400.12	355-46-4	$C_6F_{13}SO_3H$
PFHpS	Perfluoroheptanesulfonic acid	450.12	375-92-8	$C_7F_{15}SO_3H$
PFOS	Perfluorooctanesulfonic acid	500.13	1763-23-1	$C_8F_{17}SO_3H$
PFNS	Perfluorononanesulfonic acid	550.14	68259-12-1	$C_9F_{19}SO_3H$
HFPO-DA	Tetrafluoro-2-(heptafluoropropoxy) propanoic acid	330.05	13252-13-6	$C_6HF_{11}O_3$
NaDONA	Sodium dodecafluoro-3H-4,8-dioxanonanoate	395.1	958445-44-8	$C_7H_5F_{12}NO_4$
PF4OPeA	Perfluoro (4-oxapentanoic) acid	280.04	377-73-1	$C_4HF_7O_3$
PF5OHxA	Perfluoro (5-oxa-6-methoxyhexanoic) acid	380.04	863090-89-5	$C_5HF_9O_3$
3,6-OPFHpA	Perfluoro (3,6-dioxaheptanoic) acid	296.04	151772-58-6	$C_5HF_9O_4$

MPFOS	Sodium perfluoro-1-(1,2,3,4-$^{13}C_4$)octanesulfonate	526.08	960315-53-1	$^{13}C_4{}^{12}C_4F_{17}SO_3Na$

S2. Sampling Determination and Collection

Due to the geographic scale of this project, major river systems were not extensively sampled. Instead, sampling points were strategically selected to capture inflow and outflow from each river basin, and to reflect possible PFAS inputs from known or suspected source regions. Thus, the sampling locations were selected based on land use (agricultural vs. urban vs. forest), inlets and outlets of main rivers, hydrographical and geographical relevance, and industrial activity. Figure 4.4 illustrates the criteria for sampling selection.

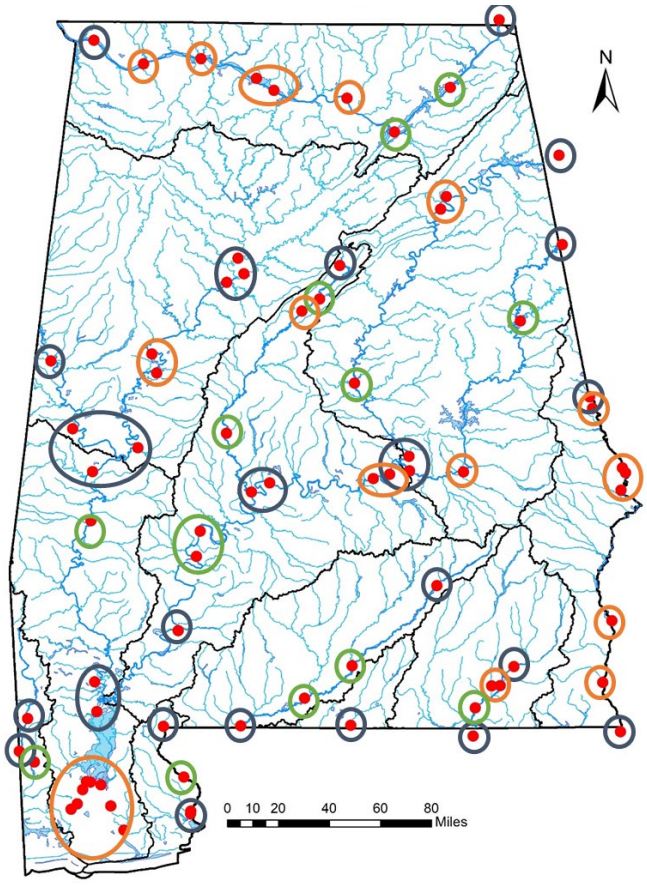

Figure 4.4. Sample locations, in red, determined to reflect (i) inlets and outlets, confluences, and headwaters of rivers (blue circles), (ii) areas of low urban development (green circles), and (iii) urbanized areas or industrial activity (orange circles).

Figure 4.5. HDPE Sampler

Table 4.3. Sampling Information. Geographic coordinates collected in WGS 84 projection. A field blank was collected at the first sampling location in each sampling trip, as indicated by an asterisk.

Sample ID	Location	Longitude	Latitude	Date	Time (CST)	Sampling
CT_6*	Tallapoosa River, Tallapoosa (Georgia)	33.74139	-85.336281	6/27/2020	12:10 PM	Bridge
CT_7	Tallapoosa River, Wedowee	33.30686	-85.574866	6/27/2020	1:40 PM	Bridge
CT_8	Tallapoosa River	32.44973	-85.898041	6/27/2020	4:13 PM	Bridge
CT_9	Tallapoosa River, Blue Ridge	32.45539	-86.202964	6/27/2020	5:09 PM	Riverbank
AC_1A	Alabama River, Prattville	32.43579	-86.315984	6/27/2020	5:44 PM	Bridge
CT_1*	Coosa River, Coosa (Georgia)	34.24861	-85.355577	6/28/2020	11:35 PM	Bridge
CT_2	Coosa River, Gadsden	34.01274	-85.995171	6/28/2020	12:57 PM	Bridge
CT_3	Coosa River, Southside	33.94254	-86.026126	6/28/2020	1:54 PM	Bridge
CT_4	Coosa River, Clayton (After Lay Dam)	32.95371	-86.515252	6/28/2020	4:17 PM	Bridge
CT_5	Coosa River, Wetumpka	32.53842	-86.206968	6/28/2020	5:31 PM	Bridge

AC_1B*	Alabama River, Prattville	32.43579	-86.315984	7/8/2020	10:30 AM	Bridge
AC_2	Alabama River, Montgomery	32.41137	-86.408425	7/8/2020	11:16 AM	Bridge
AC_3	Alabama River, Selma	32.38676	-86.997498	7/8/2020	12:28 PM	Bridge
AC_4	Alabama River, Millers Ferry	32.11354	-87.391959	7/8/2020	1:47 PM	Public Access Area
AC_5	Alabama River, Pine Hill	31.96977	-87.412779	7/8/2020	2:20 PM	Boat Ramp
AC_6	Alabama River, Claiborne	31.54806	-87.516747	7/8/2020	3:59 PM	Boat Ramp
AC_7	Cahaba River, Trussville	33.62233	-86.599476	7/9/2020	10:43 AM	Walking Bridge
AC_8	Cahaba River, Birmingham	33.432234	-86.714251	7/9/2020	11:17 AM	Boat Ramp
AC_9	Cahaba River, Hoover	33.36338	-86.813929	7/9/2020	12:05 PM	Bridge
AC_10	Cahaba River, West Blocton	32.66811	-87.241447	7/9/2020	2:12 PM	Bridge
AC_11	Cahaba River, Beloit	32.33574	-87.100699	7/9/2020	3:11 PM	Boat Ramp
CH_1*	Chattahoochee River, West Point	32.87525	-85.18144	7/27/2020	9:45 AM	Boat Ramp
CH_2	Chattahoochee River, Valley	32.80982	-85.16551	7/27/2020	10:20 AM	Kayak
CH_3	Chattahoochee River, Phenix City	32.47258	-84.99634	7/27/2020	11:37 AM	Walking Bridge
CH_4	Chattahoochee River, Columbus	32.44418	-84.97725	7/27/2020	11:58 AM	Marina
CH_5	Chattahoochee River, Fort Mitchel	32.34660	-85.00274	7/27/2020	12:57 PM	Boat Ramp
CH_6	Chattahoochee River, Fort Gaines	31.60425	-85.05576	7/27/2020	2:25 PM	Bridge
CH_7	Chattahoochee River, Columbia	31.25454	-85.10737	7/27/2020	3:19 PM	Boat Ramp
CH_8	Chattahoochee River, Steam Mill	30.97369	-85.00608	7/27/2020	4:07 PM	Boat Ramp
CW_1*	Choctawhatchee River	31.34329	-85.61102	8/1/2020	12:50 PM	Bridge
CW_2	Choctawhatchee River	31.23624	-85.68851	8/1/2020	1:20 PM	Bridge
CW_3	Choctawhatchee River Tributary	31.23437	-85.73809	8/1/2020	1:35 PM	Bridge
CW_4	Choctawhatchee River	31.10940	-85.83100	8/1/2020	2:25 PM	Boat Ramp
CW_5	Choctawhatchee River	30.95009	-85.84270	8/1/2020	3:05 PM	Bridge
FP_1	Yellow River	31.01008	-86.537368	8/1/2020	4:29 PM	Boat Ramp

CO_1	Conecuh River	31.80399	-86.04752	8/2/2020	10:02 AM	Bridge
CO_2	Conecuh River	31.34793	-86.52942	8/2/2020	11:25 AM	Boat Ramp
CO_3	Conecuh River	31.16392	-86.79932	8/2/2020	12:40 PM	Bridge
CO_4	Conecuh River	31.00753	-87.16185	8/3/2020	9:47 AM	Boat Ramp
BT_7*	Tombigbee River	33.080575	-88.237942	8/5/2020	1:02 PM	Bridge
BT_8	Tombigbee River, Epes	32.69454	-88.114504	8/5/2020	2:15 PM	Bridge
TM_1	Tombigbee River	32.45043	-88.001152	8/5/2020	3:05 PM	Bridge
TM_2	Tombigbee River	32.17152	-88.01178	8/5/2020	4:40 PM	Boat Ramp
TM_3	Tombigbee River	31.256707	-87.989013	8/5/2020	6:53 PM	Boat Ramp
BT_1	Locust Fork	33.57470	-87.142727	8/6/2020	11:42 AM	Bridge
BT_2	Mulberry Fork	33.66304	-87.17578	8/6/2020	11:16 AM	Bridge
BT_3	Black Warrior River (Bankhead Lake)	33.52678	-87.24052	8/6/2020	12:28 PM	Boat Ramp
BT_4	Black Warrior River, Tuscaloosa	33.11957	-87.66532	8/6/2020	1:52 PM	Boat Ramp
BT_5	Black Warrior River	33.01125	-87.63816	8/6/2020	3:02 PM	Boat Ramp
BT_6	Black Warrior River	32.58716	-87.74452	8/6/2020	3:56 PM	Boat Ramp
ES_1*	Escatawpa River	31.04874	-88.370773	8/22/2020	2:45 PM	Bridge
ES_2	Escatawpa River	30.86283	-88.417744	8/22/2020	3:30 PM	Bridge
ES_3	Big Creek Lake	30.80104	-88.332825	8/22/2020	3:54 PM	Public Access Area
TM_4	Mobile River	31.08773	-87.97826	8/22/2020	1:45 PM	Boat Ramp
TM_5	Mobile River	30.69082	-88.03724	8/22/2020	6:53 PM	Public Access Area
TM_6	Spanish River, Polecat Bay	30.68731	-88.01368	8/22/2020	7:20 PM	Boat Ramp
TM_7	Apalachee River	30.67281	-87.95444	8/22/2020	7:33 PM	Under Bridge
TM_8	Mobile Bay	30.64487	-88.05884	8/22/2020	6:30 PM	Public Access Area
TM_9	Dog River	30.56482	-88.088369	8/22/2020	5:27 PM	Public Access Area
TM_10	Deer River	30.53379	-88.123917	8/22/2020	4:55 PM	Public Access Area

TM_11	Fly Creek	30.55129	-87.898556	8/23/2020	9:50 AM	Walking Bridge
TM_12	Fish River	30.41556	-87.823803	8/23/2020	10:43 AM	Public Access Area
FP_2	Perdido River	31.00372	-87.599125	8/23/2020	2:01 PM	Riverbank
FP_3	Perdido River	30.71656	-87.484393	8/23/2020	1:02 PM	Public Access Area
FP_4	Perdido River	30.52354	-87.445177	8/23/2020	12:13 PM	Boat Ramp
FP_5	Perdido River	30.50846	-87.445687	8/23/2020	11:51 AM	Boat Ramp
TN_1*	TN River, Guntersville Lake, South Pittsburgh (Tennessee)	35.01647	-85.69544	8/30/2020	7:50 AM	Boat Ramp
TN_2	TN River, Guntersville Lake, Scottsboro	34.63306	-85.97196	8/30/2020	9:03 AM	Boat Ramp
TN_3	TN River, Guntersville Lake, Guntersville	34.38055	-86.28884	8/30/2020	9:51 AM	Boat Ramp
TN_4	TN River, Wheeler Lake, Whitesburg	34.57187	-86.55872	8/30/2020	10:52 AM	Riverbank
TN_5	TN River, Wheeler Lake, Mooresville	34.61615	-86.97268	8/30/2020	11:55 AM	Boat Ramp
TN_6	TN River, Wheeler Lake, Athens	34.68456	-87.07123	8/30/2020	12:31 PM	Boat Ramp
TN_7	TN River, Wheeler Dam	34.796179	-87.386488	8/30/2020	1:32 PM	Boat Ramp
TN_8	TN River, Florence	34.767245	-87.711904	8/30/2020	2:16 PM	Boat Ramp
TN_9	TN River, Waterloo	34.901112	-87.993785	8/30/2020	3:13 PM	Boat Ramp

S3. Quantitative Analysis

Targeted Analytes were extracted and quantified based on a modification from a previously published method in Mulabagal et al. (2018), with slight modifications in liquid chromatography. Parameters are presented in Table 4.4. Figures 4.6a-b illustrate the peaks and retention times of target analytes in calibration standard solution. Seven-point calibration curves were developed in the analytical range of target analytes and presented a great fit (R^2>0.990 for all substances), as illustrated in Figure 4.7. Extracted LC-MS/MS MRM chromatograms of detected analytes in surface water samples from selected rivers are illustrated in Figures 4.8 and 4.9. Further, each sample was analyzed five times, with two method blanks (acetonitrile:water 80:20) placed in between each sample. As illustrated in Figure 4.10, analytes

were not observed in solvent blanks, indicating carryover was negligible. At each sampling trip, a field blank was also collected to capture any cross-contamination between samples. None of the analytes were identified in the field blanks (Figure 4.10), suggesting cross-contamination likely did not occur. Finally, results from recovery experiments are displayed in Table 4.5.

Table 4.4. Modified mobile phase conditions

Mobile phase	A. 5mM ammonium formate in water/acetonitrile (95/5, v/v) B. acetonitrile/water (95/5, v/v)
Gradient method conditions	Time in min (Solvent B%) 0 (20); 0.5 (20); 1 (40); 2 (50); 3 (60); 5 (70); 7 (80); 8 (99); 8.5 (99); 8.8 (20); 9 (20)
Post run	2 min
Flow rate	0.2 mL min^{-1}
Total runtime	9 min

Table 4.5. Percent Recoveries of PFAS (mean ± standard deviation) and Limit of Detection (LOD) in spiked reagent water samples (Substances were spiked at 10 ng L^{-1}).

Substance	% Recovery (Run 1)	% Recovery (Run 2)	% Recovery (Run 3)	LOD (ng L^{-1})
PFBA	100.09 ± 3.93	108.83 ± 2.42	112.61 ± 4.35	0.65
PFBS	97.50 ± 3.48	104.73 ± 2.44	109.92 ± 4.12	1.27
PFPeA	96.47 ± 2.35	105.00 ± 1.46	111.17 ± 4.99	0.65
PFPeS	99.18 ± 2.39	107.46 ± 3.51	110.82 ± 3.00	0.73
PFHxA	96.42 ± 1.07	104.34 ± 3.88	107.74 ± 4.56	0.63
PFHxS	99.17 ± 2.87	107.26 ± 2.82	110.85 ± 5.07	0.69
PFHpA	96.63 ± 1.95	106.23 ± 2.89	110.32 ± 3.67	1.62
PFHpS	98.17 ± 1.75	104.31 ± 2.39	109.51 ± 5.23	1.00
PFOA	97.69 ± 1.92	105.27 ± 2.71	110.03 ± 3.75	0.21
PFOS	98.81 ± 2.62	108.68 ± 4.22	111.38 ± 3.93	0.89
PFNA	97.67 ± 2.31	105.15 ± 2.69	109.78 ± 4.77	0.72
PFNS	100.63 ± 1.66	107.94 ± 3.58	111.17 ± 4.54	0.70
HFPO-DA	102.29 ± 0.78	110.73 ± 2.03	113.56 ± 3.49	0.55
ADONA	97.09 ± 2.26	105.71 ± 2.16	110.78 ± 4.54	0.48
PF4OPeA	92.03 ± 4.48	89.78 ± 2.45	87.26 ± 6.19	0.91
PF5OHxA	95.71 ± 4.90	92.91 ± 3.42	91.30 ± 5.13	0.75
3,6-OPFHpA	87.82 ± 4.81	85.71 ± 3.14	83.32 ± 4.72	0.69

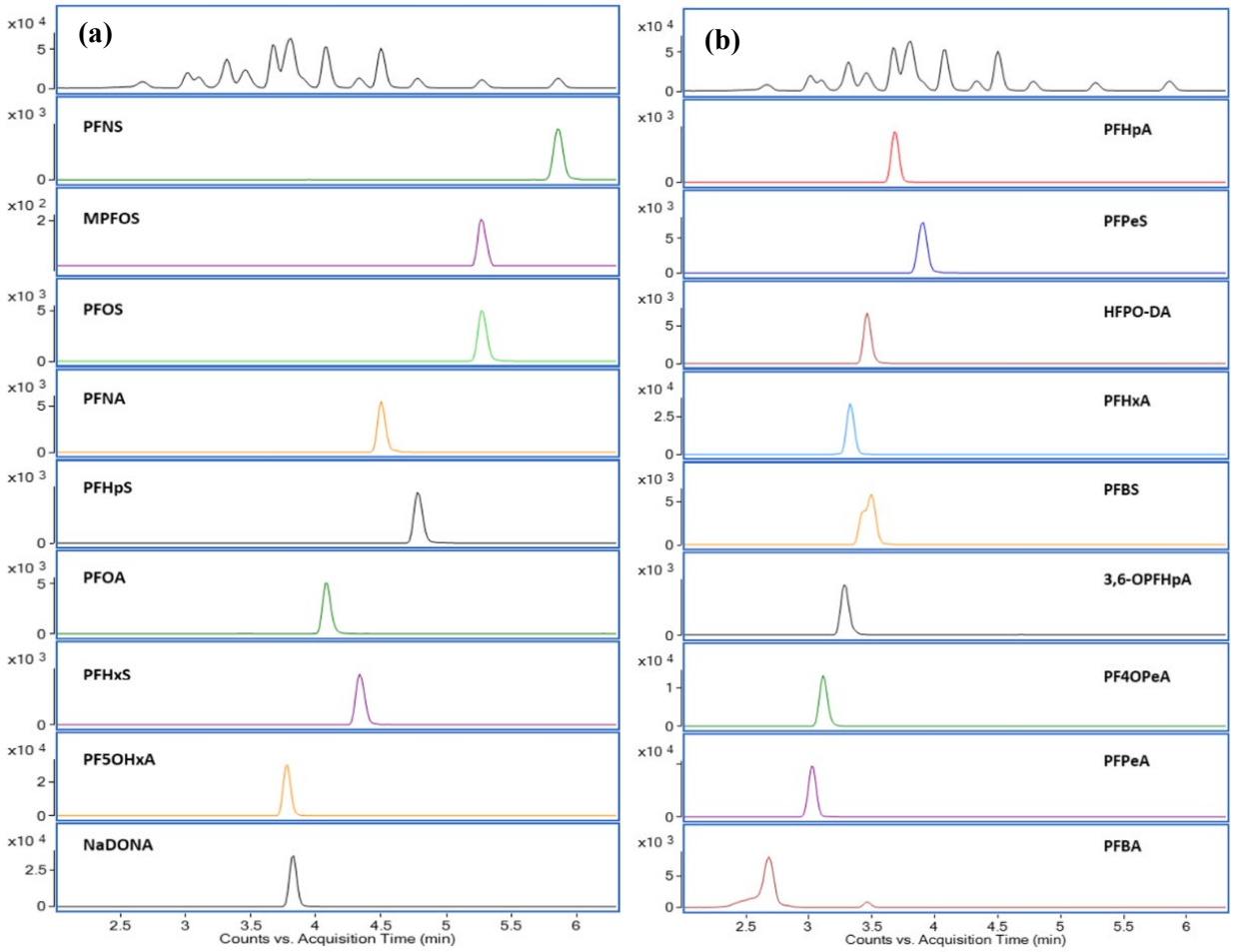

Figure 4.6. LC-MS/MS MRM Chromatograms of PFAS in Calibration Standard Solution for (a) PFNS, MPFOS, PFOS, PFNA, PFHpS, PFOA, PFHxS, PF5OHxA, and NaDONA and (b) PFHpA, PFPeS, HFPO-DA, PFHxA, PFBS, 3,6-OPFHpA, PF4OPeA, PFPeA, and PFBA.

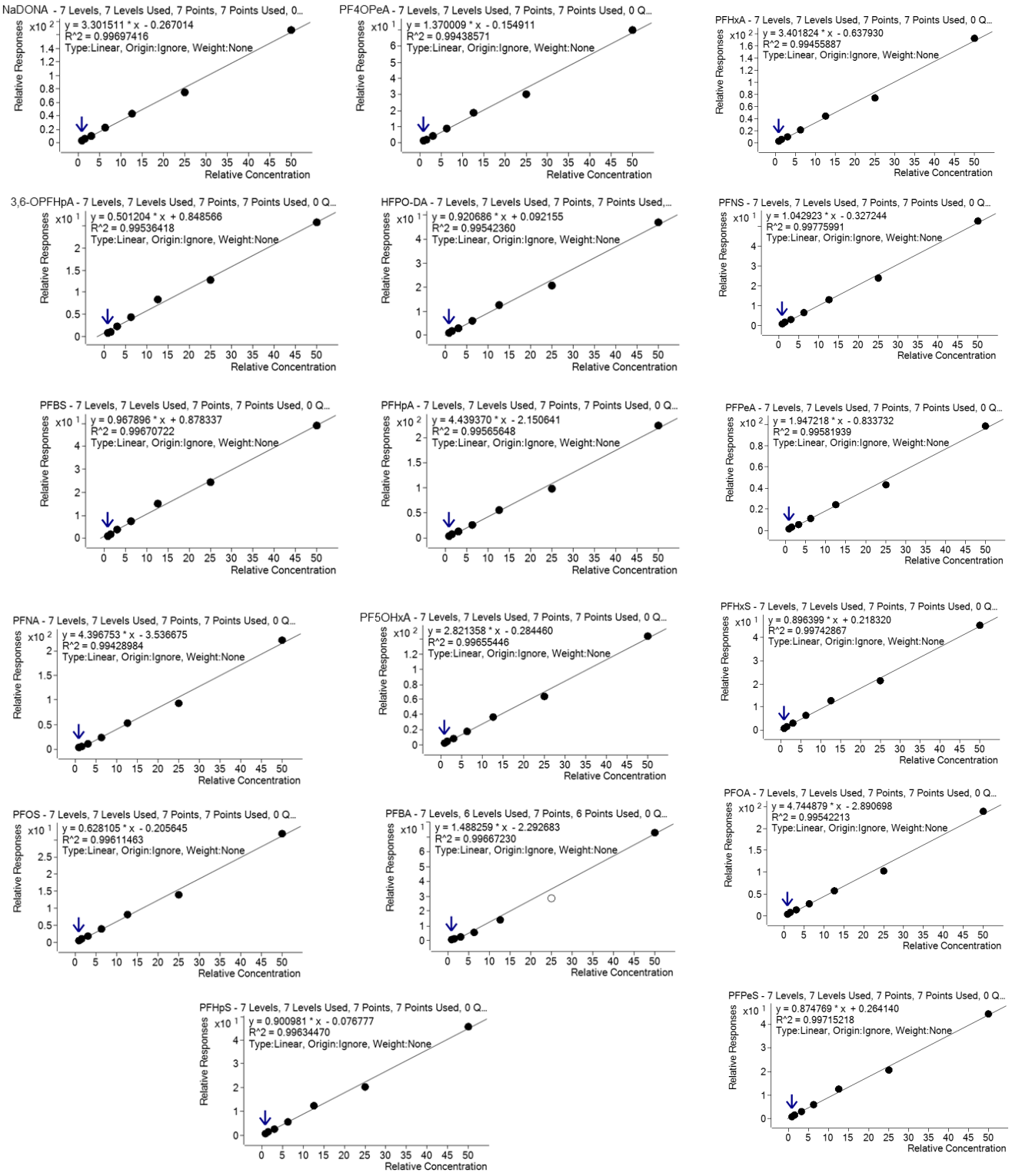

Figure 4.7. Calibration Curves for the 17 Target Analytes.

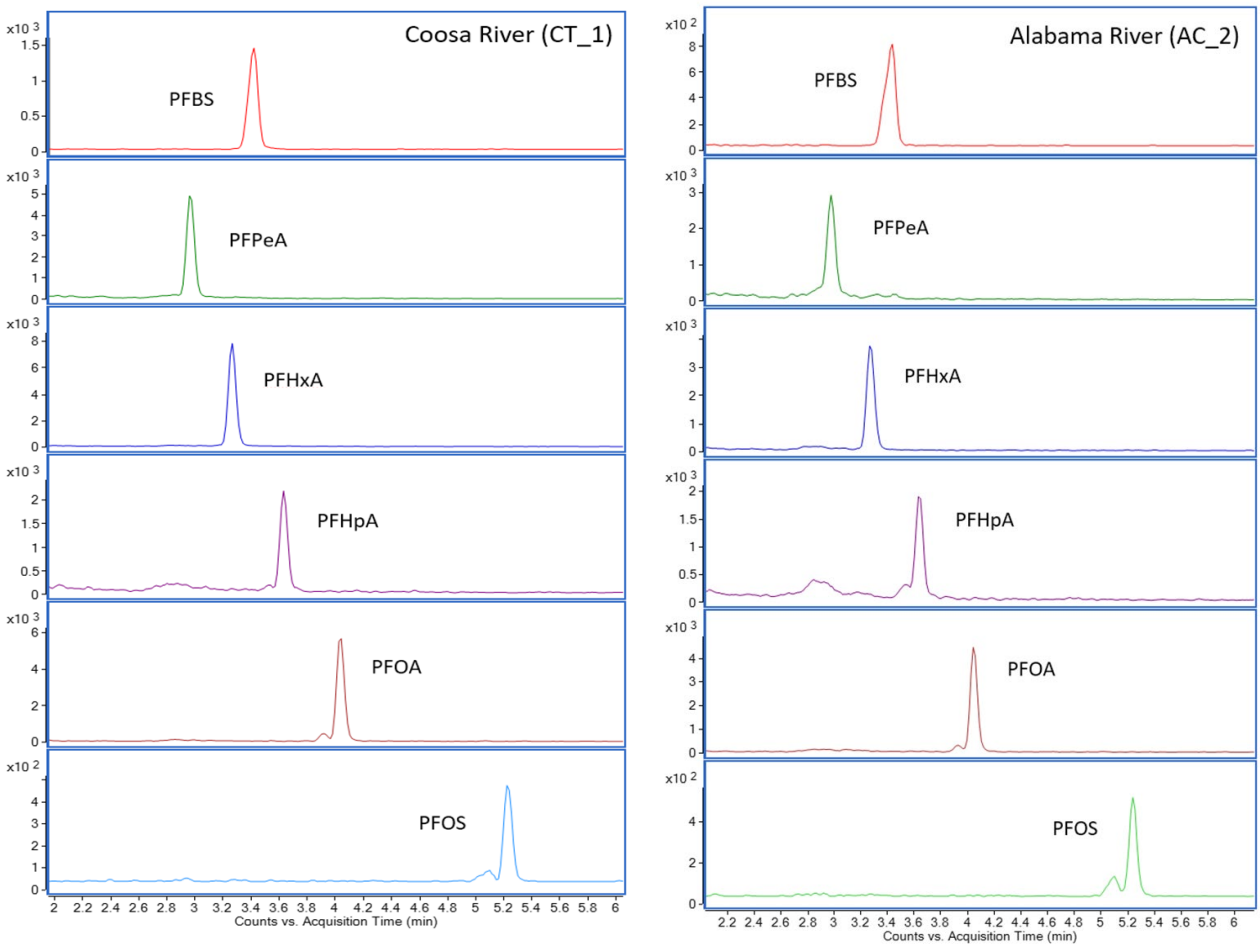

Figure 4.8. Extracted LC-MS/MS MRM Chromatograms of detected analytes in a surface water sample from the Coosa River (CT-1) and Alabama River (AC-2).

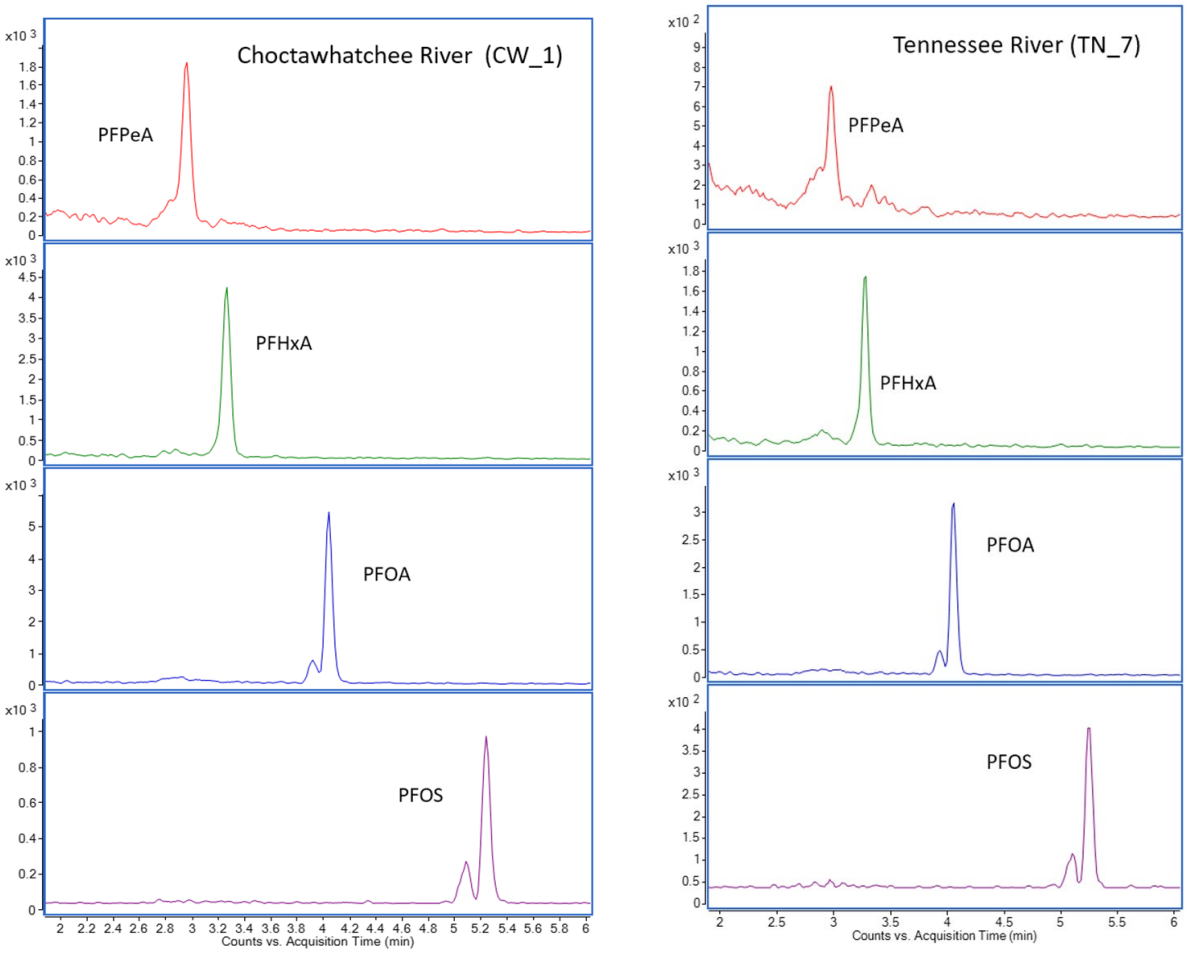

Figure 4.9. Extracted LC-MS/MS MRM Chromatograms of detected analytes in a surface water sample from the Choctawhatchee River (CW-1) and Tennessee River (TN-7).

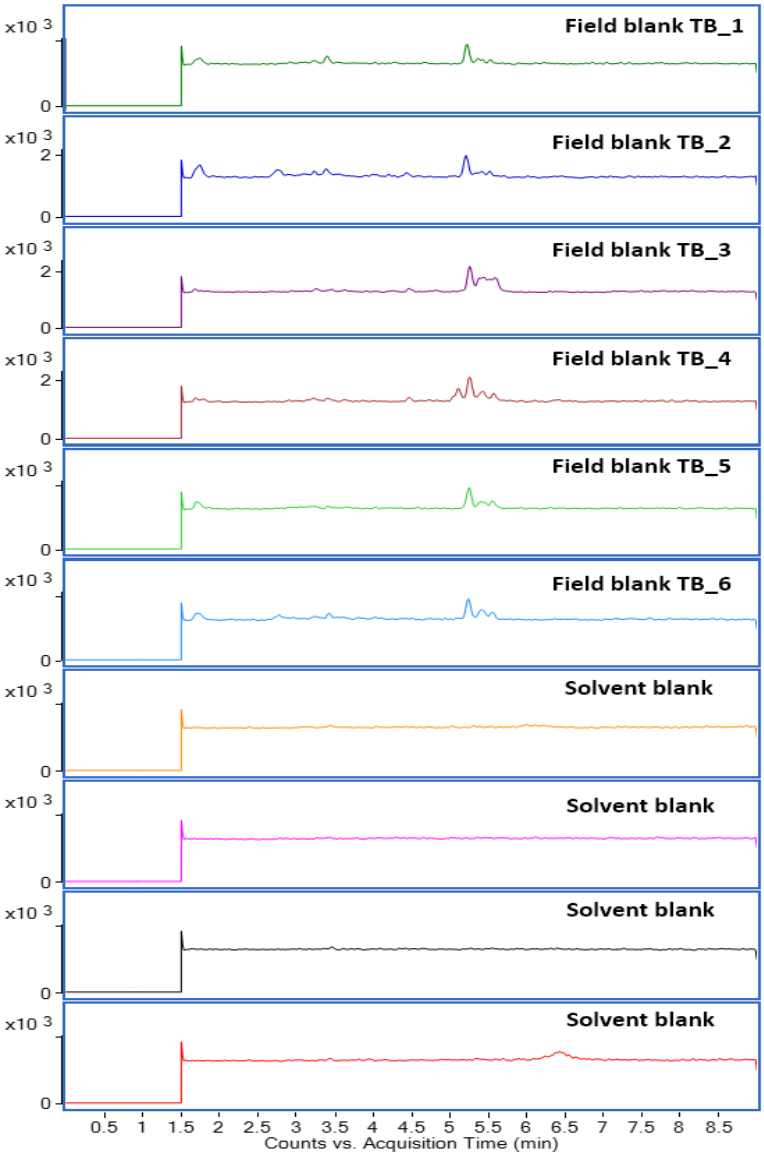

Figure 4.10. Solvent and field blanks LC-MS/MS MRM chromatograms.

S4. Data Analysis

Spatial Analyses were conducted using ArcMap v 10.7.1 (ESRI- Environmental Systems Research Institute). Hydrographic data was collected from the National Hydrography Dataset (https://apps.nationalmap.gov/downloader/#/) as an HU-8 subbasin shapefile. The catchment area discharging to each sampling point was delineated using the Hydrology toolbox in ArcMap. Digital Elevation Models (DEMs) used in the delineation process were downloaded from the USGS National Map

(https://apps.nationalmap.gov/downloader/#/) at a 1/3 arc-second resolution. DEMs were merged together (Mosaic to new Raster) and filled to remove any sinks (Hydrology > Fill). Flow direction (Hydrology > Flow Direction) and flow accumulation (Hydrology > Flow Accumulation) rasters were then generated to model water movement through the basins. Sampling points were used as the outlets of the catchment area (Hydrology>Snap Pour Points). Finally, catchment areas were delineated for each sampling point across all river basins (Figure 4.11).

After catchment areas were delineated, information on point and non-point sources was gathered. Information on industrial activity was obtained by searching the top employers in each of the 67 counties in Alabama and counties in neighboring states. Industrial facilities were grouped into paper products, automotive, plastics/packaging, chemical, flooring/textile/carpet, and others, based on their products. Locations of wastewater treatment plant (WWTP) outfalls were obtained from the Alabama Department of Environmental Management (ADEM), but only WWTP of the 100-most populous cities in Alabama were used. Municipal and Industrial Landfills information was also obtained from ADEM. Land cover data was collected from the Multi-Resolution Land Characteristics Consortium (MRLC) ("National Land Cover Database (NLCD)" 2016). The resolution of this data is 30 meters. Land cover categories were reclassified into Open Water (11), Developed (21-24), Barren Land (31), Forested (41-43), Shrub/Grassland (52, 71), Cultivated (81-82), and Wetlands (90,95). Legend information can be found at the MRLC webpage. Figure 4.12 illustrates land use information, industrial activity, and the location of WWTP outfalls, airports, landfills, and military bases. The overlay tool was used to compute the number of potential point sources (industries, airports, WWTP, military bases, and landfills). Land use rasters and catchment shapefiles were projected into WGS_1984_Albers and the Overlay Toolbox was used to calculate area in batch.

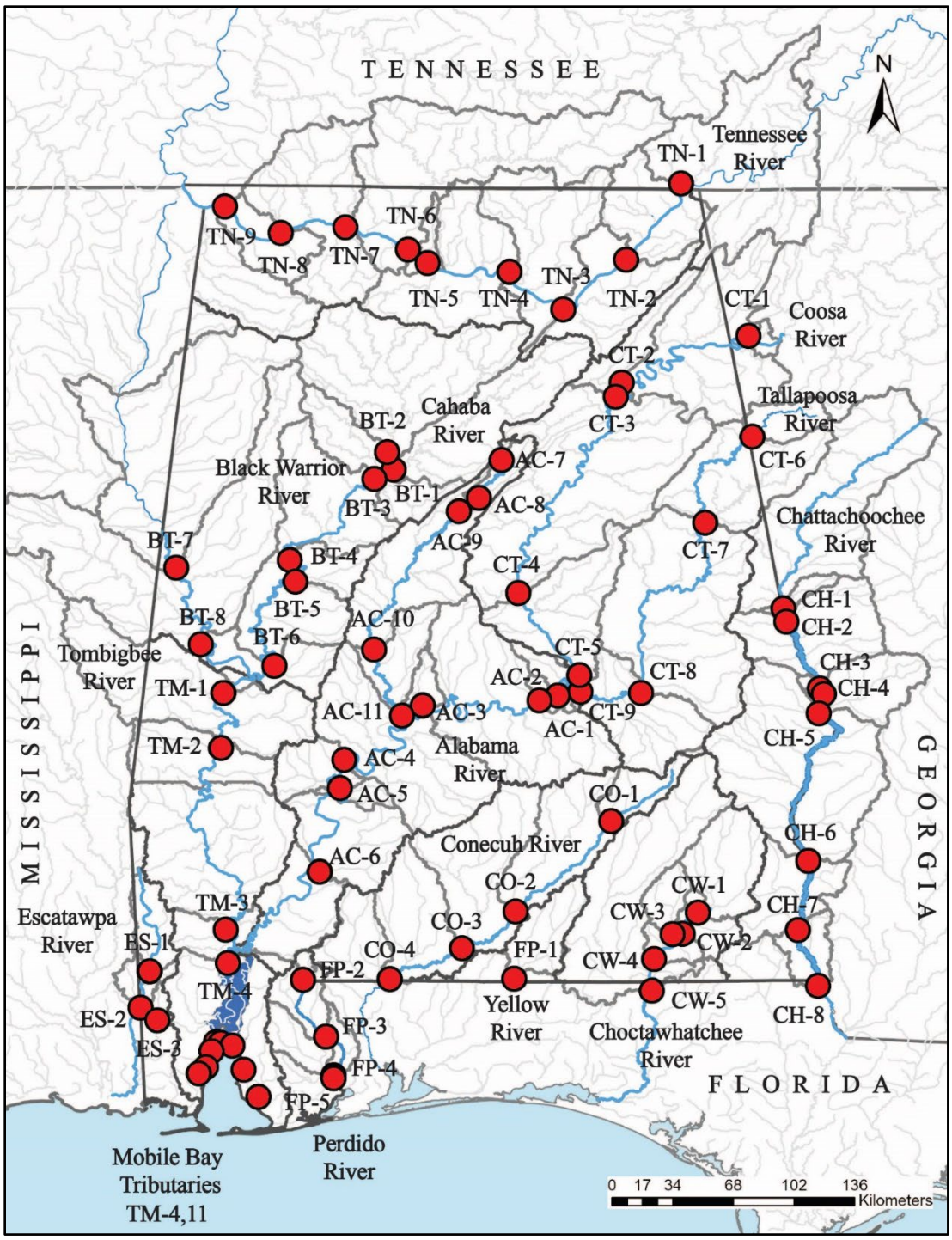

Figure 4.11. Catchment Areas for Selected Sampling Locations (in red).

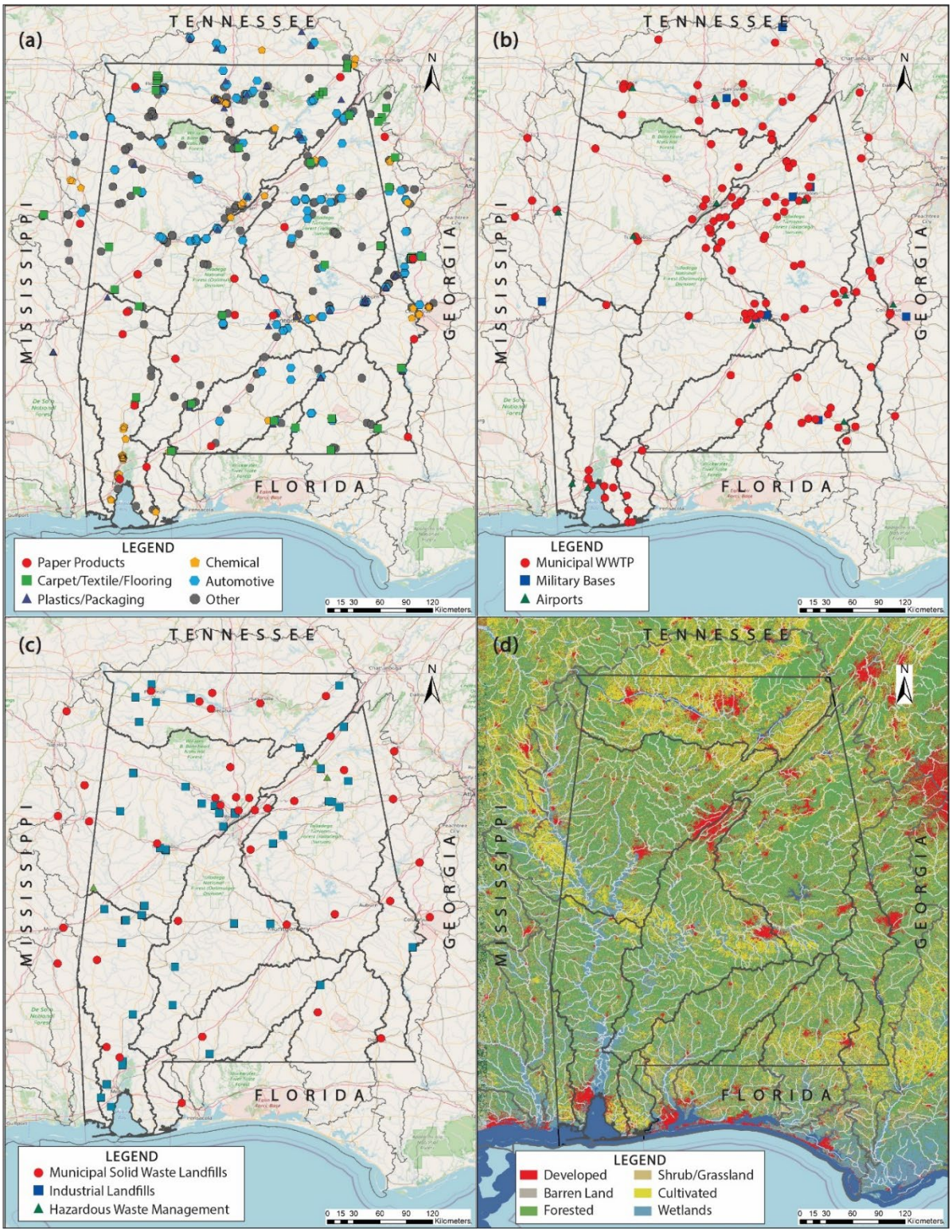

Figure 4.12. (a) Top Industrial Facilities, (b) Municipal WWTP, Military Bases, and Airports, (c) Landfills, and (d) Land Use.

S5. PFAS in Sampled River Systems in Alabama

Table 4.6. Concentration of PFAS, in ng L^{-1}, in riverine surface water in Alabama. Values are represented as mean ± standard deviation.

Sample	River System	PFBS	PFPeA	PFHxA	PFHpA	PFOA	PFOS	Sum PFAS
CT_6	Tallapoosa	n.d.	5.56 ± 0.50	n.d.	n.d.	n.d.	n.d.	5.56
CT_7	Tallapoosa	n.d.	5.91 ± 1.07	n.d.	n.d.	n.d.	n.d.	5.91
CT_8	Tallapoosa	n.d.	7.80 ± 0.58	n.d.	n.d.	5.78 ± 0.11	n.d.	13.58
CT_9	Tallapoosa	n.d.	8.55 ± 1.17	n.d.	n.d.	5.43 ± 0.08	n.d.	13.98
CT_1	Coosa	52.77 ± 4.36	34.19 ± 0.95	29.88 ± 2.03	8.83 ± 0.46	18.31 ± 0.32	11.04 ± 0.43	155.02
CT_2	Coosa	67.12 ± 6.75	52.07 ± 4.90	35.93 ± 2.92	11.91 ± 1.01	26.01 ± 2.01	20.51 ± 2.04	213.56
CT_3	Coosa	79.39 ± 1.79	54.90 ± 2.42	39.31 ± 1.00	13.10 ± 0.61	30.24 ± 1.08	20.36 ± 1.33	237.29
CT_4	Coosa	61.35 ± 1.65	35.59 ± 1.36	24.46 ± 0.69	11.31 ± 0.51	22.39 ± 0.75	29.59 ± 0.52	184.68
CT_5	Coosa	59.00 ± 3.72	33.85 ± 2.09	22.50 ± 1.32	10.44 ± 0.71	21.43 ± 1.24	18.11 ± 1.78	165.33
AC_1A	Alabama	45.06 ± 3.00	29.48 ± 2.32	19.48 ± 1.21	9.43 ± 0.78	19.20 ± 1.52	19.55 ± 2.14	142.21
AC_1B	Alabama	28.65 ± 2.13	20.81 ± 1.08	13.24 ± 0.57	7.55 ± 0.38	14.12 ± 0.39	12.04 ± 0.82	96.40
AC_2	Alabama	33.30 ± 3.53	23.49 ± 1.98	15.26 ± 1.14	7.93 ± 0.79	14.78 ± 1.13	12.98 ± 1.75	107.74
AC_3	Alabama	31.73 ± 2.79	22.31 ± 1.80	14.21 ± 0.82	7.67 ± 0.47	15.12 ± 0.90	11.42 ± 1.31	102.46
AC_4	Alabama	29.60 ± 4.16	21.27 ± 2.33	14.13 ± 1.66	8.18 ± 0.40	13.97 ± 1.12	10.86 ± 1.29	98.01
AC_5	Alabama	29.35 ± 1.00	22.65 ± 1.13	14.02 ± 0.33	7.58 ± 0.31	14.14 ± 0.31	11.99 ± 0.73	99.73
AC_6	Alabama	28.24 ± 2.31	21.13 ± 1.26	13.93 ± 0.92	7.79 ± 0.87	15.30 ± 0.44	10.65 ± 1.01	97.04
AC_7	Cahaba	n.d.	9.47 ± 1.20	n.d.	n.d.	6.37 ± 0.29	n.d.	15.85
AC_8	Cahaba	n.d.	13.05 ± 0.15	6.64 ± 0.48	n.d.	5.74 ± 0.15	n.d.	25.43
AC_9	Cahaba	n.d.	14.97 ± 1.84	7.31 ± 0.75	n.d.	7.11 ± 0.17	n.d.	29.39
AC_10	Cahaba	n.d.	8.65 ± 1.15	n.d.	n.d.	n.d.	n.d.	8.65
AC_11	Cahaba	n.d.	8.50 ± 1.63	n.d.	n.d.	n.d.	n.d.	8.50
CH_1	Chattahoochee	n.d.	14.50 ± 0.68	8.99 ± 0.52	5.26 ± 0.53	6.96 ± 0.14	n.d.	35.70
CH_2	Chattahoochee	n.d.	17.53 ± 0.80	10.76 ± 0.34	6.22 ± 0.68	8.97 ± 0.38	n.d.	43.48
CH_3	Chattahoochee	n.d.	14.98 ± 0.59	9.45 ± 0.85	5.36 ± 0.38	7.86 ± 0.46	n.d.	37.65
CH_4	Chattahoochee	n.d.	11.80 ± 1.15	5.63 ± 0.60	n.d.	4.33 ± 0.43	n.d.	21.76
CH_5	Chattahoochee	n.d.	10.84 ± 0.73	5.35 ± 0.89	n.d.	6.26 ± 0.54	n.d.	22.45

CH_6	Chattahoochee	n.d.	10.66 ± 0.79	4.63 ± 0.83	n.d.	10.17 ± 0.76	n.d.	25.46
CH_7	Chattahoochee	n.d.	9.72 ± 0.81	3.73 ± 0.43	n.d.	9.28 ± 0.74	n.d.	22.74
CH_8	Chattahoochee	n.d.	8.40 ± 1.19	3.56 ± 0.56	n.d.	9.42 ± 0.58	n.d.	21.38
CW_1	Choctawhatchee	n.d.	n.d.	n.d.	n.d.	n.d.	n.d.	n.d.
CW_2	Choctawhatchee	n.d.	7.95 ± 2.26	n.d.	n.d.	n.d.	n.d.	7.95
CW_3	Choctawhatchee	n.d.	15.74 ± 0.77	14.98 ± 0.45	n.d.	14.01 ± 0.86	19.10 ± 3.46	63.83
CW_4	Choctawhatchee	n.d.	7.45 ± 0.56	n.d.	n.d.	n.d.	n.d.	7.45
CW_5	Choctawhatchee	n.d.	5.96 ± 1.01	n.d.	n.d.	n.d.	n.d.	5.96
FP_1	Yellow	n.d.	n.d.	n.d.	n.d.	n.d.	n.d.	n.d.
CO_1	Conecuh	n.d.	n.d.	n.d.	n.d.	n.d.	n.d.	n.d.
CO_2	Conecuh	n.d.	n.d.	n.d.	n.d.	n.d.	n.d.	n.d.
CO_3	Conecuh	n.d.	n.d.	n.d.	n.d.	n.d.	n.d.	n.d.
CO_4	Conecuh	n.d.	n.d.	n.d.	n.d.	n.d.	n.d.	n.d.
BT_7	Tombigbee	n.d.	5.78 ± 1.30	n.d.	n.d.	0.55 ± 0.14	n.d.	6.33
BT_8	Tombigbee	n.d.	7.65 ± 2.13	n.d.	n.d.	0.40 ± 0.18	n.d.	8.05
TM_1	Tombigbee	n.d.	8.42 ± 0.59	n.d.	n.d.	n.d.	n.d.	8.42
TM_2	Tombigbee	n.d.	7.87 ± 1.16	n.d.	n.d.	n.d.	n.d.	7.87
TM_3	Tombigbee	n.d.	9.05 ± 0.96	n.d.	n.d.	n.d.	n.d.	9.05
BT_1	Black Warrior	n.d.	23.07 ± 2.10	11.55 ± 0.88	n.d.	6.14 ± 0.38	n.d.	40.76
BT_2	Black Warrior	n.d.	2.11 ± 1.59	n.d.	n.d.	0.24 ± 0.14	n.d.	2.35
BT_3	Black Warrior	n.d.	7.41 ± 1.53	n.d.	n.d.	1.22 ± 0.23	n.d.	8.63
BT_4	Black Warrior	n.d.	6.90 ± 1.37	n.d.	n.d.	1.51 ± 0.18	n.d.	8.41
BT_5	Black Warrior	n.d.	6.49 ± 2.61	n.d.	n.d.	1.76 ± 0.11	n.d.	8.26
BT_6	Black Warrior	n.d.	5.96 ± 0.79	n.d.	n.d.	1.09 ± 0.19	n.d.	7.05
ES_1	Escatawpa	n.d.	n.d.	n.d.	n.d.	n.d.	n.d.	n.d.
ES_2	Escatawpa	n.d.	n.d.	n.d.	n.d.	n.d.	n.d.	n.d.
ES_3	Escatawpa	n.d.	n.d.	n.d.	n.d.	n.d.	n.d.	n.d.
TM_4	Mobile	n.d.	12.89 ± 1.06	4.72 ± 0.35	n.d.	6.40 ± 0.23	n.d.	24.01
TM_5	Mobile	n.d.	12.74 ± 1.41	5.03 ± 0.79	n.d.	6.45 ± 0.57	n.d.	24.22
TM_6	Spanish	n.d.	14.10 ± 1.06	4.87 ± 0.44	n.d.	6.78 ± 0.27	n.d.	25.74
TM_7	Apalachee	n.d.	14.68 ± 0.75	5.81 ± 0.88	n.d.	7.53 ± 0.43	n.d.	28.02

TM_8	Mobile Bay	n.d.	12.34 ± 0.46	4.58 ± 0.90	n.d.	6.27 ± 0.34	n.d.	23.20
TM_9	Dog	n.d.	11.73 ± 1.59	4.62 ± 0.46	n.d.	5.86 ± 0.67	n.d.	22.20
TM_10	Deer	n.d.	13.30 ± 2.33	6.50 ± 0.56	n.d.	6.19 ± 0.19	30.69 ± 2.21	56.68
TM_11	Fly	n.d.	4.39 ± 1.03	1.41 ± 0.34	n.d.	2.68 ± 0.07	n.d.	8.48
TM_12	Fish	n.d.	6.69 ± 2.17	n.d.	n.d.	3.44 ± 0.16	n.d.	10.12
FP_2	Perdido	n.d.	4.16 ± 0.57	n.d.	n.d.	2.59 ± 0.12	n.d.	6.75
FP_3	Perdido	n.d.	13.48 ± 0.66	5.48 ± 0.71	n.d.	8.38 ± 0.45	n.d.	27.34
FP_4	Perdido	n.d.	13.87 ± 1.37	6.07 ± 0.61	n.d.	9.01 ± 0.75	n.d.	28.95
FP_5	Perdido	n.d.	9.97 ± 0.26	3.18 ± 0.46	n.d.	5.85 ± 0.16	n.d.	19.00
TN_1	Tennessee	n.d.	5.26 ± 0.61	0.88 ± 0.24	n.d.	3.02 ± 0.10	n.d.	9.17
TN_2	Tennessee	n.d.	6.43 ± 0.93	1.51 ± 0.22	n.d.	3.25 ± 0.12	n.d.	11.20
TN_3	Tennessee	n.d.	6.23 ± 0.53	2.14 ± 0.59	n.d.	3.37 ± 0.05	n.d.	11.73
TN_4	Tennessee	n.d.	7.99 ± 0.49	5.75 ± 0.39	n.d.	3.22 ± 0.14	n.d.	16.95
TN_5	Tennessee	n.d.	8.24 ± 0.90	7.02 ± 0.99	n.d.	3.31 ± 0.15	n.d.	18.56
TN_6	Tennessee	n.d.	7.72 ± 0.37	4.22 ± 0.48	n.d.	3.93 ± 0.26	n.d.	15.88
TN_7	Tennessee	n.d.	8.78 ± 0.66	6.58 ± 0.70	n.d.	10.70 ± 0.88	9.51 ± 1.62	35.58
TN_8	Tennessee	n.d.	8.20 ± 0.17	6.01 ± 0.78	n.d.	9.40 ± 0.48	9.07 ± 1.37	32.68
TN_9	Tennessee	n.d.	7.56 ± 0.65	6.73 ± 0.84	n.d.	10.06 ± 0.55	7.39 ± 0.24	31.74

n.d.= not detected

Table 4.7. Spearman Correlation Matrix. A significant correlation ($p<0.05$) was observed for all pairings.

	PFBS	PFPeA	PFHxA	PFHpA	PFOA	PFOS
PFBS	1	0.61	0.63	0.9	0.62	0.81
PFPeA	0.61	1	0.85	0.67	0.83	0.59
PFHxA	0.63	0.85	1	0.69	0.89	0.7
PFHpA	0.9	0.67	0.69	1	0.65	0.72
PFOA	0.62	0.83	0.89	0.65	1	0.69
PFOS	0.81	0.59	0.7	0.72	0.69	1

S.5.1 Basin-Level Charts

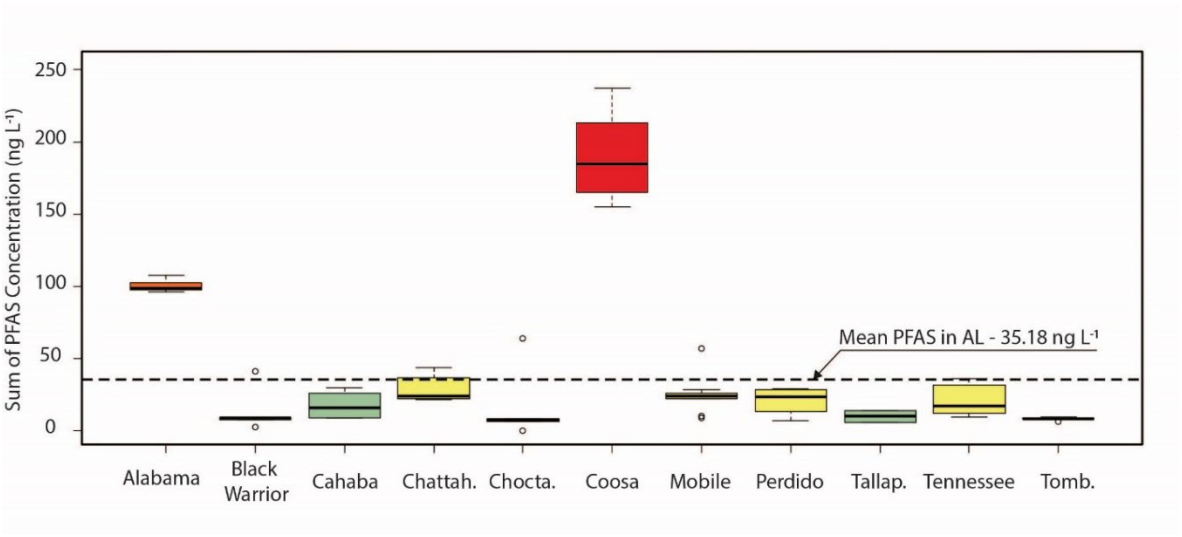

Figure 4.13. Boxplot of ∑PFAS in sampled rivers in Alabama

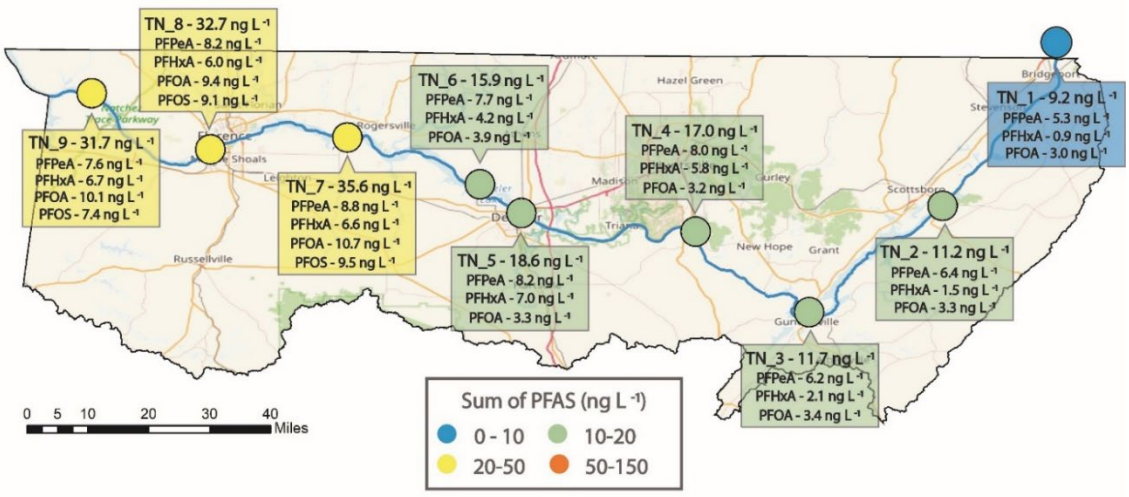

Figure 4.14. Profile and Concentration of PFAS in the Tennessee River Basin

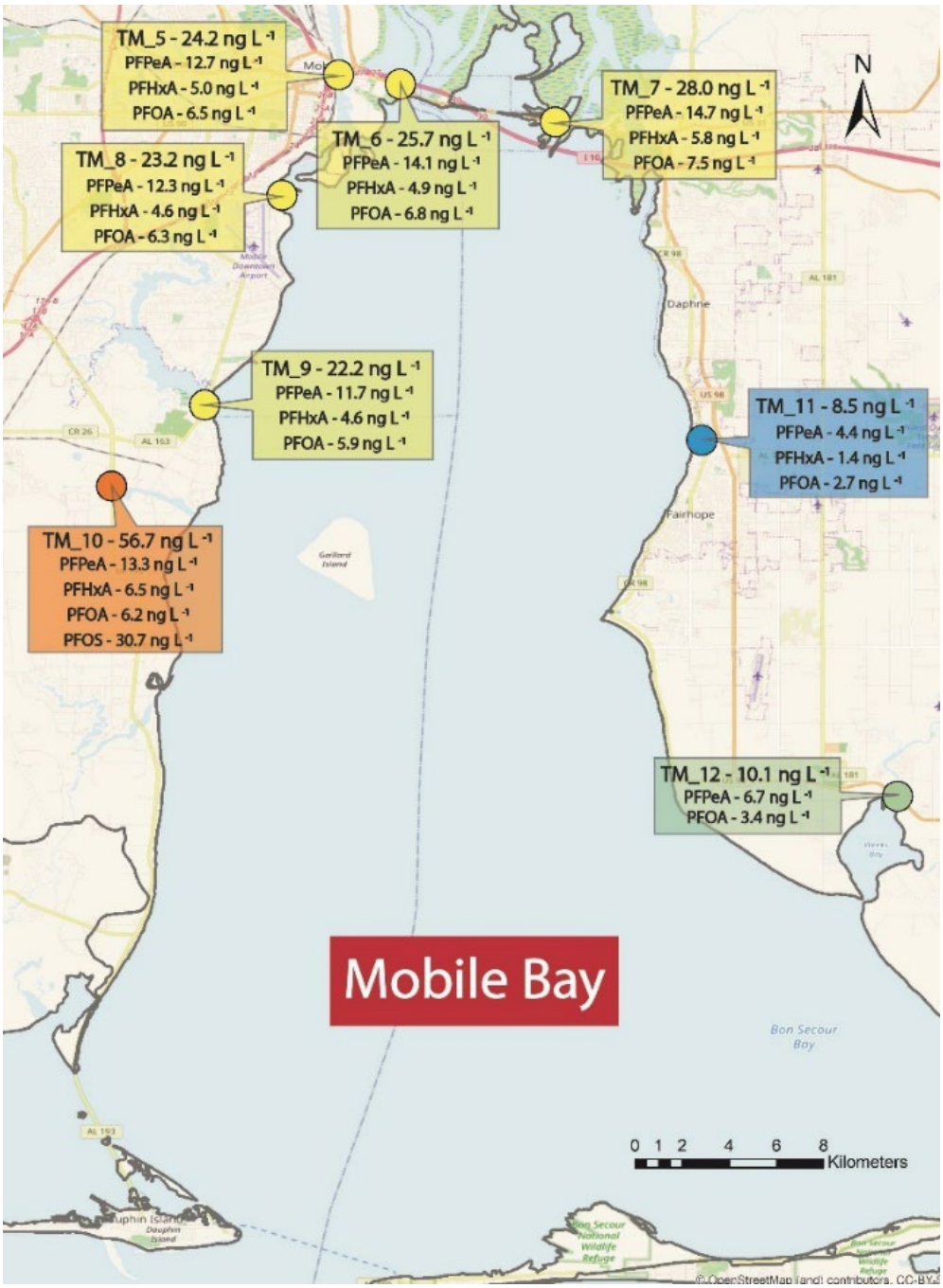

Figure 4.15. Profile and Concentration of PFAS in Mobile Bay and Tributaries.

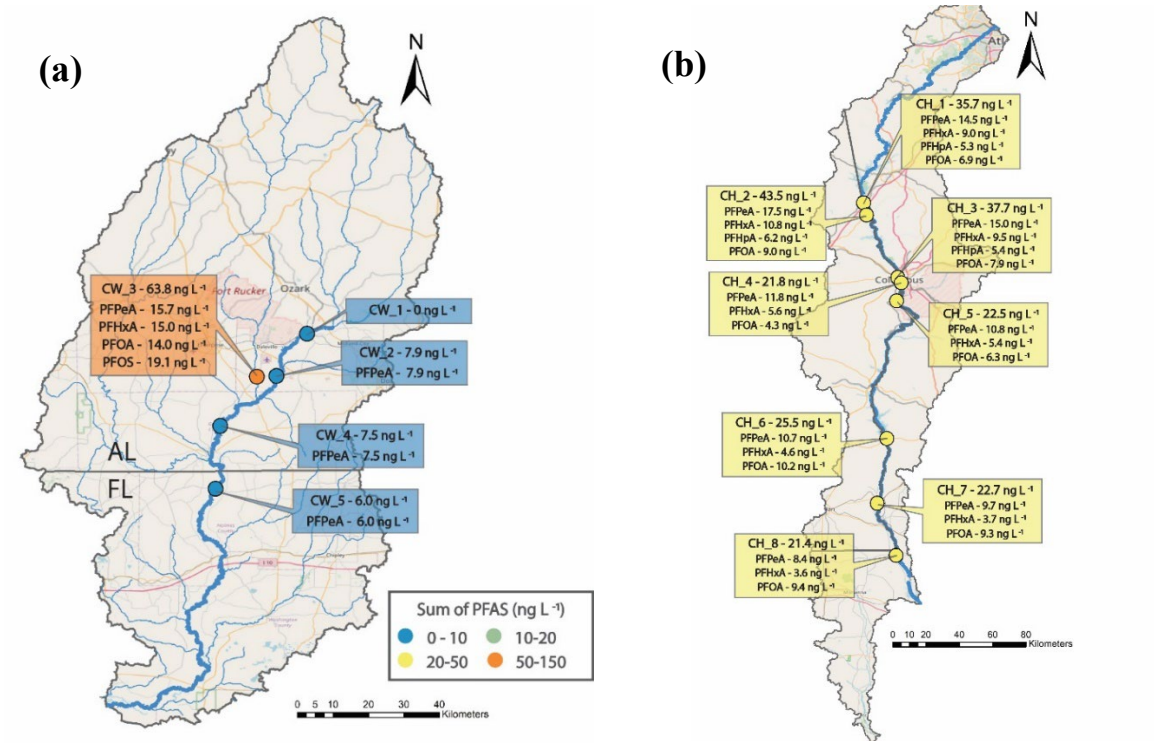

Figure 4.16. Profile and Concentration of PFAS in the (a) Choctawhatchee and (b) Chattahoochee River Basins.

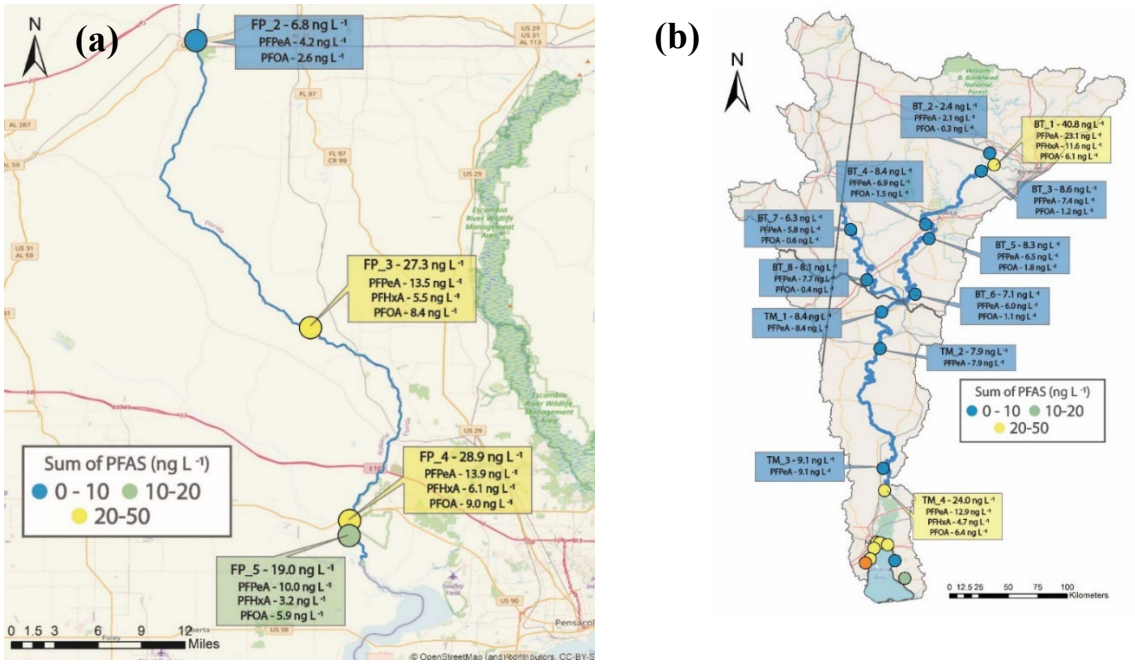

Figure 4.17. Profile and Concentration of PFAS in the (a) Perdido River and (b) Black Warrior and Tombigbee River Basins.

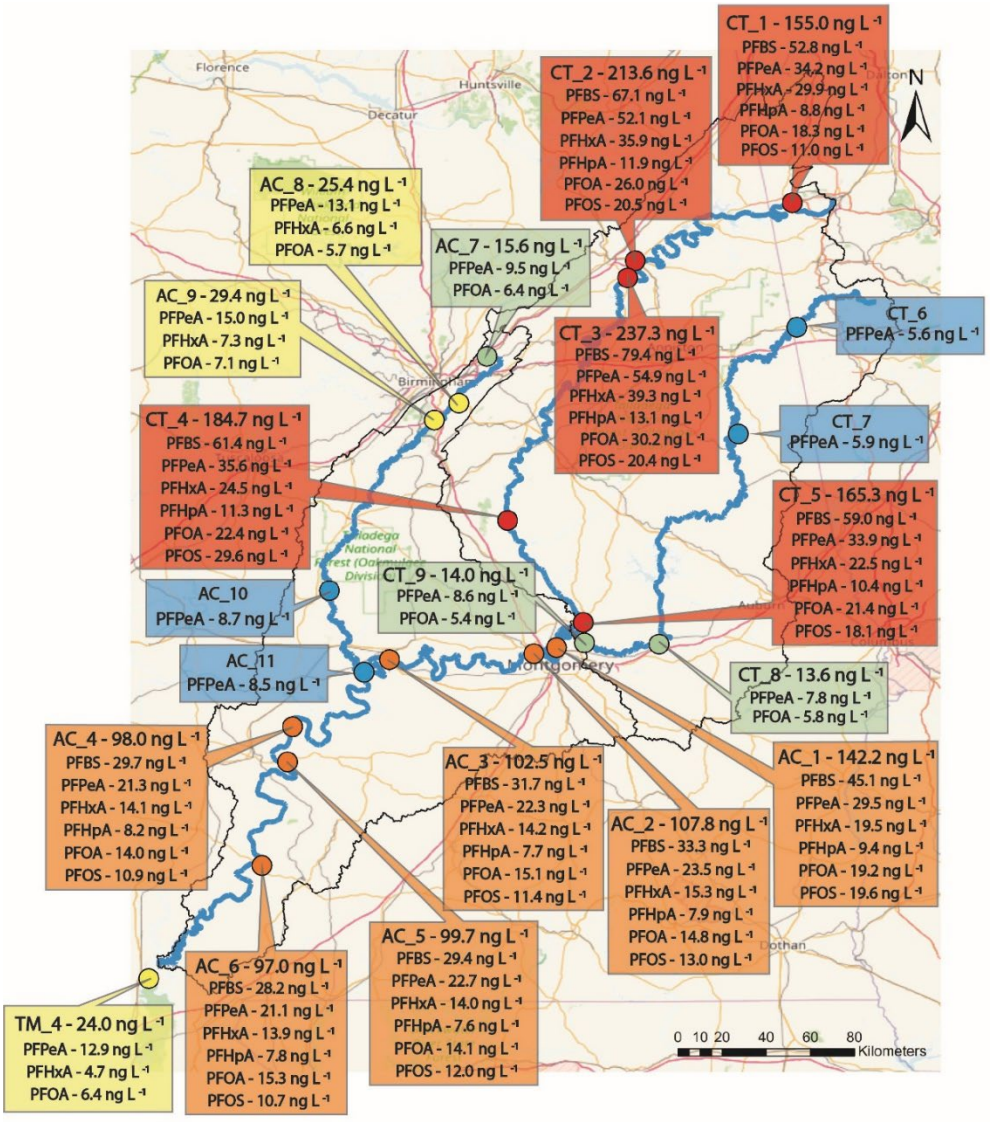

Figure 4.18. Profile and Concentration of PFAS in the Coosa, Tallapoosa, Cahaba, and Alabama River Basins

S6. Mass flux Analysis

Mass flux of PFAS ($\Phi_{\sum PFAS}$) was calculated by multiplying the sum of PFAS concentration ($\sum$PFAS) in a given location by the 48-h average volumetric discharge rate ($\overline{Q}$), as shown in the equation below. Volumetric flow rate data was acquired from the United Stated Geological Survey (USGS), when stations were located near sampling points, or from the National Water Model (NWM), supported by the

US National Oceanic and Atmospheric Administration (US-NOAA). Volumetric flow rates for AC_1 and CT_3 were calculated by adding the 48-h average flow from upstream USGS gage stations.

$$\Phi_{\sum PFAS}\ [mg\ s^{-1}] = \sum PFAS * \overline{Q} \quad (1)$$

Table 4.8. Volumetric Flow Rate and Mass Flux. Flow data was acquired from either United States Geological Survey (USGS) gages or National Water Model (NWM). NA = not available.

Sample ID	River	Sum PFAS (ng L^{-1})	48-h Flow Rate (ft^3/s)	Flow Data Source	Mass Flux (mg s^{-1})
CT_6	Tallapoosa River	5.56	225.43	USGS - 02411930	0.035
CT_7	Tallapoosa River	5.91	1531.97	NWM	0.256
CT_8	Tallapoosa River	13.58	2639.44	NWM	1.015
CT_9	Tallapoosa River	13.98	5464.27	USGS - 02419890	2.162
CT_1	Coosa River	155.02	5304.91	NWM	23.281
CT_2	Coosa River	213.56	5084.37	NWM	30.739
CT_3	Coosa River	237.29	5278.20	NWM and USGS - 02401000	35.458
CT_4	Coosa River	184.68	10963.00	Lay Dam	57.319
CT_5	Coosa River	165.33	11071.41	USGS - 02411590	51.818
AC_1A	Alabama River	142.21	15,697.69	USGS – 02411590 and 02419890	62.3
AC_1B	Alabama River	96.40	13443.44	USGS – 02411590 and 02419890	36.688
AC_2	Alabama River	107.74	13749.29	USGS – 02420000	41.937
AC_3	Alabama River	102.46	16624.40	NWM	48.222
AC_4	Alabama River	98.01	NA	NA	NA
AC_5	Alabama River	99.73	21877.56	NWM	61.771
AC_6	Alabama River	97.04	23057.14	NWM	63.343
AC_7	Cahaba River	15.85	13.09	USGS - 02423130	0.006
AC_8	Cahaba River	25.43	133.05	USGS - 02423425	0.096
AC_9	Cahaba River	29.39	178.50	USGS - 02423500	0.149
AC_10	Cahaba River	8.65	1545.77	USGS - 02425000	0.379
AC_11	Cahaba River	8.50	1376.55	NWM	0.331
CH_1	Chattahoochee River	35.70	1348.34	USGS - 02339500	1.363
CH_2	Chattahoochee River	43.48	2023.00	NWM	2.490
CH_3	Chattahoochee River	37.65	2579.72	USGS - 02341460	2.750
CH_4	Chattahoochee River	21.76	2909.07	NWM	1.792
CH_5	Chattahoochee River	22.45	3538.51	NWM	2.249
CH_6	Chattahoochee River	25.46	5060.23	USGS - 023432415	3.647
CH_7	Chattahoochee River	22.74	5597.65	USGS - 02343801	3.603
CH_8	Chattahoochee River	21.38	6204.02	NWM	3.755

CW_1	Choctawhatchee R.	n.d	219.22	USGS - 02361000	NA
CW_2	Choctawhatchee R.	7.95	495.70	NWM	0.112
CW_3	Choctawhatchee R.	63.83	109.31	NWM	0.198
CW_4	Choctawhatchee R.	7.45	850.23	NWM	0.179
CW_5	Choctawhatchee R.	5.96	1770.67	USGS - 02365200	0.299
FP_1	Yellow River	n.d.	679.84	NWM	NA
CO_1	Conecuh River	n.d.	41.585	NWM	NA
CO_2	Conecuh River	n.d.	623.308	USGS - 02372430	NA
CO_3	Conecuh River	n.d.	2590.620	NWM	NA
CO_4	Conecuh River	n.d.	2803.480	NWM	NA
BT_7	Tombigbee River	6.33	3080.82	NWM	0.552
BT_8	Tombigbee River	8.05	2033.47	NWM	0.463
TM_1	Tombigbee River	8.42	4352.57	NWM	1.037
TM_2	Tombigbee River	7.87	9122.80	USGS - 02469525	2.032
TM_3	Tombigbee River	9.05	9456.34	NWM	2.422
BT_1	Black Warrior River	40.76	583.22	NWM	0.673
BT_2	Black Warrior River	2.35	1596.29	NWM	0.106
BT_3	Black Warrior River	8.63	NA	NA	NA
BT_4	Black Warrior River	8.41	2333.14	NWM	0.555
BT_5	Black Warrior River	8.26	2491.21	NWM	0.582
BT_6	Black Warrior River	7.05	2798.74	NWM	0.559
ES_1	Escatawpa River	n.d.	192.92	NWM	NA
ES_2	Escatawpa River	n.d.	407.28	NWM	NA
ES_3	Escatawpa River	n.d.	37.49	USGS - 02479945	NA
TM_4	Mobile River	24.01	18143.90	NWM	12.333
TM_5	Mobile River	24.22	19326.66	NWM	13.250
TM_6	Spanish River	25.74	NA	NA	NA
TM_7	Apalachee River	28.02	NA	NA	NA
TM_8	Mobile Bay	23.20	NA	NA	NA
TM_9	Dog River	22.20	306.56	NWM	0.193
TM_10	Deer River	56.68	17.35	NWM	0.028
TM_11	Fly Creek	8.48	6.89	NWM	0.002
TM_12	Fish River	10.12	214.09	NWM	0.061
FP_2	Perdido River	6.75	18.79	NWM	0.004
FP_3	Perdido River	27.34	315.89	NWM	0.244
FP_4	Perdido River	28.95	716.20	NWM	0.587
FP_5	Perdido River	19.00	1253.11	NWM	0.674
TN_1	Tennessee River	9.17	NA	NA	NA
TN_2	Tennessee River	11.20	NA	NA	NA
TN_3	Tennessee River	11.73	NA	NA	NA
TN_4	Tennessee River	16.95	NA	NA	NA
TN_5	Tennessee River	18.56	NA	NA	NA
TN_6	Tennessee River	15.88	NA	NA	NA

TN_7	Tennessee River	35.58	NA	NA	NA
TN_8	Tennessee River	32.68	NA	NA	NA
TN_9	Tennessee River	31.74	NA	NA	NA

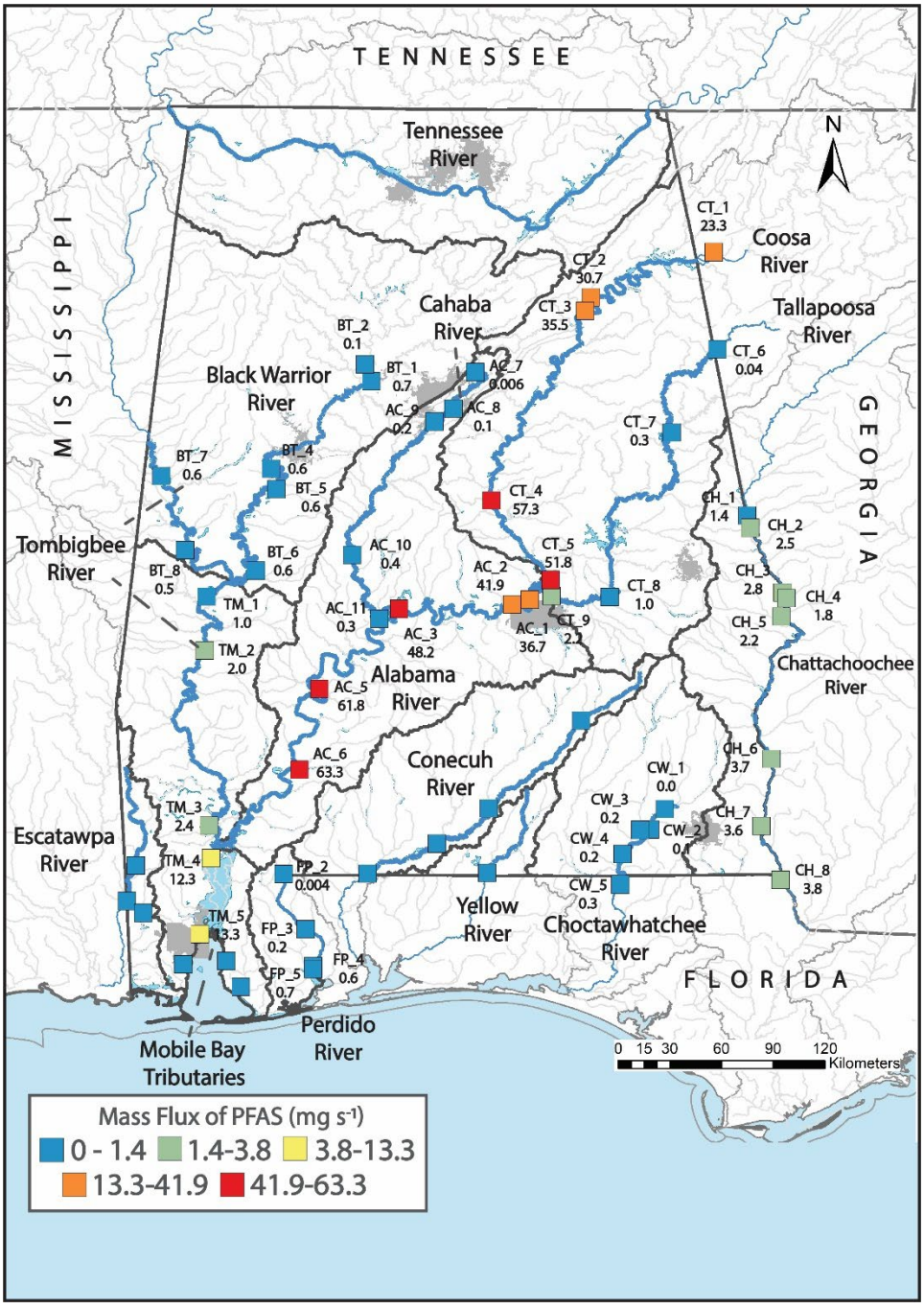

Figure 4.19. Mass Flux, in mg s^{-1}, of ∑PFAS in selected rivers in Alabama

S6.1. Alabama, Cahaba, Coosa, and Tallapoosa Rivers. The Alabama-Coosa-Tallapoosa River system is one of the most important river systems in Alabama as it runs the length of the majority of the state, passing through major cities such as Montgomery and Birmingham, before it merges with the Tombigbee River to form the Mobile River. The Coosa River was previously sampled for PFAS at a similar location to CT-1, the first sampling location in Figure 4.2a. In that study, Lasier et al. (2011) detected ∑PFAS concentration of 564 ng L^{-1} and PFOS and PFBS as major analytes, compared to the 155.02 ng L^{-1} found in this study. The authors linked the contamination to carpet manufacturers in Dalton, GA that have their effluents treated by a municipal wastewater treatment plant. Indeed, it seems likely that PFAS in the Coosa River is heavily impacted by inputs from Georgia. For instance, the first sampling point on the Coosa River, CT-1, indicates a mass flux of PFAS ($\Phi_{\sum PFAS}$) of 23.28 mg s^{-1} from Georgia into Alabama, while $\Phi_{\sum PFAS}$ in CT-2 (30.74 mg s^{-1}) also reflects possible inputs through tributaries from Georgia, including the Chattooga River. Carpet and textile industries are known to be potential sources of PFAS, due to the use of PFAS as stain-, fire-, and water-repellents in fabrics (Zheng and Salamova, 2020; Zhu et al., 2021). The fact that PFBS, used as a PFOS-alternative in the formulation of these products (DEPA, 2015), was found at high concentrations in the Coosa River further supports the hypothesis that carpet industries in Georgia are a major source of PFAS in the Coosa River. A further increase of 21.8 mg s^{-1} in the $\Phi_{\sum PFAS}$ was observed between CT-3 and CT-4. There are several potential sources between those points, including a high number of industries, WWTPs, landfills, and military bases. However, a more detailed sampling campaign is needed to determine specific sources. Similarly, a consistent increase in the $\Phi_{\sum PFAS}$ was observed in the Tallapoosa River, reaching up to 2.16 mg s^{-1} before it merged with the Coosa River. Interestingly, PFOA was only identified after sample location CT_7. Potential sources to CT_8 include inputs from the Auburn area discharged through the Chewacla and Saugahatchee creeks, local inputs from a large sewage pond in Tallassee, and inputs from a large landfill. Landfills are a major source of PFAS to the environment due to the disposal of many PFAS-containing products and waste (Lang et al., 2017). Alabama has 173 operating landfills, with many of them located in poor rural areas and accepting toxic waste from all states in the US

(Milman, 2019). A more detailed sampling approach is needed to determine the effect of landfills on PFAS contamination in Alabama's river system.

The Alabama River, formed from the confluence of the Coosa and Tallapoosa rivers exhibited relatively high $\sum_6$PFAS concentrations, with a mean of 100.23 ng L^{-1}. While the Coosa and Tallapoosa rivers were sampled on June 27th, the Alabama River was sampled on July 8th. Because of that, AC-1 was sampled twice, during each sampling event, to better understand the effect of temporal variations in the flux and concentration of PFAS. A considerable difference in the concentration and mass flux was observed between those two dates: 142.20 ng L^{-1} and 63.20 mg s^{-1} on June 27th versus 96.40 ng L^{-1} and 36.69 mg s^{-1} on July 8th. The difference could be related to variability in river flow between the sampling dates (15,697 and 13,443 ft^3 s^{-1}), controlled by two upstream dams, one on the Coosa and one on the Tallapoosa. In general, higher concentrations are expected with lower volumetric flow rates, assuming that PFAS sources are relatively constant. The fact that the opposite was observed in sample AC-1 suggests that increases in runoff could be an important vector for PFAS in that catchment. Runoff has been previously linked to be a major vector of PFAS into waterways (Kim and Kannan, 2007). Regardless, the fluxes in AC-1 are in agreement with those calculated for upstream and downstream samples. Because sample AC-1B was collected on the same day as AC-2,6, the $\Phi_{\sum PFAS}$ of 36.69 mg s^{-1} was adopted for AC-1. An increase in the $\Phi_{\sum PFAS}$ was observed at AC-2, most likely due to inputs from the City of Montgomery. AC-2 is downstream from three WWTPs receiving waste from Montgomery and Prattville, and from the Maxwell Air Force Base. A further increase to 48.22 mg s^{-1} was observed at AC-3, with a catchment primarily comprised of forested and cultivated areas, but also containing industries associated with PFAS use. PFAS flux at AC-3 is most likely impacted by industrial discharges, including a large automotive manufacturing industry, a paper mill, and an engineered plastics facility. The Alabama River also receives inputs from the Cahaba River, a 190-mile river that flows through Birmingham and Hoover, two of the largest cities in Alabama. A two-fold increase in the $\sum_6$PFAS was observed between AC-7 and AC-9 on the Cahaba River, with $\sum_6$PFAS reaching 29.39 ng L^{-1} after possible inputs from those cities. As expected, a consistent decrease in

the concentrations of PFAS was observed after AC-9, as the Cahaba River flowed downstream through progressively less urbanized and industrialized areas. After inputs from the Cahaba River, catchments for downstream points on the Alabama River become increasingly less urbanized. However, $\Phi_{\sum PFAS}$ substantially increased, reaching up to 63.34 mg s^{-1} (AC-6), the highest in the state, before merging with the Tombigbee River. Both AC-5 and AC-6 samples were collected downstream from large paper manufacturing facilities. Previous studies suggest that facilities that produce paper products could be major sources of PFAS in the environment (Clara et al., 2008; Langberg et al., 2020). Langberg et al. (2020) also noticed that paper fibers from paper mills can be a major vector for the transport and exposure of PFAS.

S.6.2. Black Warrior, Tombigbee, and Mobile Rivers. Observed PFAS contamination in the Tombigbee and Black Warrior basins were low, with mean $\sum_6$PFAS concentration of 7.94 and 12.58 ng L^{-1}, respectively. The highest $\sum_6$PFAS concentration of 40.76 ng L^{-1} was detected in Locust Fork (BT-1), a tributary to the Black Warrior River that receives inputs from the Birmingham area, including a WWTP and a large landfill. PFAS profile in Locust Fork included PFPeA, PFHxA, and PFOA, the same observed in the Cahaba River, which flows through the eastern side of Birmingham. The Tombigbee River is an important route for commercial navigation as it is connected to the Tennessee River through the man-made Tombigbee-Tennessee waterway. Low $\Phi_{\sum PFAS}$ of 0.55 and 0.46 mg s^{-1} were detected in the first two sampling points in the Tombigbee River, prior to discharges from the Black Warrior River (Figure 4.2a). A consistent increase in the $\Phi_{\sum PFAS}$ was observed between samples TM-1,3, reaching 2.42 mg s^{-1}. Although the Tombigbee River watershed is primarily rural, samples TM-1,2 were sampled immediately downstream from paper industries, and TM-3 from a chemical facility, which could have contributed to the increase in mass.

The Mobile River is formed from the confluence of the Tombigbee and Alabama Rivers, captured by the sample TM-4 (Figure 4.11). A substantial decrease in the concentration and flux of $\sum_6$PFAS was observed at that location, in comparison to the upstream levels in the Alabama River. A possible explanation for this decrease could be the high-water exchange in the region, as the area is dominated by wetlands. The

Mobile River is further divided into several tributaries before reaching Mobile Bay. The $\sum_6$PFAS levels in these tributaries were very similar, between 24.22 and 28.02 ng L^{-1} (TM-5,7). Further, the eastern side of the bay is mainly composed of residential and forested areas and sampled tributaries presented low $\sum_6$PFAS levels, ranging between 8.48 and 10.12 ng L^{-1}. The western side, where the city of Mobile is located, is much more industrialized. As expected, $\sum_6$PFAS levels were much higher in those tributaries, ranging from 22.20 to 56.68 ng L^{-1}. Although PFOA was detected in all tributaries, PFOS was only found in one sample (TM-10, PFOS concentration of 30.69 ng L^{-1}), in the Deer River, downstream of several chemical industries. The fact that PFOS was identified does not necessarily mean that those facilities are discharging PFOS into the river, since PFAS precursors like several sulfonamides can breakdown into PFOS (Benskin et al., 2012; Gilljam et al., 2016). However, the detection of PFOS is a potential concern as it can pose a risk to wildlife in the bay, as PFOS was observed to cause developmental effects in several fish species (Wang et al., 2011) and to cause cellular damage to oysters (Aquilina-Beck et al., 2020).

S.6.3 Chattahoochee River. Mean $\sum_6$PFAS levels of 28.83 ng L^{-1} (21.38-43.48 ng L^{-1}) were detected in the Chattahoochee River, with PFPeA, PFHxA, PFHpA, and PFOA as the detected analytes. The Chattahoochee River is part of the Apalachicola-Chattahoochee-Flint river system and the subject of many legal battles between the states of Florida, Alabama, and Georgia, related to shared access to water (Feldman, 2008). An increase in the $\sum_6$PFAS concentration was observed between CH-1 and CH-2, possibly the result of discharges from WWTPs in Lanett and Valley (AL) and industries in LaGrange (GA). However, $\sum_6$PFAS levels decreased and then plateaued in the direction of river flow, even after possible discharges from Columbus, GA, a city with nearly 200,000 habitants. Results from the mass flux analysis are more complex (Figure 4.3a). A consistent increase in the $\Phi_{\sum PFAS}$ was observed between CH-1 and CH-3, from 1.36 to 2.75 mg s^{-1}, followed by a decrease to 1.79 mg s^{-1} in CH-4. Although samples CH-3 and CH-4 were less than 3 miles apart, a 329 cfs increase in the flow and low number of potential sources could partially explain the observed decrease. Moreover, PFHpA, a potential breakdown product of coatings used on food packaging and carpets, was detected in samples CH-1,3 but not in CH-4. The volumetric flow rate

doubled between CH-4 and CH-8, followed by an increase in the $\Phi_{\sum PFAS}$ to 3.76 mg s^{-1}. Several potential sources were present in between those points, including industrial and municipal landfills, WWTPs, military bases, and industries.

S.6.4. Choctawhatchee River. The Choctawhatchee River watershed is located in southern Alabama and discharges into the Choctawhatchee Bay, in Florida. The watershed is situated in a mostly rural area, with forested and cultivated areas accounting for 70% of the overall land use. Mean PFAS concentrations of 17.04 ng L^{-1} were detected in samples from the Choctawhatchee Basin, ranging from below quantification levels to 63.83 ng L^{-1}. The first sample, CW-1, was associated with drainage from primarily forested and agricultural portions of the catchment and did not present any measurable level of PFAS. An increase in the $\Phi_{\sum PFAS}$ was observed in CW-2 after inputs from the Little Choctawhatchee River, a tributary that, among others, receives discharges from a municipal WWTP serving Dothan, AL. In addition to sampling the actual river, Claybank Creek was also sampled to access the effects of tributaries on PFAS pollution. A mass flux of 0.20 mg s^{-1} was calculated for sample CW-3 in Claybank Creek (Figure 4.3b), downstream from the Fort Rucker military base and the City of Enterprise WWTP. High concentrations of PFAS, primarily in groundwater, have been found near military installations in the US due to the use of AFFF (Barzen-Hanson et al., 2017; Houtz et al., 2013; Moody and Field, 1999). The next sample, CW-4, captured the fluxes of both CW-2 and CW-3. CW-4 presented a $\Phi_{\sum PFAS}$ of 0.18 mg s^{-1}, lower than what would have been estimated by simply adding fluxes from the upstream samples. This difference, however, is explained by flow inputs from tributaries between those points. For instance, CW-2 and CW-3 presented flow rates of 496 and 109 cfs, while the flow rate in CW_4 was 850 cfs. This indicates that the inflow from tributaries of about 245 cfs contained little to no PFAS. Finally, an increase in the PFAS flux was identified between CW-4 and CW-5, after inputs from the Pea River and Double Bridges Creek. The Pea River drains approximately 60% of the Alabama component of the Choctawhatchee River watershed, receiving inputs from several industries, landfills, and WWTPs. The increase in the $\Phi_{\sum PFAS}$ to 0.30 mg s^{-1} in CW-5 is most likely a reflection of such inputs.

S.6.5. Perdido River. Mean $\sum_6$PFAS levels of 20.51 ± 10.16 ng L^{-1} (6.75-28.95 ng L^{-1}) were detected in the Perdido River which separates Florida and Alabama, and eventually discharges into Perdido Bay on the northern Gulf of Mexico. The Perdido River is a transboundary river in which potential sources are present in both states, and it exemplifies the need for inter-state strategies to mitigate PFAS contamination. Although $\Phi_{\sum PFAS}$ in the first sample (FP-2) is negligible, it increased to 0.24 mg s^{-1} at FP-3. This increase is most likely a reflection of discharges from Bushy Creek, which receives inputs from a carpet manufacturing facility and a WWTP from the city of Atmore, AL. The mass flux further increased to 0.59 mg s^{-1}, after likely inputs from a landfill in Florida. A final increase in the mass flux was identified at FP-5, reaching 0.67 mg s^{-1}. The Styx River, a 41-mile river that drains 260 mi^2 of the Perdido watershed, is most likely associated with this increase, as it is the main tributary between FP-4 and FP-5. The small increase in the flux suggests that the amount of PFAS provided by the Styx River is low, which is supported by the lack of potential PFAS sources throughout its catchment.

4.6 References

3M. Letter to the US EPA - TSCA Section 8(e) -- Perfluorooctane Sulfonate 1998.

3M. Letter to the US EPA: Phase-out Plan for POSF-Based Products, 2000.

ADEM. ADEM Announces Precedent-Setting Consent Order with 3M. Alabama Department of Environmental Management, 2020, pp. 5.

ADEM. Final Report: 2020 Per- and Polyfluoroalkyl Substances (PFAS) Sampling Program. Alabama Department of Environmental Management, 2021.

Ahrens L, Taniyasu S, Yeung LW, Yamashita N, Lam PK, Ebinghaus R. Distribution of polyfluoroalkyl compounds in water, suspended particulate matter and sediment from Tokyo Bay, Japan. Chemosphere 2010; 79: 266-72.

Aquilina-Beck AA, Reiner JL, Chung KW, DeLise MJ, Key PB, DeLorenzo ME. Uptake and Biological Effects of Perfluorooctane Sulfonate Exposure in the Adult Eastern Oyster Crassostrea virginica. Arch Environ Contam Toxicol 2020; 79: 333-342.

Bai X, Son Y. Perfluoroalkyl substances (PFAS) in surface water and sediments from two urban watersheds in Nevada, USA. Sci Total Environ 2021; 751: 141622.

Barzen-Hanson KA, Roberts SC, Choyke S, Oetjen K, McAlees A, Riddell N, et al. Discovery of 40 Classes of Per- and Polyfluoroalkyl Substances in Historical Aqueous Film-Forming Foams (AFFFs) and AFFF-Impacted Groundwater. Environ Sci Technol 2017; 51: 2047-2057.

Benskin JP, Ikonomou MG, Gobas FA, Woudneh MB, Cosgrove JR. Observation of a novel PFOS-precursor, the perfluorooctane sulfonamido ethanol-based phosphate (SAmPAP) diester, in marine sediments. Environ Sci Technol 2012; 46: 6505-14.

Blum A, Balan SA, Scheringer M, Trier X, Goldenman G, Cousins IT, et al. The Madrid Statement on Poly- and Perfluoroalkyl Substances (PFASs). Environ Health Perspect 2015; 123: A107-11.

Braun JM. Early-life exposure to EDCs: role in childhood obesity and neurodevelopment. Nature Reviews Endocrinology 2017; 13: 161.

Brumovsky M, Karaskova P, Borghini M, Nizzetto L. Per- and polyfluoroalkyl substances in the Western Mediterranean Sea waters. Chemosphere 2016; 159: 308-316.

Casal P, Zhang Y, Martin JW, Pizarro M, Jimenez B, Dachs J. Role of Snow Deposition of Perfluoroalkylated Substances at Coastal Livingston Island (Maritime Antarctica). Environ Sci Technol 2017; 51: 8460-8470.

Chen H, Yao Y, Zhao Z, Wang Y, Wang Q, Ren C, et al. Multimedia Distribution and Transfer of Per- and Polyfluoroalkyl Substances (PFASs) Surrounding Two Fluorochemical Manufacturing Facilities in Fuxin, China. Environ Sci Technol 2018; 52: 8263-8271.

Clara M, Scheffknecht C, Scharf S, Weiss S, Gans O. Emissions of perfluorinated alkylated substances (PFAS) from point sources--identification of relevant branches. Water Sci Technol 2008; 58: 59-66.

Crone BC, Speth TF, Wahman DG, Smith SJ, Abulikemu G, Kleiner EJ, et al. Occurrence of per-and polyfluoroalkyl substances (PFAS) in source water and their treatment in drinking water. Critical reviews in environmental science and technology 2019; 49: 2359-2396.

DEPA. Short-chain Polyfluoroalkyl Substances (PFAS). Danish Environmental Protection Agency, 2015, pp. 106.

Feldman DL. Barriers to adaptive management: lessons from the Apalachicola–Chattahoochee–Flint Compact. Society and Natural Resources 2008; 21: 512-525.

Fischer HB, List JE, Koh CR, Imberger J, Brooks NH. Mixing in inland and coastal waters: Academic press, 1979.

Gao L, Liu J, Bao K, Chen N, Meng B. Multicompartment occurrence and partitioning of alternative and legacy per-and polyfluoroalkyl substances in an impacted river in China. Science of The Total Environment 2020; 729: 138753.

Gilljam J, Leonel J, Cousins IT, Benskin JP. Is Ongoing Sulfluramid Use in South America a Significant Source of Perfluorooctanesulfonate (PFOS)? Production Inventories, Environmental Fate, and Local Occurrence. Environ Sci Technol 2016; 50: 653-9.

Gobelius L, Hedlund J, Durig W, Troger R, Lilja K, Wiberg K, et al. Per- and Polyfluoroalkyl Substances in Swedish Groundwater and Surface Water: Implications for Environmental Quality Standards and Drinking Water Guidelines. Environ Sci Technol 2018; 52: 4340-4349.

Gong X, Yang C, Hong Y, Chung ACK, Cai Z. PFOA and PFOS promote diabetic renal injury in vitro by impairing the metabolisms of amino acids and purines. Sci Total Environ 2019; 676: 72-86.

Guelfo JL, Adamson DT. Evaluation of a national data set for insights into sources, composition, and concentrations of per- and polyfluoroalkyl substances (PFASs) in U.S. drinking water. Environ Pollut 2018; 236: 505-513.

Hansen KJ, Johnson H, Eldridge J, Butenhoff J, Dick L. Quantitative characterization of trace levels of PFOS and PFOA in the Tennessee River. Environmental Science & Technology 2002; 36: 1681-1685.

Higgins CP, Luthy RG. Sorption of perfluorinated surfactants on sediments. Environmental science & technology 2006; 40: 7251-7256.

Houtz EF, Higgins CP, Field JA, Sedlak DL. Persistence of perfluoroalkyl acid precursors in AFFF-impacted groundwater and soil. Environ Sci Technol 2013; 47: 8187-95.

Hu XC, Andrews DQ, Lindstrom AB, Bruton TA, Schaider LA, Grandjean P, et al. Detection of Poly- and Perfluoroalkyl Substances (PFASs) in U.S. Drinking Water Linked to Industrial Sites, Military Fire Training Areas, and Wastewater Treatment Plants. Environ Sci Technol Lett 2016; 3: 344-350.

Johns K, Stead G. Fluoroproducts - the extremophiles. Journal of Fluorine Chemistry 2000; 104: 5-18.

KEMI. Occurrence and use of highly fluorinated substances and alternatives. Swedish Chemical Agency, 2015, pp. 112.

Kim S-K, Kannan K. Perfluorinated acids in air, rain, snow, surface runoff, and lakes: relative importance of pathways to contamination of urban lakes. Environmental science & technology 2007; 41: 8328-8334.

Lane SN, Parsons DR, Best JL, Orfeo O, Kostaschuk R, Hardy RJ. Causes of rapid mixing at a junction of two large rivers: Río Paraná and Río Paraguay, Argentina. Journal of Geophysical Research: Earth Surface 2008; 113.

Lang JR, Allred BM, Field JA, Levis JW, Barlaz MA. National Estimate of Per- and Polyfluoroalkyl Substance (PFAS) Release to U.S. Municipal Landfill Leachate. Environ Sci Technol 2017; 51: 2197-2205.

Langberg HA, Arp HPH, Breedveld GD, Slinde GA, Hoiseter A, Gronning HM, et al. Paper product production identified as the main source of per- and polyfluoroalkyl substances (PFAS) in a Norwegian lake: Source and historic emission tracking. Environ Pollut 2020; 273: 116259.

Lasier PJ, Washington JW, Hassan SM, Jenkins TM. Perfluorinated chemicals in surface waters and sediments from northwest Georgia, USA, and their bioaccumulation in Lumbriculus variegatus. Environ Toxicol Chem 2011; 30: 2194-201.

Lee YM, Lee JY, Kim MK, Yang H, Lee JE, Son Y, et al. Concentration and distribution of per- and polyfluoroalkyl substances (PFAS) in the Asan Lake area of South Korea. J Hazard Mater 2020; 381: 120909.

Lindstrom AB, Strynar MJ, Delinsky AD, Nakayama SF, McMillan L, Libelo EL, et al. Application of WWTP biosolids and resulting perfluorinated compound contamination of surface and well water in Decatur, Alabama, USA. Environ Sci Technol 2011; 45: 8015-21.

Liu J, Wang N, Szostek B, Buck RC, Panciroli PK, Folsom PW, et al. 6-2 Fluorotelomer alcohol aerobic biodegradation in soil and mixed bacterial culture. Chemosphere 2010; 78: 437-44.

Liu Y, Zhang Y, Li J, Wu N, Li W, Niu Z. Distribution, partitioning behavior and positive matrix factorization-based source analysis of legacy and emerging polyfluorinated alkyl substances in the dissolved phase, surface sediment and suspended particulate matter around coastal areas of Bohai Bay, China. Environ Pollut 2019; 246: 34-44.

Ma X, Shan G, Chen M, Zhao J, Zhu L. Riverine inputs and source tracing of perfluoroalkyl substances (PFASs) in Taihu Lake, China. Sci Total Environ 2018; 612: 18-25.

McCarthy C, Kappleman W, DiGuiseppi W. Ecological Considerations of Per- and Polyfluoroalkyl Substances (PFAS). Current Pollution Reports 2017; 3: 289-301.

Milman O. 'We're not a dump' – poor Alabama towns struggle under the stench of toxic landfills. The Guardian, 2019.

Moody CA, Field JA. Determination of perfluorocarboxylates in groundwater impacted by fire-fighting activity. Environmental science & technology 1999; 33: 2800-2806.

Moody CA, Martin JW, Kwan WC, Muir DC, Mabury SA. Monitoring perfluorinated surfactants in biota and surface water samples following an accidental release of fire-fighting foam into Etobicoke Creek. Environmental science & technology 2002; 36: 545-551.

Mulabagal V, Liu L, Qi J, Wilson C, Hayworth JS. A rapid UHPLC-MS/MS method for simultaneous quantitation of 23 perfluoroalkyl substances (PFAS) in estuarine water. Talanta 2018; 190: 95-102.

Munoz G, Budzinski H, Babut M, Lobry J, Selleslagh J, Tapie N, et al. Temporal variations of perfluoroalkyl substances partitioning between surface water, suspended sediment, and biota in a macrotidal estuary. Chemosphere 2019; 233: 319-326.

Munoz G, Giraudel JL, Botta F, Lestremau F, Devier MH, Budzinski H, et al. Spatial distribution and partitioning behavior of selected poly- and perfluoroalkyl substances in freshwater ecosystems: a French nationwide survey. Sci Total Environ 2015; 517: 48-56.

Nakayama SF, Strynar MJ, Reiner JL, Delinsky AD, Lindstrom AB. Determination of perfluorinated compounds in the Upper Mississippi River Basin. Environmental science & technology 2010; 44: 4103-4109.

Newton S, McMahen R, Stoeckel JA, Chislock M, Lindstrom A, Strynar M. Novel Polyfluorinated Compounds Identified Using High Resolution Mass Spectrometry Downstream of Manufacturing Facilities near Decatur, Alabama. Environ Sci Technol 2017; 51: 1544-1552.

Pan Y, Zhang H, Cui Q, Sheng N, Yeung LWY, Guo Y, et al. First Report on the Occurrence and Bioaccumulation of Hexafluoropropylene Oxide Trimer Acid: An Emerging Concern. Environ Sci Technol 2017; 51: 9553-9560.

Pan Y, Zhang H, Cui Q, Sheng N, Yeung LWY, Sun Y, et al. Worldwide Distribution of Novel Perfluoroether Carboxylic and Sulfonic Acids in Surface Water. Environ Sci Technol 2018; 52: 7621-7629.

Pedersen KE, Letcher RJ, Sonne C, Dietz R, Styrishave B. Per- and polyfluoroalkyl substances (PFASs) - New endocrine disruptors in polar bears (Ursus maritimus)? Environ Int 2016; 96: 180-189.

Pouchoulin S, Le Coz J, Mignot E, Gond L, Riviere N. Predicting Transverse Mixing Efficiency Downstream of a River Confluence. Water Resources Research 2020; 56: e2019WR026367.

Ross I, McDonough J, Miles J, Storch P, Thelakkat Kochunarayanan P, Kalve E, et al. A review of emerging technologies for remediation of PFASs. Remediation Journal 2018; 28: 101-126.

Seo SH, Son MH, Choi SD, Lee DH, Chang YS. Influence of exposure to perfluoroalkyl substances (PFASs) on the Korean general population: 10-year trend and health effects. Environ Int 2018; 113: 149-161.

Steenland K, Winquist A. PFAS and cancer, a scoping review of the epidemiologic evidence. Environ Res 2021; 194: 110690.

USEPA. Human Health Toxicity Values for Perfluorobutane Sulfonic Acid and Related Compound Potassium Perfluorobutane Sulfonate. U.S. Environmental Protection Agency, 2021.

Wang F, Shih K, Ma R, Li XY. Influence of cations on the partition behavior of perfluoroheptanoate (PFHpA) and perfluorohexanesulfonate (PFHxS) on wastewater sludge. Chemosphere 2015; 131: 178-83.

Wang N, Liu J, Buck RC, Korzeniowski SH, Wolstenholme BW, Folsom PW, et al. 6:2 fluorotelomer sulfonate aerobic biotransformation in activated sludge of waste water treatment plants. Chemosphere 2011; 82: 853-8.

Wang Z, Cousins IT, Scheringer M, Hungerbühler K. Fluorinated alternatives to long-chain perfluoroalkyl carboxylic acids (PFCAs), perfluoroalkane sulfonic acids (PFSAs) and their potential precursors. Environment international 2013; 60: 242-248.

Wu Z, Wu W. Theoretical analysis of pollutant mixing zone considering lateral distribution of flow velocity and diffusion coefficient. Environmental Science and Pollution Research 2019; 26: 30675-30683.

Xu J, Guo CS, Zhang Y, Meng W. Bioaccumulation and trophic transfer of perfluorinated compounds in a eutrophic freshwater food web. Environ Pollut 2014; 184: 254-61.

Zhao Z, Cheng X, Hua X, Jiang B, Tian C, Tang J, et al. Emerging and legacy per- and polyfluoroalkyl substances in water, sediment, and air of the Bohai Sea and its surrounding rivers. Environ Pollut 2020; 263: 114391.

Zheng G, Salamova A. Are Melamine and Its Derivatives the Alternatives for Per- and Polyfluoroalkyl Substance (PFAS) Fabric Treatments in Infant Clothes? Environ Sci Technol 2020; 54: 10207-10216.

Zhu Y, Ro A, Bartell SM. Household low pile carpet usage was associated with increased serum PFAS concentrations in 2005-2006. Environ Res 2021; 195: 110758.

Zushi Y, Ye F, Motegi M, Nojiri K, Hosono S, Suzuki T, et al. Spatially detailed survey on pollution by multiple perfluorinated compounds in the Tokyo Bay basin of Japan. Environ Sci Technol 2011; 45: 2887-93.

Chapter 5. Source Profiling, Transport, and Distribution of Perfluoroalkyl Substances (PFAS) in a section of the Tallapoosa River Basin

Manuscript in Preparation

5.1 Introduction

Per- and polyfluoroalkyl substances (PFAS) are a group of nearly 5,000 anthropogenic organic substances produced since the late 1940s (Lindstrom et al., 2011; OECD, 2018). These substances generally present a hydrophilic functional group and a hydrophobic and lipophobic chain containing at least one fluorinated moiety $C_nF_{2n-1}^-$ (Buck et al., 2011). The strength and stability of the C-F bonds, the strongest in organic chemistry, provide these substances with stability to chemical, biological, and thermal degradation (Buck et al., 2011; Guelfo and Adamson, 2018). Given their unique properties, PFAS have been widely used in a variety of consumer products, including firefighting foams, non-stick cookware, oil- and water-proof products, and personal care products, among others (Gluge et al., 2020; Johns and Stead, 2000). These substances were used, produced, and discharged throughout decades without much regulatory oversight. Although there is evidence that the major PFAS producers were aware of the potential health effects of PFAS in humans via animal models studies (Sunderland et al., 2019), it was not until 1998 that 3M reported to the United States Environmental Protection Agency (US EPA) evidence regarding the bioaccumulation potential of certain PFAS (3M, 1998). Throughout the last two decades, several studies have been conducted to better understand the behavior and fate of PFAS in the environment (Kurwadkar et al., 2022) and their effects on humans and wildlife (Fenton et al., 2021; Sunderland et al., 2019). These studies have linked PFAS to several adverse health effects, including obesity, endocrine disruption, cholesterol, and testicular and kidney cancers (Fenton et al., 2021; Sunderland et al., 2019).

Regulatory agencies have tried to keep pace with the fluorochemical industry, with several agencies limiting or eliminating the production and use of many PFAS worldwide. In 2006, the US EPA released a global stewardship program to completely phase out the production of PFOA by 2015 (USEPA, 2006). Perfluorooctanesulfonic acid (PFOS) and its salts were added in Annex B of the Stockholm Convention in

2009, limiting their production, while perfluorooctanoic acid (PFOA) and its salts were included in Annex A in 2019, eliminating their production in several countries (Torres et al., 2022). In response to regulatory actions, fluorochemical manufacturers started to replace regulated PFAS with new or unregulated PFAS. The most common emerging PFAS include short-chain perfluoroalkyl acids (PFAAs) and novel analytes with fluorinated segments joined by ether linkages (Pan et al., 2018; Wang et al., 2017). The US EPA recently released interim non-enforceable lifetime health advisory limits of 0.004 ng L^{-1} for PFOA, 0.02 ng L^{-1} for PFOS, 10 ng L^{-1} for hexafluoropropylene oxide dimer acid (GenX), and 2,000 ng L^{-1} for perfluorobutanesulfonic acid (PFBS) (USEPA, 2022). Note that these standards include PFBS and GenX, emerging analytes widely used as PFOS and PFOA replacements, respectively (Pan et al., 2018; Wang et al., 2015). Despite regulatory efforts, PFAS continue to be omnipresent in the environment. They have been detected in every continent, from urban areas in North America (Zhang et al., 2016) and Europe (Castiglioni et al., 2015) to remote areas in Antarctica (Cai et al., 2012). PFAS ubiquity is related to their recalcitrance and large number of sources. PFAS can reach the environment through several pathways, most commonly through direct discharge from fluorochemical manufacturers and other industries that use PFAS in their products, airports, fire-fighting training facilities, and military installations from the use of Aqueous Film Forming Foam (AFFF), wastewater treatment plants and landfills, among others (Hu et al., 2016; Prevedouros et al., 2006).

Our research team conducted a statewide analysis of the distribution and transport of PFAS in Alabama, detecting at least one analyte in 88% of surface water samples with ∑PFAS ranging from non-detect (n.d.) to 237 ng L^{-1} (Viticoski et al., 2022). Several areas of interest emerged from this analysis, including in the Tallapoosa River basin where an increase in the aqueous concentration and mass flux of PFAS was observed as the river moved through the basin (Viticoski et al., 2022). A section of the Tallapoosa River near the Thurlow Dam drawn particular attention due to the presence of two potential sources: the Tallassee Sewage Disposal Pond and the Stone's Throw Landfill. The Stone's Throw Landfill is privately owned and receives up to 1,500 tons of waste daily from all counties in Alabama and three

counties in Georgia (ADEM, 2020). This landfill has been the center of several lawsuits, in which residents alleged that the Alabama Department of Environmental Management (ADEM) violated Title VI of the Civil Rights Act of 1964 Civil Rights by modifying (USEPA, 2017) and renewing the landfill's permit (USEPA, 2018). The US EPA ultimately found "insufficient evidence" of discrimination on the basis of race (USEPA, 2017). The landfill leachate was historically sent to the Tallassee Sewage Disposal Pond for treatment with chlorine prior to its discharge into the Tallapoosa River (Alabama Supreme Court, 2020). The sewage pond also receives waste from 1,782 residential and 18 commercial customers. There is currently litigation against Stone's Throw Landfill for the alleged disposal of illegal contaminants into the river (Alabama Supreme Court, 2020).

Although many studies have investigated the distribution of PFAS in the environment, especially in the last decade, there are still many questions regarding their sources and transport mechanisms. Most studies have historically expressed PFAS contamination in terms of aqueous concentrations, which might not be sufficient to track their transport in the environment as concentrations are highly influenced by the volumetric flow. Mass Flux Analysis can be used as a complementary approach, as it integrates volumetric flow and aqueous concentration (Viticoski et al., 2022). Further, chemical fingerprinting can be used to better understand the sources of PFAS in the environment, even if the presence and amounts of individual PFAS analytes in specific products are unknown (Charbonnet et al., 2021). For instance, PFBS is known to be used in the formulation of Scotchgard^{TM} (Jensen and Warming, 2015), and the presence of PFBS downstream of carpet industries can be used as further evidence of discharge. Thus, this study aims to enhance the understanding of the distribution and transport of PFAS at the watershed level and use chemical fingerprinting to identify potential sources of PFAS. Results will also help in understanding the limitations and uncertainties associated with the use of mass flux analysis in tracking the transport of PFAS in the environment.

5.2 Methods

5.2.1 Chemicals and Reagents

Analytical grade PFAS standards were purchased from Wellington Laboratories (Ontario, Canada). Target analytes include six short-chain PFAA (PFBA, PFPeA, PFHxA, PFHpA, PFBS, and PFPeS), six long-chain PFAA (PFOA, PFNA, PFHxS, PFHpS, PFOS, and PFNS), and five emerging perfluoroethers (HFPO-DA, NaDONA, PF4OPeA, PF5OHxA, and 3,6-OPFHpA). The molecular weight, chemical structure, nomenclature, and CAS of analytes are listed in Table 5.2. Mobile phase modifiers (ammonium formate) were purchased from Agilent Technologies (Wilmington, DE), while high purity LC-MS grade solvents (water, methanol, and acetonitrile) were purchased from VWR international (Suwanee, GA).

5.2.2 Sampling Campaigns

Eleven surface water samples were collected in a section of the Tallapoosa River Basin (Figure 5.1a) on August 8th, 2021. Of these, two were collected in the Thurlow Reservoir (T1 and T3), three in the Tallapoosa River downstream of Thurlow Dam (T4, T6, and T11), and the remaining six in tributaries of interest (Graveyard, Stone, Mill, and Chewacla Creeks and Gleeden Branch). A complete list of coordinates and time/date of sampling is available in Table 5.3. Surface water samples (2 L) were collected using a sampling device comprised of a 1-gallon high-density polyethylene (HDPE) bottle attached to weights and a 100-ft rope. Samples were either collected from bridges, riverbanks, or a boat (T1 and T3). The sampling device was thoroughly rinsed with deionized (DI) water three times between each sample. Water quality parameters such as temperature, pH, and conductivity were measured in situ using a Hanna HI98130 combo tester (Hanna Instruments, Inc.). Field blanks were collected in each sampling trip to assess potential cross-contamination during sampling, transport, and storage by transferring 2 L of DI water from the sampler to a labeled HDPE storage container.

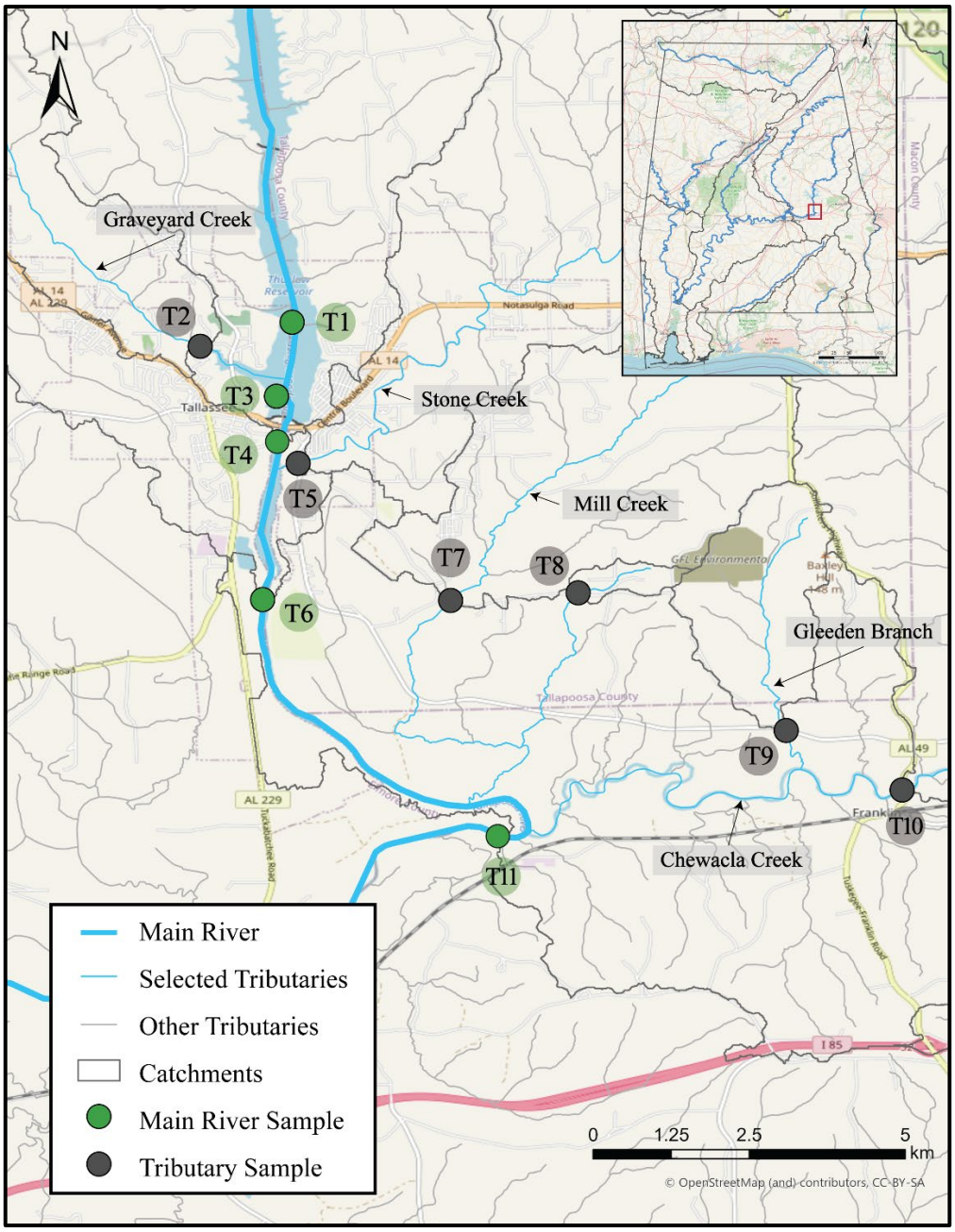

Figure 5.1. Sampling Locations in a section of the Tallapoosa River Basin

5.2.3 Quantitative Analysis

Samples were filtered under vacuum through 0.7 µm GE Whatman glass microfiber filters (GE, Boston, MA, USA) within 24 hours upon arrival to the laboratory to remove large debris and suspended solids. The Tallapoosa River samples were spiked with a mass-labeled internal standard (MPFOS) and processed through solid-phase extraction (SPE) following the methodology described in Viticoski et al. (2022), with

slight modifications. Target analytes were quantified using an Agilent ultrahigh performance liquid chromatography triple quadrupole mass spectrometer (UHPLC-MS/MS), composed of a 1290 Infinity II high-speed pump (Model G7120) coupled to a triple quadrupole mass spectrometer (Model G6460) and Jet-Stream Electrospray Ionization source. Detailed information on sample preparation and analysis is presented in S3.

5.2.4 Data Analysis

Concentrations below detection limits were treated as zero to avoid bias. Potential correlations among the concentrations of detected analytes were analyzed through Spearman Correlation coefficients in R v.4.0.2 (R Foundation for Statistical Computing). LC-MS/MS data were processed using Agilent Mass Hunter software version B.07.1. Spatial analyses were conducted using ArcGIS Pro 2.9 (Esri - Environmental Systems Research Institute). PFAS mass fluxes were calculated by multiplying the total concentration in a given point by the respective 48-h average volumetric flow rate (Eq. 1). Flow rate information was obtained from the United States Geological Survey (USGS), when available, or from the National Water Model (NWM) supported by the United States National Oceanic and Atmospheric Administration (US-NOAA).

$$\Phi_{\sum \mathrm{PFAS}} [mg\ s^{-1}] = \sum \mathrm{PFAS} * \overline{\mathrm{Q}} \qquad \text{(Eq. 1)}$$

5.3 Results and Discussion

5.3.1 PFAS Profile in the Tallapoosa River

Four perfluorocarboxylic acids (PFCAs) were detected in all samples (n=11), including the short-chains PFPeA, PFHxA, and PFHpA and the long-chain PFOA. Perfluorosulfonic acids (PFSAs) and perfluoroethers were not detected in any samples. Table 5.1 illustrates the overall profile of detected analytes at each sampling location. PFHxA had the highest mean concentration of 9.4 ng L^{-1}, ranging from 5.1 to 33.6 ng L^{-1}. PFHxA was detected at similar ranges in several locations across the globe, including 8.0-47.3 ng L^{-1} in the Yellow River in China (Zhao 2016), n.d.-26.0 ng L^{-1} in selected waterbodies in New Jersey (Goodrow et al., 2020), and 4.8-26.2 ng L^{-1} near a landfill in Hangzhou City, China (Xu et al., 2021).

The prevalence of PFHxA in the environment can be partially attributed to this substance being widely used as a PFOA replacement in several consumer products, including in the coating of food packaging and paper products (Xiao et al., 2012). Despite regulations in its production and use, PFOA presented the second-highest mean concentration of 7.5 ng L^{-1} (range 4.9-19.2 ng L^{-1}). Similar ranges were detected in Poyang Lake in China (1.8-17 ng L^{-1}) (Tang et al., 2022), in the Truckee River in Nevada (1.6-19.2 ng L^{-1}) (Bai and Son, 2021), and in the Delaware River (2.12-14.9 ng L^{-1}) (Pan et al., 2018). The presence of PFOA in the Tallapoosa River does not necessarily mean direct inputs of PFOA by nearby sources, as it could be related to the breakdown of labile precursors (Guelfo and Adamson, 2018) and the decomposition of PFOA-based consumer products in the Stone's Throw Landfill. Furthermore, PFPeA was detected at concentrations ranging from 2.7 to 22.1 ng L^{-1} (mean 7.0 ng L^{-1}) and PFHpA from 4.0 to 14.1 ng L^{-1} (mean 5.55 ng L^{-1}). Both substances were detected at similar ranges in selected waterbodies in New Jersey (Goodrow et al., 2020) and in the Truckee River in Nevada (Bai and Son, 2021).

Table 5.1. Aqueous concentration (ng L^{-1}) of the detected PFAS in the Tallapoosa River Basin samples.

Sample ID	Waterbody	PFPeA	PFHxA	PFHpA	PFOA	∑PFAS
T1	Thurlow Reservoir	4.8	6.2	4.7	5.9	21.6
T2	Graveyard Creek	5.0	5.6	4.3	5.7	20.6
T3	Thurlow Reservoir	5.2	6.0	4.4	5.7	21.3
T4	Tallapoosa River	4.8	6.0	4.4	5.8	21.0
T5	Stone Creek	3.4	5.1	3.9	4.9	17.4
T6	Tallapoosa River	4.6	5.9	4.3	5.7	20.5
T7	Mill Creek Reach	22.1	33.6	14.1	19.1	89.0
T8	Mill Creek	5.3	6.3	4.1	5.2	21.0
T9	Gleeden Branch	2.7	6.2	4.0	5.2	18.1
T10	Chewacla Creek	13.2	14.8	7.8	12.5	48.2
T11	Tallapoosa River	6.0	7.4	5.0	6.9	25.3

Significant ($p<0.05$) positive correlations were observed among the concentrations of all detected analytes, with Spearman correlation coefficients ranging from 0.67 for PFHxA-PFHpA to 0.99 for PFHpA-PFOA (Table 5.4). As previously mentioned, only PFCAs were detected in the surface water samples. The prevalence of PFCAs in landfill leachate and landfill-impacted surface water has been observed in previous

studies (Xu et al., 2021). For example, PFCAs accounted for 89% of the total PFAS concentration in surface water samples around a landfill in China (Xu et al., 2021) and 86% in leachate samples from several landfills in Spain (Fuertes et al., 2017). Moreover, short-chain PFCAs accounted for, on average, 73% of the total PFAS concentration in the surface water samples. This pattern has been widely observed in surface water, including in Las Vegas Wash (Bai and Son, 2021) and the Xi-Daling River system in China (Gao et al., 2020). Short-chain PFAS have been widely employed as alternatives to long-chain PFAS due to worldwide regulatory actions in the production and use of legacy PFAS (Blum et al., 2015; Wang et al., 2017). The ubiquity of short-chain PFAS in the environment is troublesome, as these substances are not easily removed from contaminated media, are highly mobile, and can present adverse health effects in humans and wildlife (Ateia et al., 2019; Blum et al., 2015; USEPA, 2021).

5.3.2 Spatial Distribution and Transport of PFAS in the Tallapoosa River

$\sum_4$PFAS ranged from 17.4 ng L^{-1} in Stone Creek (T5) to 89.0 ng L^{-1} in Gleeden Branch (T9), with an overall mean of 29.5 ng L^{-1} and a median of 21.0 ng L^{-1}, respectively (Figure 5.2). Similar mean ∑PFAS were observed in the basins of the Huai River (27.8 ng L^{-1}, n=9), Pearl River (35.8 ng L^{-1}, n=13), and Lambro River (28.1 ng L^{-1}, n=7) (Castiglioni et al., 2018; Pan et al., 2018; Yu et al., 2013). Many studies have evaluated the occurrence of PFAS in riverine surface water, with reported concentrations varying in orders of magnitude (Joerss et al., 2020; Penland et al., 2020). Thus, comparisons must be made carefully, as different methods, sample sizes, and target analytes are usually employed in different studies. Moreover, PFAS mass fluxes ($\Phi_{\sum 4PFAS}$), calculated by multiplying the aqueous concentration in each sampling location by its respective volumetric flow rate, reached up to 3.0 mg s^{-1} in T11 (Figure 5.3 and Table 5.5).

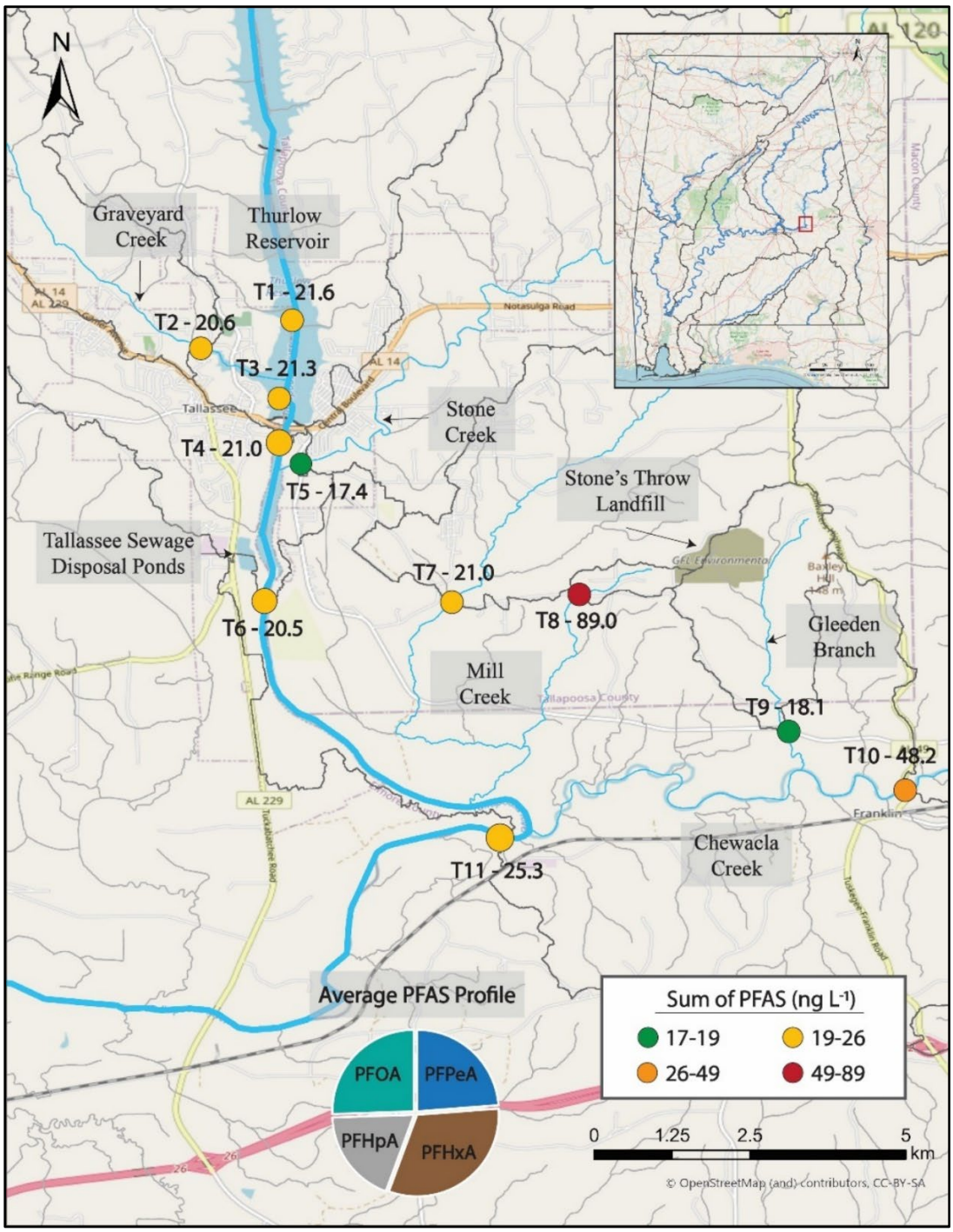

Figure 5.2. Spatial Distribution of PFAS in a section of the Tallapoosa River Basin. Sampled reaches are displayed in light blue, additional reaches in light gray, and catchment areas in black.

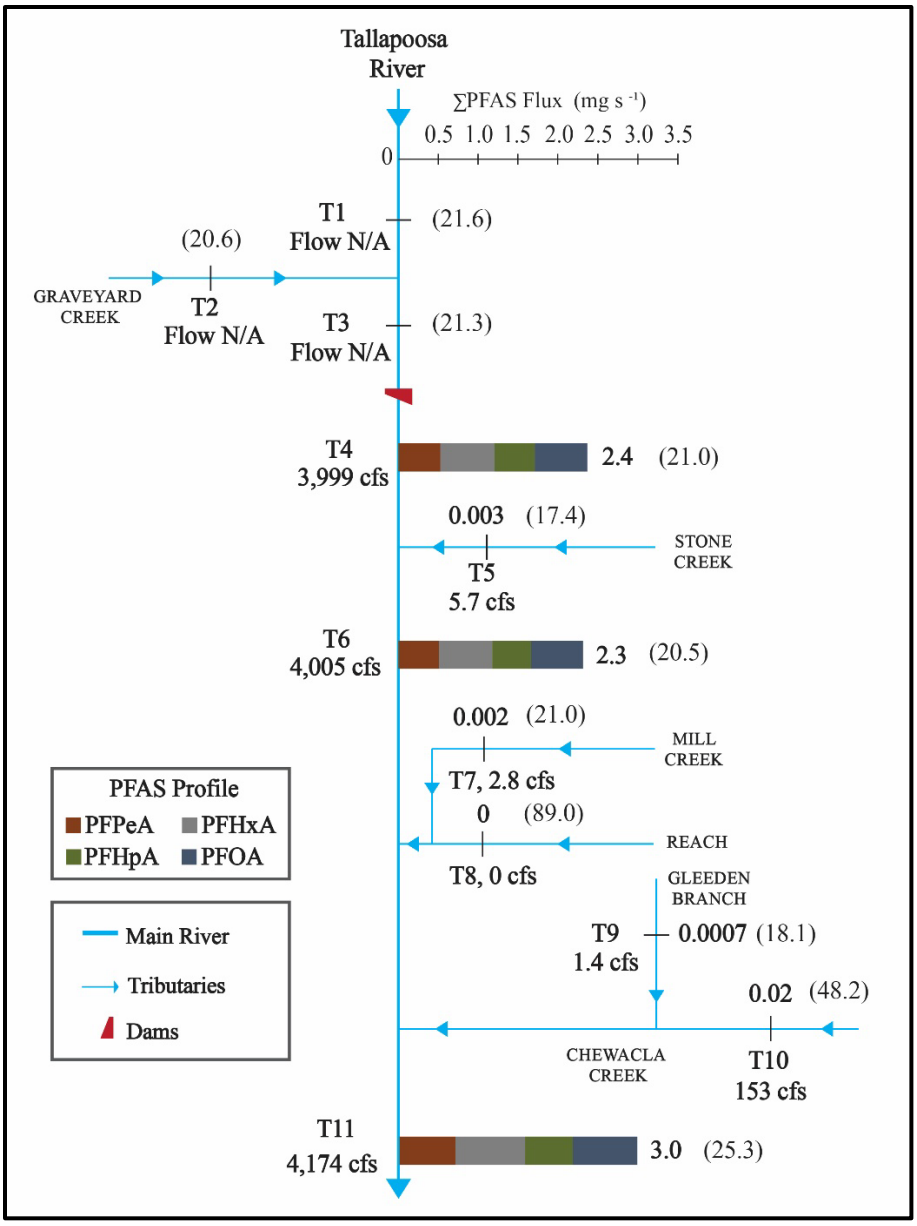

Figure 5.3. Mass Flux of PFAS in a portion of the Tallapoosa River Basin. Flow rate (cfs), mass flux (mg s^{-1}), and aqueous concentration (ng L^{-1}) are displayed for each sampling location following the format $\Phi_{\sum 4PFAS}$ ($\sum_4$PFAS).

Samples collected above and immediately below Thurlow Dam had similar PFAS concentrations, ranging from 21.3-21.6 ng L^{-1} in the Thurlow Reservoir (T1 and T3) to 21.0 ng L^{-1} in the Tallapoosa River (T4). The impact of dams on the overall transport of PFAS has not yet been fully explored. Campo et al. (2016) observed that regulation dams in the Jucar River Basin promoted the accumulation of PFAS in

sediments, and Nakayama et al. (2010) noted an increase in the aqueous concentration of PFAS downstream of a dam, possibly due to the resuspension of solids. Jin et al. (2020) observed that PFAS concentrations were almost five times higher in the storage period than in the discharge period, and that riparian soils can act as both sinks and sources of PFAS, varying with the operation cycle of the dam. More studies are needed to fully understand the impact of dams on the transport of PFAS. Moreover, potential inputs from the Tallassee Sewage Pond were captured by samples T4 and T6. The low variation in the $\sum_4$PFAS (21.0 ng L^{-1} in T4 and 20.5 ng L^{-1} in T6) and $\Phi_{\sum 4PFAS}$ (2.4 mg s^{-1} in T4 and 2.3 mg s^{-1} in T6) between these samples indicates minimal discharge of PFAS at time of sampling. It is unclear whether the Tallassee sewage pond continues to treat leachate from Stone's Throw Landfill, given the current litigation.

Samples T7-T9 captured potential inputs from Stone's Throw Landfill. Similar PFAS concentrations were identified in T7 and T9 (21.0 and 18.1 ng L^{-1}, respectively) but much higher in T8 (89.0 ng L^{-1}). The absence of additional sources in their catchments and proximity to the landfill indicate that most of the detected PFAS contamination is most likely related to the landfill. T8 was collected in a stagnant small reach heavily impacted by groundwater recharge. High PFAS concentrations have been detected in groundwater near landfills, including between 17.3–163 ng L^{-1} in Hangzhou City, China (Xu et al., 2021), 160-240 ng L^{-1} in Melbourne, Australia (Hepburn et al., 2019), and 6.3-1,210 ng L^{-1} in Guangzhou, China (Liu et al., 2022). The study in Guangzhou also detected 637 emerging PFAS in landfill leachate and nearby groundwater through non-target analysis (Liu et al., 2022). Despite the relatively high aqueous concentrations, mass discharges from these reaches (T7-T9) were low ($\Phi_{\sum 4PFAS}$ 0-0.002 mg s^{-1}). Relatively high $\sum_4$PFAS of 48.2 ng L^{-1} were detected in Chewacla Creek (T10), a tributary that receives potential discharges from several industries and a WWTP in Auburn (Figure S1).

The last sampling point (T11), located downstream of Chewacla Creek, had $\sum_4$PFAS of 25.3 ng L^{-1} (PFPeA – 6.0 ng L^{-1}, PFHxA – 7.4 ng L^{-1}, PFHpA – 5.0 ng L^{-1}, and PFOA – 6.9 ng L^{-1}) and $\Phi_{\sum 4PFAS}$ of 3.0 mg s^{-1}. This location was chosen due to its proximity to the drinking water intake for the city of Tuskegee. ADEM has conducted an extensive analysis of PFAS in drinking water sources in Alabama, including in

Tuskegee's Water Treatment Plant. ∑PFAS reached 18.1 ng L^{-1} (PFHxA – 4.1 ng L^{-1}, PFHpA – 3.2 ng L^{-1}, PFOA – 8.1 ng L^{-1}, and PFOS – 2.7 ng L^{-1}) in March 2022 and 4.1 ng L^{-1} (PFOA – 2.0 ng L^{-1} and PFOS – 2.1 ng L^{-1}) in May 2022 (ADEM, 2022). In 2020, our research group sampled a location 4 miles downstream of T11, finding $\sum_4$PFAS of 13.6 ng L^{-1} (PFPeA - 7.8 ng L^{-1} and PFOA - 5.8 ng L^{-1}) and $\Phi_{\sum 4PFAS}$ of 1.0 mg s^{-1} (Viticoski et al., 2022). The high variability in the concentrations and profile of PFAS in the Tallapoosa River could be partially related to variations in volumetric flow rates due to Thurlow Dam. Nonetheless, results from these different datasets indicate the consistent occurrence of PFAS in the Tallapoosa River. Concentrations of PFAS in the Graveyard (T2) and Stone (T5) creeks seem to be highly impacted by mixing from the Tallapoosa River, as supported by the absence of apparent sources in their catchments.

5.4 Conclusions

PFAS were observed to be ubiquitous in surface water samples collected in the Tallapoosa River Basin, with $\sum_4$PFAS between 17.4-89.0 ng L^{-1} and $\Phi_{\sum 4PFAS}$ reaching up to 3.0 mg s^{-1}. The Tallassee Sewage Discharge Pond seems to have little impact on the concentration of PFAS in the Tallapoosa River at the time of sampling. However, it is unclear whether or not the sewage pond was accepting leachate from Stone's Throw Landfill at the time of sampling due to lawsuits. $\sum_4$PFAS between 18.1-89.0 ng L^{-1} were detected in surface water samples downstream of Stone's Throw Landfill. All four analytes detected in this study are PFCAs. Several studies have previously observed the prevalence of PFCAs in surface and groundwater near landfills and in landfill leachate (Xu et al., 2021). These results suggest that Stone's Throw Landfill is a source of PFAS in the Tallapoosa River and surrounding tributaries. $\sum_4$PFAS of 25.3 ng L^{-1} were detected near the drinking water intake for Tuskegee (T11), in which PFOA concentration reached 6.9 ng L^{-1}. This number is over 1,700 times higher than the interim LHA standard recently released by the US EPA. It is worth mentioning, however, that $\sum_4$PFAS and $\Phi_{\sum 4PFAS}$ only increased by 4.3 ng L^{-1} and 0.6 mg s^{-1}, respectively, between the first (T4) and last (T11) sampling points in the Tallapoosa River. This indicates that most of the PFAS contamination in T11 is most likely related to discharges upstream of Thurlow Dam.

Moreover, results from this study enhance the understanding of uncertainties and limitations of the Mass Flux Analysis. Some of the sampled tributaries seem to be heavily impacted by groundwater recharge, presenting generally low volumetric flow rate. Despite high aqueous concentrations, $\Phi_{\sum 4PFAS}$ in sampled tributaries were generally low, varying from 0 to 0.02 mg s^{-1}, compared to 2.3-3.0 mg s^{-1} in the Tallapoosa River. These results suggest that mass flux analysis might not be adequate in reaches that are heavily impacted by groundwater. Further research is needed to better understand the uncertainties associated with this analysis.

5.5 Future Work

The results presented in this chapter, including concentrations, profiles, and mass fluxes of PFAS will be used in a comparative study aiming to further understand the uncertainties associated with mass flux analysis and source attribution of PFAS. This analysis will compare the results from the Tallapoosa River with the Chattooga River Basin, a small river basin that originates in Georgia and discharges into Weiss Lake, in Alabama. Given that these two basins have suspected PFAS sources from different sectors, such comparison will enhance the understanding of specific profiles of PFAS linked to specific sources. For example, the PFAS profile in the Chattooga River is expected to include PFBS and PFOS as major analytes, given their ubiquity in carpet and textile facilities, as previously observed in the Conasauga and Coosa rivers (Konwick et al., 2008; Lasier et al., 2011). The Chattooga River is a free-flowing river that is not thought to be substantially impacted by groundwater recharge. Thus, results of this comparative analysis will also aid in understanding the uncertainties associated with using mass flux analysis to track the transportation of PFAS in the environment.

5.6 Supporting Information

S1. Target Analytes

Table 5.2. Molecular weight, formula, nomenclature, and CAS of the substances targeted in this study and internal standard (MPFOS).

Substance	Nomenclature	Molecular Weight	CAS	Molecular Formula
PFBA	Perfluorobutanoic acid	214.04	375-22-4	C_3F_7COOH
PFPeA	Perfluoropentanoic acid	264.05	2706-90-3	C_4F_9COOH
PFHxA	Perfluorohexanoic acid	314.05	307-24-4	$C_5F_{11}COOH$
PFHpA	Perfluoroheptanoic acid	364.06	375-85-9	$C_6F_{13}COOH$
PFOA	Perfluorooctanoic acid	414.07	335-67-1	$C_7F_{15}COOH$
PFNA	Perfluorononanoic acid	464.08	375-95-1	$C_8F_{17}COOH$
PFBS	Perfluorobutanesulfonic acid	300.10	375-73-5	$C_4F_9SO_3H$
PFPeS	Perfluoropentanesulfonic acid	350.11	2706-91-4	$C_5F_{11}SO_3H$
PFHxS	Perfluorohexanesulfonic acid	400.12	355-46-4	$C_6F_{13}SO_3H$
PFHpS	Perfluoroheptanesulfonic acid	450.12	375-92-8	$C_7F_{15}SO_3H$
PFOS	Perfluorooctanesulfonic acid	500.13	1763-23-1	$C_8F_{17}SO_3H$
PFNS	Perfluorononanesulfonic acid	550.14	68259-12-1	$C_9F_{19}SO_3H$
HFPO-DA	Tetrafluoro-2-(heptafluoropropoxy) propanoic acid	330.05	13252-13-6	$C_6HF_{11}O_3$
NaDONA	Sodium dodecafluoro-3H-4,8-dioxanonanoate	395.1	958445-44-8	$C_7H_5F_{12}NO_4$
PF4OPeA	Perfluoro (4-oxapentanoic) acid	280.04	377-73-1	$C_4HF_7O_3$
PF5OHxA	Perfluoro (5-oxa-6-methoxyhexanoic) acid	380.04	863090-89-5	$C_5HF_9O_3$
3,6-OPFHpA	Perfluoro (3,6-dioxaheptanoic) acid	296.04	151772-58-6	$C_5HF_9O_4$
MPFOS	Sodium perfluoro-1-(1,2,3,4-$^{13}C_4$)octanesulfonate	526.08	960315-53-1	$^{13}C_4{}^{12}C_4F_{17}SO_3Na$

S2. Sampling Information

Table 5.3. Sampling Information for the Tallapoosa River Basin. Geographic coordinates collected in WGS 84 projection.

Sample ID	Reach	Longitude	Latitude	Date	Time (CST)
T1	Thurlow Reservoir	-85.886959	32.549603	8/8/2021	12:04 PM
T2	Graveyard Creek	-85.899926	32.545509	8/8/2021	11:52 AM
T3	Thurlow Reservoir	-85.889066	32.538113	8/8/2021	12:17 PM
T4	Tallapoosa River	-85.888814	32.531904	8/8/2021	10:05 AM
T5	Stone Creek	-85.885703	32.528941	8/8/2021	9:45 AM
T6	Tallapoosa River	-85.890868	32.509128	8/8/2021	1:13 PM
T7	Mill Creek	-85.845468	32.509881	8/8/2021	5:27 PM
T8	Mill Creek	-85.863911	32.509051	8/8/2021	5:46 PM
T9	Gleeden Branch	-85.815315	32.490342	8/8/2021	3:37 PM
T10	Chewacla Creek	-85.798624	32.481722	8/8/2021	3:20 PM
T11	Tallapoosa River	-85.85706	32.475098	8/8/2021	4:33 PM

S3. Quantitative Analysis

Samples were processed and analyzed following the methods presented in Viticoski et al. (2022) and Mulabagal et al. (2018). In summary, Oasis WAX cartridges (6 cc, 150 mg; Waters Corporation, Milford, MA, US) were pre-conditioned with 0.1% ammonium hydroxide in methanol (4 mL) followed by methanol (4 mL) and LC grade water (4 mL). Cartridges were then loaded with 2 L of each sample (500 mL per cartridge) and washed with a 25 mM ammonium acetate buffer (pH 4.0) in LC-grade water (4mL) and dried under vacuum. Target analytes were extracted from cartridges with 1.5 mL of methanol followed by 1.5 mL of 0.1% ammonium hydroxide in methanol. Extracts were filtered through 0.2 μm Agilent glass fiber nylon syringe filters and spiked with MPFOS prior to analysis. Target analytes were then quantified using an Agilent ultrahigh performance liquid chromatography, triple quadrupole mass spectrometer (UHPLC-MS/MS), composed of a 1290 Infinity II high-speed pump (Model G7120) coupled to a triple quadrupole mass spectrometer (Model G6460) and Jet-Stream Electrospray Ionization source. Each sample was analyzed five times in multiple reaction monitoring (MRM) mode, with two method blanks (acetonitrile:water 80:20) in between samples. A 7-point calibration was run.

S4. Results

S.4.1 Spearman Correlation Coefficients

Table 5.4. Spearman Correlation Matrix. A significant correlation ($p<0.05$) was observed for all pairings.

	PFPeA	PFHxA	PFHpA	PFOA
PFPeA	1.00	0.70	0.77	0.75
PFHxA	0.70	1.00	0.67	0.68
PFHpA	0.77	0.67	1.00	0.99
PFOA	0.75	0.68	0.99	1.00

S.4.2 Catchments and Sources

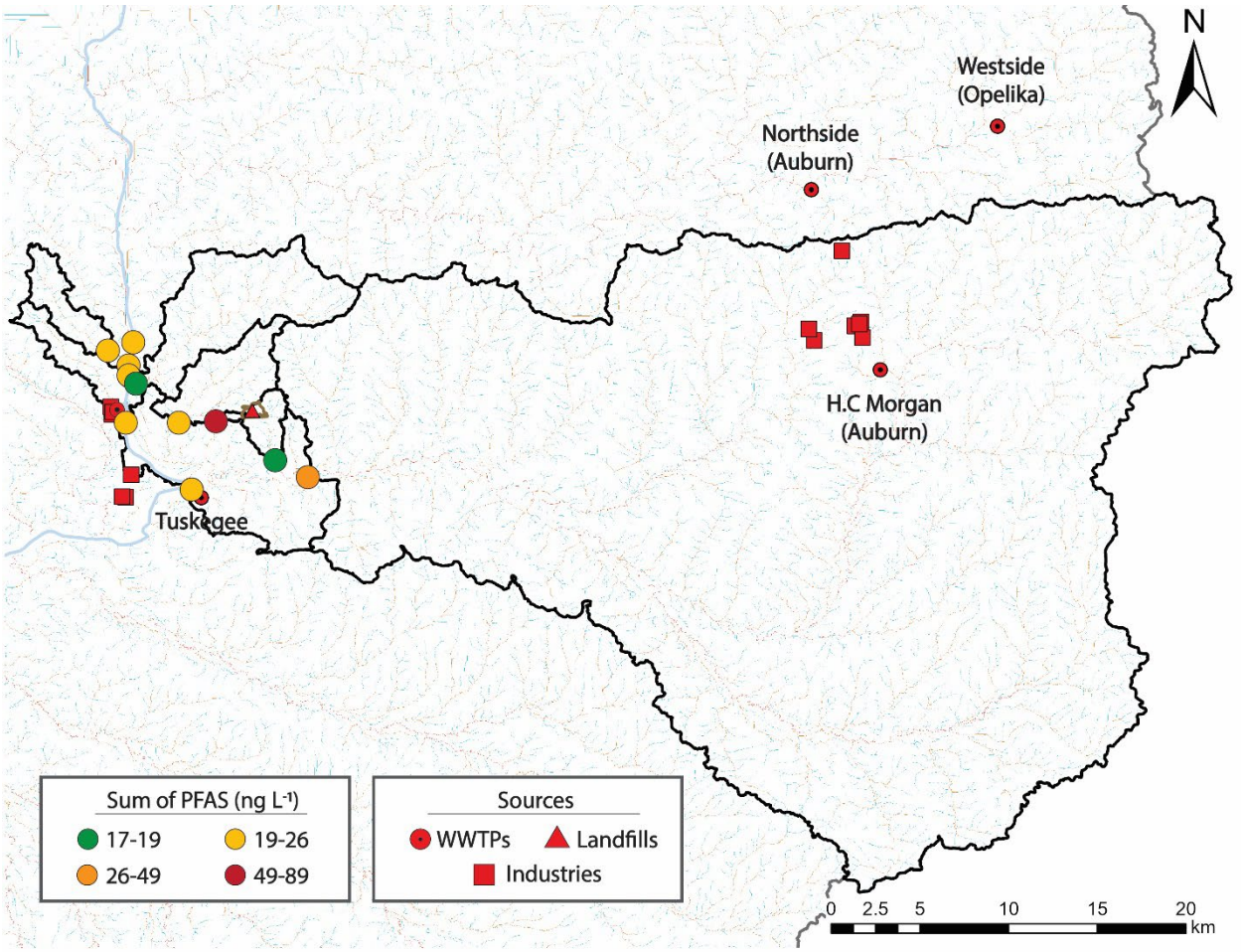

Figure 5.4. Sources and catchments of the Tallapoosa River samples

S.4.3 Mass Flux Analysis

Table 5.5. Results of Mass Flux Analysis for the Tallapoosa River Basin. NA – Not Available.

Sample ID	Reach	Flow rate (cfs)	48-h Flow Rate (cfs)	Source	Mass Flux (mg s^{-1})
T1	Thurlow Reservoir	NA	NA	NWM	NA
T2	Graveyard Creek	NA	NA	NWM	NA
T3	Thurlow Reservoir	NA	NA	NWM	NA
T4	Tallapoosa River	3941.12	3999.13	NWM	2.383
T5	Stone Creek	5.65	5.65	NWM	0.003
T6	Tallapoosa River	3939.35	4005.27	NWM	2.325
T7	Mill Creek	0	0	NWM	0.000
T8	Mill Creek	2.83	2.83	NWM	0.002
T9	Gleeden Branch	1.41	1.41	NWM	2.991
T10	Chewacla Creek	145.5	152.69	NWM	0.001
T11	Tallapoosa River	4098.97	4174.44	NWM	0.208

5.7 References

3M. Letter to the US EPA - TSCA Section 8(e) – Perfluorooctane Sulfonate, 1998.

ADEM. Permitted Municipal Solid Waste Landfills in the State of Alabama. In: Management ADoE, editor, 2020.

ADEM. Per- and Polyfluoroalkyl Substances (PFAS) in Drinking Water. In: Management ADoE, editor, 2022.

Alabama Supreme Court. Jerry Tarver, Sr. v. Advanced Disposal Services South, LLC, et al. Alabama Supreme Court, 2020.

Ateia M, Maroli A, Tharayil N, Karanfil T. The overlooked short- and ultrashort-chain poly- and perfluorinated substances: A review. Chemosphere 2019; 220: 866-882.

Bai X, Son Y. Perfluoroalkyl substances (PFAS) in surface water and sediments from two urban watersheds in Nevada, USA. Sci Total Environ 2021; 751: 141622.

Blum A, Balan SA, Scheringer M, Trier X, Goldenman G, Cousins IT, et al. The Madrid Statement on Poly- and Perfluoroalkyl Substances (PFASs). Environ Health Perspect 2015; 123: A107-11.

Buck RC, Franklin J, Berger U, Conder JM, Cousins IT, de Voogt P, et al. Perfluoroalkyl and polyfluoroalkyl substances in the environment: terminology, classification, and origins. Integr Environ Assess Manag 2011; 7: 513-41.

Cai M, Yang H, Xie Z, Zhao Z, Wang F, Lu Z, et al. Per- and polyfluoroalkyl substances in snow, lake, surface runoff water and coastal seawater in Fildes Peninsula, King George Island, Antarctica. J Hazard Mater 2012; 209-210: 335-42.

Campo J, Lorenzo M, Perez F, Pico Y, Farre M, Barcelo D. Analysis of the presence of perfluoroalkyl substances in water, sediment and biota of the Jucar River (E Spain). Sources, partitioning and relationships with water physical characteristics. Environ Res 2016; 147: 503-12.

Castiglioni S, Davoli E, Riva F, Palmiotto M, Camporini P, Manenti A, et al. Mass balance of emerging contaminants in the water cycle of a highly urbanized and industrialized area of Italy. Water Res 2018; 131: 287-298.

Castiglioni S, Valsecchi S, Polesello S, Rusconi M, Melis M, Palmiotto M, et al. Sources and fate of perfluorinated compounds in the aqueous environment and in drinking water of a highly urbanized and industrialized area in Italy. J Hazard Mater 2015; 282: 51-60.

Charbonnet JA, Rodowa AE, Joseph NT, Guelfo JL, Field JA, Jones GD, et al. Environmental Source Tracking of Per- and Polyfluoroalkyl Substances within a Forensic Context: Current and Future Techniques. Environ Sci Technol 2021; 55: 7237-7245.

Fenton SE, Ducatman A, Boobis A, DeWitt JC, Lau C, Ng C, et al. Per- and Polyfluoroalkyl Substance Toxicity and Human Health Review: Current State of Knowledge and Strategies for Informing Future Research. Environ Toxicol Chem 2021; 40: 606-630.

Fuertes I, Gomez-Lavin S, Elizalde MP, Urtiaga A. Perfluorinated alkyl substances (PFASs) in northern Spain municipal solid waste landfill leachates. Chemosphere 2017; 168: 399-407.

Gao L, Liu J, Bao K, Chen N, Meng B. Multicompartment occurrence and partitioning of alternative and legacy per- and polyfluoroalkyl substances in an impacted river in China. Sci Total Environ 2020; 729: 138753.

Gluge J, Scheringer M, Cousins IT, DeWitt JC, Goldenman G, Herzke D, et al. An overview of the uses of per- and polyfluoroalkyl substances (PFAS). Environ Sci Process Impacts 2020; 22: 2345-2373.

Goodrow SM, Ruppel B, Lippincott RL, Post GB, Procopio NA. Investigation of levels of perfluoroalkyl substances in surface water, sediment and fish tissue in New Jersey, USA. Sci Total Environ 2020; 729: 138839.

Guelfo JL, Adamson DT. Evaluation of a national data set for insights into sources, composition, and concentrations of per- and polyfluoroalkyl substances (PFASs) in U.S. drinking water. Environ Pollut 2018; 236: 505-513.

Hepburn E, Madden C, Szabo D, Coggan TL, Clarke B, Currell M. Contamination of groundwater with per- and polyfluoroalkyl substances (PFAS) from legacy landfills in an urban re-development precinct. Environ Pollut 2019; 248: 101-113.

Hu XC, Andrews DQ, Lindstrom AB, Bruton TA, Schaider LA, Grandjean P, et al. Detection of Poly- and Perfluoroalkyl Substances (PFASs) in U.S. Drinking Water Linked to Industrial Sites, Military Fire Training Areas, and Wastewater Treatment Plants. Environ Sci Technol Lett 2016; 3: 344-350.

Jensen AA, Warming M. Short-chain Polyfluoroalkyl Substances (PFAS). The Danish Environmental Protection Agency 2015.

Jin Q, Liu H, Wei X, Li W, Chen J, Yang W, et al. Dam operation altered profiles of per- and polyfluoroalkyl substances in reservoir. J Hazard Mater 2020; 393: 122523.

Joerss H, Schramm TR, Sun L, Guo C, Tang J, Ebinghaus R. Per- and polyfluoroalkyl substances in Chinese and German river water - Point source- and country-specific fingerprints including unknown precursors. Environ Pollut 2020; 267: 115567.

Johns K, Stead G. Fluoroproducts—the extremophiles. Journal of Fluorine Chemistry 2000; 104: 5-18.

Konwick BJ, Tomy GT, Ismail N, Peterson JT, Fauver RJ, Higginbotham D, et al. Concentrations and patterns of perfluoroalkyl acids in Georgia, USA surface waters near and distant to a major use source. Environmental Toxicology and Chemistry: An International Journal 2008; 27: 2011-2018.

Kurwadkar S, Dane J, Kanel SR, Nadagouda MN, Cawdrey RW, Ambade B, et al. Per- and polyfluoroalkyl substances in water and wastewater: A critical review of their global occurrence and distribution. Sci Total Environ 2022; 809: 151003.

Lasier PJ, Washington JW, Hassan SM, Jenkins TM. Perfluorinated chemicals in surface waters and sediments from northwest Georgia, USA, and their bioaccumulation in Lumbriculus variegatus. Environ Toxicol Chem 2011; 30: 2194-201.

Lindstrom AB, Strynar MJ, Libelo EL. Polyfluorinated compounds: past, present, and future. Environ Sci Technol 2011; 45: 7954-61.

Liu T, Hu LX, Han Y, Dong LL, Wang YQ, Zhao JH, et al. Non-target and target screening of per- and polyfluoroalkyl substances in landfill leachate and impact on groundwater in Guangzhou, China. Sci Total Environ 2022; 844: 157021.

Mulabagal V, Liu L, Qi J, Wilson C, Hayworth JS. A rapid UHPLC-MS/MS method for simultaneous quantitation of 23 perfluoroalkyl substances (PFAS) in estuarine water. Talanta 2018; 190: 95-102.

Nakayama SF, Strynar MJ, Reiner JL, Delinsky AD, Lindstrom AB. Determination of perfluorinated compounds in the Upper Mississippi River Basin. Environmental science & technology 2010; 44: 4103-4109.

OECD. Toward a new comprehensive global database of per-and polyfluoroalkyl substances (PFASs): Summary report on updating the OECD 2007 list of per-and polyfluoroalkyl substances (PFASs). Organisation for Economic Cooperation and Development (OECD) 2018.

Pan Y, Zhang H, Cui Q, Sheng N, Yeung LWY, Sun Y, et al. Worldwide Distribution of Novel Perfluoroether Carboxylic and Sulfonic Acids in Surface Water. Environ Sci Technol 2018; 52: 7621-7629.

Penland TN, Cope WG, Kwak TJ, Strynar MJ, Grieshaber CA, Heise RJ, et al. Trophodynamics of Per- and Polyfluoroalkyl Substances in the Food Web of a Large Atlantic Slope River. Environ Sci Technol 2020; 54: 6800-6811.

Prevedouros K, Cousins IT, Buck RC, Korzeniowski SH. Sources, fate and transport of perfluorocarboxylates. Environmental science & technology 2006; 40: 32-44.

Sunderland EM, Hu XC, Dassuncao C, Tokranov AK, Wagner CC, Allen JG. A review of the pathways of human exposure to poly- and perfluoroalkyl substances (PFASs) and present understanding of health effects. J Expo Sci Environ Epidemiol 2019; 29: 131-147.

Tang A, Zhang X, Li R, Tu W, Guo H, Zhang Y, et al. Spatiotemporal distribution, partitioning behavior and flux of per- and polyfluoroalkyl substances in surface water and sediment from Poyang Lake, China. Chemosphere 2022; 295: 133855.

Torres F, Guida Y, Weber R, Machado Torres JP. Brazilian overview of per- and polyfluoroalkyl substances listed as persistent organic pollutants in the stockholm convention. Chemosphere 2022; 291: 132674.

USEPA. 2010/2015 PFOA Stewardship Program. In: Agency USEP, editor, 2006.

USEPA. Re: Closure of Administrative Complaint, EPA File No. 06R-03-R4 In: Agency USEP, editor, 2017.

USEPA. Re: Preliminary Findings Letter, EPA Administrative Complaint No.16R-17-R4 In: Agency USEP, editor, 2018.

USEPA. Human Health Toxicity Values for Perfluorobutane Sulfonic Acid and Related Compound Potassium Perfluorobutane Sulfonate., 2021.

USEPA. EPA Announces New Drinking Water Health Advisories for PFAS Chemicals, $1 Billion in Bipartisan Infrastructure Law Funding to Strengthen Health Protections. In: USEPA, editor, 2022.

Viticoski RL, Wang D, Feltman MA, Mulabagal V, Rogers SR, Blersch DM, et al. Spatial distribution and mass transport of Perfluoroalkyl Substances (PFAS) in surface water: A statewide evaluation of PFAS occurrence and fate in Alabama. Sci Total Environ 2022; 836: 155524.

Wang Z, Cousins IT, Scheringer M, Hungerbuehler K. Hazard assessment of fluorinated alternatives to long-chain perfluoroalkyl acids (PFAAs) and their precursors: status quo, ongoing challenges and possible solutions. Environ Int 2015; 75: 172-9.

Wang Z, DeWitt JC, Higgins CP, Cousins IT. A Never-Ending Story of Per- and Polyfluoroalkyl Substances (PFASs)? Environ Sci Technol 2017; 51: 2508-2518.

Xiao F, Halbach TR, Simcik MF, Gulliver JS. Input characterization of perfluoroalkyl substances in wastewater treatment plants: source discrimination by exploratory data analysis. Water Res 2012; 46: 3101-9.

Xu C, Liu Z, Song X, Ding X, Ding D. Legacy and emerging per- and polyfluoroalkyl substances (PFASs) in multi-media around a landfill in China: Implications for the usage of PFASs alternatives. Sci Total Environ 2021; 751: 141767.

Yu N, Shi W, Zhang B, Su G, Feng J, Zhang X, et al. Occurrence of perfluoroalkyl acids including perfluorooctane sulfonate isomers in Huai River Basin and Taihu Lake in Jiangsu Province, China. Environ Sci Technol 2013; 47: 710-7.

Zhang X, Lohmann R, Dassuncao C, Hu XC, Weber AK, Vecitis CD, et al. Source attribution of poly- and perfluoroalkyl substances (PFASs) in surface waters from Rhode Island and the New York Metropolitan Area. Environ Sci Technol Lett 2016; 3: 316-321.

Chapter 6. Summary and Contributions to the Scientific Knowledge

This work improved the understanding of the distribution, transport, and fate of PFAS in the natural environment, as well as uncertainties and limitations associated with tracking these substances in the environment. Specific contributions include:

6.1 Improved knowledge of the global distribution, profile, and ERCs of PFAS in the environment

Hundreds of studies have investigated the occurrence and distribution of PFAS in the environment in the last two decades. Although important conclusions can be drawn from these studies individually, information on their overall global distribution is lacking. Further, given the complexity and the large number of PFAS substances, PFAS have been detected in the environment at concentrations ranging from pg L^{-1} (Yamazaki et al., 2019) to mg L^{-1} (Joerss et al., 2020). The wide range of detected PFAS concentrations has led to a high degree of uncertainty around what constitutes ERCs of PFAS. Information on ERCs is essential for studies conducting controlled experiments, in which parameters must mimic environmental conditions to ensure results are meaningful and representative.

In Chapter 3, research data from 228 peer-reviewed journals were used to better understand the (i) profiles, (ii) spatial distribution, and (iii) ERCs of PFAS in surface water, sediment, and groundwater. To accomplish this, specific information, including location, total and individual PFAS concentrations, author, year, and media, was extracted from each of the 228 studies. Although PFAAs were the most targeted and frequently detected PFAS in all analyzed matrices, novel fluorinated alternatives and precursors have increasingly been detected in the environment at high frequencies. Further, PFAS were detected in 43 countries across all continents spanning over two decades (1999-2021). Most studies were concentrated on select regions, including the Bohai and Yellow seas in China, Eastern Unites States, and Western Europe. Regarding their concentrations, ∑PFAS reached up to 2,270 μg L^{-1} in surface water, 7,090 μg L^{-1} in groundwater, and 2,450 ng gdw^{-1} in sediment. Worldwide information on PFAS concentrations was used to develop ERCs, recommended not to exceed 2,721 and 48,606 ng L^{-1} in studies evaluating PFAS in

surface water and groundwater, respectively, and 137.9 ng gdw^{-1} in sediments to guarantee environmental relevance.

This assessment illustrates the extent of the global distribution of PFAS in the natural environment and provides essential information that can help guide future PFAS research. As most studies have been concentrated in areas historically associated with PFAS contamination, the true global extent of PFAS contamination is still unknown. Fluorochemistry is rapidly changing, with emerging PFAS, such as HFPO-DA, HFPO-TA, F-53B, 6:2 FTSA, TFA, PFPrA, and FHxSA, being frequently detected in the environment. The ERCs provided in this assessment can be used in the design of controlled experiments to ensure that results are meaningful and represent environmental conditions.

6.2 Enhanced understanding of the spatial distribution of PFAS in Alabama and their transport behavior in large, interconnected river systems

Alabama is a particular hotspot for PFAS in the United States. Some of the highest concentrations in surface water recorded in the United States (up to 31,906 ng L^{-1}) were identified near Decatur in northern Alabama (Hansen et al., 2002; Lindstrom et al., 2011; Newton et al., 2017). PFAS were also identified in drinking water sources of several municipalities in the state (ADEM, 2022). Moreover, studies generally express PFAS contamination solely in terms of aqueous concentration, which is heavily impacted by the volumetric flow rate. Considering aqueous concentration alone can lead to erroneous conclusions regarding the transport behavior and sources of PFAS into the environment. Alternatively, mass flux can be used as a complementary metric as it integrates aqueous concentration and volumetric flow rate.

In Chapter 4, a statewide analysis of PFAS in Alabama was conducted to better understand the (i) spatial distribution of seventeen PFAS in surface water in the major river systems in the state, (ii) transport characteristics of PFAS in large, interconnected systems, and (iii) potential source areas of PFAS in Alabama. Strategic sampling locations were determined to capture inlets and outlets of rivers flowing into and out of Alabama, confluence and headwaters of rivers, and areas of contrasting land use (urban vs.

forested vs. rural). The 74 surface water samples were collected between June 27th and August 30th, 2020, covering all major river basins in the state. Samples were filtered under vacuum to remove suspended solids and large debris, processed through SPE, and analyzed for target analytes using a UHPLC-MS/MS. PFAS were ubiquitous in the collected samples, with at least one PFAS detected in 88% of all samples. Short-chain PFAS accounted for the majority of the contamination in the state, in agreement with a trend that has been observed globally. Total PFAS concentration reached 237 ng L^{-1}, with mean $\sum_6$PFAS of 35.2 ng L^{-1}. PFAS distribution was not homogenous across the state. While the Coosa and Alabama rivers presented relatively high mean $\sum_6$PFAS of 191 and 100 ng L^{-1}, respectively, the remaining river systems presented mean $\sum_6$PFAS between n.d. and 28.8 ng L^{-1}. Mass fluxes were calculated by multiplying the ∑PFAS by its respective volumetric flow rate at a given location. Consistent increases in PFAS mass fluxes were generally observed as rivers flowed through the state, indicating the presence of a large number of sources across the state. The highest mass flux of 63.3 mg s^{-1} was detected on the last sample point in the Alabama River, which eventually discharges into Mobile Bay.

Results of this work identified PFAS to be ubiquitous in the state, raising important considerations regarding PFAS exposure in Alabama as many of the sampled locations are used as drinking water sources. Mass flux analysis was used to better understand the transport characteristics of PFAS in river systems and to identify potential PFAS source areas. Although background fluxes from transboundary rivers are a substantial source of PFAS into Alabama, consistent increases as rivers flowed through the state suggest the existence of several sources within the state. These inputs might not have been captured if only aqueous concentrations were considered, highlighting the usefulness of the mass flux analysis.

6.3 Insights into source attribution and transport characteristics of PFAS, and uncertainties related to the use of mass flux analysis

Several areas of interest emerged from the statewide analysis of PFAS in Alabama presented in Chapter 4, including a section of the Tallapoosa River Basin downstream from Thurlow Dam. In Chapter 5, a watershed-level analysis was conducted to enhance the understanding of (i) the sources of PFAS

through chemical profiling, (ii) transport characteristics of PFAS through a mass flux analysis, and (iii) uncertainties and limitations associated with tracking PFAS in the environment.

Eleven surface water samples were collected in a section of the Tallapoosa River Basin in August 2021, processed through SPE, and analyzed using a UHPLC-MS/MS. Four PFCAs were detected in all eleven samples, with ∑PFAS ranging from 17.4 to 89.0 ng L^{-1}. Low variation was observed between samples collected upstream and downstream from the Tallassee Sewage Pond, indicating low inputs at the time of sampling. In contrast, high ∑PFAS were detected in tributaries near the Stone's Throw Landfill. ∑PFAS of 25.3 ng L^{-1} were detected in the last sampling location, which is located near the drinking water intake for Tuskegee, AL, posing potential risks for its residents. PFAS mass fluxes were generally low in tributaries, ranging from 0 to 0.02 mg s^{-1}, despite high aqueous concentrations. Many of these tributaries seem to be affected by groundwater recharge, underlining a potential limitation on the use of mass flux analysis.

6.4 Insights into Spatial Analyses and Display of Environmental Data

All three research projects presented in this dissertation inherently have a strong spatial component. Several methodologies were developed/used to ensure that the collected data were properly displayed and analyzed. For instance, in Chapter 3, an Esri® StoryMap application containing all layers and data were developed in addition to the traditional maps present throughout the chapter. The addition of this interactive application allows the reader to better visualize the data and fully access the available information associated with each component. In Chapter 4, protocols were used to delineate the catchment area for each location in ArcGIS Pro to identify potential sources of PFAS within these catchments. The protocols and tools mentioned throughout this work can help researchers and stakeholders in the analysis and display of environmental data.

6.5 References

ADEM. Per- and Polyfluoroalkyl Substances (PFAS) in Drinking Water. In: Management ADoE, editor, 2022.

Hansen KJ, Johnson H, Eldridge J, Butenhoff J, Dick L. Quantitative characterization of trace levels of PFOS and PFOA in the Tennessee River. Environmental Science & Technology 2002; 36: 1681-1685.

Joerss H, Schramm TR, Sun L, Guo C, Tang J, Ebinghaus R. Per- and polyfluoroalkyl substances in Chinese and German river water - Point source- and country-specific fingerprints including unknown precursors. Environ Pollut 2020; 267: 115567.

Lindstrom AB, Strynar MJ, Delinsky AD, Nakayama SF, McMillan L, Libelo EL, et al. Application of WWTP biosolids and resulting perfluorinated compound contamination of surface and well water in Decatur, Alabama, USA. Environ Sci Technol 2011; 45: 8015-21.

Newton S, McMahen R, Stoeckel JA, Chislock M, Lindstrom A, Strynar M. Novel Polyfluorinated Compounds Identified Using High Resolution Mass Spectrometry Downstream of Manufacturing Facilities near Decatur, Alabama. Environ Sci Technol 2017; 51: 1544-1552.

Yamazaki E, Taniyasu S, Ruan Y, Wang Q, Petrick G, Tanhua T, et al. Vertical distribution of perfluoroalkyl substances in water columns around the Japan sea and the Mediterranean Sea. Chemosphere 2019; 231: 487-494.